Branching Out with CCTP; The Synthesis of Branched Functional Polymers

By Kayleigh McEwan

A thesis submitted in partial fulfilment of the requirements for the degree of

Doctor of Philosophy in Chemistry

Department of Chemistry

University of Warwick

December 2012

Table of Contents

List of Figures

Abbreviations

AIBN	2,2'-Azo-*bis*-isobutyrylnitrile
ATRP	Atom transfer radical polymerisation
BDDA	1,4-Butanediol diacrylate
BDDMA	1,4-Butanediol dimethacrylate
BHT	Butylated hydroxytoluene
Bis-MPA	Bis(methyloyl)propionic acid
BM	Benzyl mercaptan
BzAm	Benzylamine
CCT	Catalytic chain transfer
CCTP	Catalytic chain transfer polymerisation
CLD	Chain length distribution
CoBF	Co(II)dimethylglyoxime-difluoroboryl
Co(III)-H	Cobalt(III)-hydride
CuAAc	Copper mediated azide-alkyne click
DAm	Decylamine
DCE	1,2-Dichloroethane
DCM	Dichloromethane
DDMA	1,10-Decanediol methacrylate
DDT	Dodecanethiol
DEGDMA	Di(ethylene glycol) dimethacrylate
DEGMEMA	Di(ethylene glycol) methyl ether methacrylate
DLS	Dynamic light scattering
DMF	Dimethyl formamide
DMPP	Dimethylphenylphosphine

DMSO	Dimethyl sulfoxide
DP	Degree of polymerisation
DVB	Divinyl benzene
EGDMA	Ethylene glycol dimethacrylate
ESI-MS	Electrospray ionisation-mass spectrometry
Et. OAc.	Ethyl acetate
FT-IR	Fourier transform- infra red
GC-FID	Gas chromatograph- flame ionisation detection
GMA	Glycidyl methacrylate
GPC	Gel permeation chromatography
GTP	Group transfer polymerisation
HDDMA	1,6-Hexanediol dimethacrylate
HEMA	Hydroxyethyl methacrylate
IR	Infra red
IV	Intrinsic viscosity
LALS	Low angle light scattering
LCST	Lower critical solution temperature
LS	Light scattering
MALDI-ToF	Matrix assisted laser desorption ionisation- time of flight
MALS	Multi angle light scattering
ME	Mercaptoethanol
MeCN	Acetonitrile
MEK	Methyl ethyl ketone
MMA	Methyl methacrylate
M_n	Number average molecular weight

M_w	Weight average molecular weight
NMP	Nitroxide mediated polymerisation
NMR	Nuclear magnetic resonance
OEGMEMA	Oligoethylene glycol methyl ether methacrylate
PAm	Propylamine
PDA	Photodiode array
PDi	Polydispersity index
PEG	Poly(ethylene glycol)
PE-SH	Thiol terminated polyethylene
PGMA	Polyglycidyl methacrylate
pKa	Acid dissociation constant
PMMA	Polymethyl methacrylate
ppm	parts per million
PS	Polystyrene
RAFT	Reversible addition fragmentation chain transfer
RI	Refractive index
ROP	Ring-opening polymerisation
SEC	Size exclusion chromatography
SCROP	Self condensing ring-opening polymerisation
SCVP	Self condensing vinyl polymerisation
TCEP	Tris(2-carboxyethyl)phosphine
T_d	Decomposition temperature
TEA	Triethylamine
TEGDMA	Triethylene glycol dimethacrylate
TG	Thioglycerol

T_g	Glass transition temperature
THF	Tetrahydrofuran
TMA	Thiol-Michael addition
TMPTMA	Trimethylolpropane trimethacrylate
TMS	Tetramethyl silane
TPGDA	Tripropylene glycol diacrylate
UV	Ultra-violet
V-601	Azobis(2,4-dimethylvaleronitrile)
VOC	Volatile organic compound

Acknowledgements

First and foremost my thanks go to Dave, for giving me the opportunity to work in the Haddleton group, and for all his help and advice throughout my time here at Warwick. Dave's "just do it" attitude has become renowned throughout group members past and present, and although it is not infallible, it remains excellent advice that I'm never likely to forget.

My thanks to the Haddleton group members, who have made my time here so enjoyable. Especially Raj and Claudia, who have always provided me with support and advice when things haven't gone to plan (even though Raj's advice is a bit odd sometimes, but at least he makes me laugh!), and they never fail to come through with some emergency chocolate or snacks to keep me smiling. Stacy, Mat, George, Ant, James, Jay, Chris F, and Pete for making me feel so welcome starting my PhD at a new University, and I'm not sure whether to thank you guys for introducing me to the nightclubs in Leam or not... but it was always an experience!

Thank you to our fonts of knowledge, past and present, Paul, Beppe and Fina, who have been our organic chemistry go tos in times of need. Especially to Paul, who had the patience to edit my whole thesis, there will be cake in return!

A special thanks to everyone who helped me with the ACOMP (my unfortunately not so successful project), Steve O'Donohue, who should be an honorary Haddleton group member due to the amount of time he spends here! Ian Willoughby, Ben MacCreath Tomek, Julien and Martin, who sympathised with me over all things ACOMP related.

Massive thank yous to Jamie (SKM) for all the CCTP banter, Alex S for being my fume cupboard friend, Chris S and Chris W for providing much bowling related entertainment, Guangzhao, Muxiu, Remzi, Ed, Athina, Flo, Qiang, Jasmin, Yanzi, Jenny C, Ronan, Sarah-Jane, Dan, Jenny K, Tara and Fran. You have all helped me to get this finished and whether the contribution was big or small, it was appreciated all the same.

Finally, thank you to my family and friends; Mum, Dad, Kirsten, Conrad, Rachel, Keiran and Alex H, without your love, support and cups of tea/cider/hugs/Chinese takeaways, this would not have been possible.

Declaration

Experimental work contained in this thesis is original research carried out by the author, unless otherwise stated, in the Department of Chemistry at the University of Warwick, between October 2008 and November 2012. No material contained herein has been submitted for any other degree, or at any other institution.

Results from other authors are referenced in the usual manner throughout the text.

_____ Date: _____

Kayleigh McEwan

Abstract

Initially the aims of this thesis were to settle conflicting literature that arose based on the consistency of results obtained from the synthesis of branched polymers, using divinyl monomer ethylene glycol dimethacrylate (EGDMA), by catalytic chain transfer polymerisation (CCTP). By polymerisation of EGDMA using a range of catalyst concentrations, and introduction of comonomers, a range of branched polymers were obtained, all of which retained high levels of vinyl functionality in the resulting products. With the increasing popularity of click chemistry, the natural progression of this work lent towards the functionalisation of these branched vinyl containing polymers by thiol-Michael addition, using a range of commercial thiols, in the creation of branched highly functional polymers, which display enhanced solution properties compared to their linear counterparts, from a small commercial monomer set.

The desire to synthesise highly functional polymers led to investigation of epoxide containing monomer, glycidyl methacrylate (GMA), which has proven to be versatile to a range of functionalities. The synthesis of linear GMA homopolymers *via* CCTP resulted in polymers with the potential for dual functionalisation, at both epoxide and ω-unsaturated groups; to which, thiol-Michael addition and self-catalysed epoxide ring-opening with amines was investigated in the synthesis of a range of functional polymers, from a single polymer precursor.

Finally the copolymerisation of EGDMA and GMA *via* CCTP was investigated in the synthesis of branched functional polymers, whereby the level of vinyl groups retained and epoxide functionality can be tuned through monomer ratios. Site selective functionalisation of the high level of epoxide and vinyl groups was conducted using both thiol-Michael addition and self-catalysed ring-opening of epoxides with functional amines. By site selective functionalisation with both hydrophobic and hydrophilic groups, amphiphilic branched copolymers are obtained, with the potential for the synthesis of branched polymers capable of self-assembly.

Chapter 1

---

1. Introduction

“Dear colleague. Leave the concept of large molecules alone... there can be no such thing as a macromolecule”

Advice given to Hermann Staudinger after his lecture introducing the revolutionary concept of polymers

1.1. Branched Polymers

Polymer topology is an important governing aspect of the properties and application of polymers. [1] The interest in branched polymers of a variety of architectures has grown rapidly over the past 20 years. Branched polymers can provide a range of desirable properties over their linear counterparts, such as increased solubilities, low solution viscosities, modified melt rheology and high levels of terminal functionality.[2-4] Applications of such polymers are often towards use in coatings, resins,[5, 6] flow improvers or viscosity modifiers and biomedical applications, such as drug delivery devices, utilising the "cavities" formed in densely branched structures.[7-10]

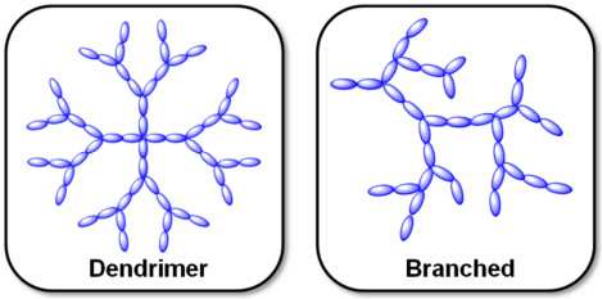

Figure 1.1: General structure of macromolecules of dendritic and branched architectures

Dendrimers are highly branched macromolecules which offer a high level of structural order, with ideally perfect symmetry and ideally a polydispersity index (PDi) of 1; hence the use of these products in drug delivery is extremely attractive.[11, 12] However, the demanding synthesis, high reagent excesses and often multiple purification steps can lead to a high cost and limitations in the applicability of these materials. Alternative architectures explored with analogous properties to dendrimers, of lower cost and comparably facile synthesis methods, have commonly included hyperbranched and star structures. The focus of this thesis is (hyper)branched polymers.

1.2. Synthesis of Branched Polymers

Classically the synthesis of branched polymers is based on Flory's AB_x monomer approach, whereby A groups are limited to reaction with B groups and the relative reactivities of A and B group are equal, also termed single monomer methodology.[13, 14] However, very few AB_x monomers are commercially available; therefore, creating a

library of hyperbranched polymers requires large amounts of monomer synthesis. Expansion of the AB_x homopolymerisation to copolymerisations of AB_x+B_y monomers also exists, termed double monomer methodology. This enables additional functionality to be introduced through the B_y unit, a more commercially available structure, therefore creating a library of hyperbranched polymers is more facile, negating the need for large amounts of monomer synthesis, thus rendering it a more industrially viable method. Examples of both AB_x and AB_x+B_y strategies have been documented using both step growth and chain growth methods.

A consideration for the synthesis of non-linear architectures, hyperbranched polycondensates in particular, is the propensity of these materials to crosslink using certain synthesis conditions. Two predominant theories exist on prediction of the gel point, the first of which was postulated by Carothers in which the critical degree of conversion at the gel point (P_{gel}) is defined by Equation 1.1.[15]

$$P_{gel} = 2/f$$

Equation 1.1: whereby P_{gel} is the critical degree of conversion at the gel point and f is the average functionality the monomers employed

The second gel theory was postulated by Flory-Stockmayer in which P_{gel} is defined through the coefficient of branching α as defined by Equation 1.2.[16-19]

$$\alpha = \frac{1}{f-1}$$

Equation 1.2: Whereby α is the critical extent of reaction and f is the functionality of the monomer of greater functionality

Flory-Stockmayer gel theory (Equation 1.2) is likely to provide an underestimation of the true gel point as cyclisation, or the formation of loops, does not contribute to gel formation. The Carothers theory (Equation 1.1) however, provides an overestimation of the value of P_{gel}. These equations become particularly useful for applications regarding thermosetting or photocurable adehesive applications as it provides a means of which to predict the gel point based on functionality and conversion.

1.2.1. Branched Polymers by Step Growth Strategies

1.2.1.1. Poly Condensation Reactions

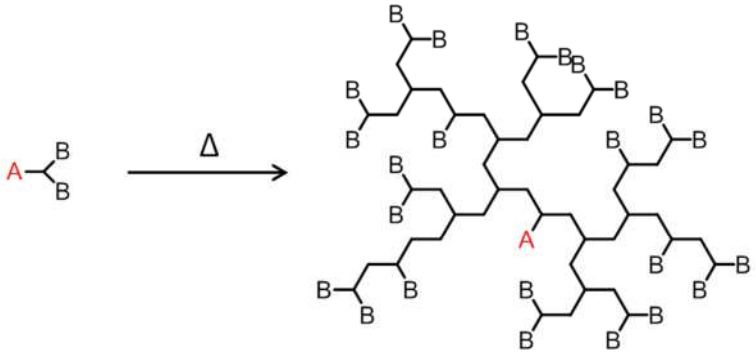

Figure 1.2: General reaction scheme for the self condensation reaction of AB_2 monomers

Polycondensation reactions using AB_x type monomers is a dominant method for the synthesis of branched polymers, with much of the focus driven towards branched polyester synthesis.[20-28] AB_x condensations have the advantage that, as A groups are limited to reaction with B groups, there is no possibility of crosslinking, providing this selectivity is upheld and no side reactions occur, for example, in branched polyester synthesis, ether formation can lead to crosslinking of B groups.[29] The end products contain dendritic (fully reacted A/B groups), terminal (unreacted B groups), linear (one reacted B group) and a focal point (a single A group) (Figure 1.2). The presence of this focal point can lead to cyclisation reactions, but this effect can be limited by monomer choice.[30-32] However, the use of AB_x type monomers leads to a molar mass build up due to the presence of the focal point and offers no control over the geometrical shape. Addition of a B_y comonomer can be used to control the molar mass, by the ratio of AB_x to B_y, and offers some control over the geometry by elimination of the focal point *via* the introduction of a central core.[33, 34]

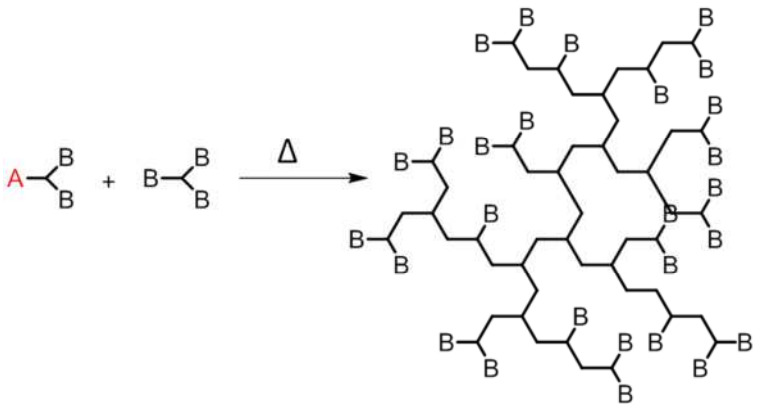

Figure 1.3: General reaction scheme for the self condensation reaction of AB_2 and B_3 monomers

In AB_x+B_y systems monomer is often added in portions in order to control the reaction.[35, 36] Peripheral functionalisation can also be introduced in a similar manner by addition of a monofunctional monomer to the polycondensation reaction (AB_x+A), however, this method for functionalisation is limited and usually results in low molar mass products.[37, 38] End group modifications have also been carried out post-polymerisation in a similar manner, offering tuneable functionality, which can have effects on solubility, T_g and T_d, without causing limitations in molar mass.[33, 38, 39]

An example of a commercial hyperbranched polymer formed by polycondensation, of perhaps the most readily available AB_2 structure, is a polymer of bis(methyloyl)propionic acid (bis-MPA), commercially known as Boltorn, originating from Perstorp (Figure 1.4). In the condensation polymerisation of bis-MPA hyperbranched/dendritic polymers containing large numbers of terminal hydroxyl functionality are formed, whose applications range from performance additives in polyurethane foams, oligomer precursors for UV-curing applications, to reactive dilutents for volatile organic compounds (VOC) control in water and solvent borne paints. Post-polymerisation functionalisation (AB_2+A) of end groups with long chain unsaturated fatty acids and polyethylene glycol (PEG) can alter the properties of resulting materials, forming water soluble, oil soluble and amphiphilic materials from a single polymer precursor.[40]

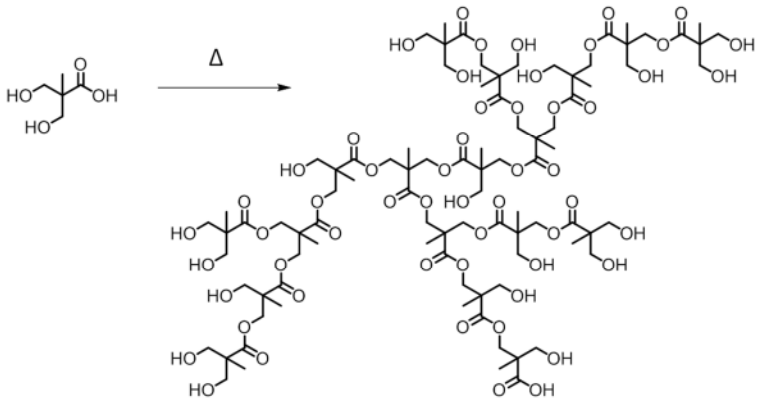

Figure 1.4: Schematic for the poly-condensation of AB_2 type monomer bis(methyloyl)propionic acid in the formation of hyperbranched polyester Boltorn

For AB_x and AB_x+B_y approaches gelation cannot be reached under Flory prerequisites, for A_x+B_y approaches, however, gelation can occur with the formation of hyperbranched structures at critical concentrations. Gelation is commonly avoided by termination of polymerisations at lower conversions, end capping with functional molecules, slow addition of monomers or use of condensation catalysts,[41] but ultimately limits its industrial applicability. A benefit of A_x+B_y reactions is the wider availability of commercial monomers, however, the resulting structural variety in the products is broader.[42] As gelation occurs at critical concentrations the resulting polymers may not be of high enough molecular weight to be considered hyperbranched, being better described as branched polymers. Limitations to the achievable molar mass at particular ratios of A to B are also prevalent, high excesses of B can eliminate the gel point but limits the molar mass, thus reducing branching further. Utilising equimolar amounts of A to B can lead to post-polymerisation crosslinking, if the level of remaining A groups is high.[14, 43, 44]

Improvements to A_x+B_y polymerisations were made by use of monomers with selectively higher reactivities of either A or B groups, or by use of monomers containing different reactivities within the A and B groups, such as AA' and B_xB' favouring A(A'-B')B_x, effectively forming a pseudo AB_x type monomer *in situ*.[45] Such polymerisations have been utilised in the alternating sequence control of branched polymers, which is difficult to access by AB_x+B_y strategies.[41]

1.2.1.2. Poly-Addition Reactions

Michael reactions are base catalysed additions of a nucleophile, Michael donor, to an α,β-unsaturated carbonyl containing compound, Michael acceptor, resulting in a Michael adduct.

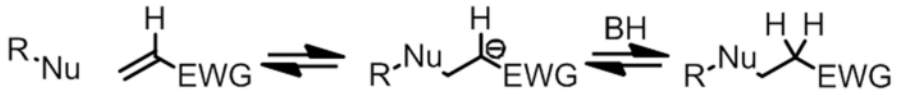

Figure 1.5: General scheme for Michael addition

A wide range of Michael donors are available, most commonly enolates; amines, thiols and phosphines can also be utilised but are referred to as 'Michael type additions'. Michael acceptors are more numerous, including acrylate esters, acrylonitrile, acrylamides, maleimides, alkyl methacrylates, cyanosulfones and vinyl sulfones.[46] Examples of branched polymers synthesised by Michael addition using AB_x, A_x+B_y and $A'A+B'B_2$ approaches are present in literature,[47-51] again with a wider commercial availability of A_x+B_y than AB_x monomers.

Michael addition has also been frequently used in the synthesis of small molecules, and has been used in the *in situ* generation of AB_2 type monomer by Gao *et al*. (Figure 1.6) by Michael addition of diethanolamine to methylacrylate. A second stage poly-condensation reaction was conducted at elevated temperatures, *via* transesterification, in the presence of a zinc acetate catalyst. It was found that at temperatures below 120 ˚C no polycondensation reaction occurred, whereas for temperatures above 165 ˚C gelation occurred. However, soluble branched polymers were obtained between the two temperatures, which degraded rapidly in water, forming self-buffered pH 7 solutions, making them potential candidates for drug delivery.[52]

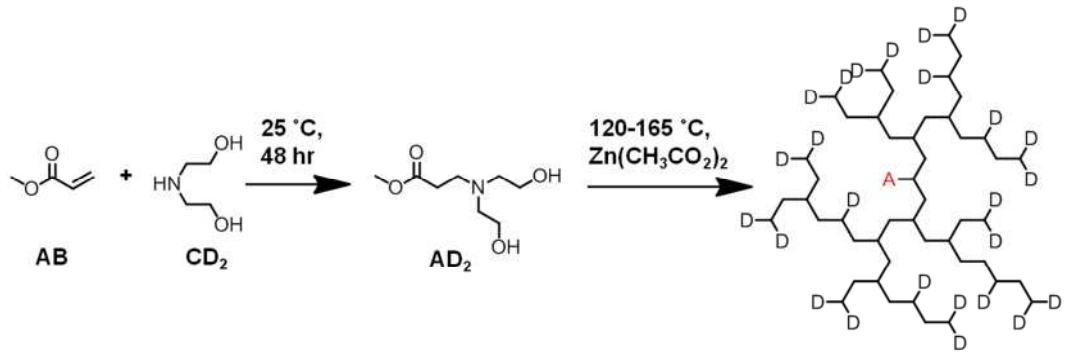

Figure 1.6: Schematic for the *in situ* formation of an AB_2 type monomer *via* Michael addition and subsequent polycondensation to yield hyperbranched polyester

Michael addition offers many benefits over other synthetic routes for the formation of branched polymers as the reaction can proceed rapidly under ambient conditions, has a low probability of side reactions and can proceed using mild reaction conditions, hence this method has been used extensively for the synthesis of dendrimers.[53] However some polymers produced are susceptible to retro-Michael addition, leading to polymer degradation.

Thiol-yne reactions allow for the addition of two functional thiols to an alkyne (Figure 1.7) and so, is well suited for application to the synthesis of multifunctional polymer structures. The reaction proceeds *via* a radical pathway, using either thermal or photoinitiation.

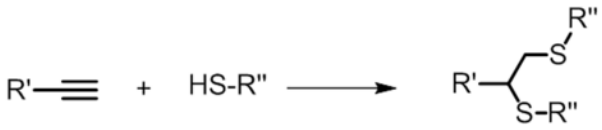

Figure 1.7: General thiol-yne reaction scheme

Thiol-yne reactions have been utilised in a variety of ways, such as the post-polymerisation modification of alkyne/thiol containing polymers [54, 55] and the synthesis of dendrimers and hyperbranched polymers. [56, 57] The advantage of this technique for the synthesis of hyperbranched systems is that branching levels are extremely high, with only low levels of linear alkene containing units observed. This is due to the initial thiol-alkyne addition being the rate determining step, followed by rapid addition of the second thiol.[58]

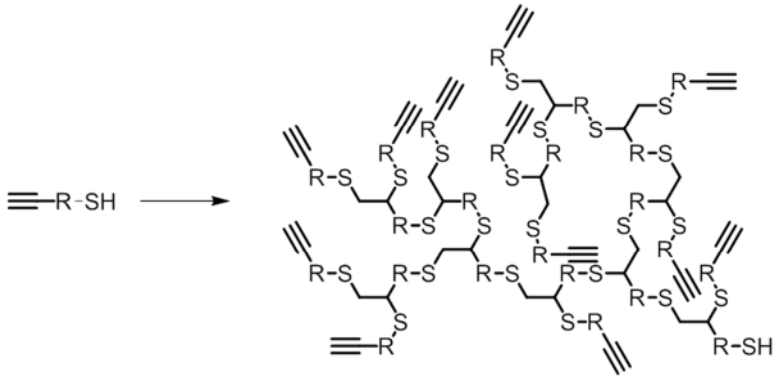

Figure 1.8: General schematic for the synthesis of hyperbranched polymers via radical thiol-yne chemistry

A further advantage of this technique is the high level of terminal alkyne functionality obtained, which can be further functionalised using thiol-yne or copper catalysed azide alkyne click (CuAAc) type chemistry, yielding functional branched polymers. It has also been postulated that resulting polymers could be utilised as macromonomers in subsequent reactions with thiol-alkynes in the formation of core-shell like structures.[59] However, polymers obtained possess high PDi's and a high sulfur content, leading to some limitations to their application, although in the case of optical applications this is an asset, as it provides a facile means to enhance the refractive index of materials.[60] Combinations of thiol-ene and thiol-yne; and thiol-halogen and thiol-yne chemistry have also emerged in the literature for the synthesis of branched polymers due to the site selective nature of the two reactions, based on use of a base/nucleophilic catalyst for thiol-ene reactions, and subsequent radical thiol-yne reaction.[61, 62]

1.2.1.3. Poly-Cyclisation Reactions

Reactions such as [4+2] Diels-Alder and Huisgen's 1,3-dipolar cycloadditions have also been utilised in the synthesis of branched polymers, with the high stereoselectivity and chemoselectivity associated with these reactions leading to their extensive use in the synthesis of dendrimers.[63]

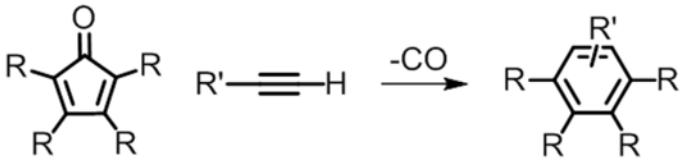

Figure 1.9: General scheme for Diels-Alder cycloaddition of substituted cyclopentadienone (diene) and substituted alkyne (dienophile)

Diels-Alder cycloaddition describes the reaction between a conjugated diene and a dienophile such as an alkene or alkyne (Figure 1.9). Diels-Alder cycloadditions have proven particularly useful for the synthesis of highly aromatic hydrocarbon structures, and, by utilising AB_x monomer structures and their combination with AB monomers, has been used for the synthesis of branched polymers, however, limitations in the obtainable molar masses are observed.[64-66]

The synthesis of polyphenylenes by Diels-Alder cycloaddition based on AB_x monomers has been of particular interest, due to the change in properties arising on the formation of hyperbranched polymers. Linear polyphenylenes possess high thermal and chemical stability and due to their extended π-conjugation can be conductive. Conversely, in dendritic and hyperbranched structures the tightly packed, twisted conformations of the phenylene units leads to a loss of conductivity, hence the resulting polymers are promising candidates for use as insulating materials. Due to the increased solubility, processability and less demanding synthesis of hyperbranched polyphenylene structures, compared to their dendritic analogues, hyperbranched structures provide a more industrially suitable material.[65, 67, 68] However, attempts to polymerise phenylene using A_2+B_3 monomers, whereby A is diene and B is dienophile functionality, led to high degrees of steric hindrance, which limited cycloaddition to the formation of linear structures in the absence of high excesses of A_2.[69]

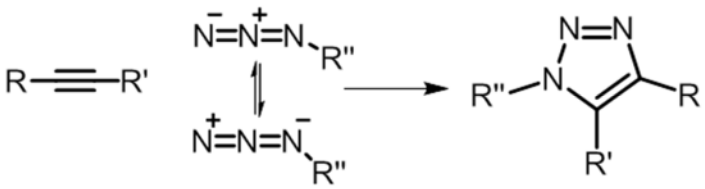

Figure 1.10: General scheme for Huisgen's 1,3 dipolar cycloaddition with a substituted alkyne and substituted azide

Huisgen's 1,3-dipolar cycloadditions describe the reaction between an azide and alkyne in the formation of a triazole ring (Figure 1.10), often referred to as copper mediated azide-alkyne click (CuAAc), due to the widely used Cu(I) catalysed reaction realised by Sharpless *et al*.,[70] although thermal reaction conditions are also employed.[71] Huisgen's cycloadditions offer a more versatile route to the synthesis of branched polymers, in that complex heterocycles and the introduction of polar functionality can be obtained, with the potential to achieve high levels of stereoselectivity. Although, as the reactivity of the starting materials is high, reactions can be susceptible to side reactions such as rearrangements, dimerisation and cyclisations.[72]

Cycloaddition of bisazines leads to a so-called criss-cross reaction, whereby a two step dual [3+2] cycloaddition *via* an instable azomethine imine 1,3-dipolar intermediate. Due to this instable azomethine imine intermediate the formation of linear chains is not observed, hence 100% branching was achieved; the linear azomethine imine cyclic system can only undergo further reaction with a second azide forming a tetracyclic system (Figure 1.11), or undergo retrosynthesis to its corresponding starting materials. However, a high level of isomerism was observed in the products.[73, 74]

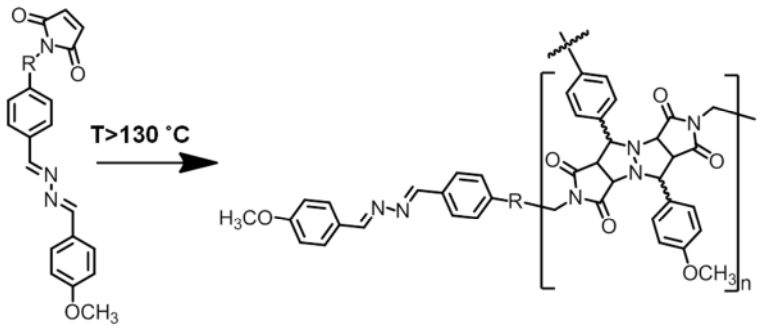

Figure 1.11: Schematic for the criss-cross cycloaddition of AB_2 type bisazine maleimide monomer

Work by Voit *et al*. on the Huisgen's cycloaddition of AB_2 monomer, 3,5-bis(propargyloxy) benzyl azide, used both thermal polymerisation and Cu(I) catalysis for the formation of branched polymers. However, Cu(I) catalysis led to the formation of insoluble products, presumably through formation of high molar masses or side reactions. Despite this, full stereocontrol was achieved; whereas for thermally induced cycloaddition, and the use of substituted alkynes, stereocontrol was not achieved.[75] Additionally polymerisation of AB_2 monomers, whereby B groups were azide

functionalities, were susceptible to post-polymerisation gelation, presumably due to reaction or decomposition of terminal azide groups. To avoid post-polymerisation gelation, or to provide additional functionality, terminal functional alkyne/azides can be reacted with their corresponding monofunctional groups, effectively end capping polymer chains and introducing terminal functionality.[76]

1.2.2. Branched Polymers by Chain Growth Strategies

The realisation of self condensing vinyl polymerisation (SCVP) by Fréchet in 1995 led to an increase in the application of chain growth methods to the synthesis of hyperbranched polymers,[77] including techniques such as self condensing ring-opening polymerisation (SCROP) and chain transfer.

1.2.2.1. Self Condensing Vinyl Polymerisation (SCVP)

SCVP is based on the use of inimers, a vinyl monomer which bears initiator functionality; this allows for chain growth through the double bond and step growth through addition of the initiator site to double bonds, which, dependant on the functionality, can proceed in a cationic, anionic or radical fashion. Dependant on the reactivity ratios of A* and B* groups the degree of branching can vary. Typically SCVP inimer homopolymerisations possess broad PDi's, due to their non-living characteristics and are subject to side reactions such as radical coupling and an increasing likelihood of gelation for long timescales, even with the use of AB_x monomers, for which gelation should not occur according to Flory prerequisites.[78] Copolymerisations of inimers with traditional vinyl monomers leads to a reduction in PDi, compared with inimer homopolymerisations, and the degree of branching can be tailored through the ratio of inimer to vinyl monomer.[79, 80] The synthesis of inimers suitable for specific polymerisation techniques has led to the combination of SCVP with group transfer polymerisation (GTP), atom transfer radical polymerisation (ATRP), nitroxide mediated polymerisation (NMP) and reversible addition fragmentation termination (RAFT), with additional control of PDi's imparted by use of 'living' polymerisation methods.[81-87]

Combinations of both NMP and RAFT with SCVP led to the incorporation of weak links in the resulting polymer chains due to labile nitroxide or RAFT moieties at branch points;[83, 88] in the case of combination of SCVP with NMP these weak links were

utilised by thermal homolysis, allowing the severing of branch points from the main chain.[89, 90] The nitroxide moieties at branch points were also used for further propagation of alternative monomers near to the branch point.[91] Modifications to RAFT/SCVP monomers, placing dithioesters at the chain end, removed labile RAFT moieties from branch points and has been utilised in the formation of block copolymer hyperbranched structures, with stimuli responsive properties.[92-94]

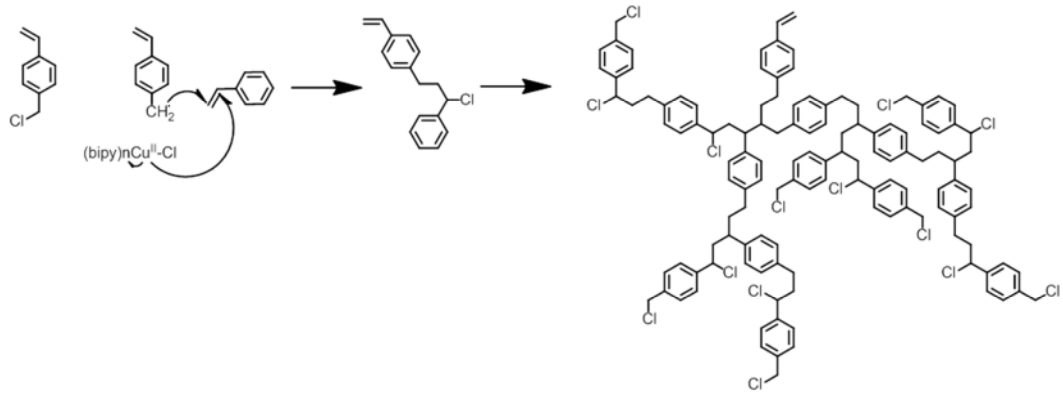

Figure 1.12: Example of SCVP with ATRP inimer *p*-chlorostyrene, copolymerisation with styrene in the formation of an AB_2 type monomer and polymerisation to form a branched structure via ATRP

The combination of ATRP and SCVP initially led to the formation of predominantly linear structures. In order to maintain a steady concentration of active catalyst Cu(I), required for the formation of branched structures, a high initiator concentration and additional Cu(0) was used, which oxidises deactivated Cu(II) species.[84, 95, 96] Due to the use of halide initiating species in ATRP the copolymerisation of fluorinated monomers, such as pentafluorostyrene, with ATRP/SCVP inimers such as *p*-chloromethyl styrene or *p*-bromomethylstyrene, has been used in the production of highly fluorinated hyperbranched polymers.[97, 98]

1.2.2.2. Self Condensing Ring-Opening Polymerisation (SCROP)

SCROP also employs inimers in order to combine step growth and chain growth methods but rather than vinyl groups, as used in SCVP, chain growth functionalities take part in reversible ring-opening reactions.[99] Most inimers/monomers used in SCROP are latent AB_x structures, that once ring-opened provide further branch points from latent secondary heteroatoms formed (Figure 1.13).[100, 101] The application of A_x+B_y based monomers has also been investigated.[102-104]

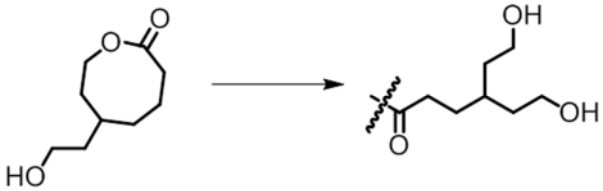

Figure 1.13: Latent AB_2 structure of ROP monomer 5-(2-hydroxyethyl)-ε-caprolactone

Ring-opening polymerisations are more complex than classical condensation reactions, due to the reversibility of ring-opening reactions and the increased likelihood of internal cyclisations reactions.[31] Similar approaches to SCVP are employed for gaining additional control over the polymerisation, including addition of a core molecule to limit molar mass build-up and cyclisation reactions, and slow monomer addition to control the PDi and geometry.[105, 106]

Combinations of SCROP and living polymerisation techniques are also found in the literature, typically towards the synthesis of star polymers or miktoarm stars.[107, 108] RAFT and ROP have been used in subsequent reactions for the synthesis of star polymers, by copolymerisation of ethyl acrylate and hydroxyethyl acrylate in the formation of low molecular weight chains, which were then utilised as ROP initiators for the polymerisation of L-lactide. Additionally, low molecular weight ethyl acrylate/ hydroxyethyl acrylate chains were extended using styrene, prior to ring-opening of L-lactide, in the formation of miktoarm stars.[108] In a similar fashion ATRP was used in order to synthesise star like ε-caprolactone from a bis(hydroxylmethyl) central core, by capping the chain ends with dendrons possessing terminal bromine groups, further polymerisation *via* ATRP led to the formation of branched block copolymers with low PDi's.[109]

1.2.2.3. Chain Transfer

Chain transfer reactions have also been employed for the synthesis of branched polymers using di- or multivinyl monomers by addition of chain transfer agents, the main benefit of which is the commercial availability of suitable monomers. However, chain transfer can occur in many cases of free radical polymerisation in low levels as a side reaction. Chain transfer arises when hydrogen or another atom, X, is transferred from a molecule in the system to the growing radical chain, chain growth is terminated

and the radical transferred onto the species from which hydrogen or X was extracted (Equation 1.3).[110]

$$M_n^{\cdot} + R_1X \xrightarrow{k_{tr}} M_nX + R_1^{\cdot}$$

Equation 1.3: Chain transfer from propagating radical chains to chain transfer species R_1X, whereby k_{tr} is the rate constant of chain transfer

Chain transfer can take place from propagating chains to monomer, solvent and initiator, having a direct effect on the degree of polymerisation (DP_n) by lowering the number of polymer molecules produced per kinetic chain length. For normal chain transfer the rate of polymerisation remains unchanged and the DP_n is reduced, although cases exist whereby the rate of polymerisation is affected by chain transfer, dependant on the relative rates of propagation, chain transfer and reinitiation (Table 1.1).

k_p:k_{tr}	k_a:k_p	Resulting Chain Transfer	Effect on R_p	Effect on DP_n
$k_p >> k_{tr}$	$k_a \approx k_p$	Normal chain transfer	None	Decrease
$k_p << k_{tr}$	$k_a \approx k_p$	Telomerisation	None	Large decrease
$k_p >> k_{tr}$	$k_a < k_p$	Retardation	Decrease	Decrease
$k_p << k_{tr}$	$k_a < k_p$	Degradative chain transfer	Large decrease	Large decrease

Table 1.1: Effect of chain transfer on rate of polymerisation, R_p, and DP_n of resulting polymers based on the relative rates of propagation, k_p, transfer, k_{tr}, and reinitiation, k_a

Chain transfer does not occur in all free radical polymerisations and the degree to which this mechanism occurs also varies. In some cases chain transfer is an undesired reaction, but often it can be an asset, to which the deliberate addition of chain transfer agent provides further control over the average DP_n. Thiols are commonly utilised as chain transfer agents in free radical polymerisations,[111] as they readily transfer a hydrogen to propagating radical chains, yielding a saturated polymer chain and thiyl radical (Equation 1.4), hence the chain transfer agent is consumed as the reaction proceeds. The magnitude of a chain transfer agents efficiency depends on the structure of both the transfer agent and the attacking radical, and is commonly termed the chain transfer constant (C_s). This C_s can be measured by various methods for each monomer employed, with collections of measured C_s values available in literature. Thiols possess the highest chain transfer constants of all conventional chain transfer agents.

$$M_n^{\cdot} + HS - R \rightarrow M_n - H + S^{\cdot} - R$$

Equation 1.4: Chain transfer using a thiol chain transfer agent, hydrogen abstraction from functional thiol and generation of a 'dead' saturated polymer chain and thiyl radical species

Conventional chain transfer is commonly employed to control the molecular weight of polymer chains by producing more polymer chains per kinetic chain length, which has an effect on the viscosity of the solution. This can in turn mitigate the Norrish-Trommsdorff or gel effect,[112, 113] whereby localised increases in the viscosity of a polymer solution leads to an overall increase in the rate of polymerisation, with potentially dangerous outcomes.

Utilising the high chain transfer constants of thiols, the copolymerisation of monovinyl monomers with low levels of multivinyl, branching, monomers can be conducted by what is now commonly known as the 'Strathclyde route', due to its development at Strathclyde University (Figure 1.14).[114-121] Gelation of materials, which would occur rapidly using free radical conditions, is delayed by a reduction in the number of molecules produced per kinetic chain length, hence the number of branch units incorporated into each chain is controlled. Tailoring of these materials was achieved by the ratio of branching monomer to monovinyl monomer, providing a cost effective route to the synthesis of branched copolymers using commercial vinyl monomers. However, high PDi's are observed in comparison to condensation type methods, due to the non-selective nature of the monomers employed. Furthermore, as the chain transfer agent is non-catalytic in nature, initiation by thiyl radicals is likely, leading to incorporation of thiol chain transfer agents into polymer products. The choice of chain transfer agent can be utilised for the incorporation of functionality to chain ends, however, a mixture of functional products will be obtained.[4]

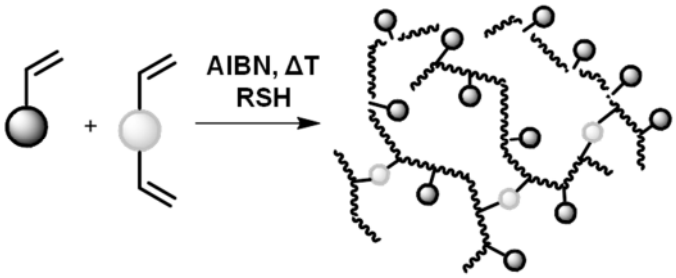

Figure 1.14: Schematic of the "Strathclyde route" for the synthesis of lightly branched polymers. Free radical copolymerisation of monovinyl monomer with branching monomer in combination with significant levels of chain transfer agent (RSH)

As well as conventional chain transfer, catalytic chain transfer polymerisation (CCTP) has been utilised in the synthesis of branched polymers. Due to the catalytic nature of the Co(II) chain transfer agent, and its higher efficiency compared to conventional thiols,[122] lower relative amounts of catalyst can be employed in the synthesis of highly branched polymers. Homopolymerisations of di- and trivinyl monomer are achievable, by a reduction in the number of molecules produced per kinetic chain length, although it should be noted the amounts of chain transfer agent employed for branched systems are high in comparison to linear concentrations.[123, 124] Hence CCTP provides an industrially applicable technique for the synthesis of branched polymers in a one pot fashion, using commercial vinyl monomers, a highly efficient, odourless catalyst, with the retention of activated vinyl groups providing a handle for functionalisation of these materials. Hence, this will be the focal polymerisation method in this thesis.

1.3. Catalytic Chain Transfer Polymerisation

1.3.1. CCTP - A Brief History

CCTP utilises Co(II) macrocycles as chain transfer agents, providing a convenient method for the synthesis of low molecular weight, vinyl terminated polymers, termed macromonomers, using low amounts (ppm levels) of catalyst.[125-127] CCTP originated in Moscow in 1975, from research into the effects of the addition of transition metal compounds to free radical polymerisations. On addition of Co(II) porphyrins, promoted by Ponomarev, an interesting inhibition effect was observed for the polymerisation of methyl methacrylate (MMA), with only monomeric products yielded. The significance of this seemingly negative effect was realised and a series of largely unnoticed

publications followed in Russian literature.[128-132] Further Russian patents described by Gridnev, one of CCTP's cofounders, added to its dormancy in the literature.[122] In 1979 CCTP was brought to light in the industrial domain, with early patents filed by the Glidden paint company on Co(II) cobaloximes and application of CCTP for the synthesis of oligomers, presumably for high solids coatings applications.[133-135] However, the patent was brief, with limited claims to the parent cobaloxime,[133, 135] hence, on the discovery of more hydrolytically stable cobaloximes specific compounds were claimed.[136, 137] Patents filed by DuPont had claimed a variety of R group substituent's, however, claiming phenyl rather than aryl, with a patent filed on the same day using the term aryl, led to a further family of patents on aryl R group substituent's claimed by ICI/Zeneca.[138, 139] To date CCTP has been utilised in a variety of industrial applications including printing and toner processes,[140] the thermoformation of sheets of MMA for the manufacture of items such as sinks, baths and shower trays,[141] additives in road/pavement manufacture[142] and automotive base/colour/top coats.[143-147] Macromonomers formed *via* CCTP have been used for conjugation to hair in hair care applications,[148] the formation of star polymers as rheology modifiers[149] and the synthesis of hydrogels for the manufacture of contact lenses, wound dressings and biocompatible adhesives.[150, 151]

1.3.2. CCTP - Mechanism

A main advantage of CCTP in comparison to conventional chain transfer polymerisation is that the Co(II) macrocycles employed as chain transfer agents are catalytic, with C_s values several orders of magnitude higher than traditionally used mercaptans. Co(II) macrocycles rapidly and reversibly combine with growing radical chains forming a Co(III) alkyl complex. β-hydrogen abstraction yields a dormant vinyl terminated polymer chain, or macromonomer/chain transfer product, and Co(III)-hydride, which is capable of initiating further monomer units or reinitiation of chain transfer products. The commonly accepted mechanism for CCTP of methacrylates is outlined in Figure 1.15.[152, 153] The effect of CCTP, as with normal chain transfer, is the reduction of molecular weight without affecting the kinetic chain length or the rate of polymerisation. The catalytic nature of CCTP was verified in 1980, on isolation of the regenerated Co(II) porphyrin complex post-polymerisation.[128-130, 132]

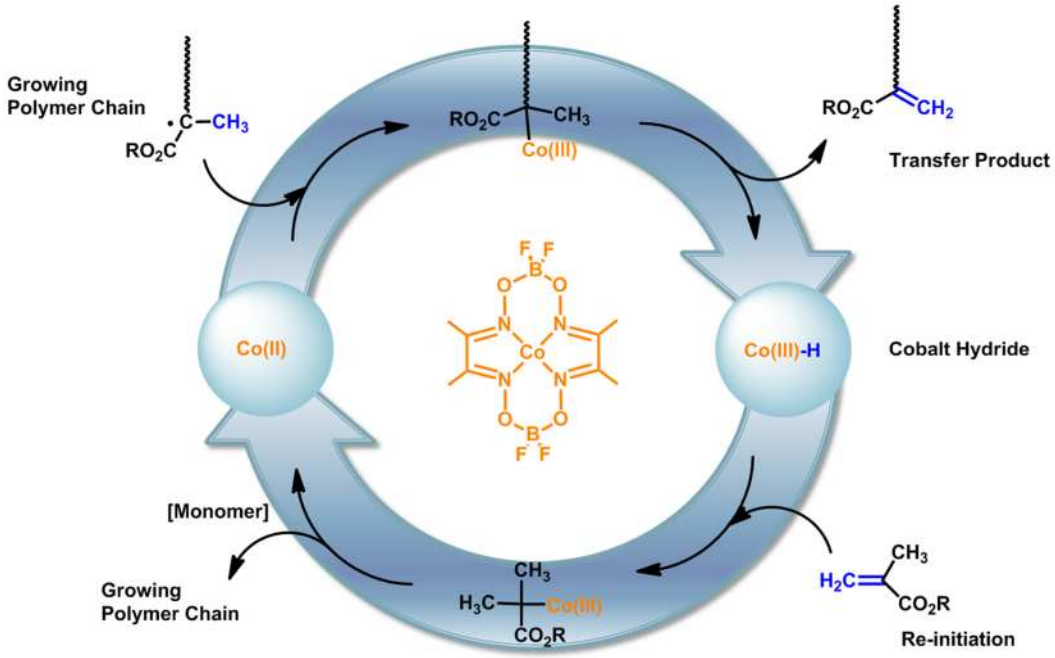

Figure 1.15: Generally accepted mechanism of CCTP for methacrylic monomers

It should be noted that anomalies are observed in the proposed mechanism. It is unlikely that hydrogen abstraction occurs *via* β-hydride elimination, abstraction *via* a radical pathway is more likely, although no conclusive evidence of a radical pathway exists, it is supported by kinetic isotope effect experiments by Gridnev.[154]

1.3.3. CCTP – Catalysts

Effective catalytic chain transfer agents are invariably low-spin Co(II) complexes with octahedral geometry, derived from a square planar ligand and two available axial sites.[155] Co(II) is d^7 with the potential to exist in either a high spin, with three unpaired electrons, or low spin conformation, with one unpaired electron (Figure 1.16). Interestingly, this is an important consideration in designing a catalytic chain transfer agent, as the nature of the ligands surrounding the central cobalt can easily result in spin crossover from low spin to high spin, as the relative energy levels are close together; to date no reason has been found for this empirical observation.

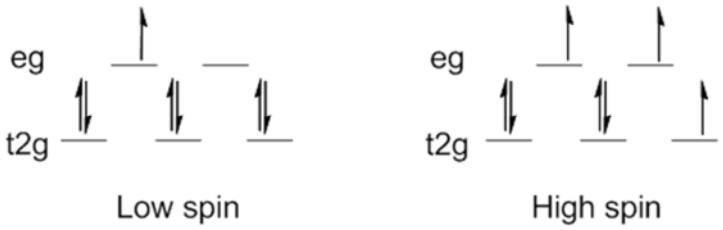

Figure 1.16: Electronic configuration of Co(II) complexes in both low (left) and high spin (right) configurations

On first discovery of CCTP the Co(II) complexes were based on porphyrin complexes e.g. Co(II) hematoporphyrin IX tetramethyl ether (**1**). This first generation of CTA's produced C_s values of 2.4 E3,[156] but due to the expensive isolation and purification of porphyrins, the cost was considered too high for application of CCTP in industry. Other disadvantages included their high colour, and insolubility in a range of solvents, hence alternative catalysts were required. Based on the criteria for active CCTP catalysts outlined above, cobaloximes were investigated.

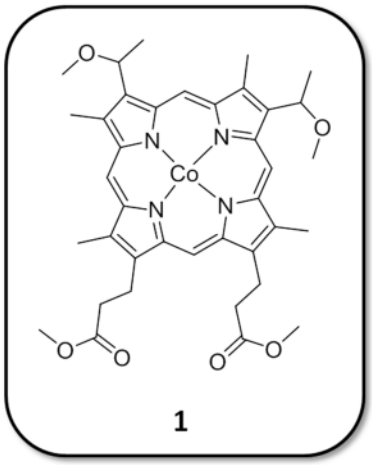

1

The second generation of Co(II) complexes were cobaloximes, (**2**), which are an order of magnitude more active than porphyrins (C_s 2.0E4 - 2.3E3), with the added benefit that the synthesis is less costly, they are low in colour compared to porphyrins, have good solubility and their properties can be tuned through the axial and equatorial ligands, in turn affecting the chain transfer constant, which has also been shown to increase the stability of catalyst solutions to oxidation in air.[122, 157-159] A disadvantage to this generation of cobaloximes was they are susceptible to hydrolysis and oxidation; hence the third generation of cobaloximes incorporates a BF_2 bridge, which stabilizes

the cobaloxime towards these reactions (C_s 4 E4).[158] These complexes were given the general name CoBF, which is commonly used to describe CTA's of general structure **3**.

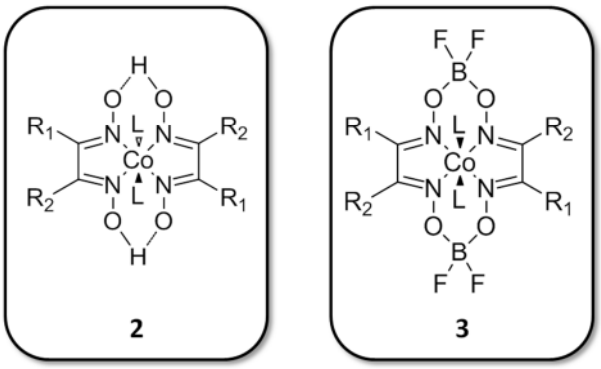

1.3.3.1. Measuring Catalyst Activity

The most commonly used measure of catalytic activity, and a commonly used indicator of catalyst purity, is measurement of the C_s, defined as the ratio of the rate constant for chain transfer to the rate constant for propagation ($k_{tr,s}/k_p$). C_s values for conventional chain transfer agents, such as mercaptans, are an order of magnitude of 1 - 10 for methacrylates, in contrast, C_s values for cobaloximes can be four orders of magnitude greater, and are not consumed during the reaction. This makes them highly effective catalysts, hence only ppm amounts are often required to achieve large reductions in molecular weight.[127]

Typically C_s values are determined using variations of the Mayo equation as described in Equation 1.5, from which a linear Mayo plot of the $1/DP_n$ vs. [S]/[M] can be plotted, the gradient of which is a measure of the C_s value for that particular chain transfer agent under the conditions used in the polymerisation. The intercept gives the $1/DP_{n0}$, defined as the DP_n in the absence of chain transfer agent.

$$\frac{1}{DP_n} = \frac{1}{DP_{n0}} + C_s \frac{[S]}{[M]}$$

Equation 1.5: General form of the Mayo equation, whereby DP_n is the number average degree of polymerisation of the polymer, DP_{n0} is the number average degree of polymerization in the absence of chain transfer agent, and [S] and [M] are the concentrations of chain transfer agent and monomer respectively.

Polymerisations carried out in order to obtain Mayo plots should ideally be conducted under the same conditions, preferably using more than three chain transfer agent concentrations, and should be terminated at low conversions in order to ensure that [S]/[M] remains constant throughout the polymerisation. DP_n can be calculated in one of two ways, either by division of the M_n, usually obtained by size exclusion chromatography (SEC), by the monomer mass or division of the M_w by two times the monomer mass. Use of M_w as a measure of DP_n is only justified when the polymerisation is fully controlled by chain transfer, hence a PDi value of approximately two is obtained, however, in general practice this method has proved more accurate than measurements based on M_n as it is less susceptible to baseline deviations.[127, 160, 161]

The C_s can also be measured by chain length distribution (CLD), also described as molecular weight distribution, which can be obtained directly *via* SEC.[127, 158, 160, 162] The CLD of a polymer contains a history of the kinetic events which have occurred throughout the polymerisation. Information on chain transfer kinetics can be readily extracted from the CLD of a polymer. Equation 1.6 was derived by Gilbert *et al*. differentiation of which gives the limiting slope of P_i *vs.* i (Equation 1.7)[162]

$$\lim_{n\to\infty} P_i \propto exp\left(\frac{k_{tr,M}[M] + k_{tr,s}[S]}{k_p[M]}\, i\right)$$

Equation 1.6: Instantaneous CLD, P_i, obtained by SEC whereby $k_{tr,M}$ is the transfer rate to monomer, $k_{tr,S}$ is the transfer rate to CTA and k_p is the rate of propagation

$$\frac{d(ln\ P_i)}{di} = -\left(\frac{k_{tr,M}[M] + k_{tr,S}[S]}{k_p[M]}\right) = -\left(C_M + C_S\frac{[S]}{[M]}\right)$$

Equation 1.7: Limiting slope of P_i *vs*. i, where C_M is chain transfer to monomer.

The slope of this can be represented by Equation 1.8 as $P_i = (1\text{-}T)\ T_i\text{-}1$:

$$\frac{d(lnP_i)}{di} = lnT$$

Equation 1.8

Where,

$$T = \frac{R_p}{R_p + R_{tr} + R_t}$$

Equation 1.9: R_p, R_{tr} and R_t are the rates of propagation, transfer and termination respectively

Hence, the slope of a plot of $\ln P_i$ *vs.* i gives lnT. From this the transfer constant can be obtained from the slope of the plot lnT *vs.* [S]/[M], preferably for more than three concentrations of chain transfer catalyst, where the intercept will be $1/DP_{n0}$.[163]

An advantage to using this method for estimation of the C_s is that essential information can be obtained by analysis of a small portion of the CLD, providing high molecular weight data is used. As the whole CLD is not analysed this method is less sensitive to noise, poor baseline selection and the presence of artefacts in the SEC spectra. The catalytic activity of Co(II) complexes can vary dramatically depending on a number of factors such as sterics and electronics of ligands, solvent, viscosity, monomer and impurities.[155, 156, 164-167] As it is difficult to measure purity of catalytic chain transfer agents, often measurement of C_s is the most reliable measure.

1.3.4. CCTP – Monomers

Suitable monomers for CCTP must be able to readily facilitate the transfer of a hydrogen atom, since this is the key mechanistic step of CCTP. Monomers containing α-methyl groups, such as methacrylates, are the most effective monomers for CCTP due to the formation of tertiary radicals, leading to labile C-Co bonds and facile hydrogen transfer (Figure 1.17).[168] Use of monomers without α-methyl groups, such as acrylates, leads to the formation of secondary propagating radicals, which form more stable C-Co bonds, leading to a lower apparent catalyst activity and less active in-chain double bonds.[161, 169] A comprehensive list of monomers utilised in CCTP reactions and their measured C_s values can be found in the appendices of this work.

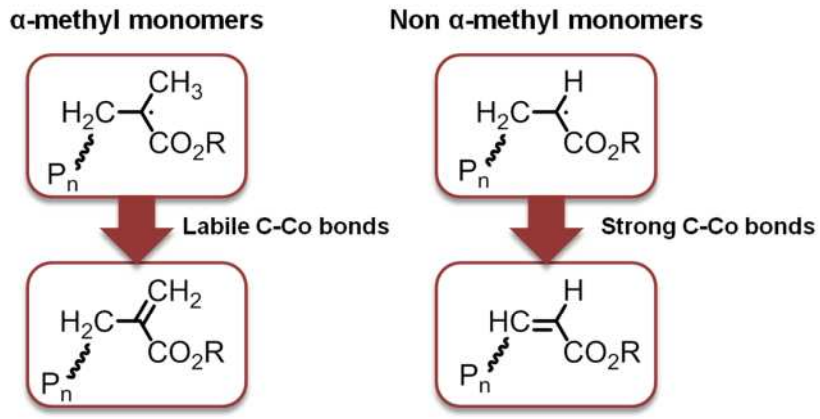

Figure 1.17: General scheme for the outcome of CCTP with α-methyl and non α-methyl monomers

1.3.4.1. Macromonomers

Not only is the CCTP technique itself an important technique in industry, but the macromonomers produced have also found a variety of unique uses. It was realised that copolymerisation of CCTP macromonomers with acrylic monomers yields comb like architectures (Figure 1.18),[170] whereas copolymerisation of macromonomers with methacrylic monomers is poor, as rather than copolymerising, macromonomers act as chain transfer agents.[171, 172]

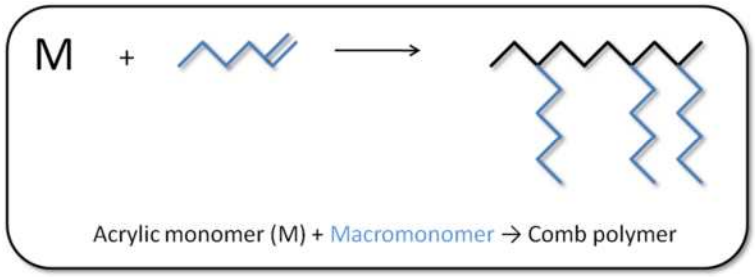

Figure 1.18: Synthesis of comb polymers by copolymerisation of an acrylic monomer with a CCTP macromonomer

For copolymerisations of CCTP macromonomers with methacrylic monomers, the macromonomer acts as a chain transfer agent by an addition-fragmentation chain transfer mechanism (Figure 1.19), with a measurable chain transfer constant.[122, 173]

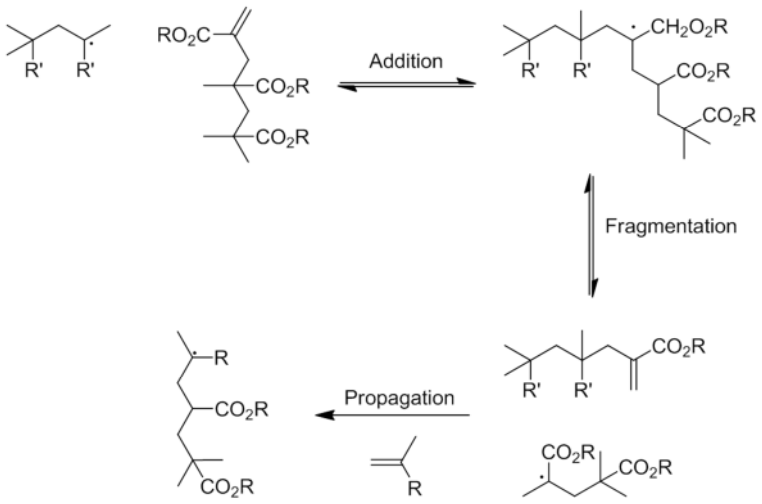

Figure 1.19: Addition fragmentation chain transfer mechanism for CCTP based oligomers, copolymerisation with methacrylic monomers

A good example of the use of CCTP macromonomers to limit the molecular weight of a polymerisation is α-methylstyrene dimer, which has been used in a range of industrial applications, such as polystyrene manufacture, [174] to control hardening and polymerisation temperature in dental adhesives cured by UV radiation,[175] and as part of a copolymer used as a fibre retention agent in the production of paper from pulp.[176] α-methylstyrene has also been used in the food packaging industry. Ethylene-vinyl acetate copolymers possess good gas-barrier properties and melt processability. These copolymers can be processed into melt films, sheets, pipes, tubes and bottles for use in the food packaging industry, however conventional ethyl-vinyl acetate copolymers streak on extrusion, leaving deformities on the surface. If the CCTP synthesised α-methylstyrene macromonomer, is added after polymerisation but before saponification, polymers with no surface deformities are obtained, although it is unknown why this occurs.[177]

Macromonomers have also been used in the synthesis of telechelic polymers using benzyl mercaptan dimer in the synthesis of *α*,*ω*-dicarboxyl telechelic PMMA. This reaction proceeds through an addition fragmentation reaction whereby the macromonomer dimer splits in half. One half forms the *ω*-terminal end of each macromolecule whilst the other is released as a functional initiating radical.[178]

1.3.4.2. Macromonomers for the Synthesis of Star Polymers

Synthesis of star polymers can be achieved by use of CCTP macromonomers using an arm first method. Macromonomers are copolymerised with an acrylic divinyl monomer which forms a crosslinked core with macromonomer arms (Figure 1.20). Work by Antonelli *et al.* used CCTP to create a range of star polymers for use as rheology modifiers.[149] Random block macromonomers are first synthesised by CCTP, copolymerising three monomers, iso-butyl methacrylate, 2-ethylhexyl methacrylate and hydroxyethyl methacrylate (HEMA), the ratio of which can alter the properties of the polymer, the molecular weight of which is in the range of 4,000-20,000 Da. A copolymerisation of the resulting macromonomers with a divinyl monomer such as butanediol diacrylate (BDDA) yields a crosslinked core, where at least three macromonomer arms have been incorporated into the polymerisation creating star polymers.

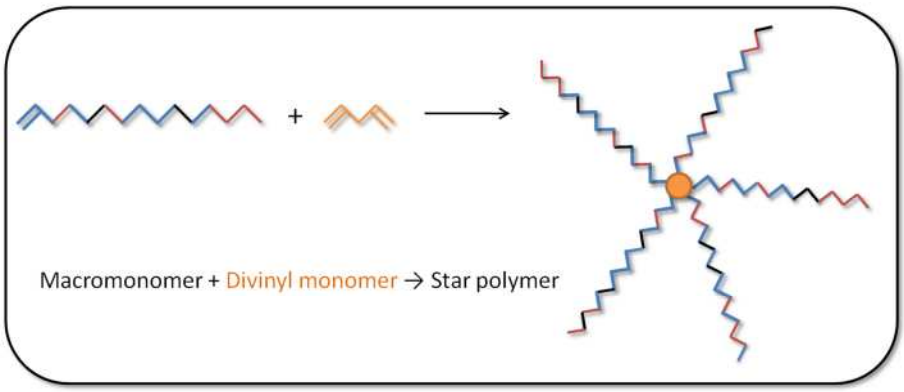

Figure 1.20: Star polymers synthesised by grafting to approach, by copolymerisation of divinyl acrylic monomers and CCTP macromonomers

Preferably the star contains between 10-50% weight of core and 50-90% weight of macromonomer arm. The resulting star polymer can be used in conventional coatings to modify the rheology or properties of the composition. They may also be used as toughening in plastic sheeting, adhesives and as an additive in motor oils to improve viscosity.

1.4. The Synthesis of Branched Polymers by CCTP in Literature

Conducting the polymerisation of di/tri-vinyl monomers *via* a free radical mechanism leads to instantaneous crosslinking of the product, but by utilisation of CCTP the molecular weight and hence the branching of these materials can be reduced to oligomeric products, dependent on the level of catalyst employed. The first published instance of the use of CCTP for the synthesis of branched polymers was by Golokov *et al*., to which triethylene glycol dimethacrylate (TEGDMA) was polymerised using a cobalt(II) hematoporphyrin tetramethyl ester complex as a chain transfer agent. Although soluble oligomers could be obtained, the reactions were inconsistent and the resulting polymers not fully characterised, containing no structural information.[179] Further to this work a patent was filed in 1986 by Abbey utilising the same monomer with a Co(II) catalyst which was generated *in situ*. The levels of catalyst used led to the formation of only low molecular weight products such as dimer, hence the majority of polymers yielded were linear.[180]

In 1998 a further patent was filed by Guan as part of E. I. Du Pont Nemours and Company, pertaining to the synthesis of multifunctional hyperbranched polymers by CCTP of di-or tri-vinyl monomers, including homopolymerisations and copolymerisations of a range of multivinyl monomers with monovinyl monomers.[181] The polymers produced in this work exhibited low solution viscosities and a high level of vinyl functionality, hence it was postulated that these materials exhibited potential for application to automotive coatings and photopolymerisations. This work was also published in part in 2002.[124] Guan used a concentration of cobalt catalyst that he postulated would lead to cascade trimerisation of the monomer. As every trimerisation contains a branching point, with termination occurring predominately *via* β-hydride abstraction, branched polymers are formed which possess high levels of vinyl functionality, both internal and external.

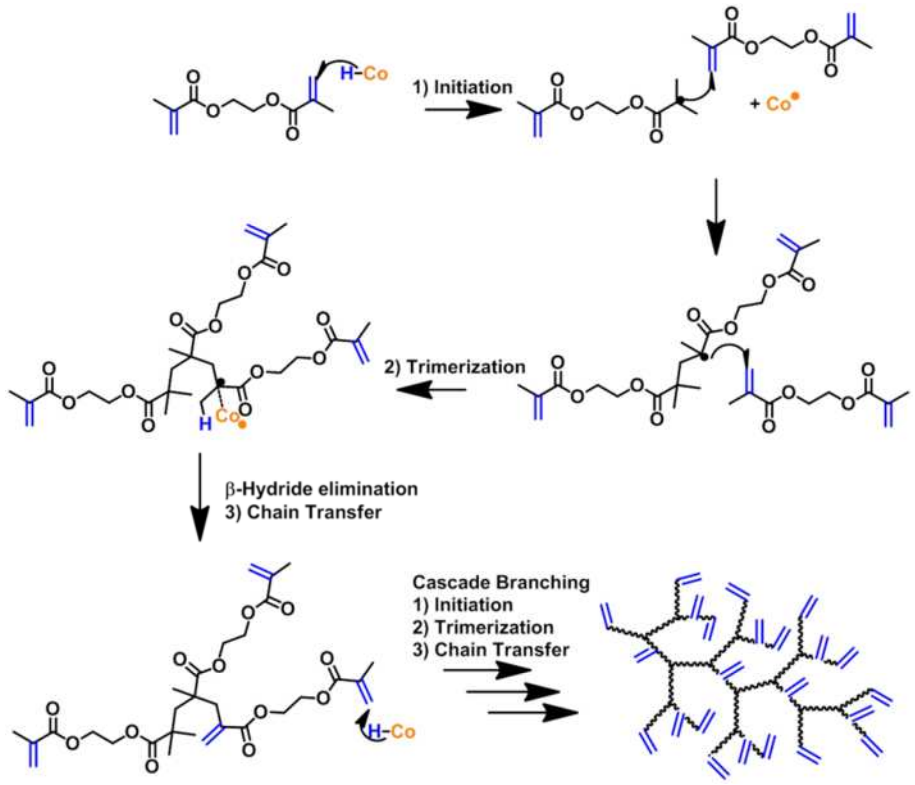

Figure 1.21: Mechanism for the CCTP of EGDMA, cascade trimerisation theory postulated by Guan,[124] leading to the formation of branched vinyl terminated polymers

The intrinsic viscosities (IV's) of ethylene glycol dimethacrylate (EGDMA) homopolymers synthesised were measured using SEC equipped with viscometry detection. It was found that the IV of branched Poly-EGDMA's synthesised were significantly lower than their linear counterparts. A further feature observed was that there was virtually no dependence of IV on molecular weight, whereas for linear polymers IV increases linearly with molecular weight in good solvents, following the Mark-Houwink equation with an α value of approximately 0.7.[182] The use of CCTP of divinyl monomers provides a novel method for the synthesis of branched polymers whereby, in the case of homopolymers, molecular weight is directly proportional to the level of branching therefore providing a tool for the control of polymer topology through molecular weight control.

In 2002, work on the polymerisation of divinyl monomers by CCTP was expanded through a collaboration between the University of Strathclyde, Viscotek and Ineos Acrylics, whereby branched copolymers of MMA and branching monomer tripropylene glycol diacrylate (TPGDA) were synthesised by both CCTP and conventional chain

transfer polymerisation, also known as the "Strathclyde route", using dodecanethiol (DDT) as the chain transfer agent.[114] Approximately 5 wt% of branching monomer TPGDA was incorporated into the copolymerisation with MMA, with resulting polymers retaining high levels of vinyl functionality. It was found that several factors had an effect on the level of branching of the polymers synthesised; by increasing the level of crosslinking monomer, an increase in branching was observed and low molecular weight products were predominately linear, with branching increasing with molecular weight. Reduction in the CoBF concentration led to variable M_n's, although M_w's increased as expected, hence the effect of varying CoBF was found to have little effect on branching and only on molecular weights.

The copolymerisation of acrylates and methacrylates *via* CCTP caused the formation of gradient compositional polymers, as the reactivity ratios are approximately 0.5 and 2.0 respectively,[183] therefore at low conversions resulting instantaneous copolymers were found to be methacrylate rich, and at high conversions the formation of acrylate rich copolymers was observed by fractionation and analysis by SEC. Use of acrylates in CCTP also leads to the formation of thermodynamically stronger C-Co bonds due to the lack of an α-methyl hydrogen for the CoBF species to abstract;[184] hence a lower apparent catalyst activity can be expected, this has the likely consequence that towards the end of the polymerisation, when the number of propagating acrylates increases, the system will be effectively starved of CoBF and termination by combination may predominate, leading to increased PDi's.[185] Hence, although CCTP has the benefit over conventional chain transfer of employing a greatly reduced amount of catalyst, the control over composition and PDi for the copolymerisation of acrylates and methacrylates led to the conclusion that conventional chain transfer provided more control in this case.

A publication pertaining to the synthesis of branched polymers by CCTP also arose from the Russian Academy of Sciences by Kurmaz *et al*., concerning the copolymerisations of styrene and branching monomers EGDMA and TEGDMA copolymers.[186] Comparisons were made between the free radical polymerisation and CCTP of styrene and EGDMA, finding that by use of a cobalt catalyst (cobalt(II) tetramethyl hematoporphyrin IX, [$Co^{II}P$]) the gel effect was suppressed, leading to the formation of polymers with superior molecular mobility and elasticity, and that by

increasing the level of [$Co^{II}P$] the modulus of elasticity and forced elasticity was diminished due to the formation of lower molecular weight products.

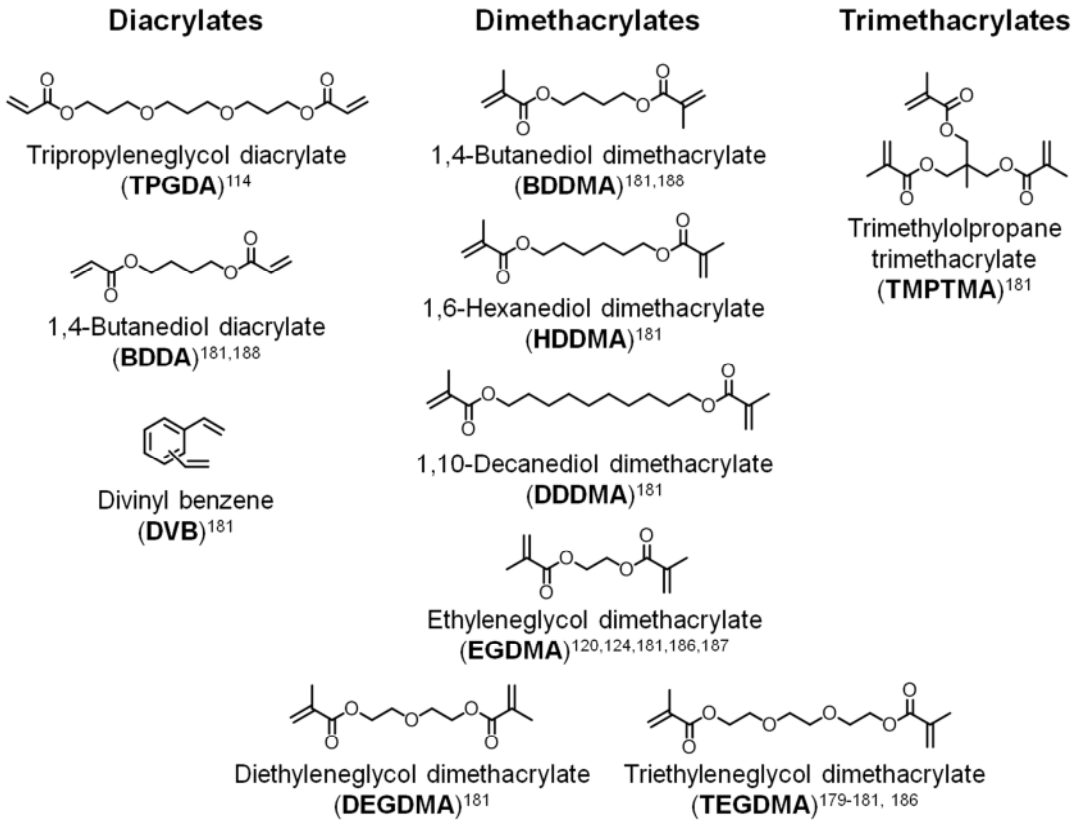

Figure 1.22: Structures of di- and trivinyl monomers employed in published accounts of CCTP, in the formation of branched polymers

Further research into the scope of branched polymers by CCTP was carried out by Kurmaz *et al*. in 2004, whereby copolymerisations of EGDMA and dodecane methacrylate (DDMA) were investigated.[187] Kurmaz *et al*. postulated that the steric bulk of DDMA would limit interaction of the polymeric radical with pendant vinyl groups, which would restrict cyclisation and crosslinking reactions. Attempts to carry out these reactions in bulk proved less controlled and the gel effect was no longer suppressed only delayed, suggesting a dependence of the reaction on diffusion control of the catalyst. An important realisation was also made that the resulting polymers could be utilised as macromonomers for the formation of star, hyperbranched, graft or block copolymer systems.

In 2005, a conflicting piece of literature was published by Sherrington *et al*. whereby a comparison was made between use of CCTP and conventional chain transfer polymerisation, the "Strathclyde route", using dodecanethiol (DDT) as the chain transfer agent in the synthesis of branched copolymers of EDGMA and MMA.[120] It was found that the reproducibility of obtaining soluble copolymers using these conditions was poor, in contrast to results reported by Guan for the homopolymerisation of EGDMA by CCTP. Sherrington surmised that perhaps backbiting cyclisation reactions were responsible for the results seen by Guan, as this would lead to a 'reduced tendency to crosslink'. Their endeavours into conventional chain transfer polymerisation were more fruitful, with soluble polymers being obtained. Multi-detector SEC was used to characterise the synthesised polymers by measurement of the g' values, which gives an indication of branching in polymers based on a comparison of their IV compared to a linear counterpart, which will be discussed in more detail later in this work. The general trend observed was that polymers synthesised by the Strathclyde route possessed the lowest g' values, and hence, were more branched than those synthesised by CCTP. This is not unexpected as the level of crosslinker employed in their conventional chain transfer polymerisation was greater than in their CCTP's.

Further work on the homopolymerisation of divinyl monomers was carried out by Kurmaz *et al*. in 2006, with a comparative study of the homopolymerisations of butane-1,4-diol dimethacrylate (BDDMA) and BDDA, whereby soluble polymers were obtained.[188] However, although a wealth of examples exists for the synthesis of branched polymers by CCTP; the high levels of vinyl functionality retained have not been exploited, which in part, is the aim of this thesis.

1.5. Post-Polymerisation Functionalisation of Vinyl Groups

Post-polymerisation functionalisations have become commonplace since the realisation of click chemistry in 2001 by Sharpless *et al*. and its rapid growth in the following years,[70] with the method of modification being highly dependent on the functionality already interred to the polymer *via* the polymerisation method or by monomer choice. Previous literature highlights the high level of vinyl functionality retained on polymerisation of multi-vinyl monomers and their copolymerisation with monovinyl

monomers *via* CCTP, providing an excellent handle for the post-polymerisation functionalisation of these materials in the formation of branched functional polymers.

The most common method for the functionalisation of unsaturated vinyl groups in post-polymerisation modifications is by addition of functional thiols to the olefinic bonds, commonly termed thiol-ene additions. The reasons as to why thiol-ene type reactions are so prevalent in comparison to other Michael type additions is its tolerance to a variety of reaction conditions, solvents and functionalities, also its orthogonal nature, which has led to its extensive use in dendrimer synthesis, where high selectivity is required.[189] Typically thiol-ene or "thiol-ene click" describes reactions conducted *via* radical pathways, [53, 190-193] but can also be achieved using mild base or nucleophilic catalysis, commonly known as thiol-Michael addition.[46, 194] In contrast to radical thiol-ene reactions, the use of activated vinyl groups is required for thiol-Michael addition,[195] examples of these activated-enes include (meth)acrylate, fumarate esters and maleimide derivatives.[196, 197]

1.5.1. Radical Thiol-ene "Click"

Radical sources in thiol-ene reactions can be generated by thermal initiation or by photoinitiation. An added benefit of photoinitiation is that ambient reaction conditions can be used, with reactions only proceeding in the presence of UV light. The mechanism proceeds by a typical chain process, with initiation resulting in the formation of a thiyl radical. Propagation occurs *via* addition of the thiyl radical to a olefinic bond, yielding an intermediate carbon centred radical, with the desired termination by chain transfer to a further thiol in the formation of the thiol-ene product and generation of a thiyl radical (Figure 1.23). Termination can also occur *via* coupling or disproportion reactions, commonly leading to the formation of disulfides. For radical thiol-ene reactions, addition can proceed with virtually any olefinic bond, although steric hindrance plays an important role in the efficiency of these reactions.[196]

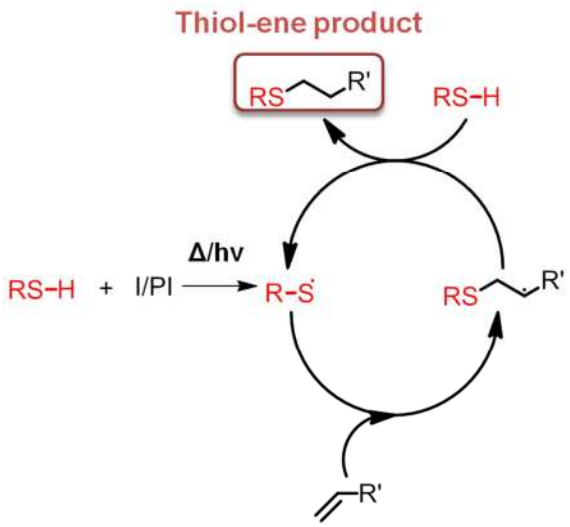

Figure 1.23: Radical thiol-ene "click" to an olefinic bond, proposed mechanism, whereby I is thermal initiation, PI is photoinitiation

A variety of polymerisation techniques have been utilised in the synthesis of polymers containing unsaturated groups, most commonly by polymerisation of monomers bearing pendant unactivated alkene groups. Campos *et al*. demonstrated the broad utility of the radical thiol-ene reaction by functionalisation of copolymers of styrene and 1-[(3-butenyloxy)methyl]-4-vinyl benzene synthesised by RAFT; MMA, but-3-enyl methacrylate synthesised by ATRP; and Sn mediated ROP of ε-caprolactone and 6-allyl-ε-caprolactone, using thiols such as thioglycolic acid, 3-mercaptopropyltrimethoxysilane, *N*-(9-fluoroenylmethoxycarbonyl)cysteine, 1-adamantanethiol and thioglycerol. Functionalisations were carried out using both photoinitiation and thermal initiation, all obtaining high yields, however, photoinitiation proved to be the more quantitative method.[198]

Small molecule thiol-ene reactions have also been used in the formation of biological conjugates including thiol modification of sugar moieties such as monoglycosides, disaccharides and glycosyl amino acids, highlighting the applicability of this technique to the synthesis of biologically applicable polymers.[199]

1.5.2. Thiol-Michael Addition

Base catalysed thiol-Michael addition uses a weak base such as triethylamine (TEA) to facilitate the deprotonation of a thiol,[200, 201] with subsequent formation of a triethylammonium cation and a thiolate anion, a powerful nucleophile. The thiolate anion can then attack activated vinyl groups forming a strong enolate base capable of thiol deprotonation, which yields the thiol-ene product whilst generating additional thiolate anions, forming a catalytic process (Figure 1.24).[46]

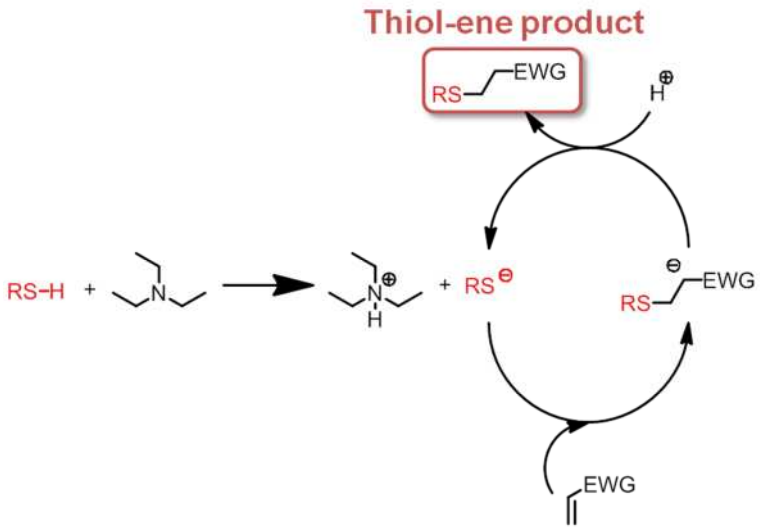

Figure 1.24: Base catalysed hydrothiolation of an activated vinyl group, proposed mechanism, where EWG is electron withdrawing group

Nucleophilic thiol-Michael addition employs strong nucleophilic catalysts such as primary amines, secondary amines, certain phosphines and very recently nitrogen centred nucleophiles, in the creation of strong bases. Nucleophilic attack at the activated vinyl groups generates a strong zwitterionic enolate base, capable of deprotonating thiols in the formation of thiolate anions.[54, 202-206] Once formed, thiolate anions can participate in the rapid formation of thiol-Michael addition products by the hydrothiolation of activated vinyl groups (Figure 1.25).

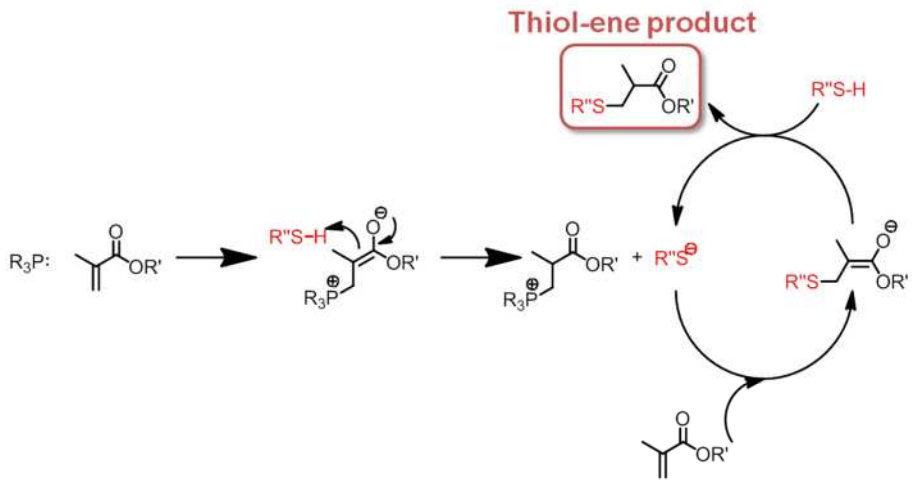

Figure 1.25: Thiol-Michael addition of a methacrylic vinyl group *via* phosphine catalysis, proposed mechanism

Although primary and secondary amines are efficient catalysts in nucleophilic thiol-Michael additions, weakly basic phosphine catalyst dimethylphenylphosphine (DMPP) has been found to be a superior catalyst for such systems.[207] Although the use of any of the variety of nucleophilic catalysts has the advantage of being robust in the presence of protic species such as water, retaining high efficiencies.[208] Deprotonation of the thiol is a rate determining effect which can affect efficiency, with the pKa of the thiol being of particular importance for basic or nucleophile catalysed systems.[209-211] It should be noted however, that as nucleophilic adducts are formed in the nucleophilic thiol-Michael addition reactions, the nucleophiles employed cannot strictly be described as catalysts, although their use initiates the catalytic formation of thiolate anions.

Due to the latent thiol functionality of polymers synthesised by RAFT polymerisation, accessible by aminolysis, their utilisation in post-polymerisation modification by thiol-Michael addition has been extensive.[212] This along with other prevalent post-polymerisation modifications using thiol-Michael addition will be discussed further later in this work, however, one salient feature is the range of catalysts available for this type of reaction, including primary and secondary amines, phosphines and in some cases thiol dissociation is promoted by the use of polar aprotic solvents. Hence, catalyst choice can be tailored for the reaction conditions used, with mild, water soluble catalysts such as tris(2-carboxyethyl)phosphine (TCEP) employed for bioconjugation of polyethylene glycol acrylate to disulfide containing salmon calcitonin, whereby the

phosphine catalyst acts as both a reducing agent and thiol-Michael catalyst,[208] again highlighting the scope of this reaction to the synthesis of bioconjugates.

1.6. References

1. Guan, Z., *J. Polym. Sci., Part A: Polym. Chem.* **2003,** *41* (22), 3680.
2. Odian, G., *Principles of Polymerisation*. 4th ed.; John Wiley & Sons: 2004.
3. Voit, B. I.; Lederer, A., *Chem. Rev.* **2009,** *109* (11), 5924.
4. England, R. M.; Rimmer, S., *Polym. Chem.* **2010,** *1* (10), 1533.
5. Bruchmann, B.; Königer, R.; Renz, H., *Macromol. Symp.* **2002,** *187* (1), 271.
6. Bruchmann, B., *Macromol. Mater. Eng.* **2007,** *292* (9), 981.
7. Mulkern, T. J.; Tan, N. C. B., *Polymer* **2000,** *41* (9), 3193.
8. Hong, Y.; Coombs, S. J.; Cooper-White, J. J.; Mackay, M. E.; Hawker, C. J.; Malmström, E.; Rehnberg, N., *Polymer* **2000,** *41* (21), 7705.
9. Chen, S.; Zhang, X.-Z.; Cheng, S.-X.; Zhuo, R.-X.; Gu, Z.-W., *Biomacromolecules* **2008,** *9* (10), 2578.
10. Wang, Y.; Grayson, S. M., *Adv. Drug Delivery Rev.* **2012,** *64* (9), 852.
11. Boas, U.; Heegaard, P. M. H., *Chem. Soc. Rev.* **2004,** *33* (1), 43.
12. Svenson, S. n.; Tomalia, D. A., *Adv. Drug Delivery Rev.* **2005,** *57* (15), 2106.
13. Flory, P. J., *Principles of Polymer Chemistry*. 1st ed.; Cornell University Press: Ithaca, New York, 1953.
14. Flory, P. J., *J. Am. Chem. Soc.* **1952,** *74*, 2718.
15. Carothers, W. H., *Transactions of the Faraday Society* **1936,** *32* (0), 39.
16. Flory, P. J., *J. Am. Chem. Soc.* **1939,** *61*, 3334.
17. Flory, P. J., *J. Am. Chem. Soc.* **1940,** *62*, 2261.
18. Flory, P. J., *J. Am. Chem. Soc.* **1941,** *63*, 3083.
19. Jacobson, H.; Beckmann, C. O.; Stockmayer, W. H., *J. Chem. Phys.* **1950,** *18* (12), 1607.
20. Hawker, C. J.; Lee, R.; Fréchet, J. M. J., *J. Am. Chem. Soc.* **1991,** *113* (12), 4583.
21. Kambouris, P.; Hawker, C. J., *J. Chem. Soc., Perkin Trans.* **1993,** *1*, 2717.
22. Kricheldorf, H. R.; Zang, Q.-Z.; Schwarz, G., *Polymer* **1982,** *23* (12), 1821.
23. Kricheldorf, H. R.; Stöber, O., *Macromol. Rapid Commun.* **1994,** *15* (1), 87.
24. Wooley, K. L.; Hawker, C. J.; Lee, R.; Fréchet, J. M. J., *Polym. J.* **1994,** *26* (2), 187.
25. Turner, S. R.; Voit, B. I.; Mourey, T. H., *Macromolecules* **1993,** *26* (17), 4617.
26. Malmström, E.; Johansson, M.; Hult, A., *Macromolecules* **1995,** *28* (5), 1698.
27. Malmström, E.; Hult, A., *Macromolecules* **1996,** *29* (4), 1222.
28. Feast, W. J.; Stainton, N. M., *J. Mater. Chem.* **1995,** *5* (3), 405.

29. Komber, H.; Ziemer, A.; Voit, B., *Macromolecules* **2002,** *35* (9), 3514.
30. Percec, V.; Chu, P.; Kawasumi, M., *Macromolecules* **1994,** *27* (16), 4441.
31. Dušek, K.; Šomvársky, J.; Smrčková, M.; Simonsick Jr, W. J.; Wilczek, L., *Polym. Bull.* **1999,** *42* (4), 489.
32. Miravet, J. F.; Fréchet, J. M. J., *Macromolecules* **1998,** *31* (11), 3461.
33. Kricheldorf, H. R.; Bolender, O.; Wollheim, T., *Macromolecules* **1999,** *32* (12), 3878.
34. Gittins, P. J.; Alston, J.; Ge, Y.; Twyman, L. J., *Macromolecules* **2004,** *37* (20), 7428.
35. Cheng, K.-C., *Polymer* **2003,** *44* (4), 1259.
36. Cheng, K.-C.; Chuang, T.-H.; Chang, J.-S.; Guo, W.; Su, W.-F., *Macromolecules* **2005,** *38* (20), 8252.
37. Saha, A.; Ramakrishnan, S., *Macromolecules* **2008,** *41* (15), 5658.
38. Orlicki, J. A.; Thompson, J. L.; Markoski, L. J.; Sill, K. N.; Moore, J. S., *J. Polym. Sci., Part A: Polym. Chem.* **2002,** *40* (8), 936.
39. Yamaguchi, N.; Wang, J.-S.; Hewitt, J. M.; Lenhart, W. C.; Mourey, T. H., *J. Polym. Sci., Part A: Polym. Chem.* **2002,** *40* (16), 2855.
40. www.perstorp.com/upload/boltorn_201202.pdf.
41. Gao, C.; Yan, D., *Prog. Polym. Sci.* **2004,** *29* (3), 183.
42. Komber, H.; Voit, B.; Monticelli, O.; Russo, S., *Macromolecules* **2001,** *34* (16), 5487.
43. Schmaljohann, D.; Voit, B., *Macromol. Theory Simul.* **2003,** *12* (9), 679.
44. Reisch, A.; Komber, H.; Voit, B., *Macromolecules* **2007,** *40* (19), 6846.
45. Rannard, S. P.; Davis, N. J., *J. Am. Chem. Soc.* **2000,** *122* (47), 11729.
46. Mather, B. D.; Viswanathan, K.; Miller, K. M.; Long, T. E., *Prog. Polym. Sci.* **2006,** *31* (5), 487.
47. Kim, Y.-B.; Kim, H. K.; Nishida, H.; Endo, T., *Macromol. Mater. Eng.* **2004,** *289* (10), 923.
48. Trumbo, D., *Polym. Bull.* **1991,** *26* (3), 265.
49. Trumbo, D. L., *Polym. Bull.* **1991,** *26* (5), 481.
50. Liu, Y.-L.; Tsai, S.-H.; Wu, C.-S.; Jeng, R.-J., *J. Polym. Sci., Part A: Polym. Chem.* **2004,** *42* (23), 5921.
51. Wu; Liu, Y.; He; Chung; Goh, *Macromolecules* **2004,** *37* (18), 6763.
52. Gao, C.; Xu, Y.; Yan, D.; Chen, W., *Biomacromolecules* **2003,** *4* (3), 704.
53. Killops, K. L.; Campos, L. M.; Hawker, C. J., *J. Am. Chem. Soc.* **2008,** *130* (15), 5062.
54. Yu, B.; Chan, J. W.; Hoyle, C. E.; Lowe, A. B., *J. Polym. Sci., Part A: Polym. Chem.* **2009,** *47* (14), 3544.
55. Semsarilar, M.; Ladmiral, V.; Perrier, S., *Macromolecules* **2010,** *43* (3), 1438.
56. Chen, G.; Kumar, J.; Gregory, A.; Stenzel, M. H., *Chem. Commun.* **2009,** (41), 6291.

57. Konkolewicz, D.; Gray-Weale, A.; Perrier, S. b., *J. Am. Chem. Soc.* **2009,** *131* (50), 18075.

58. Fairbanks, B. D.; Sims, E. A.; Anseth, K. S.; Bowman, C. N., *Macromolecules* **2010,** *43* (9), 4113.

59. Hoogenboom, R., *Angew. Chem., Int. Ed.* **2010,** *49* (20), 3415.

60. Lowe, A. B.; Hoyle, C. E.; Bowman, C. N., *J. Mater. Chem.* **2010,** *20* (23), 4745.

61. Han, J.; Zhao, B.; Gao, Y.; Tang, A.; Gao, C., *Polym. Chem.* **2011,** *2* (10), 2175.

62. Han, J.; Zhao, B.; Tang, A.; Gao, Y.; Gao, C., *Polym. Chem.* **2012,** *3* (7), 1918.

63. Goodall, G. W.; Hayes, W., *Chem. Soc. Rev.* **2006,** *35* (3), 280.

64. Morgenroth, F.; Müllen, K., *Tetrahedron* **1997,** *53* (45), 15349.

65. Martin, S. J.; Godschalx, J. P.; Mills, M. E.; Shaffer, E. O.; Townsend, P. H., *Advanced Materials* **2000,** *12* (23), 1769.

66. Stumpe, K.; Komber, H.; Voit, B. I., *Macromol. Chem. Phys.* **2006,** *207* (20), 1825.

67. Berresheim, A. J.; Müller, M.; Müllen, K., *Chem. Rev.* **1999,** *99* (7), 1747.

68. Stumpe, K.; Eichhorn, K.-J.; Voit, B., *Macromol. Chem. Phys.* **2008,** *209* (17), 1787.

69. Komber, H.; Stumpe, K.; Voit, B., *Macromol. Chem. Phys.* **2006,** *207* (20), 1814.

70. Kolb, H. C.; Finn, M. G.; Sharpless, K. B., *Angew. Chem., Int. Ed.* **2001,** *40* (11), 2004.

71. Huisgen, R., *Proc. Chem. Soc.* **1961,** (October), 357.

72. Voit, B., *New J. Chem.* **2007,** *31* (7), 1139.

73. Maier, G.; Zech, C.; Voit, B.; Komber, H., *Macromol. Chem. Phys.* **1998,** *199* (12), 2655.

74. Maier, G.; Zech, C.; Voit, B.; Komber, H., *Macromol. Symp.* **2001,** *163* (1), 75.

75. Scheel, A. J.; Komber, H.; Voit, B. I., *Macromol. Rapid Commun.* **2004,** *25* (12), 1175.

76. Voit, B.; Fleischmann, S.; Komber, H.; Scheel, A.; Stumpe, K., *Macromol. Symp.* **2007,** *254* (1), 16.

77. Fréchet, J. M. J.; Henmi, M.; Gitsov, I.; Aoshima, S.; Leduc, M. R.; Grubbs, R. B., *Science* **1995,** *269* (5227), 1080.

78. Müller, A. H. E.; Yan, D.; Wulkow, M., *Macromolecules* **1997,** *30* (23), 7015.

79. Simon, P. F. W.; Müller, A. H. E., *Macromolecules* **2001,** *34* (18), 6206.

80. Puskas, J. E.; Grasmüller, M., *Macromol. Symp.* **1998,** *132* (1), 117.

81. Simon, P. F. W.; Radke, W.; Müller, A. H. E., *Macromol. Rapid Commun.* **1997,** *18* (9), 865.

82. Sakamoto, K.; Aimiya, T.; Kira, M., *Chem. Lett.* **1997,** *26* (12), 1245.

83. Hawker, C. J.; Fréchet, J. M. J.; Grubbs, R. B.; Dao, J., *J. Am. Chem. Soc.* **1995,** *117* (43), 10763.

84. Weimer, M. W.; Fréchet, J. M. J.; Gitsov, I., *J. Polym. Sci., Part A: Polym. Chem.* **1998,** *36* (6), 955.

85. Matyjaszewski, K.; Nakagawa, Y.; Gaynor, S. G., *Macromol. Rapid Commun.* **1997,** *18* (12), 1057.

86. Gaynor, S. G.; Edelman, S.; Matyjaszewski, K., *Macromolecules* **1996,** *29* (3), 1079.

87. Carter, S.; Rimmer, S.; Sturdy, A.; Webb, M., *Macromol. Biosci.* **2005,** *5* (5), 373.

88. Wang, Z.; He, J.; Tao, Y.; Yang, L.; Jiang, H.; Yang, Y., *Macromolecules* **2003,** *36* (20), 7446.

89. Tao, Y.; He, J.; Wang, Z.; Pan, J.; Jiang, H.; Chen, S.; Yang, Y., *Macromolecules* **2001,** *34* (14), 4742.

90. Li, C.; He, J.; Li; Cao, J.; Yang, Y., *Macromolecules* **1999,** *32* (21), 7012.

91. Niu, A.; Li, C.; Zhao, Y.; He, J.; Yang, Y.; Wu, C., *Macromolecules* **2001,** *34* (3), 460.

92. Carter, S.; Hunt, B.; Rimmer, S., *Macromolecules* **2005,** *38* (11), 4595.

93. Carter, S. R.; England, R. M.; Hunt, B. J.; Rimmer, S., *Macromol. Biosci.* **2007,** *7* (8), 975.

94. Rimmer, S.; Carter, S.; Rutkaite, R.; Haycock, J. W.; Swanson, L., *Soft Matter* **2007,** *3* (8), 971.

95. Matyjaszewski, K.; Gaynor, S. G.; Kulfan, A.; Podwika, M., *Macromolecules* **1997,** *30* (17), 5192.

96. Matyjaszewski, K.; Pyun, J.; Gaynor, S. G., *Macromol. Rapid Commun.* **1998,** *19* (12), 665.

97. Cheng, C.; Wooley, K. L.; Khoshdel, E., *J. Polym. Sci., Part A: Polym. Chem.* **2005,** *43* (20), 4754.

98. Powell, K. T.; Cheng, C.; Wooley, K. L., *Macromolecules* **2007,** *40* (13), 4509.

99. Chang, H.-T.; Fréchet, J. M. J., *J. Am. Chem. Soc.* **1999,** *121* (10), 2313.

100. Liu, M.; Vladimirov, N.; Fréchet, J. M. J., *Macromolecules* **1999,** *32* (20), 6881.

101. Sunder, A.; Hanselmann, R.; Frey, H.; Mülhaupt, R., *Macromolecules* **1999,** *32* (13), 4240.

102. Löwenhielm, P.; Nyström, D.; Johansson, M.; Hult, A., *Prog. Org. Coat.* **2005,** *54* (4), 269.

103. Chang, H.-L.; Chao, T.-Y.; Yang, C.-C.; Dai, S. A.; Jeng, R.-J., *Eur. Polym. J.* **2007,** *43* (9), 3988.

104. Chen, H.; Jia, Z.; Yan, D.; Zhu, X., *Macromol. Chem. Phys.* **2007,** *208* (15), 1637.

105. Tokar, R.; Kubisa, P.; Penczek, S.; Dworak, A., *Macromolecules* **1994,** *27* (2), 320.

106. Dworak, A.; Walach, W.; Trzebicka, B., *Macromol. Chem. Phys.* **1995,** *196* (6), 1963.

107. Zou, P.; Yang, L.-P.; Pan, C.-Y., *J. Polym. Sci., Part A: Polym. Chem.* **2008,** *46* (23), 7628.

108. Kakwere, H.; Perrier, S., *J. Polym. Sci., Part A: Polym. Chem.* **2009,** *47* (23), 6396.

109. Hedrick, J. L.; Trollsås, M.; Hawker, C. J.; Atthoff, B.; Claesson, H.; Heise, A.; Miller, R. D.; Mecerreyes, D.; Jérôme, R.; Dubois, P., *Macromolecules* **1998,** *31* (25), 8691.

110. Flory, P. J., *J. Am. Chem. Soc.* **1937,** *59* (2), 241.

111. Meijs, G. F.; Rizzardo, E.; Le, T. P. T., *Polym. Int.* **1991,** *26* (4), 239.

112. Norrish, R. G. W.; Brookman, E. F., *Proc. Roy. Soc. London* **1939,** *171* (945), 147.

113. Trommsdorff, V. E.; Köhle, H.; Lagally, P., *Makromol. Chem.* **1948,** *1* (3), 169.

114. Costello, P. A.; Martin, I. K.; Slark, A. T.; Sherrington, D. C.; Titterton, A., *Polymer* **2002,** *43* (2), 245.

115. Isaure, F.; Cormack, P. A. G.; Sherrington, D. C., *J. Mater. Chem.* **2003,** *13* (11), 2701.

116. Slark, A. T.; Sherrington, D. C.; Titterton, A.; Martin, I. K., *J. Mater. Chem.* **2003,** *13* (11), 2711.

117. Isaure, F. o.; Cormack, P. A. G.; Sherrington, D. C., *Macromolecules* **2004,** *37* (6), 2096.

118. O'Brien, N.; McKee, A.; Sherrington, D. C.; Slark, A. T.; Titterton, A., *Polymer* **2000,** *41* (15), 6027.

119. Graham, S.; Cormack, P. A. G.; Sherrington, D. C., *Macromolecules* **2004,** *38* (1), 86.

120. Camerlynck, S.; Cormack, P. A. G.; Sherrington, D. C.; Saunders, G., *J. Macromol. Sci., Part B: Phys.* **2005,** *44* (6), 881

121. Baudry, R.; Sherrington, D. C., *Macromolecules* **2006,** *39* (4), 1455.

122. Gridnev, A. A.; Ittel, S. D., *Chem. Rev.* **2001,** *101* (12), 3611.

123. Z.Guan US5767211, **1998**.

124. Guan, Z., *J. Am. Chem. Soc.* **2002,** *124*, 5616.

125. Haddleton, D. M.; Kukulj, D.; Davis, T. P.; Maloney, D. R., *Trends in Polym. Sci.* **1995,** *3*, 365.

126. Heuts, J. P. A.; Roberts, G. E.; Biasutti, J. D., *Aust. J. Chem.* **2002,** *55* (7), 381.

127. Suddaby, K. G.; Maloney, D. R.; Haddleton, D. M., *Macromolecules* **1997,** *30* (4), 702.

128. Smirnov, B. R.; Belgovskii, I. M.; Ponomarev, G. V.; Marchenko, A. P.; Enikolopyan, N. S., *Dokl. Akad. Nauk SSSR* **1980,** *254* (7), 127.

129. Smirnov, B. R.; Morozova, I. S.; Marchenko, A. P.; Markevich, M. A.; Pushchaeva, L. M.; Enikolopyan, N. S., *Dokl. Akad. Nauk SSSR* **1980,** *253* (4), 891.

130. Smirnov, B. R.; Morozova, I. S.; Pushchaeva, L. M.; Marchenko, A. P.; Enikolopyan, N. S., *Dokl. Akad. Nauk SSSR* **1980,** *255* (3), 609.

131. Smirnov, B. R.; Plotnikov, V. D.; Ozerkovskii, B. V.; Roshchupkin, V. P.; Enikolopyan, N. S., *Vysokomol. Soedin., Ser. A* **1981,** *23* (11), 2588.

132. Enikolopyan, N. S.; Smirnov, B. R.; Ponomarev, G. V.; Belgovskii, I. M., *J. Polym. Sci., Polym. Chem. Ed.* **1981,** *19* (4), 879.

133. Lin, J. C.; Abbey, K. J. US 4680354, **1987**.

134. Abbey, K. J.; Trumbo, D. L.; Carlson, G. M.; Masola, M. J.; Zander, R. A., *J. Polym. Sci., Part A: Polym. Chem.* **1993,** *31* (13), 3417.

135. Carlson, G. M.; Abbey, K. J. US 4526945, **1985**.

136. Janowicz, A. H. EP 261942, **1988**.

137. Haddleton, D. M.; Muir, A. V. G.; Leeming, S. W.; O'Donnell, J. P.; Richards, S. N. WO 9613527, **1996**.

138. Haddleton, D. M.; Muir, A. V. G.; Leeming, S. W. WO 9517435, **1995**.

139. Haddleton, D. M.; Padget, J. C.; Overbeek, G. C. WO 9504767, **1995**.

140. Cheng, C.-M.; Tshudy, D. J. US 5928829, **1999**.

141. Lynch, J. P.; Irvine, D. J.; Beverly, G. M. WO 9804603, **1998**.

142. Airey, G. D.; Wilmot, J.; Grenfell, J. R. A.; Irvine, D. J.; Barker, I. A.; Harfi, J. E., *Eur. Polym. J.* **2011,** *47* (6), 1300.

143. Huybrechts, J.; Bruylants, P.; Vaes, A.; De Marre, A., *Prog. Org. Coat.* **2000,** *38* (2), 67.

144. Huybrechts, J.; Bruylants, P.; Kirshenbaum, K.; Vrana, J.; Snuparek, J., *Prog. Org. Coat.* **2002,** *45* (2-3), 173.

145. Mironychev, V. Y.; Mogilevich, M. M.; Smirnov, B. R.; Shapiro, Y. Y.; Golikov, I. V., *Polym. Sci. U.S.S.R.* **1986,** *28* (9), 2103.

146. Lewin, L. A.; Devlin, B. P.; Parquet JR, D. A.; Adams, J. L. US 20050027074, **2005**.

147. Devlin, B. P.; Antonelli, J. A.; Scopazzi, C. WO9303081, **1993**.

148. Slavin, S.; Khoshdel, E.; Haddleton, D. M. EP10161308 **2010**.

149. Antonelli, J. A.; Scopazzi, C. US 5310807, **1994**.

150. Yamashita, S.; Shibatani, K.; Takakura, K.; Imai, K. 4279795, **1981**.

151. Muratore, L. M.; Steinhoff, K.; Davis, T. P., *J. Mater. Chem.* **1999,** *9*, 1687.

152. Burczyk, A. F.; O'Driscoll, K. F.; Rempel, G. L., *J. Polym. Sci., Polym. Chem. Ed.* **1984,** *22* (11), 3255.

153. Parshall, G. W.; Ittle, S. D., *Homogenous Catalysis: The Applications and Chemistry of Catalysis by Soluble Transition Metal Complexes*. 2nd ed.; Wiley: 1992.

154. Gridnev, A. A.; Ittel, S. D.; Fryd, M.; Wayland, B. B., *Organometallics* **1996,** *15* (1), 222.

155. Gridnev, A. A.; Ittel, S. D.; Fryd, M.; Wayland, B. B., *Organometallics* **1993,** *12* (12), 4871.

156. Haddleton, D. M.; Maloney, D. R.; Suddaby, K. G.; Muir, A. V. G.; Richards, S. N., *Macromol. Symp.* **1996,** *111*, 37.

157. Gridnev, A. A., *J. Polym. Sci., Part A: Polym. Chem.* **2000,** *38* (10), 1753.

158. Sanayei, R. A.; O'Driscoll, K. F., *J. Macromol. Sci., Chem.* **1989,** *26* (8), 1137

159. Suddaby, K. G.; Haddleton, D. M.; Hastings, J. J.; Richards, S. N.; O'Donnell, J. P., *Macromolecules* **1996,** *29* (25), 8083.

160. Heuts, J. P. A.; Kukulj, D.; Forster, D. J.; Davis, T. P., *Macromolecules* **1998,** *31* (9), 2894.

161. Heuts, J. P. A.; Forster, D. J.; Davis, T. P.; Yamada, B.; Yamazoe, H.; Azukizawa, M., *Macromolecules* **1999,** *32* (8), 2511.

162. Clay, P. A.; Gilbert, R. G., *Macromolecules* **1995,** *28*, 552.

163. Moad, G.; Moad, C. L., *Macromolecules* **1996,** *29* (24), 7727.

164. Ng, F. T. T.; Rempel, G. L.; Mancuso, C.; Halpern, J., *Organometallics* **1990,** *9* (10), 2762.

165. Suddaby, K. G.; O'Driscoll, K. F.; Rudin, A., *J. Polym. Sci., Part A: Polym. Chem.* **1992,** *30* (4), 643.

166. Heuts, J. P. A.; Forster, D. J.; Davis, T. P., *Macromol. Rapid Commun.* **1999,** *20* (6), 299.

167. Pierik, S. C. J.; Vollmerhaus, R.; van Herk, A. M., *Macromol. Chem. Phys.* **2003,** *204* (8), 1090.

168. Moad, C. L.; Moad, G.; Rizzardo, E.; Thang, S. H., *Macromolecules* **1996,** *29* (24), 7717.

169. Morrison, D. A.; Davis, T. P.; Heuts, J. P. A.; Messerle, B.; Gridnev, A. A., *J. Polym. Sci., Part A: Polym. Chem.* **2006,** *44* (21), 6171.

170. Cacioli, P.; Hawthorne, D. G.; Laslett, R. L.; Rizzardo, E.; Solomon, D. H., *J. Macromol. Sci., Part A: Pure Appl. Chem.* **1986,** *23* (7), 839

171. Haddleton, D. M.; Maloney, D. R.; Suddaby, K. G.; Clarke, A.; Richards, S. N., *Polymer* **1997,** *38* (25), 6207.

172. Smeets, N. M. B.; Jansen, T. G. T.; Sciarone, T. J. J.; Heuts, J. P. A.; Meuldijk, J.; Van Herk, A. M., *J. Polym. Sci., Part A: Polym. Chem.* **2010,** *48* (5), 1038.

173. Moad, C. L.; Moad, G.; Rizzardo, E.; Thang, S. H., *Macromolecules* **1996,** *29* (24), 7717.

174. Ishigaki, H.; Okkada, H.; Suyama, S. JP 03212402, **1991**.

175. Nagashima, M.; Kazama, H. JP11071220, **1997**.

176. Shinike, H.; Takeda, K.; Sakuraba, N. JP11124791, **1997**.

177. Yoshimi, K.; Kazeto, O.; Katayama, M. EP1101773, **1999**.

178. Haddleton, D. M.; Topping, C.; Kukulj, D.; Irvine, D., *Polymer* **1998,** *39* (14), 3119.

179. Golokov, I. V.; Semyannikov, V. A.; Mogilevich, M. M., *Vysokomol. Soedin., Ser. A Ser. B* **1985,** *27* (4), 304.

180. Abbey, K. J. US 4608423, **1986**.

181. Z.Guan **US5767211, 1998**.

182. Hiemenz, P. C.; Lodge, T. P., *Polymer Chemistry*. 2nd ed.; CRC Press: Taylor & Francis Group: 2007.

183. Brandrup, J.; H, I. E., *Polymer Handbook*. 3rd ed.; Wiley Interscience: Chichester, 1989.

184. Slavin, S.; McEwan, K. A.; Haddleton, D. M., Cobalt Catalyzed Chain Transfer Polymerization: A Review. In *Polymer Science: A Comprehensive Reference*, 1st ed.; Matyjaszewski, K.; MÖller, M., Eds. Elsevier: 2012; Vol. 3, pp 249.

185. Moad, G.; Solomon, D. H., *The Chemistry of Free Radical Polymerizations*. First ed.; Elsevier Science Ltd: Oxford, 1995.

186. Kurmaz, S. V.; Perepelitsina, E. O.; Bubnova, M. L.; Estrina, G. A.; Roshchupkin, V. P., *Mendeleev Commun.* **2002,** *12* (1), 21.

187. Kurmaz, S. V.; Perepelitsina, E. O.; Bubnova, M. L.; Estrina, G. A., *Mendeleev Commun.* **2004,** *14* (3), 125.

188. Kurmaz, S.; Perepelitsina, E., *Russ. Chem. Bull.* **2006,** *55* (5), 835.

189. Kade, M. J.; Burke, D. J.; Hawker, C. J., *J. Polym. Sci., Part A: Polym. Chem.* **2010,** *48* (4), 743.

190. Uygun, M.; Tasdelen, M. A.; Yagci, Y., *Macromol. Chem. Phys.* **2010,** *211* (1), 103.

191. Hoyle, C. E.; Lee, T. Y.; Roper, T., *J. Polym. Sci., Part A: Polym. Chem.* **2004,** *42* (21), 5301.

192. Morgan, C. R.; Magnotta, F.; Ketley, A. D., *J. Polym. Sci., Polym. Chem. Ed.* **1977,** *15* (3), 627.

193. Griesbaum, K., *Angew. Chem. Int. Ed.* **1970,** *9* (4), 273.

194. Michael, A., *J. Prakt. Chem.* **1887,** *35* (1), 349.

195. Posner, T., *Ber. Dtsch. Chem. Ges* **1905,** *38* (1), 646.

196. Lowe, A. B., *Polym. Chem.* **2010,** *1*, 17.

197. Hoyle, C. E.; Lowe, A. B.; Bowman, C. N., *Chem. Soc. Rev.* **2010,** *39* (4), 1355.

198. Campos, L. M.; Killops, K. L.; Sakai, R.; Paulusse, J. M. J.; Damiron, D.; Drockenmuller, E.; Messmore, B. W.; Hawker, C. J., *Macromolecules* **2008,** *41* (19), 7063.

199. Dondoni, A.; Marra, A., *Chem. Soc. Rev.* **2012,** *41* (2), 573.

200. Dix, L. R.; Ebdon, J. R.; Hodge, P., *Eur. Polym. J.* **1995,** *31* (7), 653.

201. Witczak, Z. J.; Lorchak, D.; Nguyen, N., *Carbohydr. Res.* **2007,** *342* (12-13), 1929.

202. Klemarczyk, P., *Polymer* **2001,** *42* (7), 2837.

203. Stewart, I. C.; Bergman, R. G.; Toste, F. D., *J. Am. Chem. Soc.* **2003,** *125* (29), 8696.

204. Gimbert, C.; Lumbierres, M.; Marchi, C.; Moreno-Mañas, M.; Sebastián, R. M.; Vallribera, A., *Tetrahedron* **2005,** *61* (36), 8598.

205. Chan, J. W.; Hoyle, C. E.; Lowe, A. B., *J. Am. Chem. Soc.* **2009,** *131* (16), 5751.

206. Xi, W.; Wang, C.; Kloxin, C. J.; Bowman, C. N., *ACS Macro Letters* **2012,** *1* (7), 811.

207. Chan, J. W.; Yu, B.; Hoyle, C. E.; Lowe, A. B., *Chem. Commun.* **2008,** (40), 4959.

208. Jones, M. W.; Mantovani, G.; Ryan, S. M.; Wang, X.; Brayden, D. J.; Haddleton, D. M., *Chem. Commun.* **2009,** (35), 5272.

209. Kreevoy, M. M.; Harper, E. T.; Duvall, R. E.; Wilgus, H. S.; Ditsch, L. T., *J. Am. Chem. Soc.* **1960,** *82* (18), 4899.

210. Kreevoy, M. M.; Eichinger, B. E.; Stary, F. E.; Katz, E. A.; Sellstedt, J. H., *J. Org. Chem.* **1964,** *29* (6), 1641.

211. Koval', I. V., *Russ. J. Org. Chem.* **2005,** *41* (5), 631.

212. Roth, P. J.; Boyer, C.; Lowe, A. B.; Davis, T. P., *Macromol. Rapid Commun.* **2011,** *32* (15), 1123.

213. Striegel, A.; Yau, W.; Kirkland, J.; Bly, D., *Modern Size-Exclusion Liquid Chromatography: Practice of Gel Permeation and Gel Filtration Chromatography* 2nd ed.; Wiley: 2009.

214. Grubisic, Z.; Rempp, P.; Benoit, H., *J. Polym. Sci., Part B: Polym. Lett.* **1967,** *5* (9), 753.

215. Striegel, A. M., *Anal. Chem.* **2005,** *77* (5), 104 A.

216. Kostanski, L. K.; Keller, D. M.; Hamielec, A. E., *J. Biochem. Biophys. Methods* **2004,** *58* (2), 159.

217. Otocka, E. P.; Hellman, M. Y., *J. Polym. Sci.: Polym. Lett. Ed.* **1974,** *12* (6), 331.

218. Saunders, G.; Cormack, P. A. G.; Graham, S.; Sherrington, D. C., *Macromolecules* **2005,** *38* (15), 6418.

219. Dubin, P. L.; Principi, J. M., *Macromolecules* **1989,** *22* (4), 1891.

220. Netopilík, M.; Podešva, J.; Lokaj, J.; Kratochvíl, P., *Polym. Int.* **2008,** *57* (10), 1152.

221. Flory, P. J.; Fox, T. G., *J. Am. Chem. Soc.* **1951,** *73* (5), 1904.

222. Fox, T. G.; Flory, P. J., *J. Am. Chem. Soc.* **1951,** *73* (5), 1915.

223. Dondos, A., *J. Chromatogr. A* **2006,** *1127*, 183.

224. Dondos, A., *Biomacromolecules* **2007,** *8* (9), 2979.

225. Simon, P. F. W.; Müller, A. H. E.; Pakula, T., *Macromolecules* **2001,** *34* (6), 1677.

226. Roovers, J.; Zhou, L. L.; Toporowski, P. M.; van der Zwan, M.; Iatrou, H.; Hadjichristidis, N., *Macromolecules* **1993,** *26* (16), 4324.

227. Ahn, S.; Lee, H.; Lee, S.; Chang, T., *Macromolecules* **2012,** *45* (8), 3550.

228. Zimm, B. H.; Stockmayer, W. H., *J. Chem. Phys.* **1949,** *17* (12), 1301.

229. Zimm, B. H., *J. Chem. Phys.* **1948,** *16* (12), 1093.

230. Zimm, B. H.; Kilb, R. W., *J. Polym. Sci.* **1959,** *37* (131), 19.

231. Yan, W.; Gardella Jr, J. A.; Wood, T. D., *J. Am. Soc. Mass Spectrom.* **2002,** *13* (8), 914.

232. Chen, H.; He, M.; Pei, J.; He, H., *Anal. Chem.* **2003,** *75* (23), 6531.

233. Adden, R.; Müller, R.; Brinkmalm, G.; Ehrler, R.; Mischnick, P., *Macromol. Biosci.* **2006,** *6* (6), 435.

234. Nielen, M. W. F.; Malucha, S., *Rapid Commun. Mass Spectrom.* **1997,** *11* (11), 1194.

235. Schriemer, D. C.; Li, L., *Anal. Chem.* **1997,** *69* (20), 4176.

236. Rashidzadeh, H.; Guo, B., *Anal. Chem.* **1998,** *70* (1), 131.

237. Kukulj, D.; Davis, T. P., *Macromol. Chem. Phys.* **1998,** *199* (8), 1697.

238. Gruendling, T.; Junkers, T.; Guilhaus, M.; Barner-Kowollik, C., *Macromol. Chem. Phys.* **2010,** *211* (5), 520.

239. Dondos, A.; Benoit, H., *Polymer* **1977,** *18* (11), 1161.

240. Dondos, A.; Skordilis, V., *Journal of Polymer Science: Polymer Physics Edition* **1985,** *23* (4), 615.

241. Mrkvičková, L., *J. Liq. Chromatogr. Relat. Technol.* **1997,** *20* (3), 403.

242. Sadron, C.; Rempp, P., *J Polym Sci* **1958,** *29*, 127.

243. Stockmayer, W. H. F., M. , *J Polym Sci C, Polym Lett* **1963,** *C1*, 137.

244. Bakac, A.; Espenson, J. H., *J. Am. Chem. Soc.* **1984,** *106* (18), 5197.

245. Yhaya, F.; Sutinah, A.; Gregory, A. M.; Liang, M.; Stenzel, M. H., *J. Polym. Sci., Part A: Polym. Chem.* **2012,** *50* (19), 4085.

246. Flores, J. D.; Treat, N. J.; York, A. W.; McCormick, C. L., *Polym. Chem.* **2011,** *2* (9), 1976.

247. Lima, V.; Jiang, X.; Brokken-Zijp, J.; Schoenmakers, P. J.; Klumperman, B.; Van Der Linde, R., *J. Polym. Sci., Part A: Polym. Chem.* **2005,** *43* (5), 959.

248. Qiu, X.-P.; Winnik, F. M., *Macromol. Rapid Commun.* **2006,** *27* (19), 1648.

249. Nicolaÿ, R., *Macromolecules* **2012,** *45* (2), 821.

250. Li, M.; De, P.; Li, H.; Sumerlin, B. S., *Polym. Chem.* **2010,** *1* (6), 854.

251. Vandenbergh, J.; Junkers, T., *Polym. Chem.* **2012,** *3* (10), 2739.

252. Ho, T. H.; Levere, M.; Soutif, J.-C.; Montembault, V.; Pascual, S.; Fontaine, L., *Polym. Chem.* **2011,** *2* (6), 1258.

253. Roth, P. J.; Davis, T. P.; Lowe, A. B., *Macromolecules* **2012,** *45* (7), 3221.

254. Ho, H. T.; Levere, M. E.; Pascual, S.; Montembault, V.; Soutif, J.-C.; Fontaine, L., *J. Polym. Sci., Part A: Polym. Chem.* **2012,** *50* (8), 1657.

255. Huang, X.; Boyer, C.; Davis, T. P.; Bulmus, V., *Polym. Chem.* **2011,** *2* (7), 1505.

256. Boyer, C.; Davis, T. P., *Chem. Commun.* **2009,** (40), 6029.

257. Boyer, C.; Granville, A.; Davis, T. P.; Bulmus, V., *J. Polym. Sci., Part A: Polym. Chem.* **2009,** *47* (15), 3773.

258. Chan, J. W.; Yu, B.; Hoyle, C. E.; Lowe, A. B., *Polymer* **2009,** *50* (14), 3158.

259. Scales, C. W.; Convertine, A. J.; McCormick, C. L., *Biomacromolecules* **2006,** *7* (5), 1389.

260. Li, M.; De, P.; Gondi, S. R.; Sumerlin, B. S., *J. Polym. Sci., Part A: Polym. Chem.* **2008,** *46* (15), 5093.

261. Boyer, C.; Bulmus, V.; Davis, T. P., *Macromol. Rapid Commun.* **2009,** *30* (7), 493.

262. Hall, D. J.; Van Den Berghe, H. M.; Dove, A. P., *Polym. Int.* **2011,** *60* (8), 1149.

263. Sumerlin, B. S.; Tsarevsky, N. V.; Louche, G.; Lee, R. Y.; Matyjaszewski, K., *Macromolecules* **2005,** *38* (18), 7540.

264. Geng, J.; Lindqvist, J.; Mantovani, G.; Haddleton, D. M., *Angew. Chem., Int. Ed.* **2008,** *47* (22), 4180.

265. Gao, H.; Matyjaszewski, K., *J. Am. Chem. Soc.* **2007,** *129* (20), 6633.

266. Coessens, V.; Nakagawa, Y.; Matyjaszewski, K., *Polym. Bull.* **1998,** *40* (2), 135.

267. Coessens, V.; Matyjaszewski, K., *Journal of Macromolecular Science, Part A* **1999,** *36* (5-6), 667.

268. Lutz, J.-F.; Börner, H. G.; Weichenhan, K., *Macromol. Rapid Commun.* **2005,** *26* (7), 514.

269. Lutz, J.-F.; BÖrner, H. G.; Weichenhan, K., *Macromolecules* **2006,** *39* (19), 6376.

270. Tsarevsky, N. V.; Sumerlin, B. S.; Matyjaszewski, K., *Macromolecules* **2005,** *38* (9), 3558.

271. Mespouille, L.; Vachaudez, M.; Suriano, F.; Gerbaux, P.; Coulembier, O.; Degée, P.; Flammang, R.; Dubois, P., *Macromol. Rapid Commun.* **2007,** *28* (22), 2151.

272. de Graaf, A. J.; Mastrobattista, E.; van Nostrum, C. F.; Rijkers, D. T. S.; Hennink, W. E.; Vermonden, T., *Chem. Commun.* **2011,** *47* (24), 6972.

273. Garamszegi, L. s.; Donzel, C.; Carrot, G. r.; Nguyen, T. Q.; Hilborn, J. n., *React. Funct. Polym.* **2003,** *55* (2), 179.

274. Liras, M.; García, O.; Quijada-Garrido, I.; París, R., *Macromolecules* **2011,** *44* (6), 1335.

275. Petton, L.; Ciolino, A. E.; Stamenović, M. M.; Espeel, P.; Du Prez, F. E., *Macromol. Rapid Commun.* **2012,** *33* (15), 1310.

276. Norman, J.; Moratti, S. C.; Slark, A. T.; Irvine, D. J.; Jackson, A. T., *Macromolecules* **2002,** *35* (24), 8954.

277. Soeriyadi, A. H.; Boyer, C.; Burns, J.; Becer, C. R.; Whittaker, M. R.; Haddleton, D. M.; Davis, T. P., *Chem. Commun.* **2010,** *46* (34), 6338.

278. Boyer, C.; Soeriyadi, A. H.; Roth, P. J.; Whittaker, M. R.; Davis, T. P., *Chem. Commun.* **2011,** *47* (4), 1318.

279. Nurmi, L.; Lindqvist, J.; Randev, R.; Syrett, J.; Haddleton, D. M., *Chem. Commun.* **2009,** (19), 2727.

280. Zhang, Q.; Slavin, S.; Jones, M. W.; Haddleton, A. J.; Haddleton, D. M., *Polym. Chem.* **2012**.

281. Zhang, Q.; Li, G.-Z.; Becer, C. R.; Haddleton, D. M., *Chem. Commun.* **2012,** *48* (65), 8063.

282. Soeriyadi, A. H.; Li, G.-Z.; Slavin, S.; Jones, M. W.; Amos, C. M.; Becer, C. R.; Whittaker, M. R.; Haddleton, D. M.; Boyer, C.; Davis, T. P., *Polym. Chem.* **2011,** *2* (4), 815.

283. Li, G.-Z.; Randev, R.; Soeriyadi, A. H.; Rees, G.; Boyer, C.; Tong, Z.; Davis, T. P.; Becer, C. R.; Haddleton, D. M., *Polym. Chem.* **2010,** *1*, 1196.

284. Mazzolini, J.; Boyron, O.; Monteil, V.; D'Agosto, F.; Boisson, C.; Sanders, G. C.; Heuts, J. P. A.; Duchateau, R.; Gigmes, D.; Bertin, D., *Polym. Chem.* **2012,** *3* (9), 2383.

285. Robert A. Schoonheydt; Rudi Van Overloop; Mathieu Van Hove; Velinden, J., *Clay Clay Miner.* **1984,** *32* (1), 74.

286. Fessler, M.; Eller, S.; Bachmann, C.; Gutmann, R.; Trettenbrein, B.; Kopacka, H.; Mueller, T.; Brueggeller, P., *Dalton Trans.* **2009,** (8), 1383.

287. Llewellyn, S. A.; Green, M. L. H.; Cowley, A. R., *Inorg. Chim. Acta* **2006,** *359* (11), 3785.

288. Godfrey, S. M.; Lane, H. P.; McAuliffe, C. A.; Pritchard, R. G., *J. Chem. Soc. Dalton Trans.* **1993,** (10), 1599.

289. Stewart, R. C.; Marzilli, L. G., *J. Am. Chem. Soc.* **1978,** *100* (3), 817.

290. Kakwere, H.; Perrier, S. b., *J. Am. Chem. Soc.* **2009,** *131* (5), 1889.

Chapter 2

2. Synthesis of Branched Polymers with High Levels of Vinyl Functionality

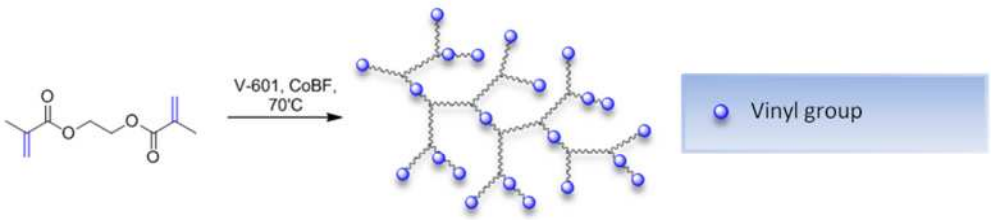

Branched polymers have been of great interest in both industry and academia as their architecture imparts low solution viscosities, increased solubility's and a high level of terminal functionality as compared to their linear counterparts. Catalytic chain transfer polymerisation (CCTP) of divinyl monomers has been used to synthesise a family of branched polymers, which retain activated vinyl functionality with the potential for functionalisation via click chemistry methods. Size exclusion chromatography (SEC) techniques are used to investigate the solution viscosities and branching of synthesised polymers.

2.1 Characterisation Techniques for Branched Polymers

2.1.1 Conventional Size Exclusion Chromatography - SEC

It is important to discuss the methods for the characterisation of branched polymers as an understanding of the theory is required to comprehend discussions from literature sources referenced within this chapter. One of the most widely used methods of characterisation for polymers is SEC, also known as gel permeation chromatography (GPC). Polymers are dissolved in a suitable solvent and injected on to a column packed with porous beads, commonly polystyrene (PS). Large molecules cannot permeate all of the mixed pore sizes and are excluded from travelling through this large network of pores and their retention time in the column is short. Smaller molecules permeate more of the pores and so their retention time in the column is longer, hence polymer separation occurs according to molecular size.[182, 213]

The most common method for the analysis of polymers is conventional SEC, whereby a concentration detector, such as refractive index (RI) is used to measure the varying concentration of polymer samples as they elute from the column using Equation 2.1.

$$\boldsymbol{RI = B(dn/dc)c}$$

Equation 2.1: Where RI is refractive index, B is an instrument constant, dn/dc is the change in RI of the solution as a function of concentration (this value varies for each polymer-solvent pair under constant conditions, common dn/dc values can be found in literature) [183], and c is the polymer concentration in solution

The elution time of the polymer sample is related to molecular weight by the calibration of the column with narrow polymer standards, of a known molecular weight. However, this method of analysis does not yield a universal curve for all polymer samples, leading to limitations in the use of conventional SEC analysis.[214] As column separation is based on hydrodynamic volume of the molecules and not molecular weight directly, accuracy of results requires, ideally, use of narrow standards of the same polymer type to the analyte, although this is not usually possible due to the low variety and number of commercially available polymer standards. Another issue arises in the analysis of non-linear polymers; again this is due to separation being based on hydrodynamic volume. Underestimation of the molecular weight occurs in the analysis of non linear polymers by conventional SEC, as a reduction in hydrodynamic volume is observed for

branched polymers compared to their linear counterparts of the same molar mass (Figure 2.1).[215, 216]

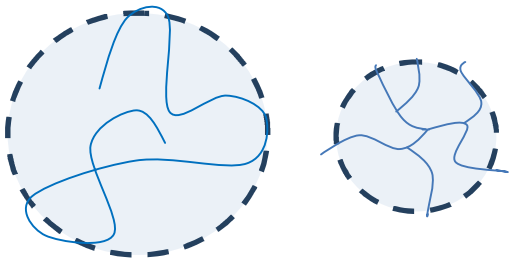

Figure 2.1: Illustration of the difference in hydrodynamic volume of a linear and branched polymer in solution

As this branching level increases the discrepancy caused by the reduction in hydrodynamic volume becomes more prominent. Another factor to consider is whether the sample is heterogeneous, not only molecular weight and architecture but also composition, such as copolymers, microstructure and tacticity, all of these factors can contribute to elution time. As conventional SEC is only accurate in a small number of cases, and cannot be considered an accurate means of measuring molecular weight for branched polymers, combinations of multiple detectors including viscometry, and multi angle light scattering (MALS) can be used.[214, 215, 217, 218]

2.1.2 Viscometry Detection in SEC - Universal Calibration

Universal calibration uses a combination of SEC with RI and viscometry detectors and is based on the hypothesis that elution volume is solely dependent on hydrodynamic volume, taking advantage of the fact that IV and molecular weight are related to the hydrodynamic volume by Equation 2.2:

$$[\eta] = K\frac{V}{M}$$

Equation 2.2: Where [η] is intrinsic viscosity, V is hydrodynamic volume, a measure of molecular size, M is molecular weight and k is a constant, whose value is independent of polymer structure.[214]

Due to the relationship between hydrodynamic volume and IV, and the fact that SEC separates molecules by size, the generation of a calibration curve for a set of standards plotting log [η].M against elution volume will be equivalent to plotting log V

against elution volume. Hence, the same calibration curve will be generated regardless of the standards used, (Figure 2.2).

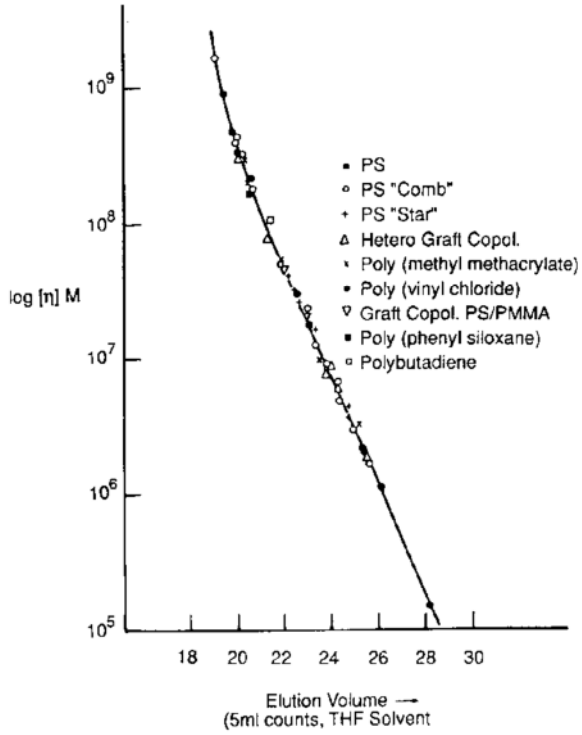

Figure 2.2 Example of universal calibration in size exclusion chromatography. Image copied from reference without editing [214]

Deviations in the universal calibration can arise when analysing macromolecules of differing shape factors, such as rod like and spherical polymers,[219, 220] as hydrodynamic volume is also proportional to the third power of the mean-square radius of gyration according to the Flory-Fox equation,[221, 222] although a wealth of literature exists of cases for the applicability of universal calibration.[116, 223-225]

The use of a viscometry detector allows the determination of the IV for the molecular weight distribution of polymer samples. These values can be used in the formation of Mark-Houwink plots using the Mark-Houwink equation (Equation 2.3).

$$M = K[\eta]^{\alpha}$$

Equation 2.3 Where M is molecular weight, [η] is intrinsic viscosity with K and α as constants.

The contraction of a branched polymer of constant branching in solution will be consistent, hence the Mark-Houwink exponent, α, will be reduced by a consistent amount, leading to a Mark-Houwink plot of the same gradient at a lower viscosity when

compared to its' linear counterpart.[226] If branching is not consistent throughout the sample, both the gradient and IV of the Mark-Houwink plot will contrast with its' linear counterpart.[3, 213] The use of universal calibration will be expanded in further detail later in this chapter.

2.1.3 Triple Detection

Triple detection is a further SEC technique widely used for the characterisation of branched polymers. This method consists of a combination of RI, Light scattering (LS) and viscometry detectors, obtaining the highest level of information from the samples. LS detection measures absolute molecular weight utilising the Rayleigh equation (Equation 2.1):

$$\boldsymbol{R(\theta)\,|_{\theta \to 0} \cong KCM}$$

Equation 2.4: The amount of light scattered by a dilute solution of analyte at a given angle θ which is termed the Rayleigh ratio, R(θ), where K is an optical constant, C is concentration and M is molecular weight

The Rayleigh equation requires the intensity of scattering at zero angle. Measurement directly in the incident beam is not possible, hence several methods to minimise the error are utilised to gain an accurate measure of molecular weight. Measurement of scattering at low angles (LALS), such as 10 degrees or less, error is minimal and is disregarded. Measurement at multiple angles, MALS, and extrapolation to zero can also be used.

In conjunction with LS and RI detection for the determination of absolute molecular weight, viscometry and RI detection are utilised in the measurement of IV, all of which can all be achieved without the need for column calibration.[213, 218, 227] Triple detection is based on the theory, originating from Zimm and Stockmayer in 1949, that chain size, or the mean squared radius of gyration (R_g^2), is affected by branching.[228, 229] As with hydrodynamic volume, the more branched a polymer, the greater the reduction in the R_g^2. This reduction in R_g^2 for branched polymers can be defined as a contraction factor, g, by Equation 2.5:

$$\boldsymbol{g = \frac{(R_g{}^2)_B}{(R_g{}^2)_L}}$$

Equation 2.5: where subscripts B and L refer to branched and linear structures respectively

Zimm and Kilb later discovered that IV could also be used to obtain equivalent information on the chain length contraction factor, g' by Equation 2.6:[230]

$$g' = \frac{[\eta]_B}{[\eta]_L}$$

Equation 2.6: where [η] is intrinsic viscosity and subscripts B and L refer to branched and linear structures respectively

Although this method cannot give an absolute branching number, it can give an indication of the extent of branching when comparing a series of branched polymers.[120, 218] It is noted that applicability of triple detection to low molecular weight polymers is poor, as light scattering detection is insensitive to low molecular weights, hence, universal calibration and the use of g' plots are often the preferred method of characterisation.[227]

2.2 Results and Discussion

Polymerisation of di- or multi-vinyl monomers leads to the formation of branched polymers, but there is a large propensity to crosslink under free radical conditions, occurring within minutes.[124, 181] CCTP provides an excellent method for the control of this type of polymerisation using relatively small amounts of catalyst and produces polymers unique in that they possess a high level of activated vinyl groups.

In this work CCTP of EGDMA, as originally described by Guan, is explored and the claims by Sherrington *et al.,* that polymerisations with crosslinker levels of 25 mol% and above yield irreproducible results, will be investigated. The resulting polymers from these CCTP polymerisations also have the potential to be used in thiol-ene click reactions, which will be discussed in the following chapter.

2.2.1 Initial Study - The Homopolymerisation of EGDMA by CCTP

The homopolymerisation of EGDMA by CCTP was reproduced, using conditions originally outlined by Guan, in order to ascertain whether conflicting literature by Sherrington *et al*. was unfounded.[120, 124] Guan's conditions employ what is considered to be a high level of CoBF, when compared to the synthesis of linear polymers by CCTP, that he postulated would lead to cascade trimerisation of the monomer, with every trimerisation providing a branch point. As the prevailing mode of termination is β-hydride abstraction branched polymers are formed containing high levels of vinyl

functionality, both internal and external (Figure 2.3). This high CoBF concentration is required in order to reduce the molecular weight to a point where gelation is circumvented.

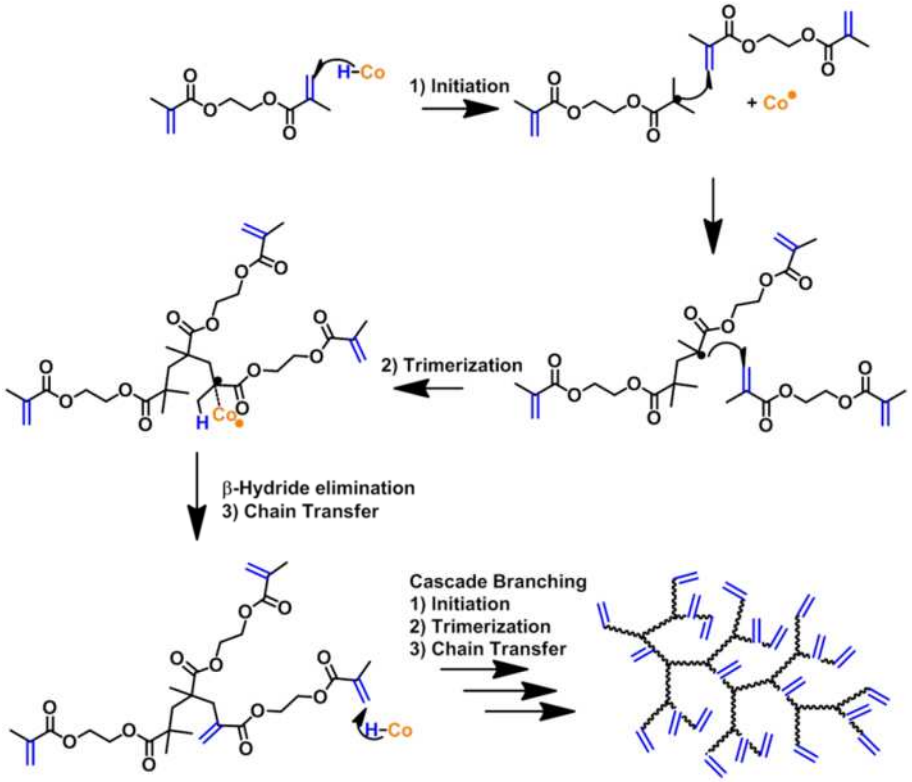

Figure 2.3: Mechanism for the CCTP of EGDMA, cascade trimerisation theory postulated by Guan, [124] leading to the formation of branched vinyl functional polymers

The results obtained using these conditions were in close correlation to those already described in the literature.[124] The product (**A**) was a low molecular weight branched polymer, with oligomeric products.

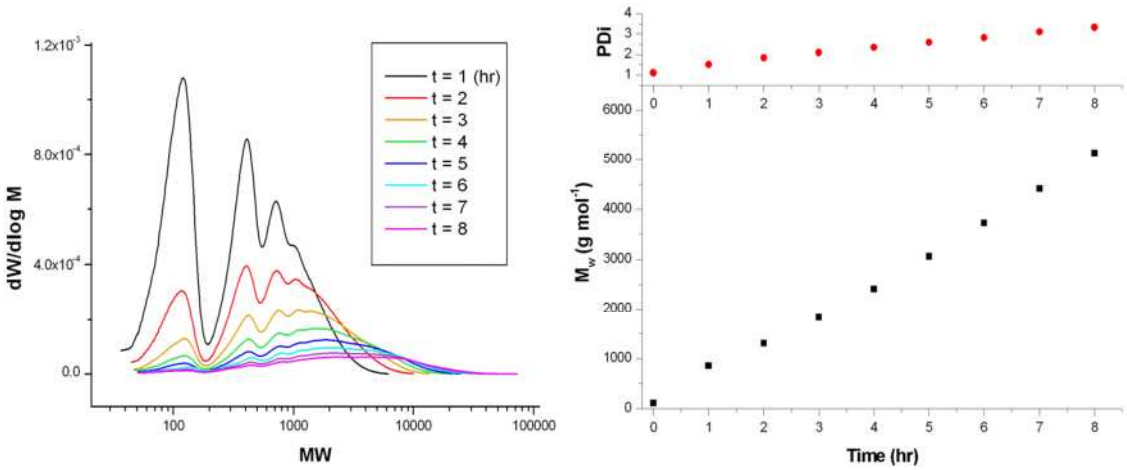

Figure 2.4: (Left) Evolution of SEC spectra over the course of EGDMA homopolymerisation A. (Right) Evolution of M_w and PDi as measured by conventional SEC over the course of EGDMA homopolymerisation A.

The evolution of the molecular weight distribution over the course of polymerisation **A** is shown in Figure 2.4 (left). Monomer decreased as the polymerisation proceeded, forming dimer, trimer, and polymeric products, with molecular weight and PDi increasing over time. After 8 hours reaction time the polymerisation was terminated, yielding a polymer of high conversion and relatively low PDi for a branched polymer. It should be noted that using these conditions the polymerisation can be conducted in a 24 hour time frame without gelation occurring, resulting in a polymer of increased molecular weight and PDi.

The molecular weight evolution over the course of the polymerisation is shown in Figure 2.4 (right). Interestingly there is a linear increase in both the M_w and PDi over the course of the reaction reaching an M_w of approximately 4900 g mol^{-1} by conventional SEC, although it should be stated that the more branched to polymer becomes the less accurate conventional SEC estimations of molecular weight will be, hence SEC monitoring only provides an indication of control in the system. Analysis of the final polymer using universal calibration yields a M_w of 6200 g mol^{-1} and an increased PDi compared to conventional SEC of 3.5 (Table 2.1).

Analysis Method	M_n ($g.mol^{-1}$)	M_w ($g.mol^{-1}$)	PDi
Conventional SEC	1700	4900	2.9
Universal Calibration	1800	6200	3.5

Table 2.1: Comparison of molecular weights obtained from conventional SEC and universal calibration

The high resolution of the SEC spectra obtained allows for deconvolution of monomer, dimer and trimer peaks, from this, the relative conversion of oligomeric products can be measured. Oligomer peaks were deconvoluted using Origin 6 software and their area ratios used to calculate conversion of oligomeric products throughout the polymerisation (Figure 2.5). Conversion was also measured accurately by gas chromatography-flame ionisation detection (GC-FID) and the two methods of measuring total conversion were found to be in close correlation (Figure 2.6).

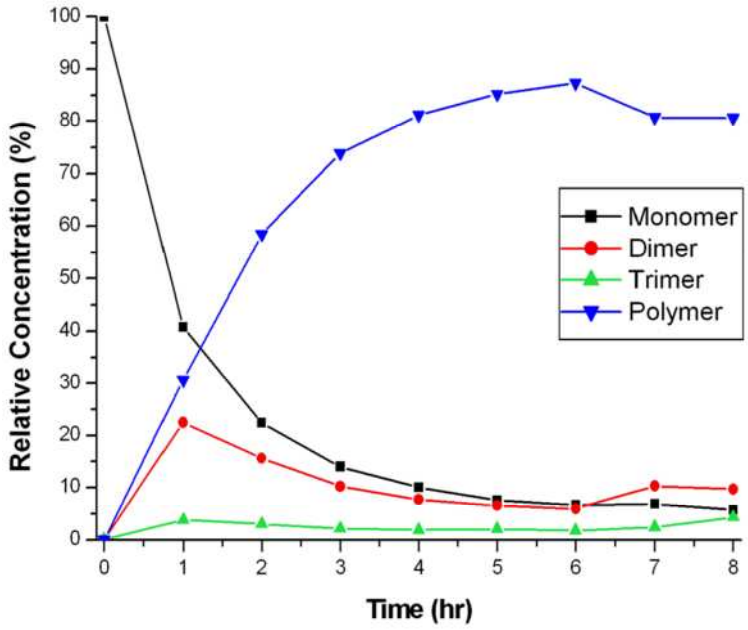

Figure 2.5: Conversion data obtained *via* SEC deconvolution for EGDMA homopolymerisation

From the SEC deconvolution it appears the concentration of dimer is highest in the early stages of the polymerisation (Figure 2.5). As the polymerisation proceeds the relative dimer concentration decreases, plateauing at approximately 10%. The concentration of trimer however, appears to be consistent throughout the polymerisation. One key observation is that crosslinking occurs only when the M_w is high and monomer concentration is relatively low (below 20%). Thus, many of the subsequent reactions were subjected to early termination (between 6 to 10 hours

duration), giving overall conversions above 90%, but decreasing the likelihood of gelation.

The decreasing monomer concentration was monitored throughout the polymerisation by GC-FID. A rapid increase in conversion is seen within the first three hours, reaching a conversion of approximately 80%. Conversion begins to plateau after three hours, reaching a final conversion of 93% at eight hours (Figure 2.6 (●)).

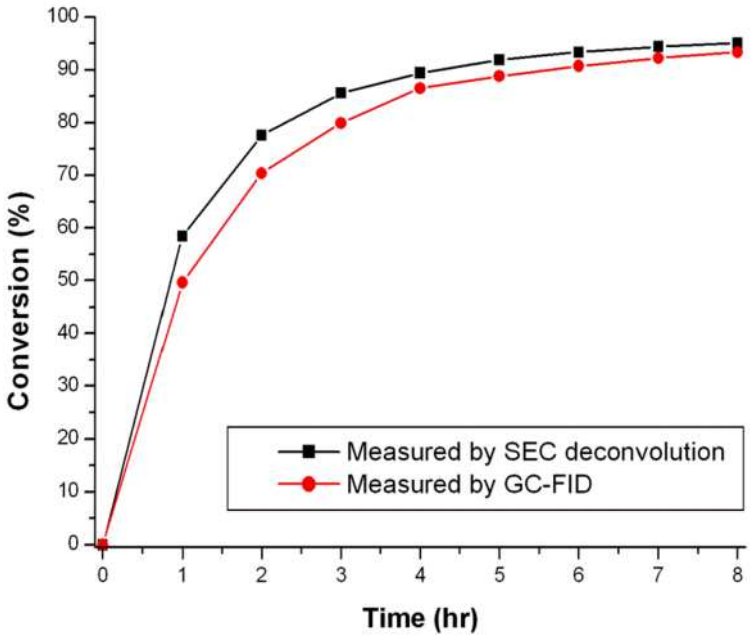

Figure 2.6: GC-FID and SEC deconvolution measured conversions for EGDMA homopolymer A

Although crosslinking can be avoided by the use of high levels of CoBF and/or termination of the polymerisation prior to gelation, care has to be taken to avoid post-polymerisation crosslinking of the vinyl groups. This manifests itself by products becoming cloudy after a few days, accompanied by the formation of a brown precipitate (Figure 2.7, left hand vial). This is consistent with oxidation of the Co(II) catalyst to a less soluble Co(III) species. Once the Co(II) concentration decreases below a certain level, crosslinking occurs. Crosslinking occurs within a month of synthesis under all storage conditions, whether in solvent, neat or under nitrogen. In order to circumvent gelation a minimum of approximately 0.2% of antioxidant, butylated hydroxytoluene (BHT), was added to polymer mixtures, which prevented gelation indefinitely (Figure 2.7, third vial from the left). Use of a smaller amount of antioxidant than 0.2% delays gelation, but inevitably leads to insoluble products.

Figure 2.7: EGDMA homopolymers with varying amounts of antioxidant. From left to right- no BHT, 0.03% BHT, 0.16% BHT, 3.5% BHT in 5 ml (approx 2.5 mL polymer) of polymer solution.

Matrix assisted laser desorption ionisation – time of flight (MALDI-ToF) was used to investigate the structure and end group fidelity of polymer **A**. In many cases MALDI-ToF can be used as a further technique for obtaining quantitative molecular weight information.[231-233] However, in the case of CCTP, quantitative information on molecular weight cannot be obtained *via* MALDI-ToF due to the broad PDi's encountered in both linear and more particularly branched polymer synthesis. MALDI-ToF is susceptible to high molecular weight discrimination, as lower mass products have a higher propensity to be detected than higher mass species.[234-236] Although the use of MALDI-ToF for molecular weight determination is limited, a great deal of structural information can still be obtained.

Initiation of polymers formed during CCTP can occur *via* two mechanisms; one being traditional free radical initiation by the azo initiator radical, in this case V-601 (Figure 2.8 (Left)), and the second *via* initiation *via* cobalt(III) hydride, [Co(III)-H], (Figure 2.8 (Right)).[157, 184, 237]

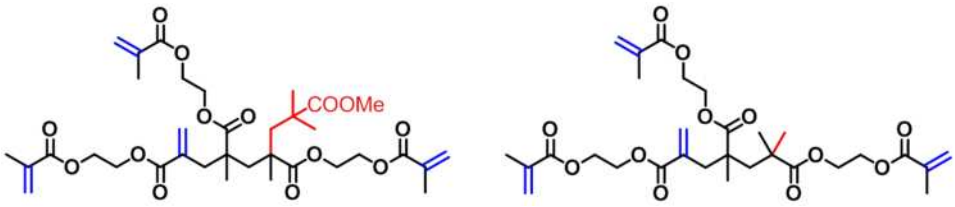

Figure 2.8: (left) Azo initiated (V-601) EGDMA trimer, m/z 594.3 (right) cobalt(III) hydride initiated EGDMA, m/z 668.3

The major peak series observed in MALDI-ToF for polymerisation **A** is that of sodiated [Co(III)-H] initiated chains, indicating the majority of chains are initiated *via* a chain transfer mechanism. A peak separation of 198 Daltons is observed for the major peak series, the repeat unit of EGDMA (Figure 2.9). V-601 initiated chains form a minor peak

series (Figure 2.10), which has a relative intensity of approximately 5% compared to the major peak series. Masses of the major peak series and V-601 initiated peak series denotes the majority of species observed in MALDI-ToF possess n+1 vinyl groups, where n is the DP_n of the chain.

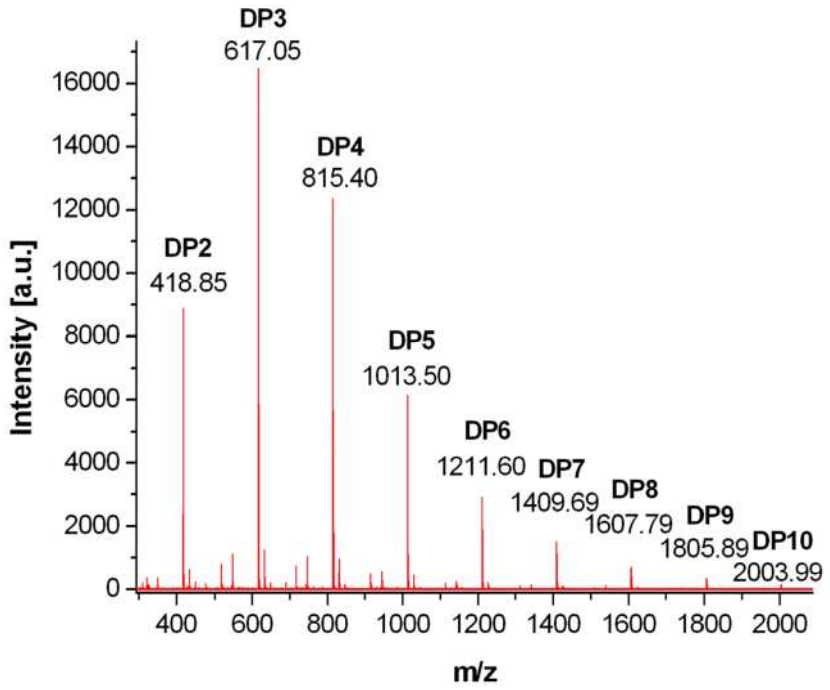

Figure 2.9: MALDI-ToF spectrum of EGDMA homopolymerisation A. Main peak distribution corresponding to sodiated [Co(III)-H] initiated EGDMA chains, 198 Dalton separation

DP	Theoretical m/z	Measured m/z
2	419.26	418.85
3	617.25	617.05
4	815.34	815.40
5	1013.43	1013.50
6	1211.52	1211.60
7	1409.61	1409.69
8	1607.70	1607.79
9	1805.79	1805.89
10	2003.88	2003.99

Table 2.2: Theoretical and measured m/z values for major peak series in the homopolymerisation of EGDMA (A) MALDI-ToF spectrum shown in Figure 2.9. Example DP3 structures for Co(III)-H and V-601 initiated poly-EGDMA given in Figure 2.8

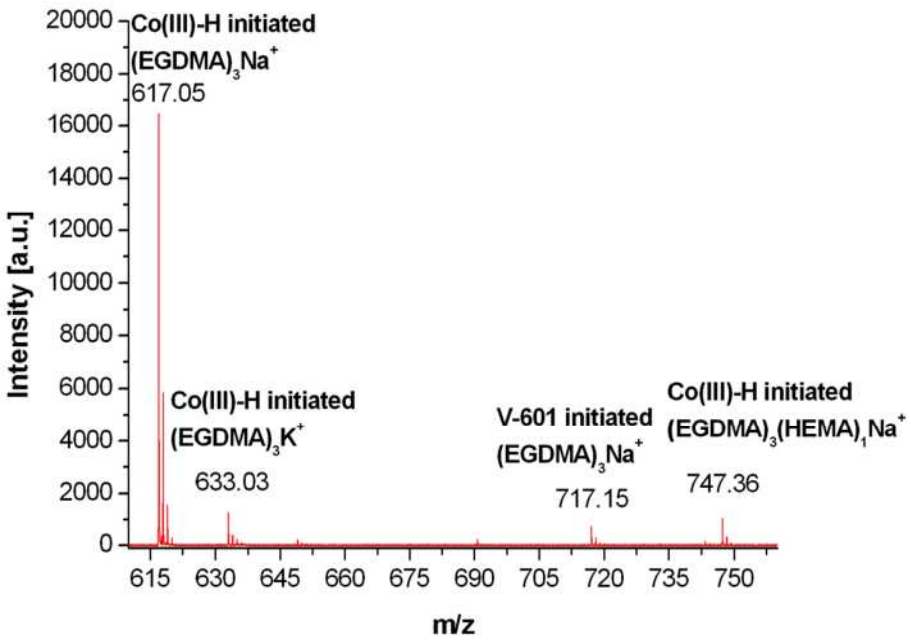

Figure 2.10: MALDI-ToF spectrum of EGDMA homopolymer A, trimer region. Trimer structures shown in Figure 2.8

A minor series of peaks is also observed corresponding to copolymerisation of EGDMA with a secondary monomer impurity, whereby low levels of hydroxyethyl methacrylate (HEMA) are incorporated into the product (Figure 2.10). This impurity, if present in large quantities, would reduce branching and the level of vinyl groups within the polymer significantly, but in this case only low levels are observed, with incorporation of one HEMA unit per chain, in a minor peak series.

^{1}H NMR also confirms the formation of EGDMA homopolymer, as described in literature,[124] with retention of a high level of vinyl groups, both internal and external; characterised by three peaks observed at 5.59, 6.12 and 6.24 ppm (Figure 2.11).

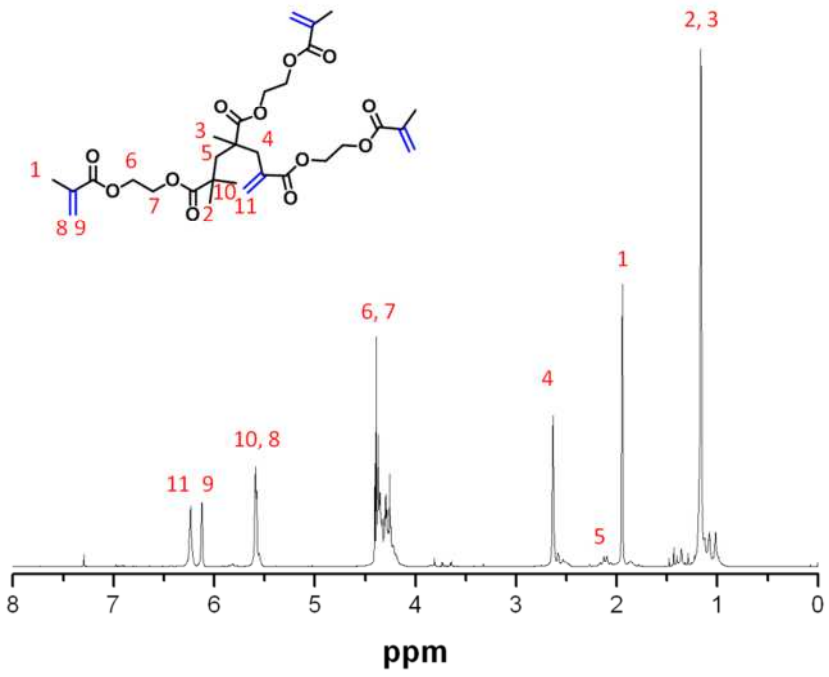

Figure 2.11: ^{1}H NMR of EGDMA homopolymer A in $CDCl_3$, volatiles removed in vacuo

2.2.2 *Effect of Monomer Concentration on the Homopolymerisation of EGDMA*

An investigation was carried out in order to determine the effect of monomer concentration on the homopolymerisation of EGDMA by CCTP. A series of polymerisations were conducted using the same conditions outlined by Guan,[124] with solvent to monomer volume as a variable. All reactions were left for 26 hours, providing gelation had not occurred prior to this. Conversion and conventional SEC results are given in Table 2.3.

Name	Monomer/Solvent (by volume)	M_n g.mol^{-1} (10 hr)	M_w g.mol^{-1} (10 hr)	PDi (10 hr)	Conversion % (10 hr)	End State of Polymer (26 hr)
B	1 : 0	N/A	N/A	N/A	N/A	Gel
C	1 : 0.33	2300	20800	9.0	93.4	Gel
D	1 : 0.5	2100	13800	6.7	96.0	Gel
E	1 : 1	2000	9700	5.0	96.6	Liquid
F	1 : 2	1800	6500	3.6	96.9	Liquid
G	1 : 3	1100	2500	2.2	96.0	Liquid

Table 2.3: Homopolymerisations of EGDMA – effect of monomer concentration on polymerisation. Molecular weights obtained from conventional SEC, conversions obtained from GC-FID

A pronounced effect of varying the monomer concentration was observed in the M_w and PDi of the polymers (Figure 2.12 (left and right)). As the volume of solvent was decreased, a rapid increase in M_w and PDi was observed; hence the onset of gelation occurs prematurely in cases of high monomer concentration (Figure 2.12 (left)). This leads to the formation of more highly branched polymers at an earlier stage in the polymerisation, leading to an increased propensity to form gel networks. As monomer volume decreases, the gradient of both M_w and PDi plots are reduced, indicating an increasing level of control over the polymerisation, which occurs without the addition of higher levels of CoBF.

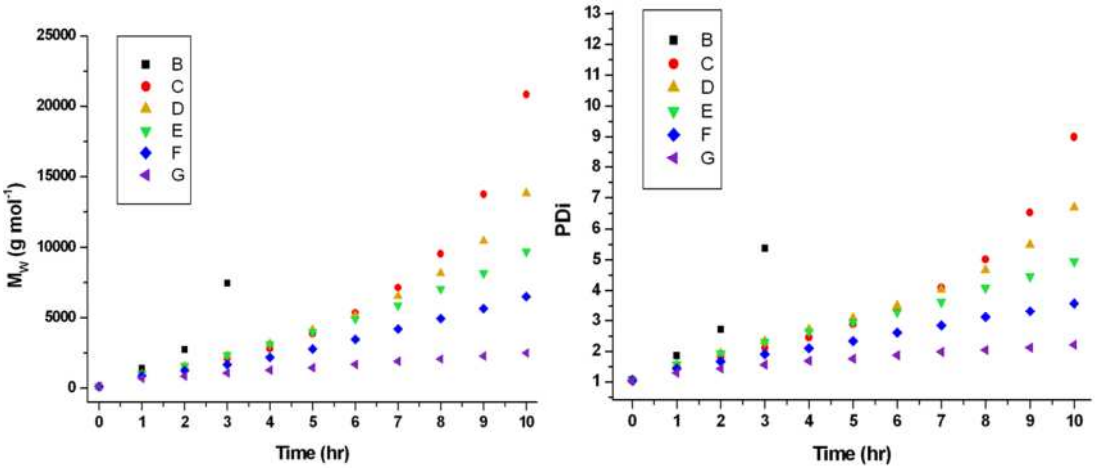

Figure 2.12: (left) Effect of monomer concentration on M_w measured *via* conventional SEC for EGDMA homopolymerisations B-G. (right) Effect of monomer concentration on PDi, measured by conventional SEC for EGDMA homopolymerisation B-G

Once conversion of the polymerisation exceeds 80% a rapid increase in M_w is seen for polymers **B**-**G** (Figure 2.13), with the severity of this increase being concentration dependent. At high monomer concentrations the severity of this increase is high, with the converse being true for low monomer concentrations; further demonstrating that decreasing monomer concentration leads to an increase in the level of control in the polymerisation.

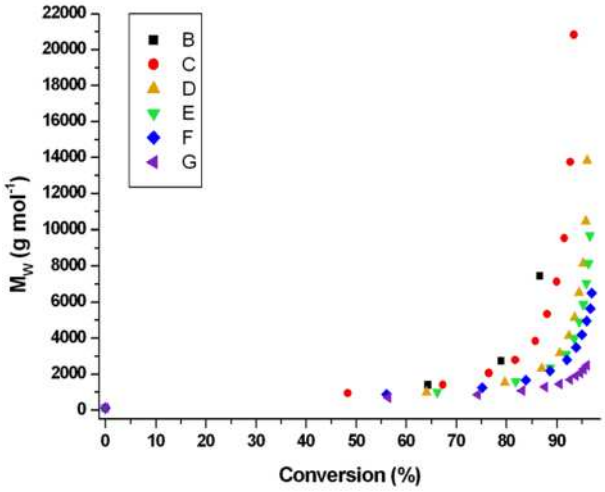

Figure 2.13: Conversion *vs.* Mw plot for EGDMA homopolymerisations B-G

Variation of the solvent concentration provides a further way to elicit control over the final molecular weight and PDi of the polymer. High molecular weights can be targeted through this method, using low solvent concentrations or carrying out the polymerisation in bulk, albeit at the cost of broadening the PDi. Conversely additional control over the molecular weight and PDi can be achieved by use of low monomer concentrations, although this enables a higher level of control over the polymerisation it is not without its disadvantages, as molecular weights obtained are low, meaning the product will contain a higher proportion of linear or lightly branched chains and the likelihood of internal cyclisation reactions increases; hence by carrying out the polymerisations at 50% volume, a balance between high conversion and control of molecular weights and PDi can be achieved, whilst reducing the probability of internal cyclisation.

2.2.3 Effect of Decreasing CoBF Concentration on the Homopolymerisation of EGDMA

Name	Ratio of CoBF to monomer (mol%)	M_n ($g.mol^{-1}$)	M_w ($g.mol^{-1}$)	PDi	Conversion (%)	Duration (hr)
A	$3.8x10^{-4}$	1800	6200	3.5	93	8
H	$3.0x10^{-4}$	1600	6900	4.4	91	6
I	$2.3x10^{-4}$	1600	11800	7.4	88	4

Table 2.4: Effect of changing CoBF concentration on molecular weights and conversion for EGDMA homopolymerisations. SEC values obtained from universal calibration

Each monomer addition provides a further point from which branching can occur, therefore the likelihood of branching increases with M_w. CoBF concentrations of $3.0x10^{-4}$ (**H**), $2.3x10^{-4}$ (**I**), $1.5x10^{-4}$ and $7.5x10^{-5}$ mol% CoBF relative to monomer were attempted in order to increase the molecular weights of resulting polymers, to circumvent gelation early termination of polymerisation was conducted (Table 2.4). Attempts to synthesise polymers using $1.5x10^{-4}$ and $7.5x10^{-5}$ mol% CoBF led to gelation within one hour, hence, too great a reduction in CoBF concentration provokes the formation of insoluble crosslinked networks.

At higher concentrations of CoBF ($3.8x10^{-4}$ (**A**) and $3.0x10^{-4}$ (**H**) mol% CoBF) the M_w and PDi increased in a linear fashion, whereas using $2.3x10^{-4}$ (**I**) mol% CoBF, M_w and PDi displayed a rapid increase after 2 hours, indicating a lower level of control over the polymerisation (Figure 2.14). This rapid increase in both M_w and PDi is indicative of the early stages of crosslinking; early termination of the polymerisation avoids crosslinking and insolubility of products, but ultimately too great a reduction in the concentration of CoBF leads to a loss of control and inevitable gelation of products.

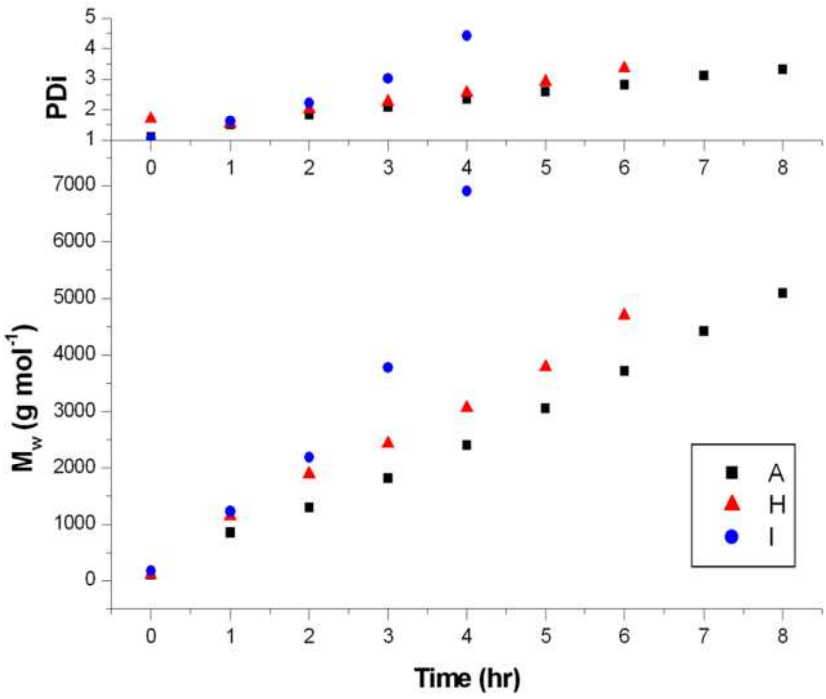

Figure 2.14: Effect of decreasing CoBF concentration on M_w and PDi evolution for EGDMA homopolymerisations A (3.8×10^{-4} mol% CoBF), H (3.0×10^{-4} mol% CoBF) and I (2.3×10^{-4} mol% CoBF), obtained by conventional SEC

Despite the increase in both M_w and PDi observed for **I**, on decreasing CoBF concentration, no significant effect is seen on comparison of the conversions for polymers **A**, **H** and **I** (Figure 2.15). This result is not unexpected, as CoBF concentration should have no effect on the conversion, if acting solely as a chain transfer agent.

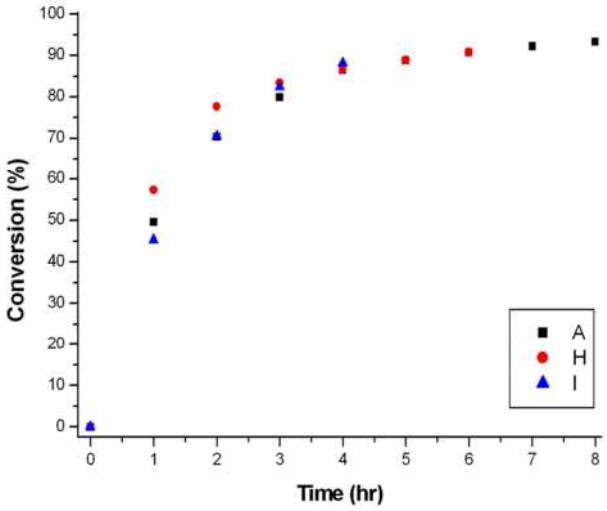

Figure 2.15: Effect of decreasing CoBF concentration on conversion measured by GC-FID of EGDMA homopolymerisations A (3.8×10^{-4} mol% CoBF), H (3.0×10^{-4} mol% CoBF) and I (2.3×10^{-4} mol% CoBF)

MALDI-ToF spectra for **H** and **I** were obtained for structural comparison to **A**. All EGDMA homopolymers possessed the same peak masses, at the same separations. The relative abundances of the most intense peak of the isotopic distribution were compared, to give an indication of the ratio of the products to one another (Table 2.5).

Polymer	Theoretical m/z	Measured m/z	Species	Relative intensity
A	617.25	617.05	[Co(III)-H] initiated $(EGDMA)_3Na^+$	100
	633.23	633.03	[Co(III)-H] initiated $(EGDMA)_3K^+$	8
	717.30	717.15	V-601 initiated $(EGDMA)_3\ Na^+$	5
	747.31	747.36	[Co(III)-H] initiated $(EGDMA)_3(HEMA)_1Na^+$	6
H	617.25	617.09	[Co(III)-H] initiated $(EGDMA)_3Na^+$	100
	633.23	633.08	[Co(III)-H] initiated $(EGDMA)_3K^+$	14
	717.30	717.19	V-601 initiated $(EGDMA)_3\ Na^+$	3
	747.31	747.41	[Co(III)-H] initiated $(EGDMA)_3(HEMA)_1Na^+$	4
I	617.25	617.07	[Co(III)-H] initiated $(EGDMA)_3Na^+$	100
	633.23	633.05	[Co(III)-H] initiated $(EGDMA)_3K^+$	14
	717.30	717.16	V-601 initiated $(EGDMA)_3\ Na^+$	4
	747.31	747.37	[Co(III)-H] initiated $(EGDMA)_3(HEMA)_1Na^+$	6

Table 2.5: MALDI-ToF product abundance data for EGDMA homopolymerisations A ($3.8x10^{-4}$ mol% CoBF), H ($3.0x10^{-4}$ mol% CoBF) and I ($2.3x10^{-4}$ mol% CoBF). Example trimer structures of poly-EGDMA initiated by both Co(III)-H and V-601 given in Figure 2.8

From the data in Table 2.5, comparisons can be made between the relative amounts of V-601 initiated EGDMA and HEMA containing EGDMA to the most abundant species, [Co(III)-H] initiated EGDMA. In polymers **A**, **H** and **I** similar relative abundances of V-601 initiated species to [Co(III)-H] initiated chains is observed of approximately 4%. HEMA incorporation is measured at approximately 5% compared to [Co(III)-H] initiated EGDMA in all three products, implying CoBF concentration has little or no effect on the initiation/termination reactions in the polymerisations.

2.2.4 Multidetector SEC Analysis of EGDMA Homopolymers

SEC analysis with RI and viscometry detection was employed to create a universal calibration from which Mark-Houwink plots can be generated. Comparisons of branched polymers **A**, **H** and **I** relative to linear PMMA, for the same molar mass, were obtained by use of the Mark-Houwink equation (Equation 2.3).[214, 238] Linear **PMMA's 1-3** were synthesised by CCTP, providing linear polymers of comparable molar masses to branched polymers, for the generation of Mark-Houwink and g' plots (Equation 2.6). The α values, derived from the gradient of these plots, were compared to linear **PMMA**

1, giving an indication of the degree of branching from the contraction observed in α value (Table 2.6 and Figure 2.16).

Name	M_n (g.mol^{-1})	M_w (g.mol^{-1})	PDi	*α*
PMMA 1	2000	3700	1.9	0.42
A	1800	6200	3.5	0.35
H	1600	6900	4.4	0.27
I	1600	11800	7.4	0.21

Table 2.6: M_w, PDi and α values for branched polymers A (3.8x10^{-4} mol% CoBF), H (3.0x10^{-4} mol% CoBF), I (2.3x10^{-4} mol% CoBF) and comparable linear PMMA 1 (2.8x10^{-6} mol% CoBF) for the same molar mass range

It should be noted however, that, on conducting an investigation of the Mark Houwink parameter α for linear PMMA's discrepancies away from those expected in the α values were observed. According to theory and text books a linear polymer fully solvated in a good solvent should have an α value of ≥ 0.5, however, linear **PMMA 1** gave a measured α value = 0.42. Previous literature exists on the applicability of universal calibration and the Mark-Houwink relationship to polymers of low molecular weight, which describes a deviation from the linear relationship between log[η] and log M for low molecular weights (<10000).[238-241] Several methods have arisen to correct the deviations observed for low molecular weight including the Benoit-Dondos equation (Equation 2.7)[239], the Sadron-Rempp equation (Equation 2.8)[241, 242] and the Stockmayer-Fixman equation (Equation 2.9),[243] however, the above equations require the use of constants, which relate to the interaction of the polymer with a specific solvent. Very few of these constants are available in the literature due to their polymer and solvent specificity and measurement of these is non-trivial.

$$\frac{1}{[\eta]} = -A_2 + A_1/M^{1/2}$$

Equation 2.7: Benoit-Dondos equation where A1 and A2 are constants relating to the polymer solvent system

$$[\eta] = A_1 + A_2 M^{\alpha}$$

Equation 2.8: Sadron-Rempp equation where A1 and A2 are constants relating to the polymer solvent system

$$[\eta] = K_\theta M^{1/2} + K' M$$

Equation 2.9: Stockmayer-Fixman equation where Kθ is a universal constant regardless of solvent and temperature and K' is a constant relating to the polymer solvent system

Hence, although the results calculated by universal calibration and the application of the Mark-Houwink equation displays this deviation from linearity at low molecular weights, it should still display trends in the hydrodynamic volume indicated by α, provided a linear standard of the same molar mass is employed and comparisons are made between similar molecular weight products. However, the molecular weights and α values obtained are unlikely to reflect the true molecular weight, providing relative molecular weights and α values between samples. Hence, a better understanding of branching can be achieved by use of universal calibration in comparison to conventional SEC.

Polymers **A**, **H** and **I** display lower α values in comparison to linear PMMA over the same molar mass range (Table 2.6), indicating a contraction in the hydrodynamic volume for EGDMA homopolymers in comparison to **PMMA 1**. The contraction in hydrodynamic volume becomes more significant as molecular weight increases, confirming the theory that an increase in molecular weight leads to an increase in branching.

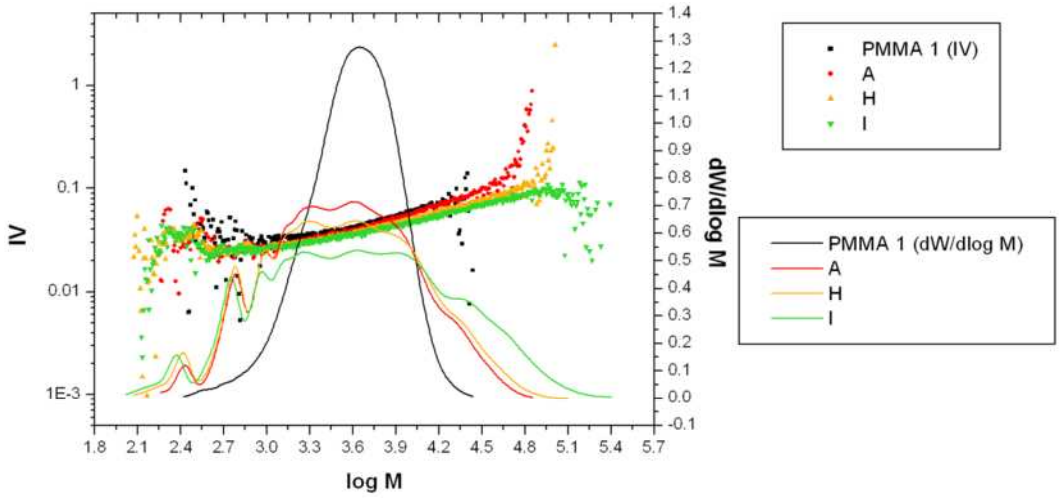

Figure 2.16: Mark-Houwink plots for polymerisations A ($3.8x10^{-4}$ mol% CoBF), H ($3.0x10^{-4}$ mol% CoBF) and I ($2.3x10^{-4}$ mol% CoBF) (EGDMA homopolymerisations) compared to linear PMMA 1

IV's for EGDMA homopolymers are also marginally reduced in comparison to linear **PMMA 1** throughout the entire molecular weight distribution (Figure 2.16). A greater reduction in IV is observed as branching increases throughout the series, with constant gradients obtained throughout each polymers IV plot, indicating that branching remains consistent as molecular weight increases.

The radius of gyration is largely responsible for controlling the IV, with *g'* (Equation 2.6) being utilised as a widely accepted qualitative indicator of the degree of chain branching for polymers of equal molar mass.[218] The *g'* of two linear polymers should yield a constant value of one, as with increasing molecular weight there is no change in the IV between the two polymers. A reduction in the *g'* for polymers **A**, **H** and **I** is observed confirming the branched nature of these materials, although molecular weights are low meaning the reduction observed is marginal. A decrease in the gradient of g' is also observed signifying that branching increases with molecular weight. This reduction in the gradient of g' becomes more pronounced as branching increases throughout the series, denoting the formation of polymers of increasing branching as CoBF concentration is reduced (Figure 2.17).

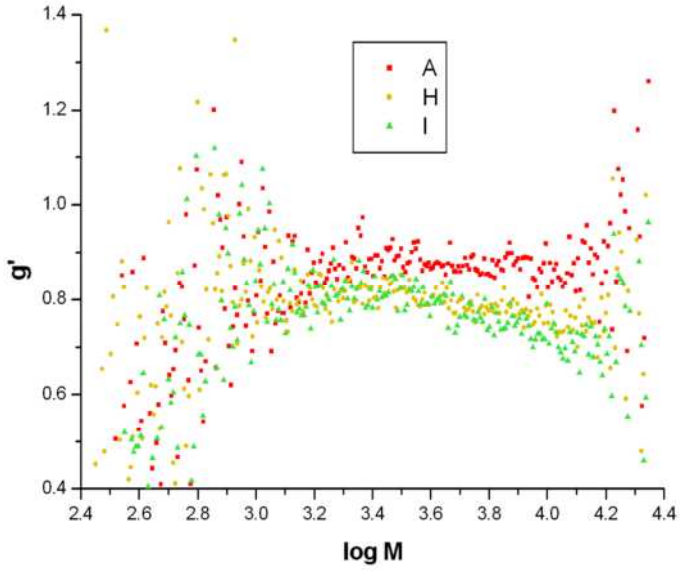

Figure 2.17: g' plots for EGDMA homopolymerisations A (3.8x10^{-4} mol% CoBF), H (3.0x10^{-4} mol% CoBF) and I (2.3x10^{-4} mol% CoBF). IV comparison to linear PMMA 1 over the same molar mass

2.2.5 Tailoring the Degree of Branching by Copolymerisation - Decreasing Branching

Monomer variation or introduction of comonomers, in CCT polymerisations is a tool for tailoring the level of branching of the resulting polymers. Reduction in the degree of branching was achieved by introduction of monofunctional comonomer, MMA, to the EGDMA polymerisation (**J**-**P**, Table 2.7). These polymerisations contained low levels of EGDMA, between 10 and 33%, in the synthesis of lightly branched polymers, similar in EGDMA content to those already quoted in literature.[120] By introduction of a branch

diluting monomer higher molecular weights can be accessed using dramatically lower levels of CoBF in comparison to EGDMA homopolymerisations.

Name	Monomer	Monomer Ratios (mol%)	CoBF: monomer (mol%)	M_n ($g.mol^{-1}$)	M_w ($g.mol^{-1}$)	PDi	Conv. (%)	Duration (hr)
J	EGDMA/ MMA	10/90	$1.6x10^{-5}$	1500	4000	2.7	91	24
K	EGDMA/ MMA	10/90	$1.2x10^{-5}$	1900	6100	3.2	95	24
L	EGDMA/ MMA	10/90	$7.7x10^{-6}$	2700	11800	4.4	95	24
M	EGDMA/ MMA	25/75	$2.7x10^{-5}$	1300	4400	3.5	96	24
N	EGDMA/ MMA	25/75	$2.1x10^{-5}$	1400	8800	6.1	97	24
O	EGDMA/ MMA	33/67	$2.7x10^{-5}$	3000	14600	4.8	96	24
P	EGDMA/ MMA	33/67	$2.1x10^{-5}$	5700	69000	12.2	96	24

Table 2.7: CCTP copolymerisations of EGDMA and MMA in the synthesis of lightly branched copolymers of varying molecular weight and EGDMA incorporation. Molecular weights obtained *via* SEC universal calibration. Conversions obtained by GC-FID

Polymerisations **J**-**K** contain low levels of EGDMA of 10 mol%, using decreasing levels of CoBF in order to access higher molecular weight products. SEC comparisons for copolymerisations **J**, **K** and **L** show controlled increases of both molecular weight and PDi, indicating a good level of control in the polymerisation (Figure 2.18). Decreasing the CoBF concentration leads to the generation of higher molecular weight chains whereby branching is increased; a good indication of this is the increase in final PDi seen throughout this series, with the lowest CoBF concentration producing the highest M_w and the highest PDi.

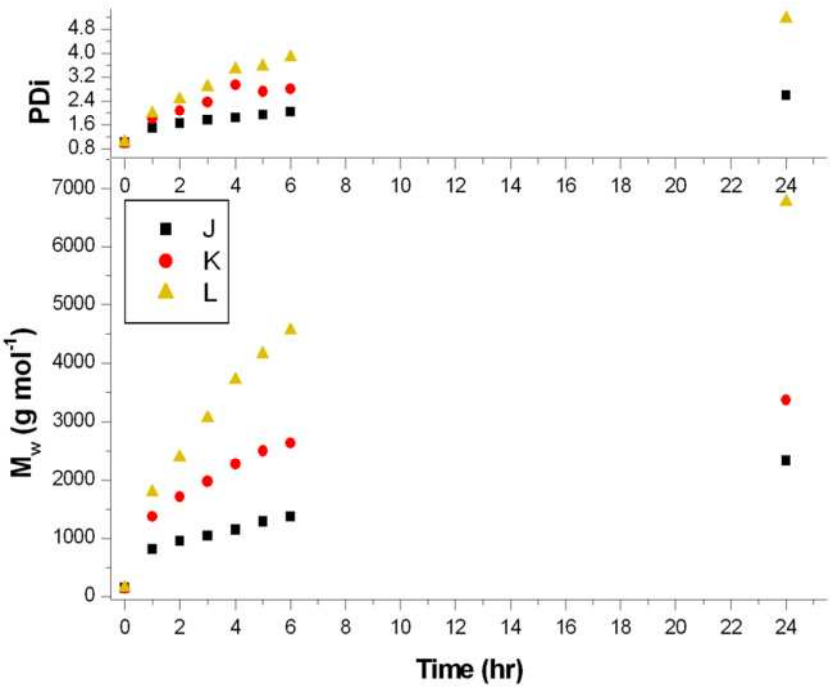

Figure 2.18: M_w and PDi data for EGDMA-MMA copolymerisations J (10/90 mol%, 1.6x10^{-5} mol% CoBF), K (10/90 mol%, 1.2x10^{-5} mol% CoBF) and L (10/90 mol%, 7.7x10^{-6} mol% CoBF) obtained from conventional SEC

In cases of copolymerisations, conversions of each monomer are monitored independently by GC-FID, providing a more detailed indication of polymer composition through rate of conversion (Figure 2.19).

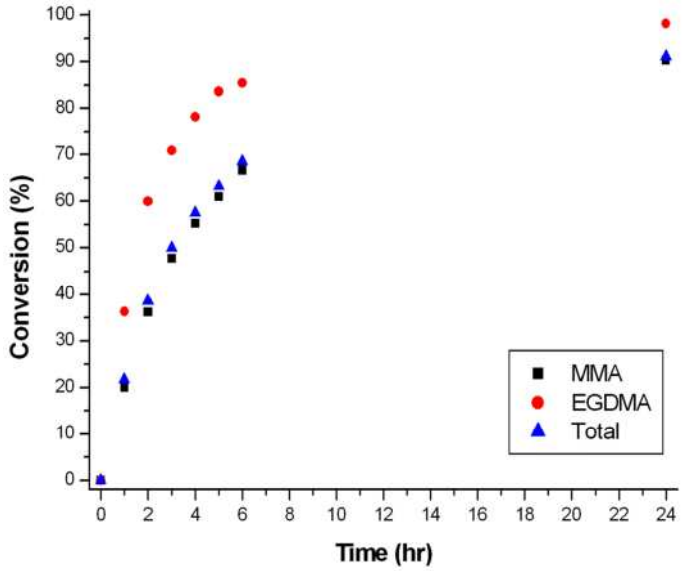

Figure 2.19: Individual and total monomer conversion measured by GC-FID monitoring of EGDMA-MMA copolymerisation J (10/90 mol%, 1.6x10^{-5} mol% CoBF)

GC-FID showed that in all copolymerisations of EGDMA and MMA the conversion of EGDMA occurs at a faster rate; a typical plot of this is shown in Figure 2.19. This effect would lead to the formation of a star like polymer, where the core is rich in EGDMA units and the periphery more MMA based. Total conversions remain fairly consistent throughout the copolymer series reaching above 90% in all EGDMA-MMA copolymers (Table 2.7).

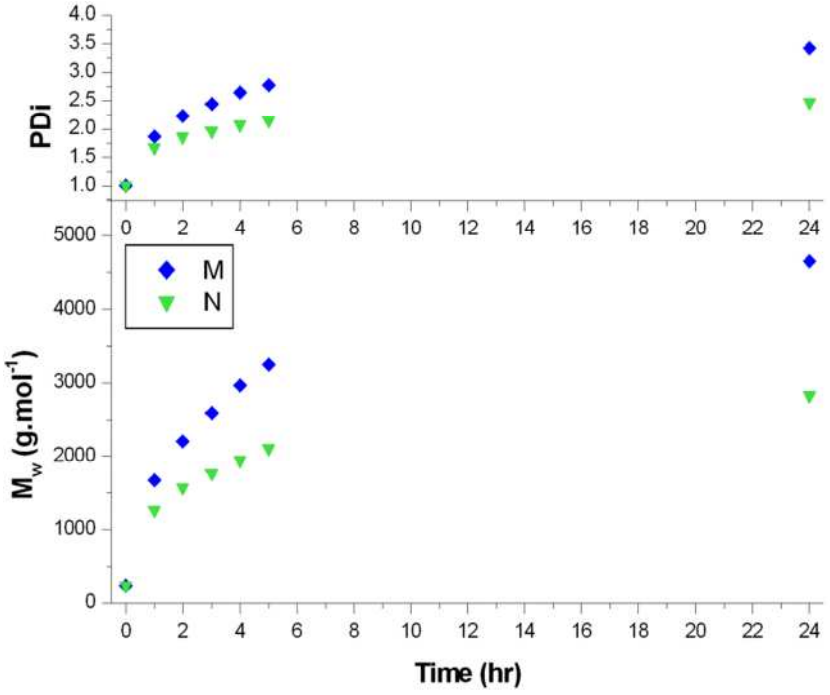

Figure 2.20: SEC M_w and PDi data for EGDMA/MMA copolymerisations M (25/75 mol%, 2.7x10^{-5} mol% CoBF) and N (25/75 mol%, 2.1x10^{-5} mol% CoBF)

At 25 mol% EGDMA both M_w and PDi remain consistent, increasing steadily throughout the polymerisation (Figure 2.20). Again, decreasing the level of CoBF in the system increases the M_w and PDi, indicative of a higher level of branching. The same trend is observed at 33 mol% EGDMA incorporation (Figure 2.21) with an increased final M_w and PDi observed by conventional SEC.

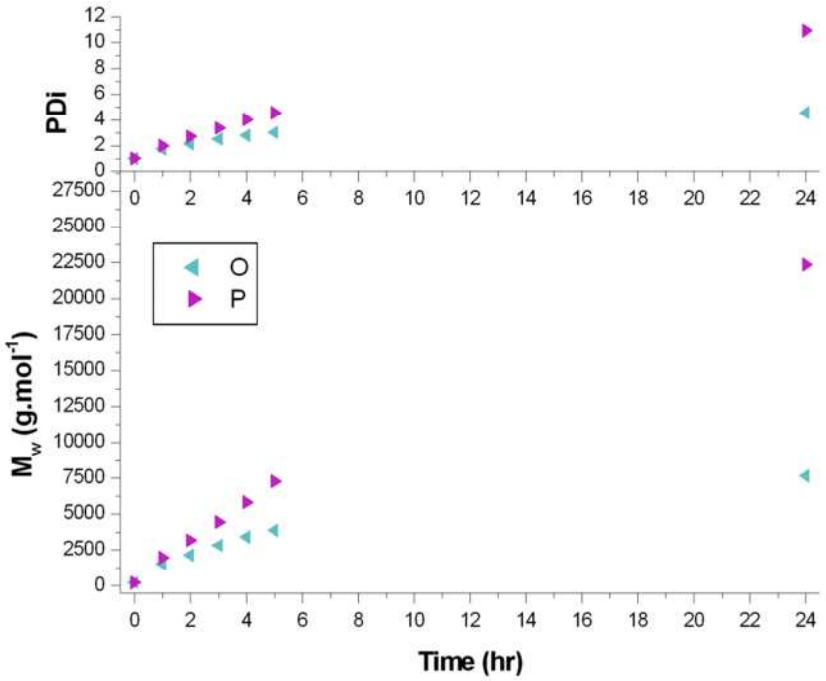

Figure 2.21: SEC M_w and PDi data for EGDMA/MMA copolymerisations O (33/67 mol%, 2.7x10^{-5} mol% CoBF) and P (33/67 mol%, 2.1x10^{-5} mol% CoBF)

Analysis of these copolymers by MALDI-ToF becomes difficult, due to overlapping peak distributions caused by the similarity in mass for polymers of increasing EGDMA and MMA units. Isotope patterns can be investigated to probe some of the structures arising from these copolymerisations, from this it can be seen that EGDMA MMA copolymers **J**-**P** all possess a common major peak series of [Co(III)-H] initiated copolymer, of increasing molecular weight (Figure 2.22). In the cases of low EGDMA content of 10 mol%, there is very little discernible formation of EGDMA homopolymers, but MMA homopolymers are present as minor peaks. Increasing the EGDMA content leads to the formation of low levels of EGDMA homopolymer, but decreases the amount of MMA homopolymer observed. Due to high molecular weight discrimination in the MALDI-ToF, indication of the branching in these products becomes difficult as high molecular weight peaks, where branching is likely to be higher, are excluded from the spectra.

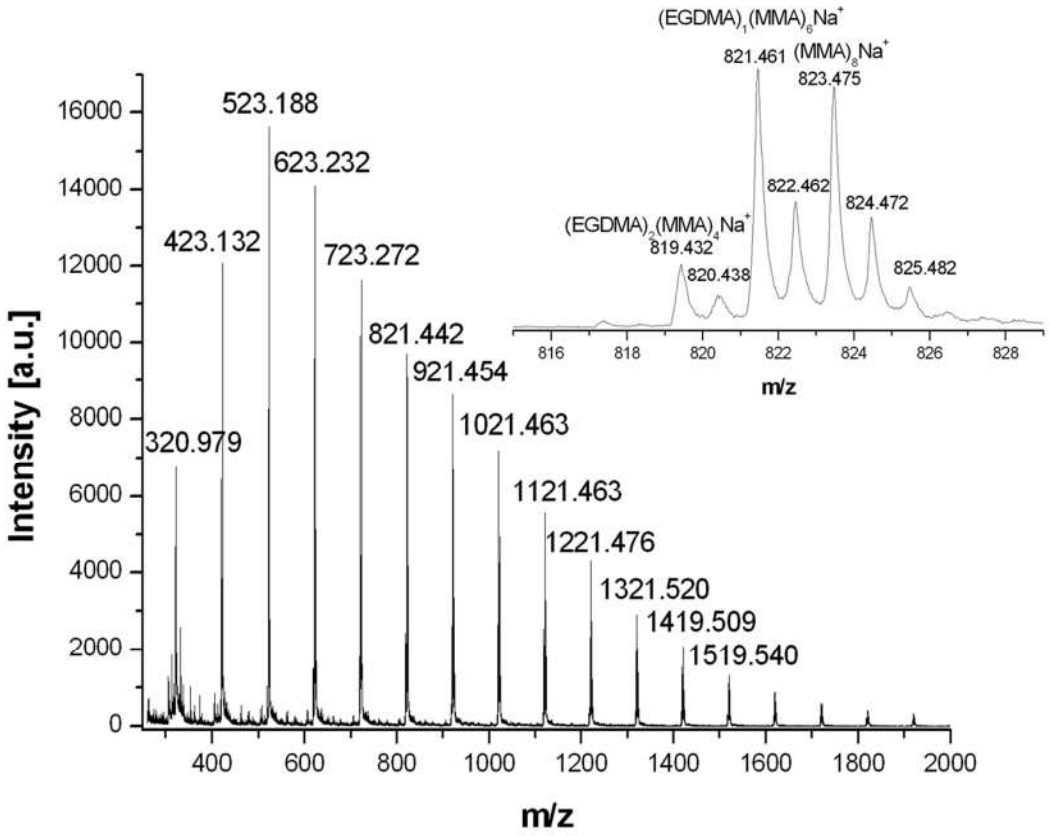

Figure 2.22: MALDI-ToF Spectrum of EGDMA/MMA copolymer J (10/90 mol%, 1.6×10^{-5} mol% CoBF) with inset of m/z 816-828 to display overlapping peak series observable in the major peak series

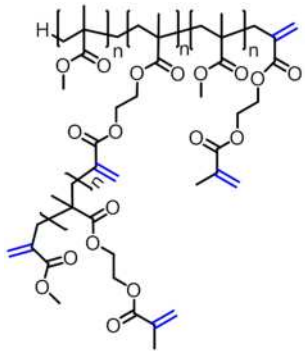

Figure 2.23: Example structure of an EGDMA MMA copolymer, $(EGDMA)_3(MMA)_3$ if n=1

DP	Theoretical m/z	Measured m/z
$(MMA)_4$	423.19	423.13
$(MMA)_5$	523.25	523.18
$(MMA)_6$	623.30	623.23
$(MMA)_7$	723.35	723.27
$(EGDMA)_1(MMA)_6$	821.39	821.44
$(EGDMA)_1(MMA)_7$	921.44	921.45
$(EGDMA)_1(MMA)_8$	1021.49	1021.46
$(EGDMA)_1(MMA)_9$	1121.55	1121.47
$(EGDMA)_1(MMA)_{10}$	1221.60	1221.47
$(EGDMA)_1(MMA)_{11}$	1321.65	1321.52
$(EGDMA)_1(MMA)_{12}$	1421.70	1419.50
$(EGDMA)_2(MMA)_{11}$	1519.74	1519.54
$(EGDMA)_2(MMA)_{12}$	1619.79	1619.54
$(EGDMA)_2(MMA)_{13}$	1719.84	1719.60

Table 2.8: Theoretical and measured m/z values for major peak series in the copolymerisation of EGDMA and MMA (J) MALDI-ToF spectrum shown in Figure 2.22. An example structure is given in Figure 2.23

2.2.6 Multidetector SEC Analysis of EGDMA-MMA Copolymers

Universal calibration was employed to investigate the branching of EGDMA-MMA copolymers **J**-**P**. Mark-Houwink plots of polymers **J**-**P** revealed reduced α values in comparison to α values of linear PMMA's over the same molar mass. A reduction in IV was observed in all cases compared to linear PMMA (Table 2.9, Figure 2.24, Figure 2.25 and Figure 2.26).

Name	M_n ($g.mol^{-1}$)	M_w ($g.mol^{-1}$)	PDi	α
PMMA 1	2000	3700	1.9	0.44
J	1500	4000	2.7	0.32
K	1900	6100	3.2	0.32
M	1300	4400	3.5	0.26
PMMA 2	7100	10300	1.4	0.46
L	2700	11800	4.4	0.33
N	1400	8800	6.1	0.31
PMMA 3	8100	14500	1.8	0.55
O	3000	14600	4.8	0.35
P	5700	69400	12.2	0.34

Table 2.9: Molecular weights, PDi and α values for branched polymers J-P and comparable linear PMMA's for the same molar mass range. J (EGDMA/MMA copolymer, 10/90 mol%, $1.6x10^{-5}$ mol% CoBF), K (EGDMA/MMA copolymer, 10/90 mol%, $1.2x10^{-5}$ mol% CoBF) and M (EGDMA/MMA copolymer, 25/75 mol%, $2.7x10^{-5}$ mol% CoBF), L (EGDMA/MMA copolymer, 10/90 mol%, $7.7x10^{-6}$ mol% CoBF), N (EGDMA/MMA copolymer, 25/75 mol%, $2.1x10^{-5}$ mol% CoBF), O (EGDMA/MMA copolymer, 33/67 mol%, $2.7x10^{-5}$ mol% CoBF) and P (EGDMA/MMA copolymer, 33/67 mol%, $2.1x10^{-5}$ mol% CoBF)

Again on investigation of the α values for linear PMMA's synthesised, low values are obtained which deviate from the expected values of ≥0.5. The values obtained also appear molecular weight dependant, with increasing α values with increasing molecular weight (0.44<0.46<0.55 respectively, Table 2.9). The deviation from linearity of the log[η] vs. logM plots is also highlighted for these low molecular weights as previously discussed in the literature.[238, 239, 241] Therefore, molecular weights and α values are unlikely to be a reflection of the true molecular weight in this case, but should provide relative values between polymer samples of similar molecular weights. However, as linear **PMMA 3** is higher in molecular weight, it's α value lies within the theoretical values for a linear polymer in a good solvent, hence the majority of its Mark-Houwink plot remains linear and the molecular weight averages are likely to be accurate in this case. This deviation from linearity is only observed for the lower molecular weight polymers synthesised.

Mark-Houwink plots for polymers **J**, **K** and **M** denote an increase in branching throughout the series, displaying decreased α values in comparison to linear **PMMA 1** of the same molar mass (Figure 2.24). Polymers **J** and **K** employ the same level of EGDMA, 10%, with **K** being of marginally higher molecular weight due to a reduced level of CoBF. Although a significant decrease in α is observed on comparison of both **J** and **K** to **PMMA 1**, no significant decrease is seen between the two, suggesting they possess similar levels of branching. Polymer **M** employs a higher level of EGDMA, 20%, with a higher level of CoBF to **K**. A significant reduction in α is observed for **M** on comparison to both **PMMA 1** and **J** and **K**, indicative of a higher level of branching, which is expected due to the increased level of EGDMA.

The IV's of these copolymers are reduced throughout the distribution in comparison to **PMMA 1**, all displaying similar IV's. Although the gradient of IV plots for polymers **J**, **K** and **M** are not constant throughout the molecular weight distribution, which would usually denote inconsistent branching within the product, in this case it may be an artefact of analysis of low molecular weight polymers, as non-linear behaviour is observed in linear **PMMA 1** (Figure 2.24). However, for a copolymer of EGDMA and MMA using such low amounts of EGDMA, inconsistencies in branching is likely.

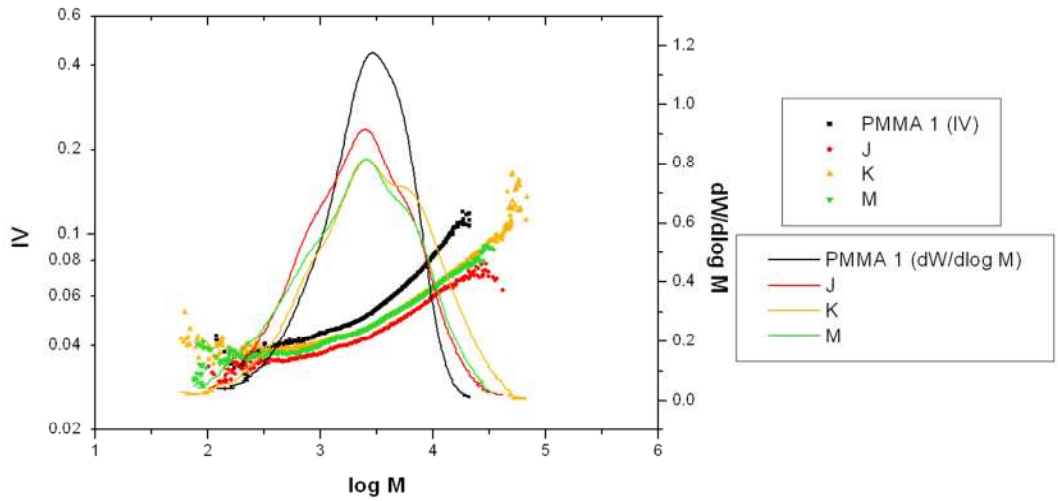

Figure 2.24: Mark-Houwink plots for polymerisations J, K and M (EGDMA/MMA copolymerisations- J: 10/90 mol% monomers, $1.6x10^{-5}$ mol% CoBF, K: 10/90 mol% monomers, $1.2x10^{-5}$ mol% CoBF, M: 25/75 mol% monomers, $2.7x10^{-5}$ mol% CoBF) compared to linear PMMA 1

A reduction in α is observed between **L** to **N** illustrating the higher level of branching achieved for **N** on use of a higher EGDMA content, 10 and 25 mol% respectively, despite a lower CoBF concentration employed for **L**, $7.7x10^{-6}$ and $2.1x10^{-5}$ respectively, with both polymers displaying a marked decrease in α compared to linear **PMMA 2**. IV's are reduced in comparison to linear **PMMA 2** throughout the whole distribution, with polymer **N** possessing a greatly reduced IV (Figure 2.25). The variation in gradient of these IV's again signifies inconsistent branching within these materials, however, **PMMA 2** also displays non-linear behaviour, albeit less prominently than at lower molar masses.

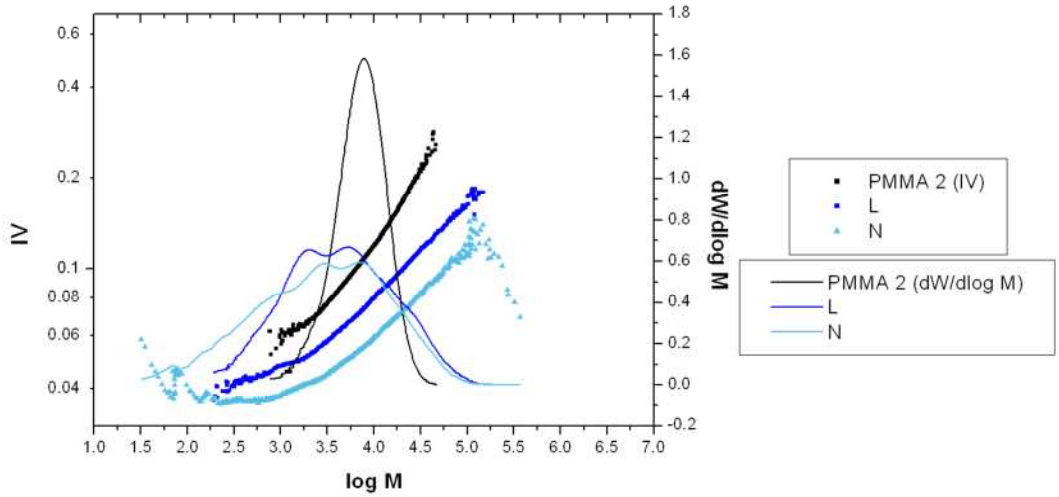

Figure 2.25: Mark-Houwink plots for polymerisations L and N (EGDMA/MMA copolymerisations- L: 10/90 mol% monomers, $7.7x10^{-6}$ mol% CoBF, N: 25/75 mol% monomers, $2.1x10^{-5}$ mol% CoBF) compared to linear PMMA 2

Copolymers **O** and **P** contain the highest level of EGDMA of 33%, with a reduced level of CoBF in **P** leading to the formation of higher molecular weights. Both copolymers **O** and **P** display reduced α values in comparison to linear **PMMA 3**, with a reduction in the α value of **P** observed on comparison to copolymer **O**, indicating a more branched structure is obtained (Figure 2.26). The IV's of both **O** and **P** are in close correlation and are markedly lower than that of **PMMA 3** throughout the molecular weight distribution, although again, variation in the gradient of these plots is observed, particularly at low molecular weights. Linear **PMMA 3** displays a constant IV gradient, therefore, the non-consistent IV's observed for polymers **O** and **P** suggest the likelihood of inconsistent branching, perhaps due to the levels of MMA homopolymer or variation in the levels of EGDMA incorporation.

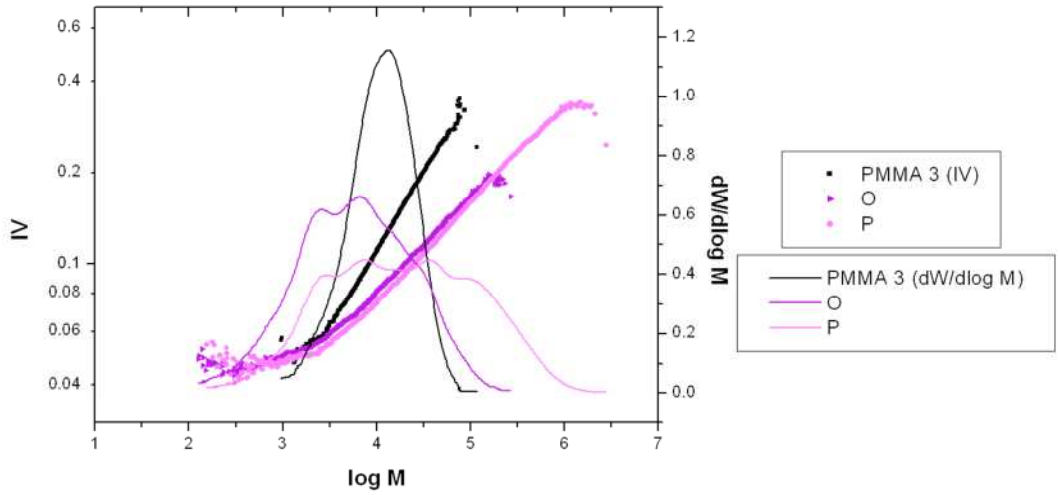

Figure 2.26: Mark-Houwink plots for polymerisations O and P (EGDMA/MMA copolymerisations- O: 33/67 mol% monomers, 2.7x10^{-5} mol% CoBF, P: 33/67 mol% monomers, 2.1x10^{-5} mol% CoBF) compared to linear PMMA 3

Comparisons of the IV's of EGDMA-MMA copolymers **J**-**P** were made to their respective linear PMMA's, for the same molar mass, and g' plots obtained (Figure 2.27). Reductions in g' for increasing molecular weight are observed in all cases, a further indication of branching in the products. Higher molecular weight polymers **O** and **P** display the most dramatic decrease in g' due to their high incorporations of EGDMA and higher molecular weights, indicating the highest levels of branching in the series (Figure 2.27 (right)).

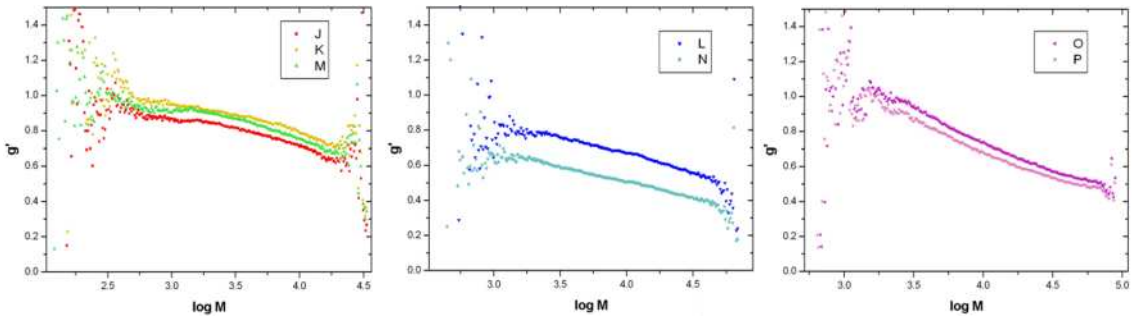

Figure 2.27: (left) g' plots generated from Mark-Houwink data for polymerisations J (EGDMA/MMA copolymer, 10/90 mol%, 1.6x10^{-5} mol% CoBF), K (EGDMA/MMA copolymer, 10/90 mol%, 1.2x10^{-5} mol% CoBF) and M (EGDMA/MMA copolymer, 25/75 mol%, 2.7x10^{-5} mol% CoBF), compared to PMMA 1 (middle) g' plot generated from Mark-Houwink data for polymerisation L (EGDMA/MMA copolymer, 10/90 mol%, 7.7x10^{-6} mol% CoBF) and N (EGDMA/MMA copolymer, 25/75 mol%, 2.1x10^{-5} mol% CoBF) compared to PMMA 2 (right) g' plots generated from Mark-Houwink data for polymerisations O (EGDMA/MMA copolymer, 33/67 mol%, 2.7x10^{-5} mol% CoBF) and P (EGDMA/MMA copolymer, 33/67 mol%, 2.1x10^{-5} mol% CoBF) compared to PMMA 3

2.2.7 Tailoring the Degree of Branching by Copolymerisation - Increasing Branching

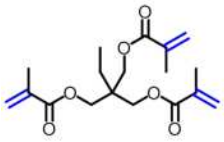

Figure 2.28: Structure of comonomer trimethylolpropane trimethacrylate

Copolymers of trimethylolpropane trimethacrylate (TMPTMA) and EGDMA were synthesised, **Q** and **R**, with an increasing level of TMPTMA content and increasing CoBF concentration. A homopolymer of TMPTMA, **S**, was also synthesised employing a high level of CoBF to prevent gelation; hence forming a range of polymers with varying degrees of branching (Table 2.10).

Name	Monomers	Monomer Ratios (mol%)	CoBF: monomer (mol%)	M_n (g.mol^{-1})	M_w (g.mol^{-1})	PDi	Conv. (%)	Duration (hr)
Q	EGDMA/ TMPTMA	80/20	4.0x10^{-4}	900	2900	3.1	76	4
R	EGDMA/ TMPTMA	67/33	5.1x10^{-4}	700	1900	2.9	73	3
S	TMPTMA	100	6.4x10^{-4}	1000	9000	9.1	78	2

Table 2.10: Effect of EGDMA copolymerisation with TMPTMA on molecular weights and conversion. SEC values obtained from universal calibration

The M_w and PDi of EGDMA-TMPTMA copolymers **Q** and **R** increase almost identically, in a controlled fashion, due to the increasing level of CoBF employed on increasing content of TMPTMA (Figure 2.29). TMPTMA homopolymer (**S**) however, displays a rapid increase in M_w and PDi, despite an increased level of CoBF, indicating a loss of control in the system, which would provoke gelation of the polymer; hence the polymerisation was subject to early termination after two hours in order to circumvent this. All polymerisations were subject to early termination in order to avoid gelation, hence lower conversions of around 80% were obtained.

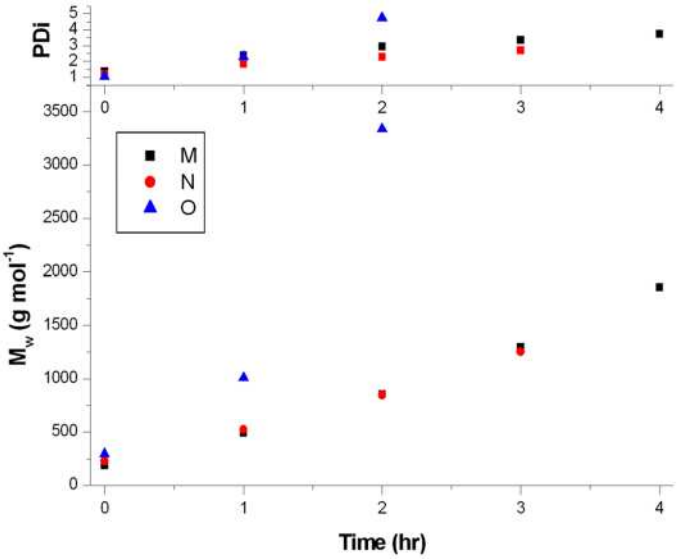

Figure 2.29: SEC Mw and PDi data for EGDMA-TMPTMA copolymers Q (80/20 mol%, $4.0x10^{-4}$ mol% CoBF) and R (67/33 mol%, $5.1x10^{-4}$ mol% CoBF) and TMPTMA homopolymerisation S ($6.4x10^{-4}$ mol% CoBF). Data obtained *via* conventional SEC

GC-FID reveals the conversion of TMPTMA in EGDMA-TMPTMA copolymers is marginally higher than that of EGDMA throughout the polymerisation; hence the polymer core is likely to possess a higher level of branching than that of the periphery (Figure 2.30).

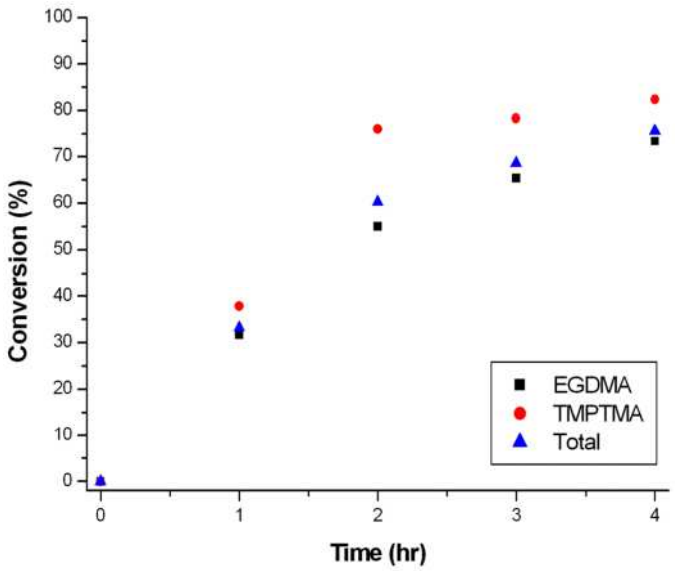

Figure 2.30: Individual monomer conversion measured by GC-FID, monitoring of EGDMA-TMPTMA copolymer Q (80/20 mol%, 4.0x10^{-4} mol% CoBF)

The structure of EGDMA-TMPTMA copolymers **Q** and **R** were probed using MALDI-ToF. Peaks series' denoting a range of EGDMA-TMPTMA copolymers are observed of varying TMPTMA content. Products containing low levels of HEMA, an impurity in EGDMA, and also low levels of an impurity found in TMPTMA, whereby one of the hydroxyl groups on the starting material 1,1,1-tris(hydroxymethyl)propane remains in the monomer, are observed. The MALDI-ToF spectrum of TMPTMA homopolymer **S** displays a major peak series indicating increasing molecular weight of TMPTMA homopolymer with a separation of 338 Daltons (Figure 2.31). Again, the single hydroxyl monomer impurity is present in this spectrum, observed as a minor peak series, peak separation 338 Daltons. MALDI-ToF confirms the majority of TMPTMA homopolymer chains possess 2n+1 vinyl groups where n is the DP_n of the chain.

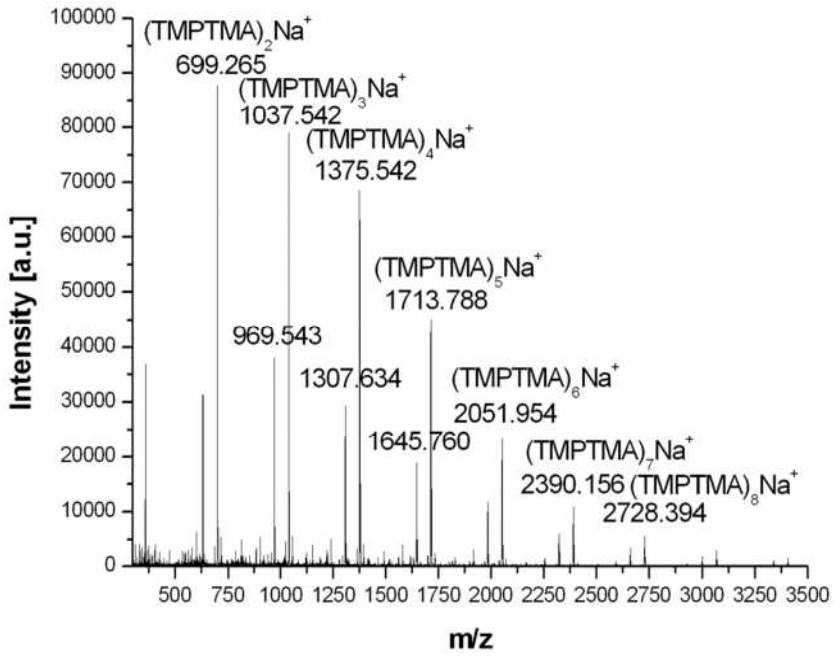

Figure 2.31: MALDI-ToF spectrum of TMPTMA homopolymer S (6.4x10^{-4} mol% CoBF)

DP	Theoretical m/z	Measured m/z
2	699.33	699.26
3	1037.50	1037.54
4	1375.68	1375.54
5	1713.85	1713.78
6	2052.02	2051.95
7	2390.19	2390.15
8	2728.37	2728.39

Table 2.11: Theoretical and measured m/z values for major peak series in the homopolymerisation of TMPTMA (S) MALDI-ToF spectrum shown in Figure 2.31

2.2.8 Multidetector SEC Analysis of EGDMA-TMPTMA Copolymers and TMPTMA Homopolymer

Universal calibration was used to obtain Mark-Houwink plots for polymerisations **Q**-**S** (Figure 2.32 and Figure 2.33), with comparisons to linear PMMA's of an equal molar mass. From the gradient of Mark-Houwink plots the hydrodynamic volume contraction factor α was obtained (Table 2.12). Again, as the molecular weight of the polymers investigated is low (<10000) the Mark-Houwink plots show a deviation from linearity. As linear **PMMA 3** and polymer **S** are higher in molecular weight this linear deviation is only observed for low molecular weights, hence the values obtained for molecular weight and α are likely to be more accurate.

Name	M_n *(g.mol^{-1})*	M_w *(g.mol^{-1})*	*PDi*	*α*
PMMA 1	2000	3700	1.9	0.44
Q	900	2900	3.1	0.27
R	700	1900	2.9	0.25
PMMA 3	8100	14500	1.8	0.55
S	1000	9000	9.1	0.25

Table 2.12: α and dn/dc values for branched polymers Q-S and comparable linear PMMA's for the same molecular weight range

EGDMA-TMPTMA copolymers **Q** and **R** display reduced α values compared to linear **PMMA 1**, illustrating the branched nature of these materials. A higher level of branching is observed in **R**, which employs both a higher CoBF concentration and higher TMPTMA content (33% TMPTMA, 5.1x10^{-4} mol% CoBF), as its α value is reduced in comparison to **Q** (20% TMPTMA, 4.0x10^{-4} mol% CoBF), most likely due to the higher TMPTMA content. A large reduction is observed in the α value of homopolymer **S** compared to linear **PMMA 3** over the same molar mass, indicating a high level of branching, as expected from a trimethacrylate homopolymer.

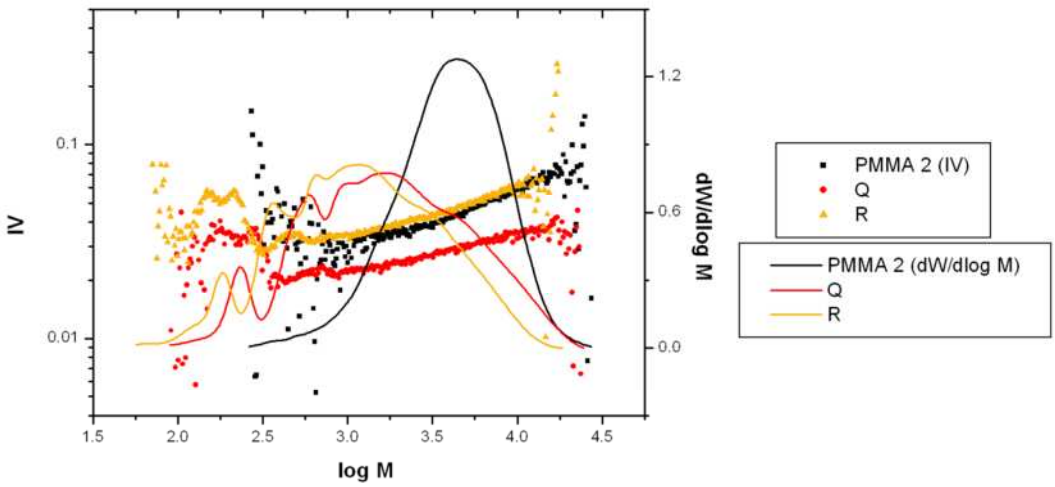

Figure 2.32: Mark-Houwink plots for copolymerisations Q (EGDMA/TMPTMA 80/20 mol%, 4.0x10^{-4} mol% CoBF) and R (EGDMA/TMPTMA 67/33 mol%, 5.1x10^{-4} mol % CoBF) compared to linear PMMA 1

The IV of polymer **Q** is reduced throughout the whole molecular weight distribution in comparison to linear **PMMA 1**, whereas copolymer **R** displays a similar IV to linear **PMMA 1**, most likely due to its low molecular weight (Figure 2.32). The gradient of the IV plot for copolymer **Q** remains fairly constant throughout the molecular weight distribution, signifying a consistent level of branching as molecular weight increases, for **R** however, deviation in the gradient of the IV plot is evident, indicating

inconsistencies in the level of branching with increasing molecular weight, again this is expected as both monomers provide different levels of branch points and due to the statistical nature of the copolymerisation, polymer composition is likely to be broad.

TMPTMA homopolymer **S** displays a greatly reduced IV in comparison to **PMMA 3** throughout the whole molecular weight distribution, indicating a more highly branched structure (Figure 2.33). Very little change is observed in the gradient of the IV plot on increasing molecular weight, suggesting consistent branching within the polymer.

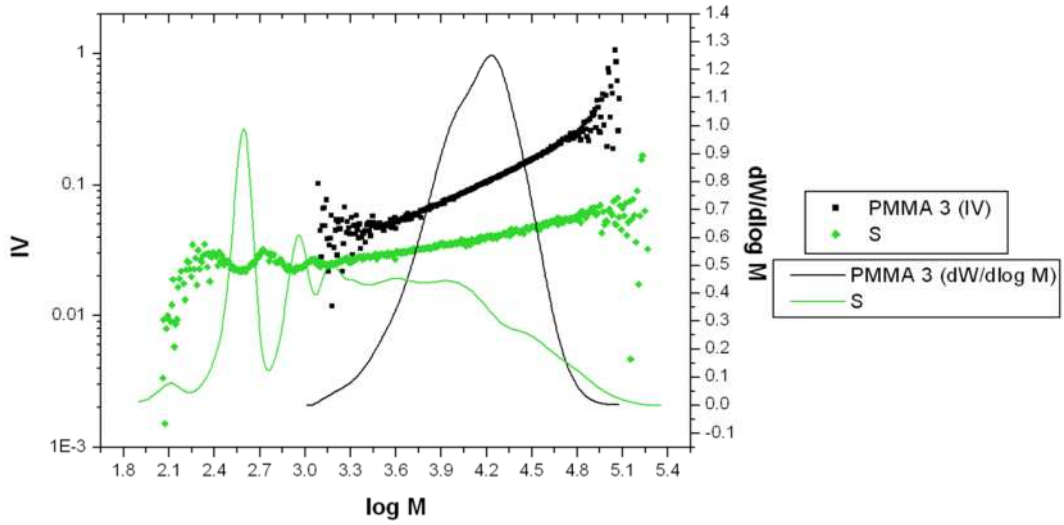

Figure 2.33: Mark Houwink plots for TMPTMA homopolymerisation S (6.4×10^{-4} mol % CoBF) compared to linear PMMA 3.

IV's obtained through universal calibration were used to generate g' plots for these polymers. A decrease in g' is observed with increasing molecular weight for polymers **Q**-**S**, indicating an increase in branching with increasing molecular weight. The largest reduction is observed in **S**, due to the increased level of branching and increased molecular weight of this polymer (Figure 2.34 (left & right)).

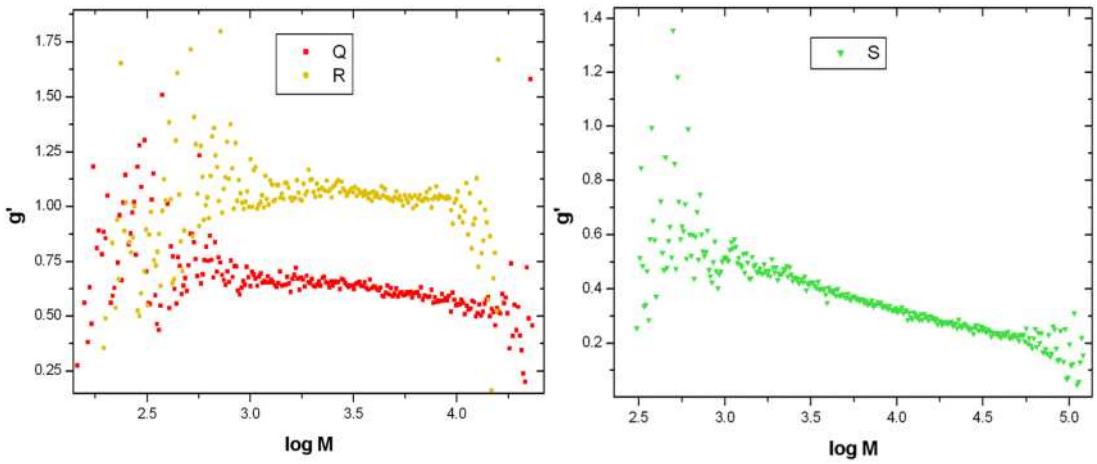

Figure 2.34: (left) g' plots generated from Mark-Houwink data for polymerisations Q (EGDMA/TMPTMA 80/20 mol% copolymer) and R (EGDMA/TMPTMA 67/33 mol%) copolymer) compared with PMMA 2 (right) g' plot generated from Mark-Houwink data for polymerisation S (TMPTMA homopolymer) compared to PMMA 3

2.3 Conclusions

EGDMA homopolymers were synthesised employing the conditions outlined by Guan,[124] obtaining consistent results over a range of polymerisations. Reduction in CoBF concentrations yielded higher molecular weight polymers with broader PDi's. Mark-Houwink plots indicate consistent and increasing branching in the products as molecular weights increase. EGDMA homopolymers synthesised retain a high level of vinyl functionality, which has the potential to be used in post polymerisation functionalisation reactions.

Copolymerisations of EGDMA and MMA led to a decrease in branching, which due to a higher rate of EGDMA conversion compared to MMA, yielded polymers with a core rich in EGDMA units and a more MMA based periphery. Use of low levels of EGDMA in this system accesses a larger range of molecular weights in comparison to those accessible *via* the synthesis of EGDMA homopolymers, due to a dramatic shift in the gel point. Mark-Houwink and g' plots confirm branching in the products, which increases on increasing EGDMA content and increasing molecular weight, however, due to the low molecular weight of the polymers synthesised a deviation from linearity for the Mark-Houwink plots is observed, therefore results obtained may not be a reflection of the true molecular weight, but should indicate trends in both molecular weight and branching between samples. IV plots suggest inconsistent branching within the products, which is most likely due to the heterogeneous nature of the copolymer, as MMA homopolymers are observed by MALDI-ToF and EDGMA incorporation is rapid,

occurring within the first four hours of the polymerisation. Vinyl functionality was retained in the polymer products, which possesses the potential to be functionalised *via* click chemistry methods, but at a lower level compared to EGDMA homopolymers.

Copolymerisations of EGDMA with tri-vinyl monomer TMPTMA and the homopolymerisation of TMPTMA led to an increase in branching. The main limitation of the use of these highly branching monomers is that only a small window of molecular weights are accessible without gelation occurring. This, alongside the fact that polymerisations require early termination in order to circumvent gelation, means high conversions are not achieved, making these systems fairly limited in their application. Hence, systems using branching diluters such as MMA and homopolymerisations of divinyl monomers provide a larger opportunity for variety in the products. Mark-Houwink and g' plots confirmed branching in TMPTMA copolymers and homopolymer, which increased on increasing molecular weight and IV plots were used to assess the consistency in branching. Again, for copolymerisations this inconsistency in branching is most likely due to variations in monomer incorporation, but consistent branching was observed for TMPTMA homopolymerisation **S**. These polymers possessed the highest level of vinyl functionality.

2.4 Experimental

General

All reagents were purchased from Aldrich and used as received unless stated. 2, 2-Azobis(2,4-dimethylvaleronitrile) (V-601) was donated from Wako and used as received. CoBF was synthesised according to literature procedure.[244]

Polymerisation Procedures

Homopolymerisations of EGDMA and TMPTMA

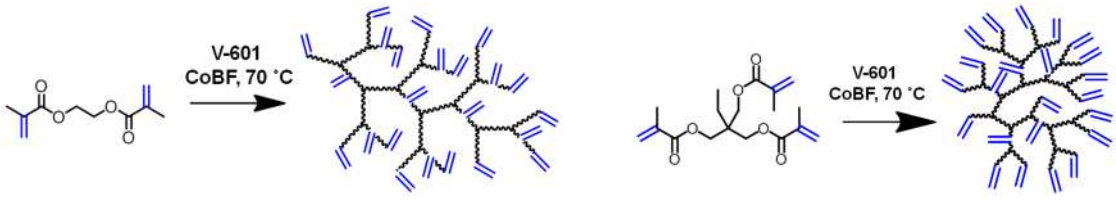

Figure 2.35: (left) General schematic for the CCT homopolymerisation of EGDMA (right) General schematic for the CCT homopolymerisation of TMPTMA

A typical scale homopolymerisation was carried out as follows.

A Schlenk tube was charged with 20 mL of monomer (EGDMA 0.106 mol, TMPTMA 0.063 mol), 19 mL dichloroethane and 1 mL anisole (1:1 solvent:monomer by volume, anisole being an internal standard for GC-FID). A minimum of three freeze pump thaw cycles were applied and the vessel backfilled with nitrogen. A separate Schlenk tube was charged with CoBF and 20 mg V-601 (0.8 mmol), with magnetic stirring. The vessel was degassed *via* a minimum of three cycles of vacuum/nitrogen, and backfilled with nitrogen. The liquids were cannulated into solids under positive nitrogen pressure and the reaction mixture stirred until homogenous. The vessel was placed in an oil bath (70 ˚C) with stirring and left to react for between 2-25 hours under nitrogen. Sampling was carried out using a degassed syringe. Solvent was removed in vacuo and the end products characterised by ^{1}H NMR, ^{13}C NMR, GC-FID, IR, MALDI-ToF and SEC.

Name	CoBF (mol%)	CoBF (mg)	CoBF (mmol)
EGDMA Homopolymers			
A-G	3.8×10^{-4}	20	0.040
H	3.0×10^{-4}	16	0.032
I	2.3×10^{-4}	12	0.024
TMPTMA Homopolymer			
S	6.4×10^{-4}	20	0.04

Table 2.13: CoBF ratio's employed in EGDMA homopolymerisations A-G, H and I and TMPTMA homopolymerisation S

Larger or smaller scale reactions were carried out using the same ratios of reagents.

Copolymerisations of EGDMA with TMPTMA

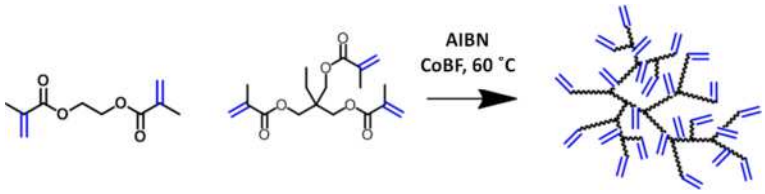

Figure 2.36: General schematic for the CCT copolymerisation of EGDMA and TMPTMA

Copolymerisations were conducted in the same fashion as above, with varying moles of monomer and mol% ratios of CoBF to monomer.

Name	Total Monomer (mol)	Monomer Ratio EGDMA/TMPTMA (mol%)	CoBF (mol%)	CoBF (mg)	CoBF (mmol)
Q	0.099	80/20	$4.0x10^{-4}$	20	0.04
R	0.079	67/33	$5.1x10^{-4}$	20	0.04

Table 2.14: Monomer and CoBF ratios employed in the copolymerisations of EGDMA and TMPTMA, polymers Q and R

Copolymerisations of EGDMA with MMA

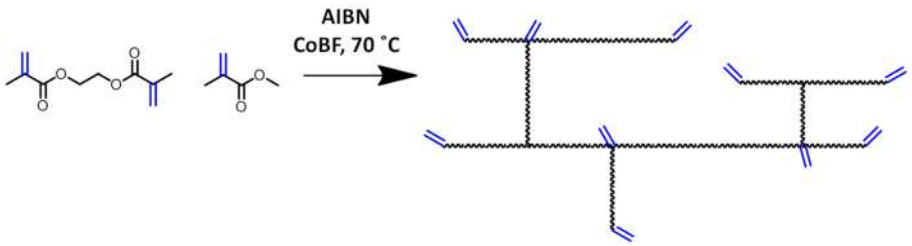

Figure 2.37: General schematic for the CCT copolymerisation of EGDMA and MMA

Due to the low amounts of CoBF employed in EGDMA MMA copolymerisations CoBF stock solutions were used. An ampoule was charged with 4.6 mg CoBF with magnetic stirring and degassed *via* three cycles of vacuum/nitrogen, the vessel was back filled with nitrogen. A separate Schlenk tube was charged with 25 mL of monomer and freeze pump thawed a minimum of three times. Degassed monomer was cannulated into solids under positive nitrogen pressure.

Polymerisations were conducted in the same manner as above, using AIBN as an initiator (50 mg, 0.3 mmol), with the addition of CoBF stock solution taking place after freeze pump thawing of reaction mixture, prior to heating, *via* degassed syringe. Polymers were precipitated into hexane or petroleum ether 40-60 ˚C and dried overnight in a vacuum oven and the end products characterised by ^{1}H NMR, ^{13}C NMR, GC-FID, IR, MALDI-ToF and SEC.

Name	Monomer Ratio EGDMA/MMA (mol%)	Total Monomer (mol)	CoBF Stock Soln. (mL)	CoBF (mol%)	CoBF (mg)	CoBF (mmol)
J	10/90	0.047	1	1.6x10-5	0.37	$7.4x10^{-4}$
K	10/90	0.047	0.75	1.2x10-5	0.28	$5.6x10^{-4}$
L	10/90	0.047	0.5	7.7x10-6	0.18	$3.6x10^{-4}$
M	25/75	0.027	1	2.7x10-5	0.37	$7.4x10^{-4}$
N	25/75	0.027	0.75	2.1x10-5	0.28	$5.6x10^{-4}$
O	33/67	0.027	1	2.7x10-5	0.37	$7.4x10^{-4}$
P	33/67	0.027	0.75	2.1x10-5	0.28	$5.6x10^{-4}$

Table 2.15: Monomer and CoBF ratios employed in the copolymerisations of EGDMA and MMA, polymers J-P

Linear PMMA Synthesis

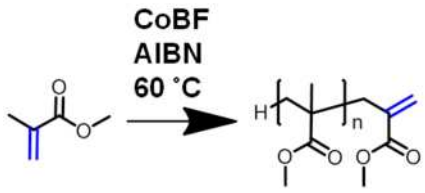

Figure 2.38: General schematic of the CCT homopolymerisation of linear PMMA

Linear PMMA's **1** and **3** were synthesised in a large scale reactor. CoBF stock solutions were used. An ampoule was charged with 10 mg (0.02 mmol) of CoBF and degassed *via* three vacuum/nitrogen cycles. 50 mL (0.467 mol) of MMA was degassed *via* three cycles of freeze pump thaw and liquids cannulated into solids under positive nitrogen pressure. A 0.5 L reactor with an oil jacket and overhead stirring was purged with nitrogen for 20 minutes. 150 mL (1.40 mol) of MMA was degassed *via* three cycles freeze pump thaw and injected into the reactor *via* degassed syringe. 150 mL of toluene was degassed *via* three cycles of freeze pump thaw and injected using degassed syringe. CoBF stock solution was added *via* degassed syringe. AIBN (0.5g, 3.04 mmol) was dissolved in a vial under nitrogen using degassed reaction mixture and injected into the reactor *via* degassed syringe. The oil jacket was set to 60 ˚C and the reaction left for 24 hours.

Linear PMMA **2** was synthesised in bulk in a Schlenk tube using freeze pump thaw techniques as above. MMA (20g, 0.20 mol), AIBN (0.1g, 0.6 mmol). CoBF stock solution was injected *via* degassed syringe to degassed reaction solution, CoBF (10 mg, 0.02 mol), MMA (50 mL, 0.467 mol).

The polymers obtained were precipitated into hexane or petroleum ether 40-60 ˚C. White solids were removed *via* filtration and volatiles removed overnight in a vacuum oven and the end products characterised by ^{1}H NMR, ^{13}C NMR, IR and SEC

Name	MMA (mol)	CoBF Stock Soln. (mL)	CoBF (mmol)	CoBF (mol%)
PMMA 1	1.40	10	$4x10^{-3}$	$2.8x10^{-6}$
PMMA 2	0.47	2	$8x10^{-4}$	$1.7x10^{-6}$
PMMA 3	1.40	2	$8x10^{-4}$	$5.7x10^{-7}$

Table 2.16: Monomer and CoBF ratios employed for the homopolymerisation of linear PMMA's 1-3

Instruments

^{1}H and ^{13}C NMR

All ^{1}H and ^{13}C NMR were recorded on Bruker DPX-300 and Bruker DPX-400 spectrometers as solutions in deuterated chloroform. Chemical shifts were calibrated using TMS and cited as parts per million (ppm).

Infra Red (IR)

IR was carried out on a Bruker Vector 22 using a Golden Gate diamond attenuated flow cell and analysed using Opus spectroscopy software.

Size Exclusion Chromatography (SEC)

All SEC were performed on Agilent 390-LC multi detector suites equipped with a PL-AS RT/MT autosampler, fitted with a PLgel 5 µm guard column and two PLgel 5 µm Mixed D columns (suitable for separations up to MW = 2.0 x 10^{6} g.mol^{-1}). All data was collected and analysed using Cirrus software (Agilent Inc). Any points within the calibration plot with an error greater than 10% were not included in the final calibrations. Third order calibration plots were used for both conventional SEC and when conducting universal calibration.

Monitoring of reactions was conducted using THF mobile phase, flow rate 1 mL.min^{-1}, ambient operating temperature, 100 µL injection volume. An RI detector was used for conventional SEC. Calibrations were set using PMMA EasiVial standards (690-1944000 g.mol^{-1}), purchased from Agilent, with a minimum of 9 points to form a third order calibration curve.

For investigation of final molecular weights by universal calibration chloroform was used as the mobile phase, flow rate of 1 mL.min^{-1}, ambient operating temperature, 100 µL injection volume. An RI detector and 4 capillary viscometer were used. Universal Calibrations were conducted using a single PS narrow standard, M_p 189,300 of known concentration for detector calibration, using PMMA EasiVial standards (690-1944000 g.mol^{-1}) of known concentrations for column calibration. A minimum of 9 points were used to form a third order universal calibration. Mark-Houwink and g' comparisons were made to linear PMMA synthesised by CCTP as above.

Matrix-Assisted Laser Desorption and Ionization Time-of-Flight (MALDI-ToF)

Mass spectra were acquired by MALDI-ToF mass spectrometry using a Bruker Daltonics Ultraflex II MALDI-ToF mass spectrometer, equipped with a nitrogen laser delivering 2 ns laser pulses at 337 nm with positive ion ToF detection performed using an accelerating voltage of 25 kV.

2, 5-Dihdroxybenzoic acid (DHB) was used as an organic matrix and sodium iodide (NaI) used as the salt. A layering method was used to spot the MALDI plate. THF was used as the solvent for sample preparation.

Gas chromatography – Flame ionisation detector (GC-FID)

GC-FID analysis was performed using a Varian 450 instrument fitted with a FactorFour^{TM} capillary column VF-1ms, of 15 m × 0.25 mm I.D., film thickness 0.25 µm from Varian. The oven temperature was programmed as follows: 40 °C (hold for 1 min) at 25 °C.min^{-1} to 200 °C. The injector was operated at 200 °C and the FID was operated at 220 °C. Nitrogen was used as carrier gas at a flow rate of 1 mL.min^{-1} and a split ratio of 1:100 was applied. Chromatographic data were processed using Galaxie Chromatography data system, version 1.9.302.530 software.

Characterisation

Characterisation of A- I (**A**: Branched PEGDMA, 3.8x10^{-4} mol% CoBF. **B**, **C**, **D** gelled, no characterisation data obtained: **E**: Branched EGDMA 50% solids, 3.8x10^{-4} mol% CoBF. **F**: Branched EGDMA 33% solids, 3.8x10^{-4} mol% CoBF. **G**: Branched EGDMA 25% solids, 3.8x10^{-4} mol% CoBF. **H**: Branched PEGDMA, 0.032 mmol CoBF. **I:** Branched PEGDMA, 0.024 mmol CoBF)

^{1}H NMR (400 MHz, TMS at 25˚C): δ 1.00-1.50 (backbone CH_3), 1.85-2.05 (terminal CH_3), 2.15-2.20 (backbone CH_2), 2.45-2.60 (backbone CH_2), 4.15-4.45 ($OC\underline{H_2}C\underline{H_2}O$), 5.50-5.60 (terminal $C\underline{H_a}H_b$=C + internal $C\underline{H_a}H_b$=C), 6.05-6.15 (terminal $CH_a\underline{H_b}$=C), 6.20-6.35 (internal $CH_a\underline{H_b}$=C)

^{13}C NMR (400 MHz $CDCl_3$ at 25˚C): δ 18.31 (terminal CH_3), 24.82, 27.22 and 30.37 (backbone CH_3), 40.67 (backbone CH_2), 41.58 and 43.05 (backbone quaternary carbons), 46.15 and 48.20 (backbone CH_2), 62.33 (OCH_2CH_2O), 126.04 (terminal $\underline{C}H_2$=C-), 128.63 (internal $\underline{C}H_2$=C-), 135.97 (terminal CH_2=$\underline{C}$-), 137.08 (internal CH_2=$\underline{C}$-), 167.09 (terminal ester carbonyl), 176.70 (internal ester carbonyl)

IR: ν_{max} (neat)/cm^{-1} 2972 (m, CH sp^3), 1715 (s, C=O), 1628 (m, C=C), 1451 (m, CH_2), 1391 (m, CH_3), 1367 (m), 1292 (m), 1141 (s, C-O), 1049 (m), 946 (m), 814 (m)

Conventional SEC: **A**: M_n 1700, M_w 4800, PDi 2.9 **E**: M_n 3600, M_w 385000 (high molecular weight exclusion present), PDi 107.9 **F**: M_n 2600, M_w 17900, PDi 6.9 **G**: M_n 1500, M_w 4100, PDi 2.8 **H**: M_n 1600, M_w 4800, PDi 3.0 **I**: M_n 1700, M_w 7000, PDi 4.1

Universal Calibration: **A:** M_n 1800, M_w 6200, PDi 3.5 **E**: M_n 1300, M_w 190000, PDi 146.5 (high molecular weight exclusion present) **F**: M_n 1930, M_w 29400, PDi 15.2 **G**: M_n 1200, M_w 6460, PDi 5.4 **H**: M_n 1600, M_w 6900, PDi 4.3 **I:** M_n 1600, M_w 11800, PDi 7.4

GC-FID (Final Conversions, %): **A** 93.3 **B**: N/A **C**: N/A **D**: N/A **E**: 98.6 **F**: 98.5 **G**: 96.7 **H**: 90.8 **I**: 88.2

Characterisation of J-P (**J**: Branched PEGDMA/PMMA 10/90 mol% monomer ratio, 2.8x10^{-5} mol% CoBF **K**: Branched PEGDMA/PMMA 10/90 mol% monomer ratio, 2.1x10^{-5} mol% CoBF **L**: Branched PEGDMA 10/90 mol% monomer ratio, 1.4x10^{-5} mol% CoBF **M**: Branched PEGDMA/PMMA 25/75 mol% monomer ratio, 2.8x10^{-5} mol% CoBF **N**: Branched PEGDMA/PMMA 25/75 mol% monomer ratio, 2.1x10^{-5} mol% CoBF **O** Branched PEGDMA/PMMA 33/67 mol% monomer ratio, 2.8x10^{-5} mol% CoBF **P**: Branched PEGDMA/PMMA 33/67 mol% monomer ratio, 2.1x10^{-5} mol% CoBF)

^{1}H NMR (400 MHz, TMS at 25˚C): δ 0.90-1.50 (backbone CH_3), 1.85-2.00 (terminal CH_3), 2.05-2.20 (backbone CH_2), 2.45-2.7 (backbone CH_2), 3.55-3.65 (OCH_3 polymer), 3.70-3.80 (OCH_3 monomer), 4.10-4.40 ($OC\underline{H_2}C\underline{H_2}O$), 5.45-5.65 (terminal $C\underline{H_a}H_b$=C, internal $C\underline{H_a}H_b$=C), 6.05-6.15 (terminal $CH_a\underline{H_b}$=C), 6.20-6.35 (internal $CH_a\underline{H_b}$=C)

^{13}C NMR (400 MHz $CDCl_3$ at 25˚C): δ 18.21 (terminal CH_3), 24.98, 29.94 and 30.53 (backbone CH_3), 40.83 (backbone CH_2), 41.74 and 43.16 (backbone quaternary carbons), 46.06 and 48.09 (backbone CH_2), 51.90 (OCH_3), 62.54 (OCH_2CH_2O), 126.19 (terminal $\underline{C}H_2$=C-), 128.75 (internal $\underline{C}H_2$=C-), 136.19 (terminal CH_2=$\underline{C}$-), 137.25 (internal CH_2=$\underline{C}$-), 167.27 (terminal ester carbonyl), 176.87 (internal ester carbonyl)

IR: ν_{max} (neat)/cm^{-1} 2960 (m, CH sp^3), 1716 (s, C=O), 1629 (m, C=C), 1451 (m, CH_2), 1391 (m, CH_3), 1367 (m), 1293 (m), 1142 (s, C-O), 1049 (m), 945 (m), 814 (m)

Conventional SEC: **J**: M_n 1800, M_w 2300, PDi 1.8 **K**: M_n 2400, M_w 4900, PDi 2.1 **L**: M_n 3400, M_w 8900, PDi 2.7 **M**: M_n 1900, M_w 3700, PDi 2.0, **N**: M_n 2400, M_w 6200, PDi 2.6 **O**: M_n 3800, M_w 10800, PDi 2.9 **P**: M_n 6300, M_w 33800, PDi 5.3

Universal Calibration: **J**: M_n 1500, M_w 4000, PDi 2.7 **K**: M_n 1900, M_w 6100, PDi 3.22 **L**: M_n 2700, M_w 11800, PDi 4.4 **M**: M_n 1300, M_w 4400, PDi 3.5 **N**: M_n 1400, M_w 8800, PDi 6.1 **O**: M_n 3000, M_w 14600, PDi 4.8 **P**: M_n 5700, M_w 69400, PDi 12.2

GC-FID (Final Conversions, %): **J**: EGDMA 98.2, MMA 90.3,Total 91.1 **K**: EGDMA 98.3, MMA 94.2, Total 94.6 **L**: EGDMA 98.4, MMA 94.4, Total 94.8 **M**: EGDMA 99.7, MMA 95.0, Total 96.2 **N**: EGDMA 99.4, MMA 95.7, Total 96.7 **O**: EGDMA 99.6, MMA 95.0, Total 96.2 **P**: EGDMA 99.4, MMA 95.5, Total 96.4

Characterisation of Q and R (**Q**: Branched PEGDMA/PTMPTMA 80/20 mol% monomer ratio, 4.0x10^{-4} mol% CoBF. **R**: Branched PEGDMA/PTMPTMA 67/33 mol% monomer ratio, 5.1 mol% CoBF)

^{1}H NMR (400 MHz, TMS at 25˚C): δ 0.90-1.65 (backbone CH_3, $C\underline{H}_2C\underline{H}_3$), 1.85-2.05 (terminal CH_3), 2.10-2.20 (backbone CH_2), 2.40-2.70 (backbone CH_2), 3.95-4.40 (OCH_2CH_2O, OCH_2), 5.45-5.65 (terminal $C\underline{H}_aH_b$=C, internal $C\underline{H}_aH_b$=C), 6.00-6.15 (terminal $CH_a\underline{H}_b$=C), 6.20-6.35 (internal $CH_a\underline{H}_b$=C)

^{13}C NMR (400 MHz $CDCl_3$ at 25˚C): δ 7.40 ($CH_2\underline{C}H_3$), 18.14 (terminal CH_3), 23.40 (TMPTMA C=O), 24.67 (backbone CH_3), 40.55 (backbone CH_2, quaternary $\underline{C}(CH_3)_2(CH_2)_2$), 42.88 (quaternary $\underline{C}(CH_2)_2(CH_3)(C{=}O)$, $C(CH_2)_4$), 48.07 (backbone CH_2), 62.23 (OCH_2CH_2O), 66.04 (OCH_2), 125.79 (terminal $\underline{C}H_2$=C-), 128.35 (internal $\underline{C}H_2$=C-), 135.95 (terminal CH_2=$\underline{C}$-), 137.06 (internal CH_2=$\underline{C}$-), 166.85 (terminal ester carbonyl), 176.42 (internal ester carbonyl)

IR: ν_{max} (neat)/cm^{-1} 2970 (m, CH sp^3), 1729 (m, C=O), 1636 (s, C=C), 1452 (s, CH_2), 1292 (m), 1142 (m, C-O), 942 (s), 813 (s)

Conventional SEC: **Q**: M_n 800, M_w 1800, PDi 2.3, **R**: M_n 800, M_w 1800, PDi 2.3

Universal Calibration: **Q**: M_n 500, M_w 2100, PDi 4.3, **R**: M_n 500, M_w 2100, PDi 4.5

GC-FID (Final Conversions, %): **Q**: EGDMA 73.4, TMPTMA 82.4, Total 75.6 **R**: EGDMA 69.6, TMPTMA 76.9, Total 73.2 **S**: 77.5

Characterisation of S (Branched PTMPTMA)

^{1}H NMR (400 MHz, TMS at 25˚C): δ 0.70-1.10 ($CH_2C\underline{H}_3$), 1.10-1.45 ($C\underline{H}_2CH_3$), 1.85-2.10 (terminal CH_3), 3.90-4.40 (OCH_2CH_2O), 5.45-5.60 (terminal $C\underline{H}_aH_b$=C + internal $C\underline{H}_aH_b$=C), 6.00-6.35 (terminal $CH_a\underline{H}_b$=C, internal $CH_a\underline{H}_b$=C)

^{13}C NMR (400 MHz $CDCl_3$ at 25˚C): δ 7.79 ($CH_2\underline{C}H_3$), 18.59 (terminal CH_3), 23.73 ($\underline{C}H_2CH_3$), 41.48 (quaternary $\underline{C}(CH_3)_2(CH_2)_2$), 64.62 ($OCH_2CH_2O$), 125.82 (terminal $\underline{C}H_2$=C-), 136.23 (terminal CH_2=$\underline{C}$-), 137.28 (internal CH_2=$\underline{C}$-), 167.28 (terminal ester carbonyl)

IR: ν_{max} (neat)/cm^{-1} 2966 (m, CH sp^3), 1715 (m, C=O), 1637 (s, C=C), 1455 (s, CH_2), 1290 (m), 1142 (m, C-O), 940 (s), 812 (s)

Conventional SEC: **S**: M_n 1100, M_w 4500, PDi 4.2

Universal Calibration: **S**: M_n 2100, M_w 11500, PDi 5.4

Characterisation of Linear PMMA's 1-3

^{1}H NMR (400 MHz, TMS at 25˚C): δ 0.70-1.5 (backbone $C\underline{H}_3$), 1.45-1.70 (terminal CH_3), 1.70-2.15 (backbone $C\underline{H}_2$), 3.40-4.80 (OCH_3), 5.50 (CH_2=C), 6.20 (CH_2=C)

^{13}C NMR (400 MHz $CDCl_3$ at 25˚C): δ 16.59 (backbone CH_3), 18.82 (terminal CH_3), 51.89 (OCH_3), 52.81 (backbone quaternary C), 54.50 (backbone CH_2), 128.40 ($\underline{C}H_2$=C), 136.39 (CH_2=$\underline{C}$), 177.06 (C=O)

IR: ν_{max} (neat)/cm^{-1} 2950 (m, CH sp^3), 1721 (m, C=O), 1482 (m), 1435 (m, CH_2), 1387 (m, CH_3), 1240 (m), 1190 (m), 1145 (m, C-O), 987 (m), 841 (m), 750 (m)

Conventional SEC: **PMMA 1**: M_n 2300, M_w 3700, PDi 1.6 **PMMA 2**: M_n 8200, M_w 11000, PDi 1.3 **PMMA 3**: M_n 8500, M_w 15000, PDi 1.8

Universal Calibration: **PMMA 1**: M_n 2000, M_w 3700, PDi 1.9 **PMMA 2**: M_n 7100, M_w 10300, PDi 1.4 **PMMA 3**: M_n 8100, M_w 14500, PDi 1.8

2.5 References

1. Striegel, A.; Yau, W.; Kirkland, J.; Bly, D., Modern Size-Exclusion Liquid Chromatography: Practice of Gel Permeation and Gel Filtration Chromatography 2nd ed.; Wiley: 2009.

2. Hiemenz, P. C.; Lodge, T. P., Polymer Chemistry. 2nd ed.; CRC Press: Taylor & Francis Group: 2007.

3. Brandrup, J.; H, I. E., Polymer Handbook. 3rd ed.; Wiley Interscience: Chichester, 1989.

4. Grubisic, Z.; Rempp, P.; Benoit, H., J. Polym. Sci., Part B: Polym. Lett. **1967,** 5 (9), 753.

5. Striegel, A. M., Anal. Chem. **2005,** 77 (5), 104 A.

6. Kostanski, L. K.; Keller, D. M.; Hamielec, A. E., J. Biochem. Biophys. Methods **2004,** 58 (2), 159.

7. Otocka, E. P.; Hellman, M. Y., J. Polym. Sci.: Polym. Lett. Ed. **1974,** 12 (6), 331.

8. Saunders, G.; Cormack, P. A. G.; Graham, S.; Sherrington, D. C., Macromolecules **2005,** 38 (15), 6418.

9. Dubin, P. L.; Principi, J. M., Macromolecules **1989,** 22 (4), 1891.

10. Netopilík, M.; Podešva, J.; Lokaj, J.; Kratochvíl, P., Polym. Int. **2008,** 57 (10), 1152.

11. Flory, P. J.; Fox, T. G., J. Am. Chem. Soc. **1951,** 73 (5), 1904.

12. Fox, T. G.; Flory, P. J., J. Am. Chem. Soc. **1951,** 73 (5), 1915.

13. Dondos, A., J. Chromatogr. A **2006,** 1127, 183.

14. Dondos, A., Biomacromolecules **2007,** 8 (9), 2979.

15. Simon, P. F. W.; Müller, A. H. E.; Pakula, T., Macromolecules **2001,** 34 (6), 1677.

16. Slark, A. T.; Sherrington, D. C.; Titterton, A.; Martin, I. K., J. Mater. Chem. **2003,** 13 (11), 2711.

17. Roovers, J.; Zhou, L. L.; Toporowski, P. M.; van der Zwan, M.; Iatrou, H.; Hadjichristidis, N., Macromolecules **1993,** 26 (16), 4324.

18. Voit, B. I.; Lederer, A., Chem. Rev. **2009,** 109 (11), 5924.

19. Ahn, S.; Lee, H.; Lee, S.; Chang, T., Macromolecules **2012,** 45 (8), 3550.

20. Zimm, B. H.; Stockmayer, W. H., J. Chem. Phys. **1949,** 17 (12), 1301.

21. Zimm, B. H., J. Chem. Phys. **1948,** 16 (12), 1093.

22. Zimm, B. H.; Kilb, R. W., J. Polym. Sci. **1959,** 37 (131), 19.

23. Camerlynck, S.; Cormack, P. A. G.; Sherrington, D. C.; Saunders, G., J. Macromol. Sci., Part B: Phys. **2005,** 44 (6), 881

24. Z.Guan **US5767211, 1998**.

25. Guan, Z., J. Am. Chem. Soc. **2002,** 124, 5616.

26. Yan, W.; Gardella Jr, J. A.; Wood, T. D., J. Am. Soc. Mass Spectrom. **2002,** 13 (8), 914.

27. Chen, H.; He, M.; Pei, J.; He, H., Anal. Chem. **2003,** 75 (23), 6531.

28. Adden, R.; Müller, R.; Brinkmalm, G.; Ehrler, R.; Mischnick, P., Macromol. Biosci. **2006,** 6 (6), 435.

29. Nielen, M. W. F.; Malucha, S., Rapid Commun. Mass Spectrom. **1997,** 11 (11), 1194.

30. Schriemer, D. C.; Li, L., Anal. Chem. **1997,** 69 (20), 4176.

31. Rashidzadeh, H.; Guo, B., Anal. Chem. **1998,** 70 (1), 131.

32. Slavin, S.; McEwan, K. A.; Haddleton, D. M., Cobalt Catalyzed Chain Transfer Polymerization: A Review. In Polymer Science: A Comprehensive Reference, 1st ed.; Matyjaszewski, K.; Möller, M., Eds. Elsevier: 2012; Vol. 3, pp 249.

33. Gridnev, A. A., J. Polym. Sci., Part A: Polym. Chem. **2000,** 38 (10), 1753.

34. Kukulj, D.; Davis, T. P., Macromol. Chem. Phys. **1998,** 199 (8), 1697.

35. Gruendling, T.; Junkers, T.; Guilhaus, M.; Barner-Kowollik, C., Macromol. Chem. Phys. **2010,** 211 (5), 520.

36. Dondos, A.; Benoit, H., Polymer **1977,** 18 (11), 1161.

37. Dondos, A.; Skordilis, V., Journal of Polymer Science: Polymer Physics Edition **1985,** 23 (4), 615.

38. Mrkvičková, L., J. Liq. Chromatogr. Relat. Technol. **1997,** 20 (3), 403.

39. Sadron, C.; Rempp, P., J Polym Sci **1958,** 29, 127.

40. Stockmayer, W. H. F., M. , J Polym Sci C, Polym Lett **1963,** C1, 137.

41. Bakac, A.; Espenson, J. H., J. Am. Chem. Soc. **1984,** 106 (18), 5197.

Chapter 3

3. Functionalisation of Branched Polymers Containing High Levels of Vinyl Functionality

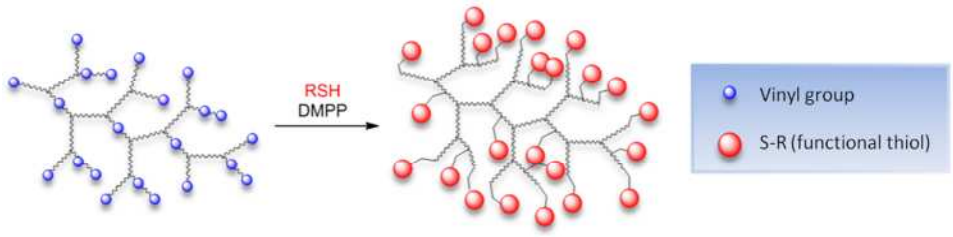

Polymers synthesised by CCTP have proven to be susceptible to thiol-Michael addition reactions due to the retention of activated terminal vinyl groups in the products. CCTP was employed in the synthesis of branched polymers using di- and multi-vinyl monomers, retaining high levels of activated vinyl groups, both internally and externally. Thiol-Michael addition was used in the exploitation of these vinyl groups by utilisation of a range of commercial thiols, creating an array of decorated polymers, with a wide scope for functionalisation.

3.1. Thiol-ene Strategies for the Synthesis of Functional Materials

3.1.1. Polymer Synthesis as a Route to Functionalisation via Thiol-ene Chemistries

Many polymerisation techniques can be used in the synthesis of functional polymers *via* thiol-ene click chemistry, providing some degree of unsaturation or thiol functionality can be incorporated into the polymer at a terminal position. Techniques such as the polymerisation of allyl containing polymers, e.g. allyl methacrylate, have been shown in the literature, where functionalisation *via* radical induced thiol-ene chemistry has been proven successful, yielding polymers where functionality can be introduced to side chains.[198, 245, 246] However, these unactivated allyl groups are limited to functionalisation *via* radical pathways and are not suitable for functionalisation using base catalysed or nucleophilic thiol-Michael addition reactions, which require the use of activated vinyl groups; hence, choice of polymerisation technique has been used to access either activated vinyl or sulfide functionalities for use in thiol-Michael reactions.

The synthesis of polymers by RAFT has been of particular interest to the application to thiol-Michael addition reactions, due to the terminal trithiocarbonate groups yielded from the RAFT mechanism; Lima *et al.* demonstrated that upon reduction of this group *via* aminolysis with hexylamine, thiol terminally functional polymers were prepared, capable of subsequent of thiol-Michael addition to activated vinyl groups.[247] This work was later continued by Qiu *et al.*, providing a one pot system for the reduction and functionalisation of terminal trithiocarbonate groups, using tris(2-carboxyethyl) phosphine hydrochloride (TCEP.HCl) as both a reducing agent and thiol-Michael addition catalyst.[248] The combination of RAFT and thiol-Michael addition was also extended by the use of trithiocarbonate containing methacrylate monomers, giving polymers comprising terminal and side chain trithiocarbonates. These polymers with a high trithiocarbonate functionality were reacted *via* several routes, reduction to their corresponding thiols and subsequent reaction *via* UV induced thiol-ene click chemistry, or *via* one pot reductions/functionalisations using a phosphine catalyst demonstrating both thiol-Michael addition and thiol exchange as routes to functionalisation of these materials.[249] Due to readily reducible terminal trithiocarbonate groups interred into the

polymer *via* the RAFT mechanism, a wealth of examples employing this type of chemistry have arisen.[250-262]

ATRP is an excellent method for the synthesis of polymers with terminal functionality, which, by use of alkyne or azide functional monomers, has been combined with CuAAc chemistry due to the common catalyst used in the two reactions.[70, 263-265] Additionally, terminal halogen groups can be easily transformed to their corresponding azide derivatives, providing a facile method for the functionalisation of these molecules,[85, 266-269] often *via* "one pot" strategies.[270-272] It has also been demonstrated that terminal halogen functionality can transformed into thiol functionality *via* reaction with thiourea and addition of sodium hydroxide for the removal of salts.[270] Thiol functionalised polymers obtained in this manner are suitable for reaction *via* thiol-ene click chemistry with vinyl or allyl containing materials.[273, 274] A further method for the transformation of halogen termini into disulfide bonds using methanethiosulfonate led to a versatility in functionalisation, as hydrolysis of methanethiosulfonate end groups yielded thiol groups which can be subsequently functionalised by thiol-ene click chemistry or thiol/disulfide exchange.[190]

Combinations of polymerisation techniques have also been investigated for the synthesis of terminal functionalities, capable of use in thiol-ene reactions. The combination of NMP and RAFT has been demonstrated for the synthesis of thiol terminated polymers. Addition of the RAFT chain transfer agent, bis(thiobenzyloyl) disulfide to NMP mixtures led to the removal of the dormant nitroxide moiety, yielding a thiobenzoylthio chain end, which can be utilised in two ways; one for chain extension of the polymer via RAFT in the formation of block copolymers, and secondly the reduction of terminal thiobenzyloyl groups via aminolysis yields thiol terminated polymers, suitable for functionalisation by thiol-ene or thiol-Michael addition.[275] Combinations of ATRP with CCTP, and RAFT with CCTP, have also been used in the formation of vinyl terminated polymers of low PDi's, in comparison to their CCTP counterparts. Polymerisations were taken to moderate conversions of approximately 70% with subsequent addition of CoBF solutions to the reaction mixtures, leading to the removal of terminal halogen groups, as prepared by ATRP and removal of RAFT end groups, with chain transfer reactions yielding vinyl terminated polymers with the potential for functionalisation *via* thiol-ene or thiol-Michael reactions.[276, 277] Hence, use of CCTP

provides the unique retention of activated terminal vinyl groups, with no need for further modification of polymers for application to post-polymerisation functionalisation by thiol-ene or thiol-Michael addition reactions.

3.1.2 Combinations of CCTP and Thiol-Michael Addition in the Literature

The prevalence of literature combining CCTP and thiol-ene chemistries, in the synthesis of functionalised polymers, has increased since work reported by Nurmi *et al*. in 2009,[278] who employed CCTP for the synthesis of TMS-protected propargyl methacrylic polymers. On deprotection of the propargyl groups, the polymers possessed high levels of alkyne functionality. Additionally termination of the chain *via* β-hydride abstraction provided terminal activated vinyl groups. The dual functionalisation of these polymers, *via* a combination of CuAAc chemistry and phosphine mediated thiol-Michael addition, resulted in end-functional glycopolymers.[279] A further method for the synthesis of end functional glycopolymers was highlighted in 2012 by Zhang *et al*., adding to the increasing popularity of epoxide containing polymers in the literature. CCTP of glycidyl methacrylate (GMA) resulted in polymers with a high epoxide content and vinyl end groups. Functionalisation of vinyl groups by phosphine mediated thiol-Michael addition, subsequent ring-opening of epoxides with sodium azide and further reaction of the azide groups *via* CuAAc with alkyne sugars led to an alternative method for the formation of end-functionalised glycopolymers *via* CCTP.[280] Zhang *et al*. also employed vinyl terminated polymers synthesised by CCTP for the functionalisation of thiol functional cyclodextrin rings *via* nucleophilic thiol-Michael addition, which were subsequently used in the ring-opening polymerisation of ε-caprolactone, giving cyclodextrin-centred star polymers.[281]

Functionalisation of thermoresponsive oligo(ethylene glycol) methyl ether methacrylate (OEGMEMA) using a combination of CCTP and nucleophilic thiol-Michael addition was also carried out, testing a variety of nucleophilic thiol-Michael addition catalysts. The tuning of lower critical solution temperatures (LCST's) was achieved by copolymerisation of OEGMEMA with di(ethylene glycol) methyl ether methacrylate (DEGMEMA), and the effects of functionalisation on the LCST of resulting polymers were investigated.[282] A range of catalysts applicable in nucleophilic thiol-Michael

additions were investigated by Li *et al*., who tested and optimised catalysts such as DMPP, TEA and hexylamine for the thiol-Michael addition of commercial thiols to MMA dimer, synthesised by CCTP, and commercially available $OEGMEMA_{475}$.[283] Attempts to use this chemistry for the formation of block copolymers however, by thiol-Michael addition of thiol terminated-polyethylene (PE-SH) to PMMA macromonomers, were unsuccessful. It was concluded that the high temperatures required to dissolve PE-SH led to the failure of thiol-Michael addition, hinting at a temperature dependency for this reaction; confirmation of this lack of reactivity of PE-SH to methacrylates leading to the investigation of acrylate based macromonomers, with success achieved *via* thiol-Michael addition of PE-SH to commercial available poly ethylene glycol (PEG) acrylates.[284]

The combination of CCTP and thiol-Michael addition, although not widely used, provides a facile method for the end functionalisation of CCTP synthesised polymers.

3.2 Results and Discussion

Polymers synthesised *via* CCTP retain terminal vinyl functionality in the product, due to β-hydride abstraction in the chain transfer mechanism. When high levels of CoBF are employed in the polymerisation of divinyl monomer, EGDMA, branched polymers are obtained, which retain high levels of both internal and external vinyl functionality. Hence, it was postulated that functionalisation of activated vinyl functionalities yielded in the CCTP of EGDMA could be achieved through phosphine mediated thiol-Michael addition, leading to the creation of branched polymers where functionality can be controlled.

This work focuses on the application and optimisation of thiol-Michael addition for the functionalisation of poly-EGDMA, synthesised by CCTP, in the formation of branched functional polymers.

3.2.1 MALDI-ToF Investigation: End Group Fidelity in the CCTP of EGDMA

As discussed in Chapter 2.1, the prevailing method of chain initiation in CCTP is *via* [Co(III)-H] initiation, leading to the loss of one vinyl group per chain, at the point of initiation. The second method of initiation is typical free radical *via* azo initiation, with the loss of one vinyl group per chain at the point of initiation and addition of an initiator fragment to the molecule. Loss of vinyl functionality *via* initiation however, is unavoidable. The leading mechanisms that may lead to problematic levels of vinyl functionality loss include termination and disproportionation reactions.

As chain transfer dominates in CCTP, chains are predominately terminated by a chain transfer mechanism, yielding a dormant species possessing terminal vinyl functionality (Chapter 2.1). Termination can also occur by azo initiator; where by growing radical chains react with initiator radicals halting polymerisation, leading to the loss of vinyl end groups (Figure 3.1).

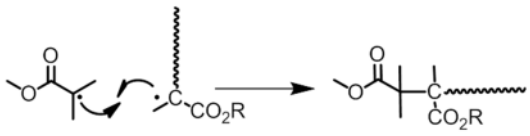

Figure 3.1: Termination of polymers *via* azo initiator V-601, leading to loss of vinyl groups

In methacrylates terminal methyl groups allow for facile disproportionation reactions, either leading to unsaturation in the growing polymer chain, the desired product, or saturation of vinyl groups; hence growing polymer chains are susceptible to disproportionation reactions (Figure 3.2). Investigation of these termination and disproportion mechanisms was carried out for EDGMA homopolymer **A**, synthesised by CCTP, by analysis of the relative abundances of isotopic distributions observed in the MALDI-ToF spectrum (Figure 3.3).

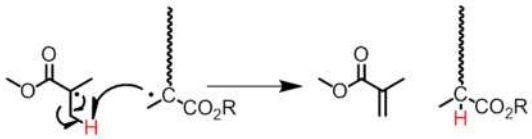

Figure 3.2: Disproportionation of polymer radical chain with primary radicals from V-601.

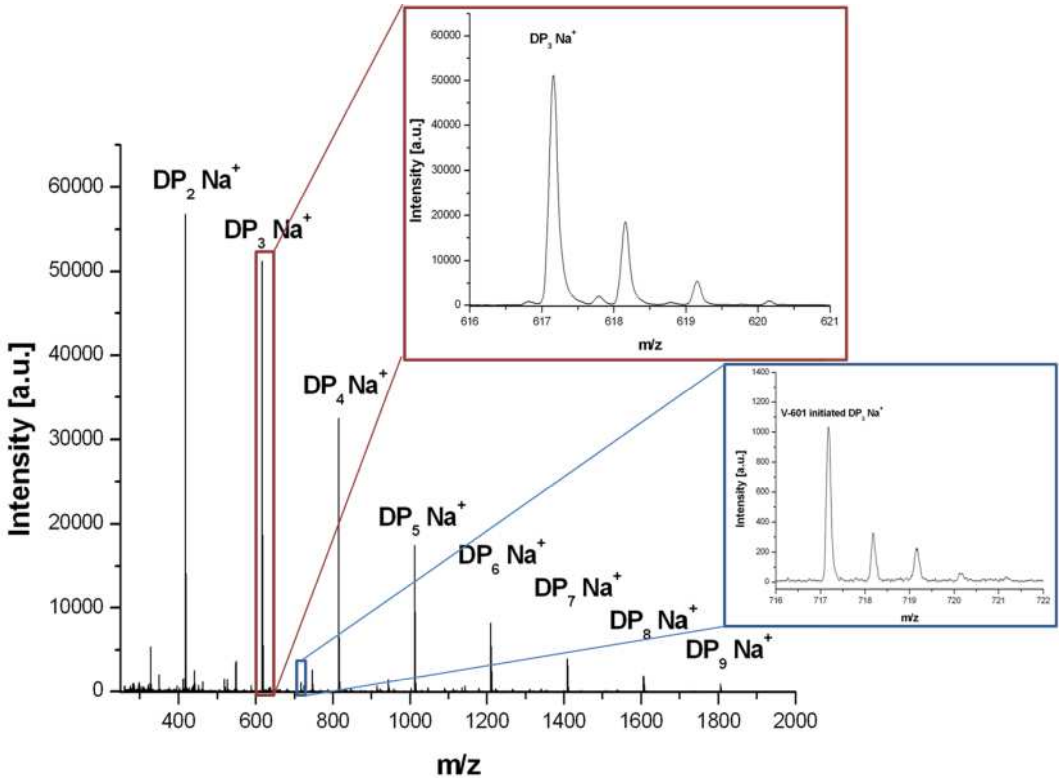

Figure 3.3: MALDI-ToF spectrum of poly-EGDMA A. Zoom regions corresponding to sodiated DP_3 [Co(III)-H] initiated chains (m/z 617.2 Daltons, Figure 3.4 (right)) and sodiated DP_3 V-601 initiated chains (m/z 717.2 Daltons, Figure 3.4 (left))

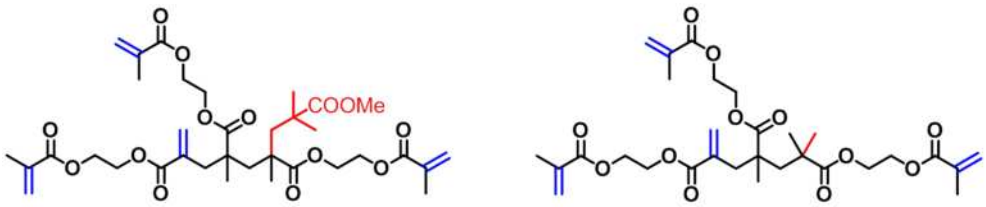

Figure 3.4: (left) Azo initiated (V-601) EGDMA trimer, m/z 594.3 Daltons (sodiated m/z 717.2 Daltons) (right) cobalt(III) hydride initiated EGDMA, m/z 668.3 Daltons (sodiated m/z 6.17.2 Daltons)

Sodiated [Co(III)-H] initiated chains, where termination occurs *via* reaction with primary V-601 radicals, would have a m/z = 719.3 Daltons. Trimer chains corresponding to primary radical initiated chains, with termination by disproportionation, would also possess an m/z of 719.3 and the same loss of vinyl functionality. The presence of these peaks would partially overlap with the mass isotope distribution for sodiated primary radical initiated, chain transfer terminated chains, for which the peak distribution begins at 717.1 Daltons (Figure 3.4 (left)). Investigation of theoretical

relative abundances of the isotopic distribution at 717.17 revealed an increase in the relative intensity observed at 719.16 Daltons, indicative of the presence of a second species corresponding to [Co(III)-H] initiated, primary radical disproportionation terminated chains and/or V-601 initiated chains, with termination by disproportionation (Table 3.1). An higher measured relative abundance is also observed at 720.15 and 721.16, the latter of which can be ascribed to multiple saturations. Peaks at 719.16 and 721.16 constitute approximately 0.1% of the peak distribution, a low level of vinyl loss, although it should be noted that these peaks are of low intensity, hence a higher degree of error is expected.

V-601 Initiated DP_3 Theoretical m/z	Theoretical abundance (%)	V-601 Initiated DP_3 Measured m/z	Measured abundance (%)
717.30	100	717.17	100
718.31	39.0	718.18	32
719.31	10.3	719.16	22
720.31	2.0	720.15	6
721.32	0.3	721.16	4

Table 3.1: Relative abundance data for MALDI-ToF peak series at m/z 717.17 Daltons corresponding to sodiated V-601 initiated EGDMA trimer, with evidence of sodiated [Co(III)-H] initiated, V-601 terminated EGDMA trimer at 719.16 Daltons

Isotopic distributions for peaks corresponding to [Co(III)-H] initiated trimers were also examined, to investigate the level of disproportionation leading to the saturation of vinyl end groups. Each saturated vinyl group will give rise to a value of +2 Daltons compared to the main distribution, causing an overlap of isotopic distributions. Comparison of theoretical abundances to the measured abundances of [Co(III)-H] initiated trimer, it is observed that some saturation may be present at +2 Daltons, approximately 0.02%, as the measured abundance is higher than the theoretical value (Table 3.2). However, a slight increase is also observed at +1 Daltons when compared to the theoretical abundance, which would not arise due to vinyl saturation. Multiple saturations are not observed, indicating a high level of end group fidelity.

Co(III)-H DP_3 Theoretical m/z	Theoretical abundance (%)	Co(III)-H DP_3 Measured m/z	Measured abundance (%)
617.25	100	617.16	100
618.26	33.3	618.16	36
619.26	7.9	619.16	11
620.26	1.4	620.16	2
621.26	0.2	621.16	0

Table 3.2: Relative abundance data for MALDI-ToF peak series at m/z 617.16 Daltons corresponding to sodiated [Co(III)-H] initiated EGDMA trimer, with evidence of saturation of vinyl groups at +2 Daltons

Although MALDI-ToF is indicative of a low level of vinyl group saturation, with examples given for DP_3 chains (Table 3.1 & Table 3.2), the overall vinyl group retention remains high (~99%), with the majority of chains possessing DP_n+1 vinyl groups.

3.2.2 Initial Study - Functionalisation of Poly-EGDMA via Thiol-Michael Addition

Due to an observable aromatic group, which has the added benefit of a UV absorption at approximately 290 nm, benzyl mercaptan was used for initial studies on the functionalisation of poly-EGDMA. As thiol-Michael addition can be conducted under ambient conditions this method was chosen for the functionalisation of poly-EGDMA, utilising DMPP as the catalyst due to reports of its superior efficiency. The formation of DMPP adducts are expected for these reactions, as consumption of DMPP is necessary for generation of thiolate anions, hence the more DMPP employed in these reactions, the more prevalent DMPP adducts are in the product.

The initial choice of solvent for the phosphine mediated thiol-Michael addition of benzyl mercaptan to poly-EGDMA was the polymerisation solvent 1,2-dichloroethane (DCE), as if successful, a one pot system could be developed whereby polymer solutions could be functionalised without the need for excessive purification. For initial studies however, all volatiles were removed in vacuo to ascertain accurate polymer masses for the calculation of the average number of vinyl group in the system. MALDI-ToF analysis confirmed the majority of chains possess DP_n+1 vinyl groups per chain. Analysis of poly-EGDMA **A** by SEC allows the calculation of the average DP_n of the polymer as both a number average and weight average. Due to the broad PDi

associated with polymerisations where chain transfer is the dominating mechanism, average values of vinyl group functionality should provide the best estimations of vinyl groups, based on DP_n+1 vinyl functionality (Table 3.3).

Name	M_n ($g.mol^{-1}$)	M_w ($g.mol^{-1}$)	PDi	Number Average Vinyl Groups	Weight Average Vinyl Groups
A	1100	2300	2.2	6.5	12.6

Table 3.3: Calculation of vinyl groups *via* SEC, based on DP_n+1 vinyl functionality using equations Equation 3.1 & Equation 3.2

The ratio of vinyl groups per chain, DP_n+1, to the DP_n of EGDMA was used to calculate the number and weight average moles of vinyl group per chain for further calculation of mole equivalents of thiol and DMPP using Equation 3.1 and Equation 3.2

$$\frac{DP_n + 1}{DP_n} = x$$

Equation 3.1: Calculation of the ratio of vinyl groups per chain to EGDMA per chain, x

$$n(EGDMA)x = n(Vinyl)$$

Equation 3.2: Calculation of average moles of vinyl groups, where n(EGDMA) is moles of EGDMA and n(vinyl) is moles of vinyl functionality

Either M_n or M_w can be used for the calculation of thiol and catalyst equivalents, both producing similar results. Calculations were conducted using M_n's and the equivalents of thiol back calculated for M_w's, as use of a number average value will provide an excess based on the most prevalent DP_n, providing a higher level of thiol excess based on weight average calculations (Table 3.4).

	Number Average Calculations		Weight Average Calculations	
Thiol	**Thiol (mol eq.)**	**DMPP (mol eq.)**	**Thiol (mol eq.)**	**DMPP (mol eq.)**
Benzyl Mercaptan	1.60	0.22	1.75	0.24

Table 3.4: Mole equivalents of benzyl mercaptan and DMPP used in initial functionalisation of poly-EGDMA A *via* phosphine mediated thiol-Michael addition.

The solutions obtained from the homopolymerisation of EGDMA are yellow/orange in colour, due to the higher levels of CoBF catalyst used (Chapter 2.2.1). On addition of DMPP to these solutions, a colour change from yellow/orange to green/brown is observed indicating the formation of a complex of DMPP, resulting in this colour change. On addition of pure DMPP to CoBF a dramatic colour change is seen from CoBF as a dark orange/brown to a deep blue/green, shaking of this solution or addition of large amounts of solvent leads to a further colour change to green/brown (Figure 3.5). A number of accounts documenting complexes of Co(II/III) compounds with phosphines are found in literature.[285-289] CoBF is a paramagnetic Co(II) complex and hence it cannot be characterised by NMR. It was postulated that if DMPP complexation occurred this would lead to a change in oxidation state change, hence the appearance of peaks corresponding to CoBF in the ^{1}H NMR spectrum. Although minor peak shifts *via* ^{1}H NMR are observed, giving an indication of some change taking place, no conclusive proof of complexation is obtained, suggesting that perhaps DMPP is acting as a ligand, this may also explain the colour change on addition of large quantities of solvent, as displacement of DMPP ligands at high concentrations is likely.

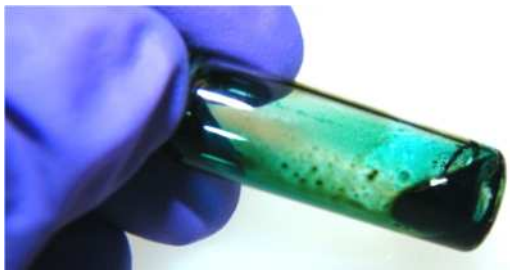

Figure 3.5: Colour change of CoBF from orange/brown powder to green/blue solution on the addition of pure colourless DMPP

The phosphine mediated thiol-Michael addition of benzyl mercaptan to poly-EGDMA (**A**) was attempted in DCE, using a 1.6 mol equivalent excess of benzyl mercaptan and 0.22 mol equivalent excess of DMPP to vinyl groups, based on a number average DP_n. A large reduction in vinyl peaks at 5.59, 6.12 and 6.24 ppm was observed by ^{1}H NMR, indicating the loss of both internal and external vinyl functionality, however, the reaction did not go to completion, reaching approximately 86% conversion overnight (Figure 3.6), with both internal and external vinyl groups remaining.

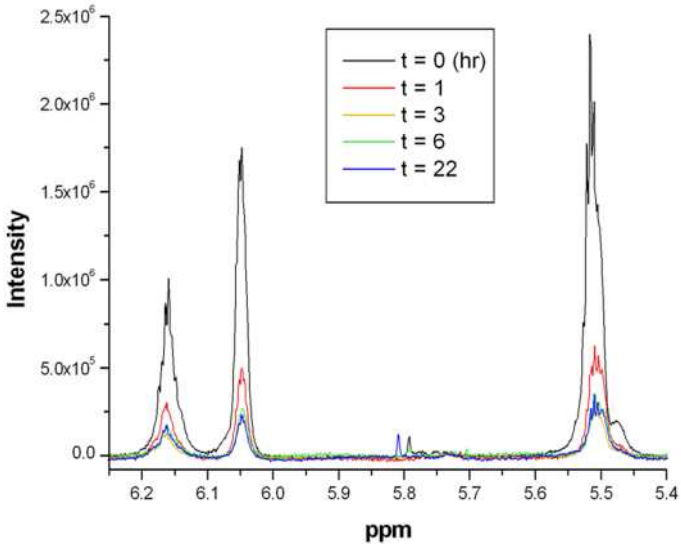

Figure 3.6: ^{1}H NMR monitoring of vinyl region for the thiol-Michael addition of benzyl mercaptan to poly-EGDMA A in DCE

The appearance of multiplet peaks at 2.4-2.8 ppm in the ^{1}H NMR spectrum also arises, corresponding to both the hydrothiolation of vinyl groups and the nucleophilic addition of DMPP to vinyl groups, with splitting of backbone CH_2 peaks adjacent to vinyl groups also observed, as illustrated in Figure 3.7.

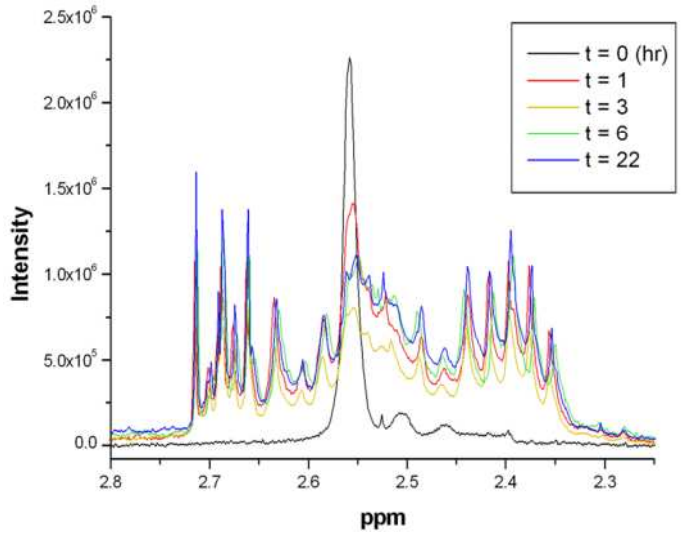

Figure 3.7: ^{1}H NMR monitoring of CH_2 region for the thiol-Michael addition of benzyl mercaptan to poly-EGDMA A in DCE

In order to increase the level of vinyl functionalisation in the thiol-Michael addition of benzyl mercaptan to poly-EGDMA the level of DMPP for this reaction could be increased, however, this would likely lead to an increase in the level of DMPP reaction

and undesired by-products; hence, an alternative solvent was used. Use of highly polar aprotic solvents such as DMSO and DMF has been shown to promote the dissociation of thiols into their corresponding thiolate anions;[196, 200, 290] hence DMSO was tested as a solvent. Use of DMSO as a solvent sees the rapid increase in the rate of the thiol-Michael addition of benzyl mercaptan to Poly-EGDMA and a complete loss of vinyl groups is observed by ^{1}H NMR within 1 hour, yielding polymer **A1** (Figure 3.8). The stark change in reaction rate on changing solvent from DCE to DMSO highlights the importance of solvent choice for thiol-Michael addition reactions; a further advantage to use of DMSO is that it is widely solvating, solubilising a range of hydrophobic and hydrophilic molecules.

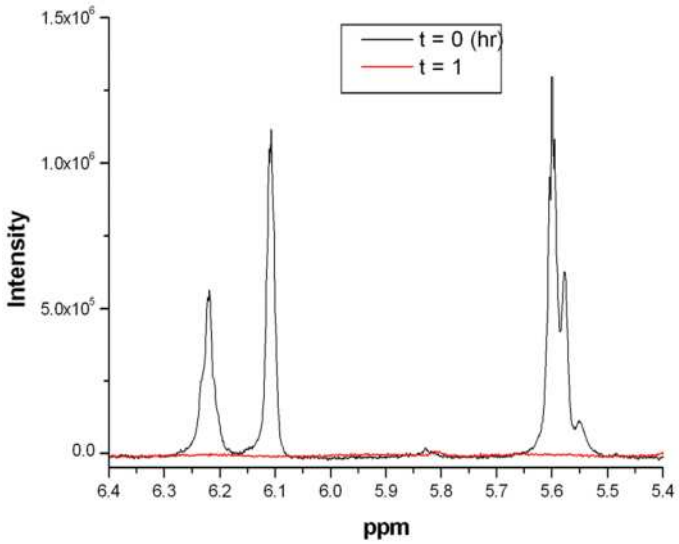

Figure 3.8: ^{1}H NMR monitoring of A1 vinyl region for the thiol-Michael addition of benzyl mercaptan to poly-EGDMA A in DMSO

Due to strong DMSO solvent peaks at approximately 2.5 ppm, investigation of the multiplet peaks observed *via* ^{1}H NMR at 2.3-2.7 ppm was not possible until DMSO had been removed from the reaction mixture by either rotary evaporation or by precipitation. On removal of DMSO, ^{1}H NMR peaks corresponding to the hydrothiolation of vinyl groups is confirmed (Figure 3.9).

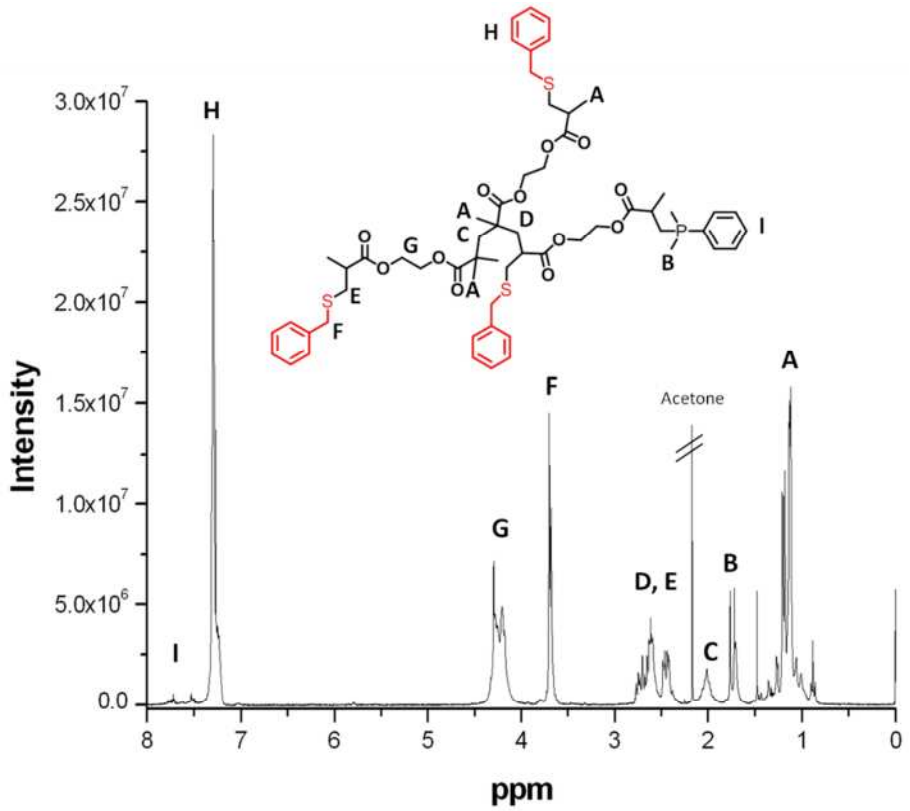

Figure 3.9: ^{1}H NMR of precipitated benzyl mercaptan functionalised poly-EGDMA, A1, (1 mol eq. vinyl groups, 1.6 mol eq. Benzyl mercaptan, 0.22 mol eq. DMPP). ^{1}H NMR spectrum in $CDCl_3$

On addition of benzyl mercaptan to poly-EGDMA (**A**) a small increase in molecular weight is observed *via* SEC (Table 3.5, Figure 3.10), further confirmation of addition of benzyl mercaptan to the polymer.

Name	M_n ($g.mol^{-1}$)	M_w ($g.mol^{-1}$)	*PDi*
A	*1200*	*2300*	*2.0*
A1	*1400*	*2400*	*1.8*

Table 3.5: Molecular weight data obtained *via* conventional SEC of poly-EGDMA A and its thiol-Michael addition with benzyl mercaptan, A1

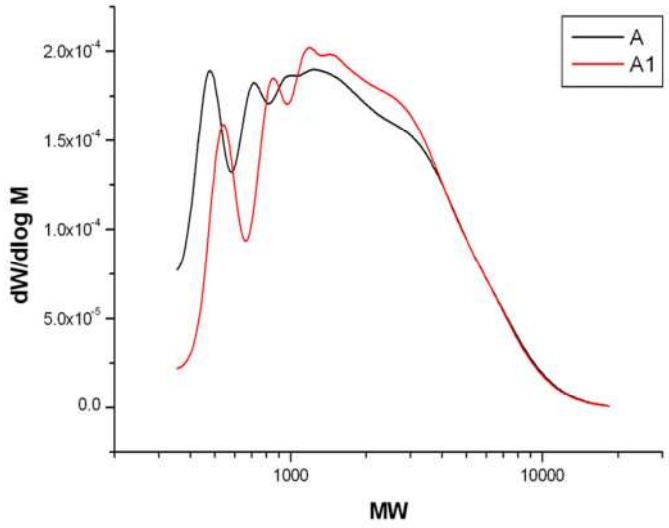

Figure 3.10: SEC comparison of unfunctionalised poly-EGDMA (A) and benzyl mercaptan functionalised poly-EGDMA (A1)

Photodiode array (PDA) detection was used in series with RI detection, for comparison of the unfunctionalised poly-EGDMA (**A**) and benzyl mercaptan functionalised poly-EGDMA (**A1**). On investigation of the PDA spectrum of unfunctionalised poly-EGDMA (**A**) a chromophore at λ = 280 nm is observed at 18 minutes retention time corresponding to the SEC eluent, THF. A strong absorbance is also seen at approximately 17 minutes retention time, with a broad absorbance of between λ = 380 and 500 nm. This retention time corresponds to the low molecular weight region of the spectrum, indicating the chromophore originates from a small molecule (Figure 3.11); comparison of this peak to a PDA spectrum of CoBF reveals that the chromophore originates from CoBF, as a result of the high level of CoBF employed in the polymerisation and the intense colour of the solution. No chromophore is observed corresponding to the retention time for the polymer, 14-17 minutes confirmed by RI detection, indicating the unfunctionalised polymer contains no UV active groups.

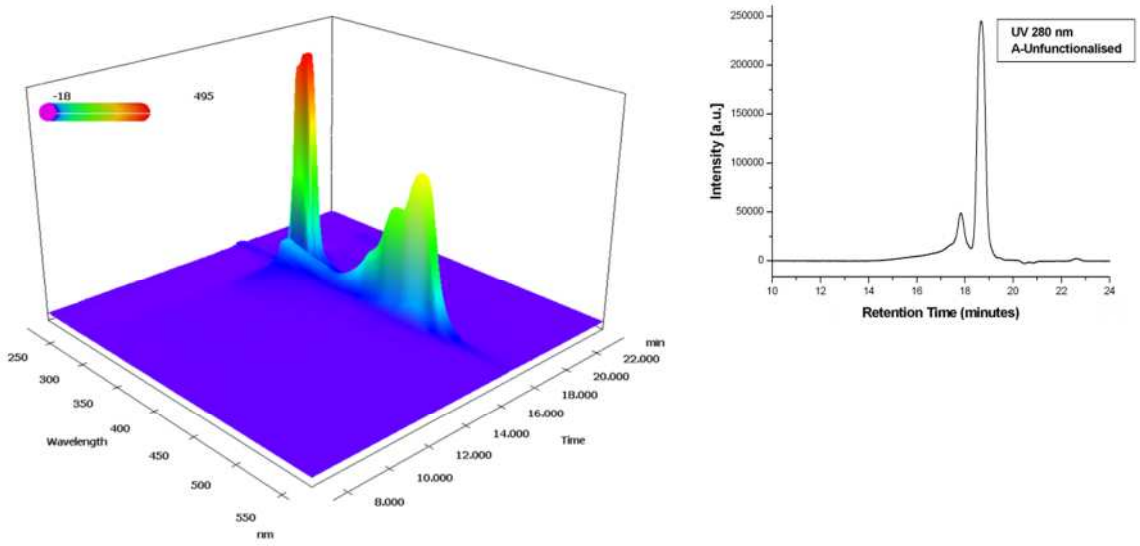

Figure 3.11: (left) SEC PDA spectrum of poly-EGDMA A. Absorbance at 18 minutes retention time, λ = 280 nm corresponding to THF, absorbance at 17 minutes retention time, λ = 380-500 nm corresponding to CoBF (right) SEC UV chromatogram extraction of data from PDA at λ 280 nm

Analysis of the PDA spectrum for benzyl mercaptan functionalised poly-EGDMA (**A1**) a chromophore at approximately 14-17 minutes retention time, λ = 290 nm was seen, corresponding to the retention time of the polymer, confirmed by RI detection, which indicates attachment of a UV active group to the polymer on addition of benzyl mercaptan. A low UV absorbance was also observed at approximately 17 minutes retention time, 380-500 nm, due to the presence of high levels of CoBF in solution (Figure 3.12).

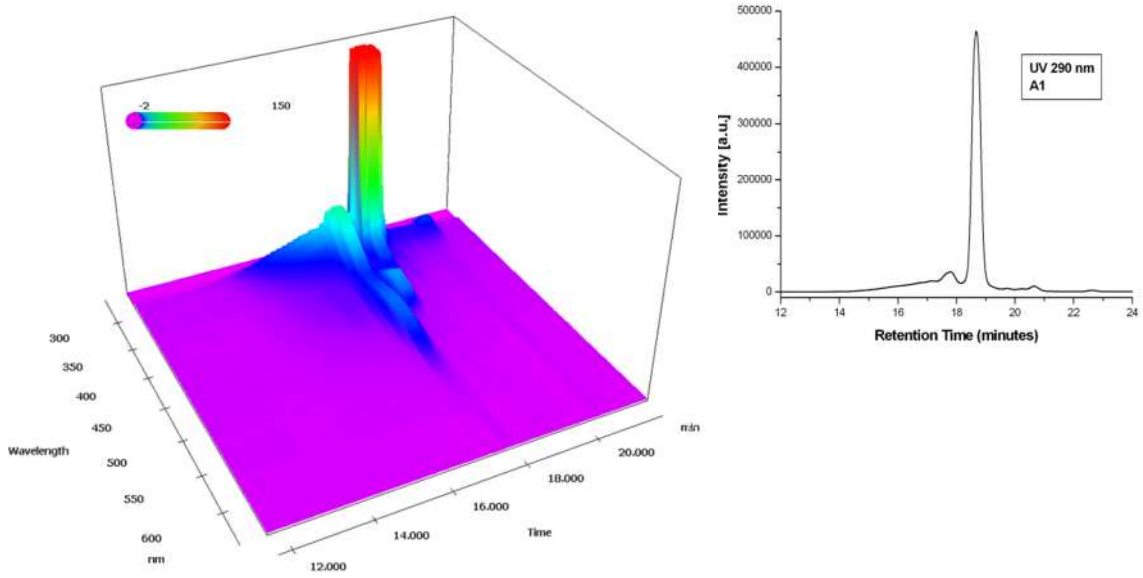

Figure 3.12: (left) SEC PDA spectrum of benzyl mercaptan functionalised poly-EGDMA A1 (0.22 mol eq. DMPP to vinyl groups). Absorbance at 18 minutes retention time, λ = 290 nm corresponding to THF eluent, absorbance at 17 minutes retention time, λ = 380-500 nm corresponding to CoBF, absorbance at 17-14 minutes retention time, λ = 290 nm corresponding to attachment of a chromophore to the polymer chain (right) UV chromatogram extraction of data from PDA at λ 290 nm

Assessment of the level of DMPP adducts formed in the thiol-Michael addition of benzyl mercaptan to poly-EGDMA *via* ^{1}H NMR and SEC with PDA detection is not trivial. DMPP signals arising in ^{1}H NMR are of low concentration, with partially overlapping peaks with both the aromatic groups arising from benzyl mercaptan and polymeric methyl groups, also both DMPP and benzyl mercaptan possess a chromophore at approximately λ = 290 nm due to their aromatic functionality, making the two products indiscernible *via* PDA detection. Hence, MALDI-ToF was employed for the investigation of **A1** (Figure 3.13).

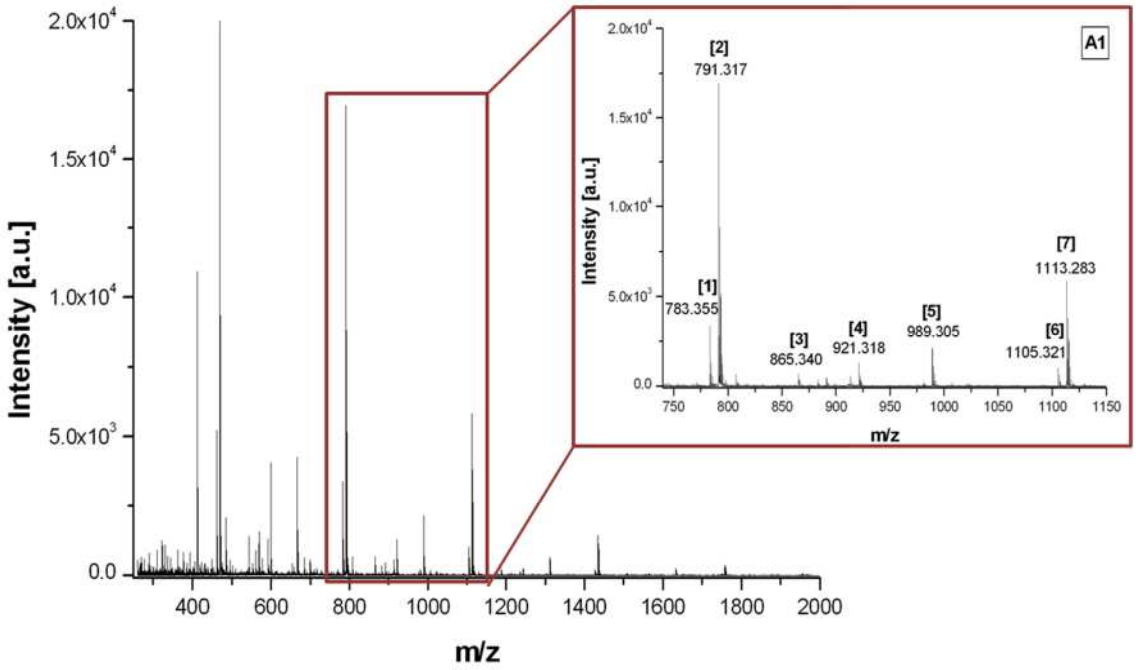

Figure 3.13: MALDI-ToF spectrum of A1, thiol-Michael addition of benzyl mercaptan to poly-EGDMA (A) (1.6 mol eq. benzyl mercaptan, 0.22 mol eq. DMPP to vinyl groups). Zoom region between 750 and 1150 Daltons. Annotations correspond to Table 3.6

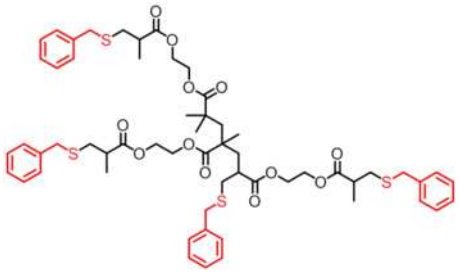

Figure 3.14: Example Structure of benzyl mercaptan functionalised poly-EGDMA, $(EGDMA)_3(BM)_4$

Name	Corresponding Structure	Theoretical m/z	Measured m/z
[A1: 1]	$(EGDMA)_2(BM)_2(DMPP)_1H^+$	783.31	783.35
[A1: 2]	$(EGDMA)_2(BM)_3Na^+$	791.27	791.31
[A1: 3]	$(EGDMA)_3(BM)_2Na^+$	865.32	865.34
[A1: 4]	$(HEMA)_1(EGDMA)_2(BM)_3Na^+$	921.33	921.31
[A1: 5]	$(EGDMA)_3(BM)_3Na^+$	989.36	989.30
[A1: 6]	$(EGDMA)_3(BM)_3(DMPP)_1H^+$	1105.43	1105.32
[A1: 7]	$(EGDMA)_3(BM)_4Na^+$	1113.39	1113.28

Table 3.6: Corresponding structures to MALDI-ToF peaks annotated in Figure 3.13 for A1 thiol-Michael addition of benzyl mercaptan to poly-EGDMA A in DMSO. m/z region 750-1150 Daltons. BM-benzyl mercaptan, HEMA-hydroxyethyl methacrylate (monomer impurity). Example structure given in Figure 3.14

Several peak distributions are present in the MALDI-ToF spectrum (Figure 3.13). The most intense peak series correlates to poly-EGDMA of increasing molecular weight containing DP_n+1 benzyl mercaptan units, **[A1: 2**, **7]** (Table 3.6). Minor peak series' correlate to poly-EGDMA of increasing molecular weight with DP_n-1 benzyl mercaptan units plus one DMPP unit per chain, with ionisation by H^+ **[A1: 1**, **6]**. Ionisation of polymer chains by H^+ is only observed when DMPP is present on the chain, due to zwitterion formation on the addition of DMPP to vinyl groups. Minor peak series' are also observed correlating to the incomplete functionalisation of poly-EGDMA with benzyl mercaptan, both DP_n-1 **[A1: 5]** and DP_n-2 **[A1: 3]** benzyl mercaptan functionalised structures are observed. Minor peaks correlating to the incorporation of one HEMA unit, a monomer impurity seen in the original MALDI-ToF spectrum of poly-EGDMA (**A**), with full functionalisation of vinyl groups with benzyl mercaptan **[A1: 4]** is also observed.

The presence of saturated species observed in the MALDI-ToF of unfunctionalised EGDMA homopolymer **A** were investigated, as these saturated groups would lead to incomplete functionalisations with benzyl mercaptan. Peaks were observed for incomplete functionalisation products **[A1: 5]**, whereby one vinyl group remains in the polymer, if saturated vinyl groups are present these would have an increased mass of +2 Daltons for each vinyl saturation. Relative intensities of functionalised dimer and trimer peaks were calculated and compared to the measured values in order to quantify the level of saturation observed in the products. Measured relative intensities correlate fairly well with calculated values, these peaks are minor peaks however and as a consequence suffer from a low signal to noise ratio. Although no increase in measured relative intensity is observed at +2 Daltons, indicating low levels of saturated products for these peak series' (Table 3.7).

$(EGDMA)_2(BM)_2Na^+$ Relative Intensities		$(EGDMA)_3(BM)_3Na^+$ Relative Intensities	
Theoretical	**Measured**	**Theoretical**	**Measured**
100.0	100	100.0	100
39.2	38	58.8	53
18.2	19	33.0	32
5.0	5	12.5	14
1.3	3	4.1	4
0.3	2	1.1	2
		0.3	0

Table 3.7: Comparison of the calculated and measured relative abundances of incompletely functionalised poly-EGDMA with benzyl mercaptan (A1). Investigation into the presence of saturated products in the MALDI-ToF spectrum

Calculation of the average number of vinyl groups per chains suggests value of 6.5 based on a number average calculation. Assuming that each DMPP employed in the thiol-Michael addition reaction forms a conjugate, an average of 1.4 DMPP units per chain is expected; based on a weight average calculations this value is significantly higher, with 3 DMPP adducts per chain is expected. These expected values are higher than the values observed *via* MALDI-ToF, in which the highest level of DMPP conjugation observed is one unit per chain, comprising a minor peak series of approximately 20% intensity compare to the major peak series. This suggests that only a small portion of DMPP is participating in the thiol-Michael addition, and that a maximum number of one DMPP adducts can be incorporated per chain. However, this result may be due to an inhomogeneous crystallisation of product on preparation of MALDI-ToF samples, as at extremely high matrix and salt concentrations (HC) an alternative spectrum is observed, whereby DMPP adducts form the major peak series (Figure 3.15, Table 3.8). This inhomogeneity of spectra was kept in mind on analysis of these products, but characterisation using low or normal matrix/salt concentrations for this technique were favoured, due to risk of saturation of the detector, it must be noted however that DMPP adducts are not quantitative in this case. Minor peak series' also differ in that V-601 initiated chains are observed **[A1(HC): 3]**, and that the majority of minor peaks contain one DMPP unit with ionisation by H^+ **[A1(HC): 3**, **5]**.

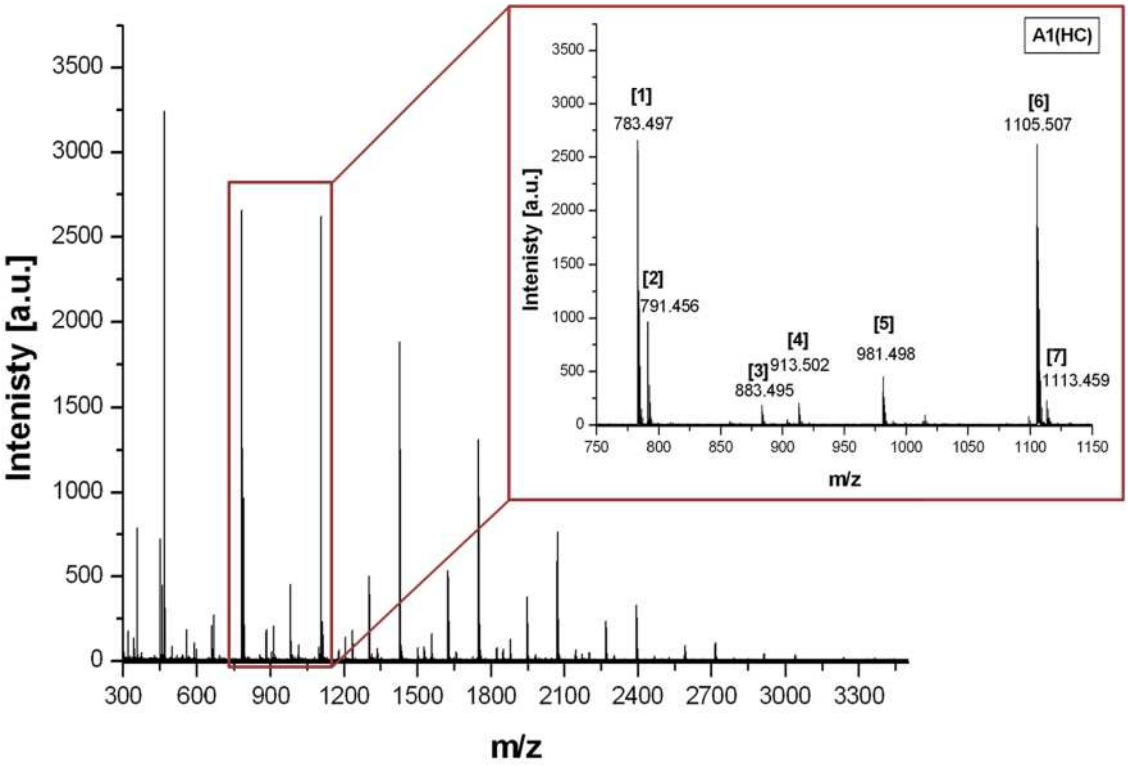

Figure 3.15: High matrix/salt concentration (HC) MALDI-ToF spectrum of A1, poly-EGDMA thiol-Michael addition with benzyl mercaptan (1.6 mol eq. benzyl mercaptan, 0.22 mol eq. DMPP to vinyl groups). Zoom region between 750 and 1150 Daltons. Annotations correspond to Table 3.8

Name	Corresponding Structure	Theoretical m/z	Measured m/z
[A1(HC): 1]	$(EGDMA)_2(BM)_2(DMPP)_1H^+$	783.31	783.49
[A1(HC): 2]	$(EGDMA)_2(BM)_3Na^+$	791.27	791.45
[A1(HC): 3]	V-601initiated$(EGDMA)_2(BM)_2(DMPP)_1H^+$	883.36	883.49
[A1(HC): 4]	$(HEMA)_1(EGDMA)_2(BM)_2(DMPP)_1H^+$	913.37	913.50
[A1(HC): 5]	$(EGDMA)_3(BM)_2(DMPP)_1H^+$	981.40	981.49
[A1(HC): 6]	$(EGDMA)_3(BM)_3(DMPP)_1H^+$	1105.43	1105.50
[A1(HC): 7]	$(EGDMA)_3(BM)_4Na^+$	1113.39	1113.45

Table 3.8: Corresponding structures to MALDI-ToF peaks (high matrix/salt concentration, HC) annotated in Figure 3.15 for A1, thiol-Michael addition of benzyl mercaptan to poly-EGDMA A in DMSO. Zoom region between 750 and 1150 Daltons BM-benzyl mercaptan, HEMA-hydroxyethyl methacrylate (monomer impurity). Example spectrum given in Figure 3.14

Functionalisation of branched poly-EGDMA **A** was successful; MALDI-ToF analysis reveals the formation of a range of products. Although DMPP adducts cannot be quantified *via* MALDI-ToF, if it is assumed that the level of DMPP incorporated into the

polymer is approximated to the amount employed, hence, the reduction of DMPP is necessary in order to obtain more homogenous functionalisation.

3.2.3 Optimisation of the Thiol-Michael Addition of Benzyl Mercaptan to Poly-EGDMA- Reduction in DMPP Concentration

Reduction of the DMPP concentration was attempted, in order to reduce the potential level of DMPP-polymer conjugation in the thiol-Michael addition of benzyl mercaptan to poly-EGDMA A, employing 0.10, 0.05 and 0.01 mole equivalents of DMPP to vinyl groups in DMSO (Table 3.9).

		Number Average Calculations		Weight Average Calculations	
Name	**Thiol**	**Thiol (mol eq.)**	**DMPP (mol eq.)**	**Thiol (mol eq.)**	**DMPP (mol eq.)**
A2	Benzyl Mercaptan	1.60	0.10	1.75	0.12
A3	Benzyl Mercaptan	1.60	0.05	1.75	0.06
A4	Benzyl Mercaptan	1.60	0.01	1.75	0.01

Table 3.9: Mol eq. of benzyl mercaptan and DMPP to vinyl groups for the thiol-Michael addition of benzyl mercaptan to poly-EGDMA A, reduced levels of DMPP

On reduction of the level of DMPP, an increase in reaction time observed by ^{1}H NMR and reduction of DMPP-polymer conjugates observed *via* MALDI-ToF was expected. Thiol-Michael addition of benzyl mercaptan to poly-EGDMA A using 0.10 (**A2**) and 0.05 (**A3**) mole equivalents of DMPP to vinyl groups was attempted, with confirmation of complete functionalisation of vinyl groups observed within one hour *via* ^{1}H NMR. Using 0.01 mole equivalents of DMPP to vinyl groups (**A4**) a conversion of approximately 98% was seen within 1 hour, with full functionalisation of vinyl groups confirmed within 2 hours (Figure 3.16) and hence no significant effect on the rate of reaction is observed on reduction of the concentration of DMPP to low levels.

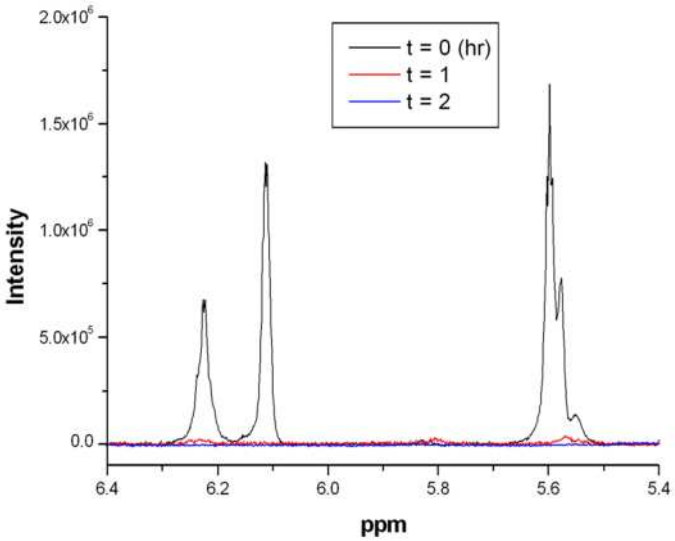

Figure 3.16: ^{1}H NMR monitoring of A4, thiol-Michael addition of benzyl mercaptan to poly-EGDMA A. Zoom of vinyl region between 5.4 and 6.4 ppm (1.6 mol eq. benzyl mercaptan, 0.01 mol eq. DMPP to vinyl groups). Complete disappearance of vinyl peaks at 2 hour reaction time

An increase in molecular weight is observed on comparison of the SEC spectra of unfunctionalised poly-EGDMA **A** and thiol-Michael addition products **A1**-**A4,** indicating addition of benzyl mercaptan to the polymer (Table 3.10, Figure 3.17).

Name	DMPP (mol eq.)	M_n ($g.mol^{-1}$)	M_w ($g.mol^{-1}$)	PDi
A	N/A	1200	2300	2.0
A1	0.22	1400	2400	1.8
A2	0.10	1400	2600	1.9
A3	0.05	1600	2800	1.8
A4	0.01	1600	2700	1.8

Table 3.10: Molecular weight comparison of poly-EGDMA A with benzyl mercaptan functionalised thiol-Michael addition products A1-A4. Molecular weights obtained *via* conventional SEC

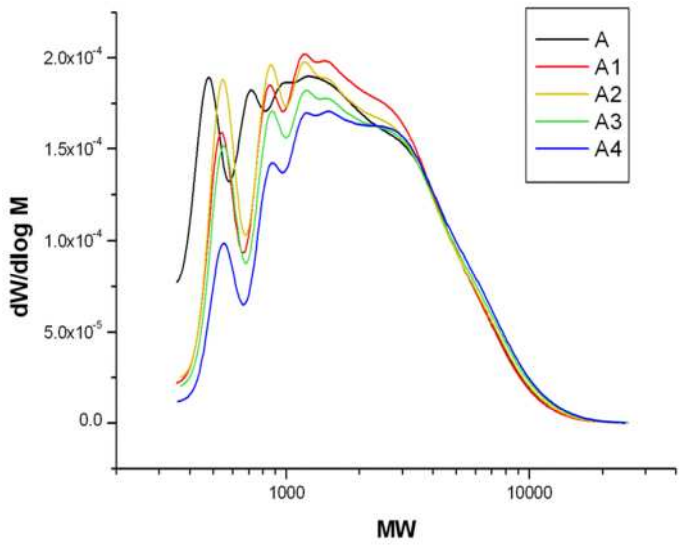

Figure 3.17: SEC comparison of A to A1-A4. Thiol-Michael additions of benzyl mercaptan to poly-EGDMA (A). A1 0.22 mol eq. DMPP to vinyl groups, A2 0.10 mol eq. DMPP to vinyl groups, A3 0.05 mol eq. DMPP to vinyl groups, A4 0.01 mol eq. DMPP to vinyl groups

Addition of a chromophore to the polymer is also confirmed by SEC analysis with PDA detection. A chromophore is observed between 17-14 minutes retention time at 290 nm, indicating attachment of a UV active species to the polymer, with absorbance's seen at 17 minutes retention time between λ = 380-500 nm, corresponding to CoBF and an absorbance at 18 minutes retention time at λ = 290 nm corresponding to THF. A typical PDA spectrum is given in Figure 3.18.

.

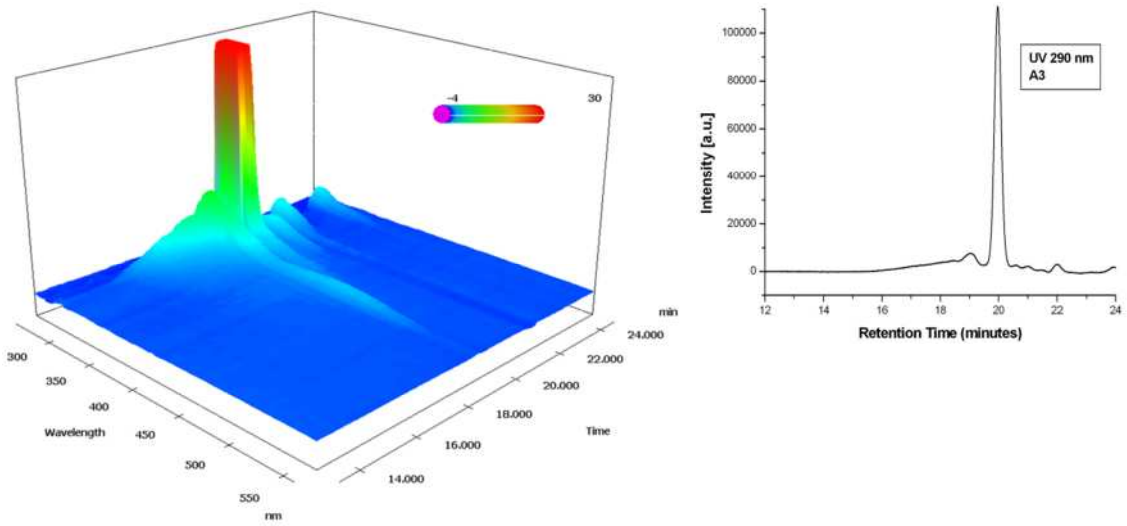

Figure 3.18: (left) SEC with PDA detection for A3, thiol-Michael addition of benzyl mercaptan to poly-EGDMA A (0.05 mol eq. DMPP to vinyl groups). Absorbance at 18 minutes retention time, 290 nm corresponding to THF eluent, absorbance at 17 minutes retention time, λ = 380-500 nm corresponding to CoBF, absorbance at 17-14 minutes retention time, λ = 290 nm corresponding to attachment of a chromophore to the polymer chain. (right) UV chromatogram extraction of data from PDA at λ 290 nm

Based on the calculation of vinyl groups using Equation 3.1 and Equation 3.2 the number average value of vinyl groups is 6.5 per chain, hence using 0.10 mole equivalents of DMPP to vinyl groups (**A2**) an average of 0.65 DMPP-polymer conjugates is expected, if every mole of DMPP employed participates in the thiol-Michael addition. Based on a weight average the average number of vinyl groups per chain is 12.5 vinyl groups per chain, using 0.10 mole equivalents of DMPP to vinyl groups leads to an expected value of 1.5 DMPP-polymer conjugates per chain. Investigation of **A2** by MALDI-ToF, as previously discussed, cannot give quantitative information on the level of DMPP adducts, but may allude to any structural defects arising from the reduction in the level of DMPP on the thiol-Michael addition of benzyl mercaptan to the poly-EGDMA **A** (Figure 3.19, Table 3.11).

The MALDI-ToF spectrum of **A2** shows a similar level of incompletely functionalised polymer to **A1**, indicating that the level of DMPP can be reduced without causing detrimental effects to the level of functionalisation. The most abundant peak series' observed in the spectrum correspond to poly-EGDMA fully functionalised with benzyl mercaptan **[A2: 2, 7]**, and full functionalisation incorporating a single DMPP-polymer

conjugate, with remaining vinyl groups functionalised with benzyl mercaptan **[A2: 1, 6]**. Minor peaks series' corresponding to poly-EGDMA, containing one unfunctionalised vinyl group **[A2: 4, 5]**, with no evidence of multiple vinyl groups remaining. An increase in the apparent level of DMPP-polymer conjugates is observed, with higher peak intensities than previously observed in the MALDI-ToF spectrum of **A1**, however, this increase is believed not to be quantitative (Figure 3.19, Table 3.11).

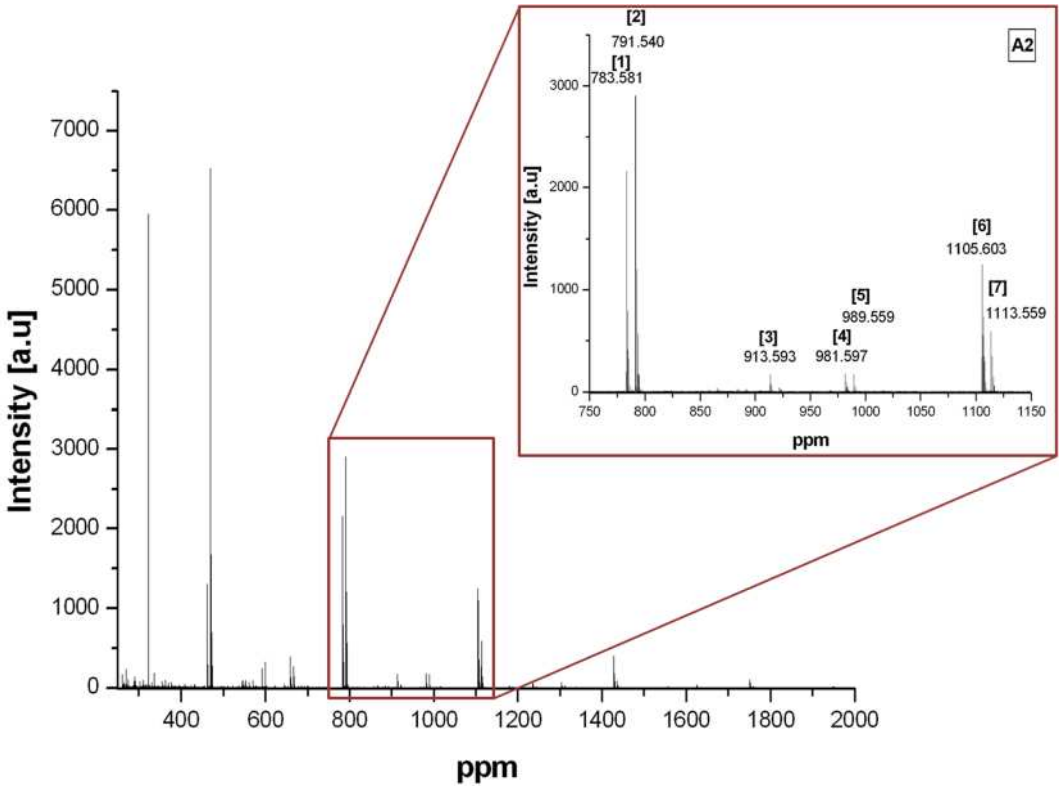

Figure 3.19: MALDI-ToF spectrum of A2, thiol-Michael addition of benzyl mercaptan to poly-EGDMA (A) (1.6 mol eq. benzyl mercaptan, 0.10 mol eq. DMPP to vinyl groups). Zoom region between 750 and 1150 Daltons. Annotations correspond to Table 3.11

Name	Corresponding Structure	Theoretical m/z	Measured m/z
[A2: 1]	$(EGDMA)_2(BM)_2(DMPP)_1H^+$	783.31	783.58
[A2: 2]	$(EGDMA)_2(BM)_3Na^+$	791.27	791.54
[A2: 3]	$(HEMA)_1(EGDMA)_2(BM)_2(DMPP)_1H^+$	913.37	913.59
[A2: 4]	$(EGDMA)_3(BM)_2(DMPP)_1H^+$	981.40	981.59
[A2: 5]	$(EGDMA)_3(BM)_3Na^+$	989.36	989.55
[A2: 6]	$(EGDMA)_3(BM)_3(DMPP)_1H^+$	1105.43	1105.60
[A2: 7]	$(EGDMA)_3(BM)_4Na^+$	1113.39	1113.55

Table 3.11: Corresponding structures to MALDI-ToF peaks annotated in Figure 3.19 for A2, thiol-Michael addition of benzyl mercaptan to poly-EGDMA A in DMSO. Mass region 750-1150 Daltons BM-benzyl mercaptan, HEMA-hydroxyethyl methacrylate (monomer impurity). Example structure given in Figure 3.14

On further reduction of the DMPP concentration to 0.05 (**A3**) and 0.01 (**A4**) mole equivalents to vinyl groups, no change is observed in the MALDI-ToF spectra (Figure 3.20, Table 3.12 and Figure 3.21, Table 3.13), indicating that reduction of the level of DMPP, even to low levels such as 1%, does not appear to effect the level of functionalisation achieved in the thiol-Michael addition of benzyl mercaptan to poly-EGDMA **A**. Use of 0.05 mole equivalents of DMPP should, as a number average based on the level of vinyl groups calculated *via* SEC results, yield 0.33 DMPP units per chain. As a weight average 0.63 DMPP-polymer conjugates are expected per chain. At 0.01 mole equivalents these values are reduced to 0.007 and 0.013 respectively.

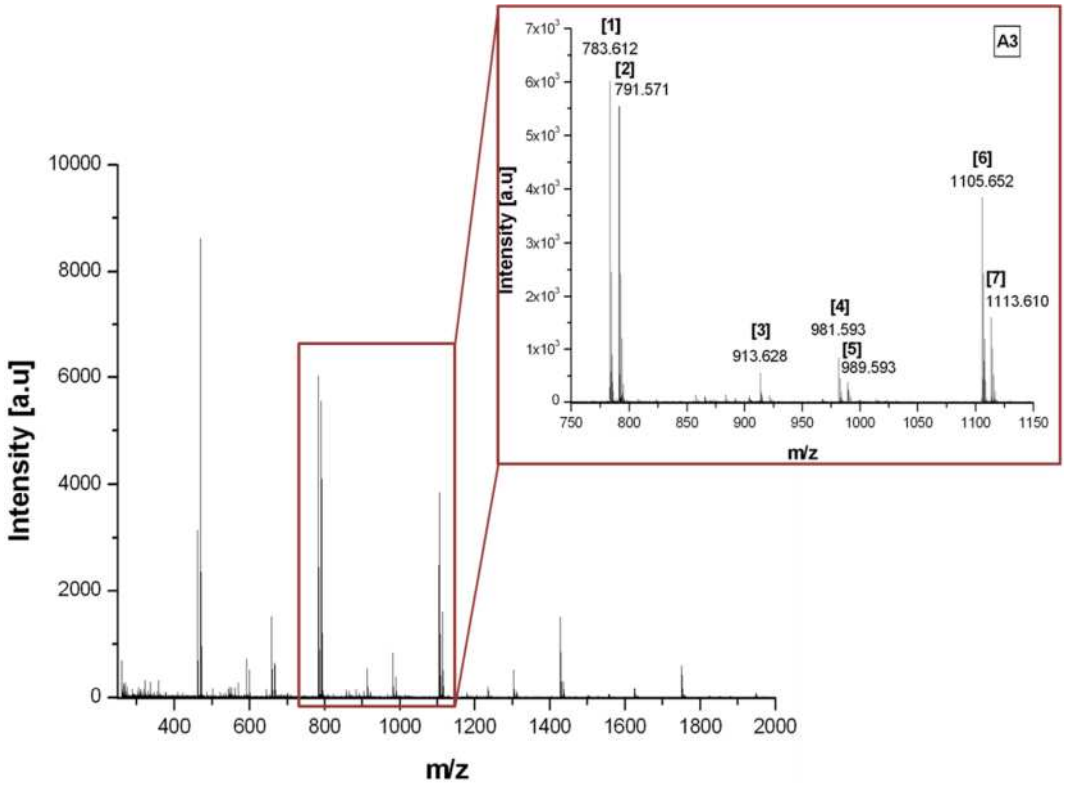

Figure 3.20: MALDI-ToF spectrum of A3, thiol-Michael addition of benzyl mercaptan to poly-EGDMA (1.6 mol eq. benzyl mercaptan, 0.05 mol eq. DMPP to vinyl groups). Zoom region between 750 and 1150 Daltons. Annotations correspond to Table 3.12

Name	Corresponding Structure	Theoretical m/z	Measured m/z
[A3: 1]	$(EGDMA)_2(BM)_2(DMPP)_1H^+$	783.31	783.61
[A3: 2]	$(EGDMA)_2(BM)_3Na^+$	791.27	791.57
[A3: 3]	$(HEMA)_1(EGDMA)_2(BM)_2(DMPP)_1H^+$	913.37	913.62
[A3: 4]	$(EGDMA)_3(BM)_2(DMPP)_1H^+$	981.40	981.59
[A3: 5]	$(EGDMA)_3(BM)_3Na^+$	989.36	989.59
[A3: 6]	$(EGDMA)_3(BM)_3(DMPP)_1H^+$	1105.43	1105.65
[A3: 7]	$(EGDMA)_3(BM)_4Na^+$	1113.39	1113.61

Table 3.12: Corresponding structures to MALDI-ToF peaks annotated in Figure 3.20 for A3 thiol-Michael addition of benzyl mercaptan to poly-EGDMA A in DMSO. Mass region 750-1150 Daltons, BM-benzyl mercaptan, HEMA-hydroxyethyl methacrylate (monomer impurity). Example structure given in Figure 3.14

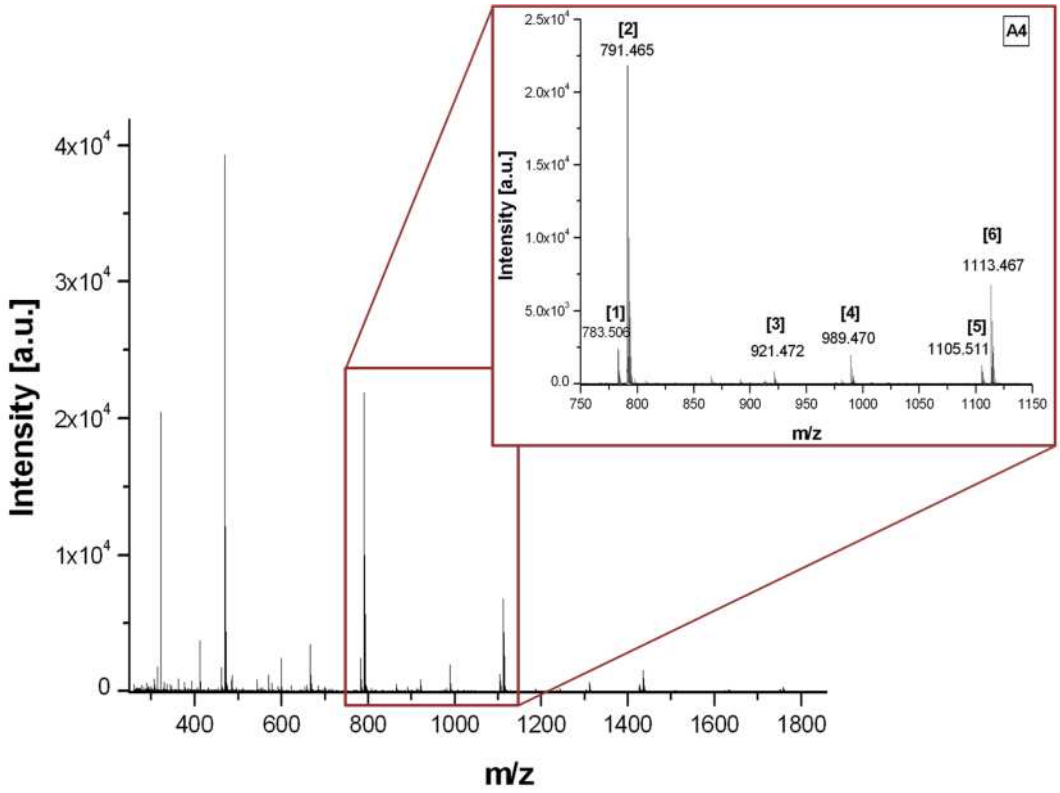

Figure 3.21: MALDI-ToF spectrum of A4, poly-EGDMA thiol-Michael addition with benzyl mercaptan (1.6 mol eq. benzyl mercaptan, 0.01 mol eq. DMPP to vinyl groups). Zoom region between 750 and 1150 Daltons. Annotations correspond to Table 3.13

Name	Corresponding Structure	Theoretical m/z	Measured m/z
[A4: 1]	$(EGDMA)_2(BM)_2(DMPP)_1H^+$	783.31	783.50
[A4: 2]	$(EGDMA)_2(BM)_3Na^+$	791.27	791.46
[A4: 3]	$(HEMA)_1(EGDMA)_2(BM)_3Na^+$	921.33	921.47
[A4: 4]	$(EGDMA)_3(BM)_3Na^+$	989.36	989.47
[A4: 5]	$(EGDMA)_3(BM)_3(DMPP)_1H^+$	1105.43	1105.51
[A4: 6]	$(EGDMA)_3(BM)_4Na^+$	1113.39	1113.46

Table 3.13: Corresponding structures to MALDI-ToF peaks annotated in Figure 3.21 for mass region 750-1150 Daltons for A4, thiol-Michael addition of benzyl mercaptan to poly-EGDMA A in DMSO. BM-benzyl mercaptan, HEMA-hydroxyethyl methacrylate (monomer impurity). Example structure given in Figure 3.14

Use of 0.01 mole equivalents of DMPP to vinyl groups yielded a consistent level of functionalisation to those formed using increased levels of DMPP observed *via* MALDI-ToF analysis, however due to the longer reaction time, subsequent reactions were conducted with 0.05 mole equivalents of DMPP.

3.2.4 Optimisation of the Thiol-Michael Addition of Benzyl Mercaptan to Poly-EGDMA- Reduction of Thiol Excess

The excess of thiol employed in the thiol-Michael addition of benzyl mercaptan to poly-EGDMA (**A**) was reduced from a 1.0:1.6 ratio of [vinyl groups]:[thiol] to a 1.0:1.0 ratio using 0.05 vinyl equivalents of DMPP (**A5**), based on the number average level of vinyl groups per chain calculated using Equation 3.1 and Equation 3.2. The complete disappearance of vinyl signals at 5.6, 6.1 and 6.2 ppm was observed *via* ^{1}H NMR within one hour, signifying successful thiol-Michael addition of benzyl mercaptan to the poly-EGDMA **A**. Upon removal of volatiles in vacuo, peaks at 2.3-2.7 ppm were observed corresponding to the hydrothiolation of vinyl groups (Figure 3.22).

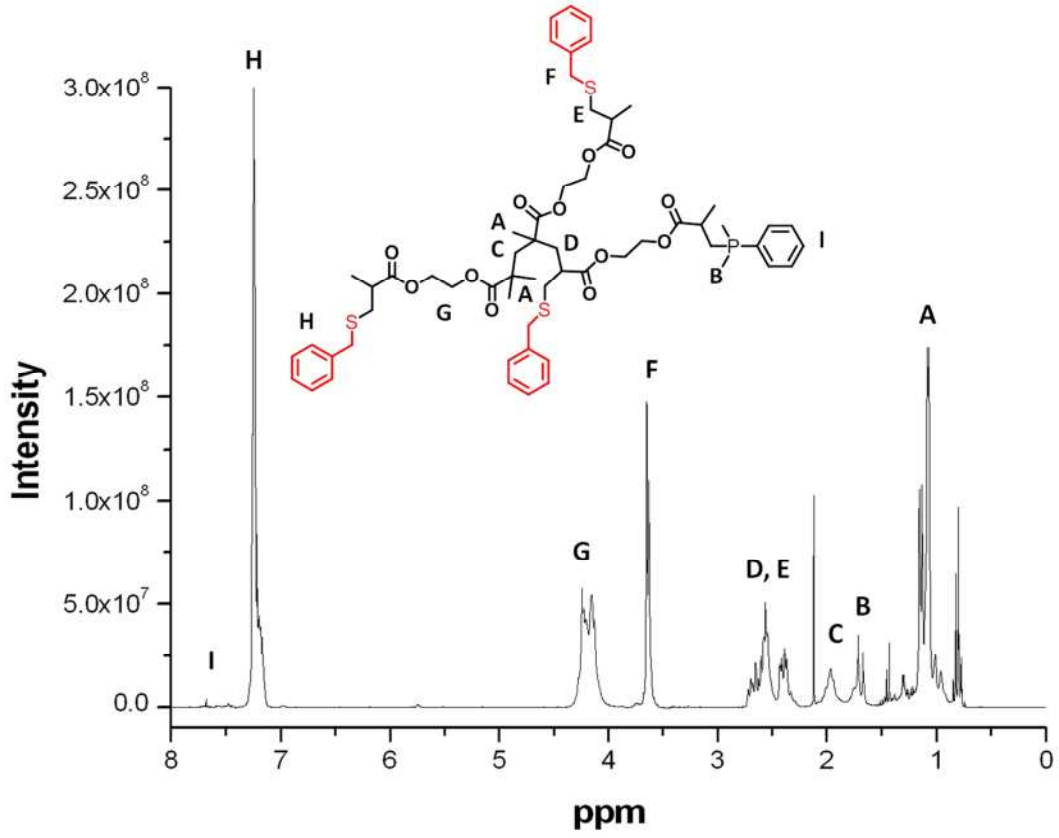

Figure 3.22: ^{1}H NMR spectrum of precipitated polymer A5, thiol-Michael addition of benzyl mercaptan to poly-EGDMA A (1.0 mol eq. Benzyl mercaptan, 0.05 mol eq. DMPP to vinyl groups). ^{1}H NMR solvent $CDCl_3$

An increase in molecular weight was also observed *via* SEC for the addition of benzyl mercaptan to poly-EGDMA **A** (Table 3.14, Figure 3.23), with the appearance of a chromophore at approximately 14-17 minutes retention time, λ = 290 nm.

Name	M_n ($g.mol^{-1}$)	M_w ($g.mol^{-1}$)	PDi
A	1200	2300	2.0
A5	1600	2700	1.8

Table 3.14: Molecular weight comparison of poly-EGDMA A with benzyl mercaptan functionalised thiol-Michael addition product A5 (1.0 mol eq. benzyl mercaptan, 0.05 mol eq. DMPP to vinyl groups). Molecular weights obtained *via* conventional SEC

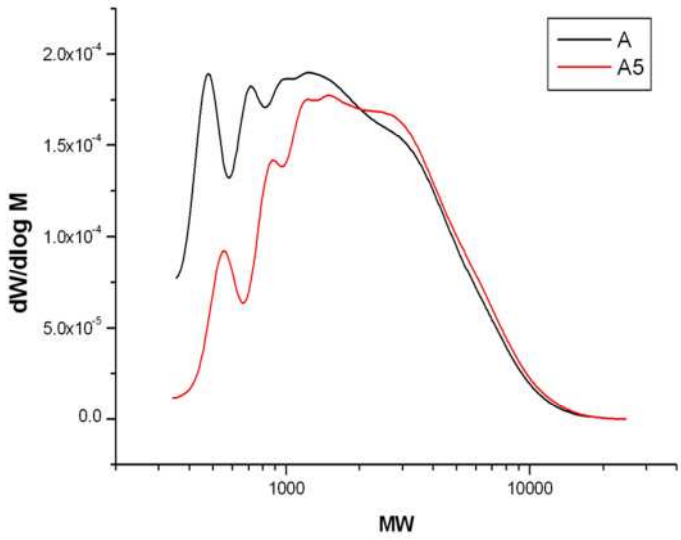

Figure 3.23: SEC comparison of poly-EGDMA A to A5, thiol-Michael addition of benzyl mercaptan to poly-EGDMA A (1.0 mol eq. benzyl mercaptan, 0.05 mol eq. DMPP)

MALDI-ToF investigation of **A5** shows that the level of functionalisation of vinyl groups in the reaction remains high, with the majority of peaks observed corresponding to fully benzyl mercaptan functionalised chains **[A5: 2, 3, 6]**, with a small portion of chains containing one DMPP moiety **[A5:1, 5]**. Minor peaks correspond to chains whereby a single vinyl group remains unfunctionalised in the product, as previously observed where an excess of thiol was employed **[A5: 4]** (Figure 3.24, Table 3.15). Hence, reductions in both the level of DMPP and excess of thiol can be made without having detrimental effects on reaction time and efficiency for the thiol-Michael addition of benzyl mercaptan to poly-EGDMA **A**.

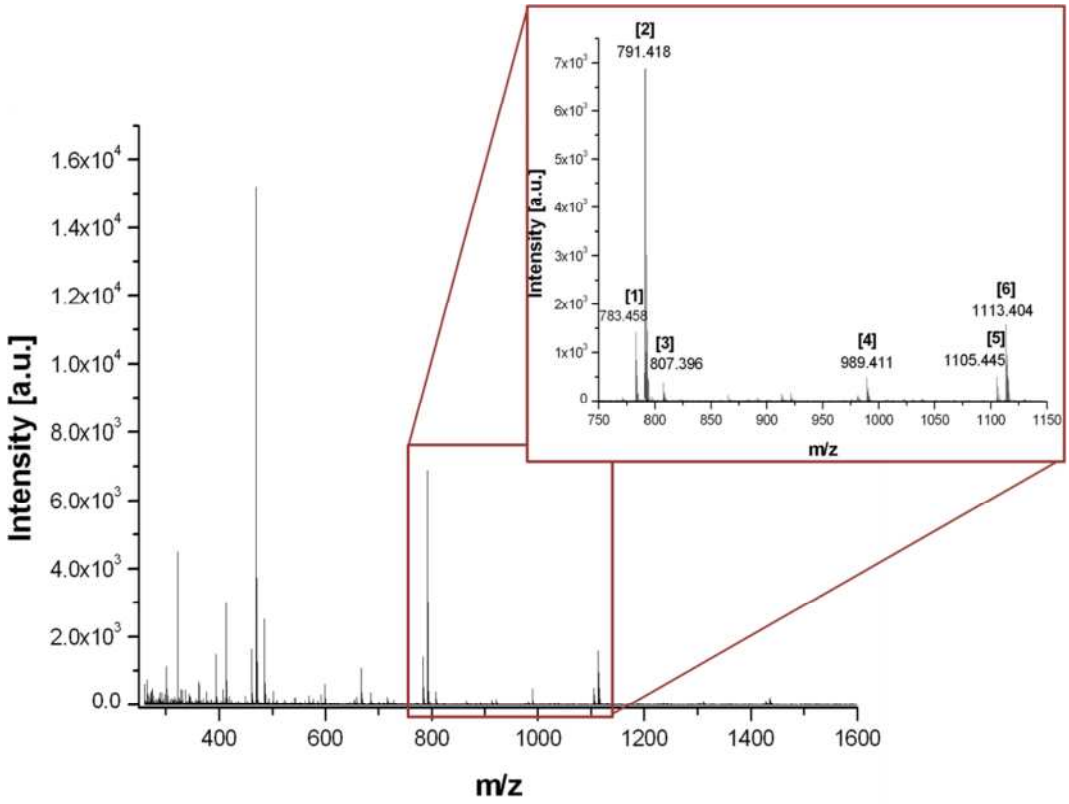

Figure 3.24: MALDI-ToF spectrum of A5, thiol-Michael addition of benzyl mercaptan to poly-EGDMA A (1.0 mol eq. benzyl mercaptan, 0.05 mol eq. DMPP to vinyl groups). Zoom region between 750 and 1150 Daltons. Annotations correspond to Table 3.15

Name	Corresponding Structure	Theoretical m/z	Measured m/z
[A5: 1]	$(EGDMA)_2(BM)_2(DMPP)_1H^+$	783.31	783.45
[A5: 2]	$(EGDMA)_2(BM)_3Na^+$	791.27	791.41
[A5: 3]	$(EGDMA)_2(BM)_3K^+$	807.24	807.39
[A5: 4]	$(EGDMA)_3(BM)_3Na^+$	989.36	989.41
[A5: 5]	$(EGDMA)_3(BM)_3(DMPP)_1H^+$	1105.43	1105.44
[A5: 6]	$(EGDMA)_3(BM)_4Na^+$	1113.39	1113.40

Table 3.15: Corresponding structures to MALDI-ToF peaks annotated in Figure 3.24 for A5, thiol-Michael addition of benzyl mercaptan to poly-EGDMA A in DMSO. Mass region 750-1150 Daltons. BM-benzyl mercaptan, HEMA-hydroxyethyl methacrylate (monomer impurity). Example sstructure given in Figure 3.14

3.2.5 Variation of the Thiol Employed for the Thiol-Michael Addition to Poly-EGDMA

The versatility of the thiol-Michael addition to poly-EGDMA (**A**) was assessed by using a range of commercially available thiols. Mercaptoethanol (**A6**), thioglycerol (**A7**) and dodecanethiol (**A8**), were chosen to cover a range of hydrophobicities/hydrophilicities. A 1:1:0.05 ratio of vinyl groups: thiol : DMPP was employed for all three thiols. Thiol-Michael addition of both mercaptoethanol and thioglycerol were complete within one hour, with the complete disappearance of vinyl groups observed *via* ^{1}H NMR. Attempts were made to conduct the thiol-Michael addition of dodecanethiol to poly-EGDMA in DMSO, however, the insolubility of dodecanethiol in such a hydrophilic solvent yielded biphasic systems, despite this the reaction reached 93% conversion within one hour as measured by ^{1}H NMR, with both internal and external vinyl groups remaining. Although high conversion was still achieved using DMSO, the solvent was changed to DMF in an attempt to increase the conversion by use of a homogenous reaction mixture.

DMF gave a homogenous system, yet full conversion was still not achieved within one hour using a 1:1 ratio of vinyl groups to thiol, reaching 87% within one hour. A higher conversion of external vinyl functionality was observed *via* ^{1}H NMR compared to internal vinyl functionality. The incomplete functionalisation of poly-EGDMA with dodecanethiol is thought to be due to a combination of steric hindrance, due to the long alkyl chain, additionally the reduced electron withdrawing nature of the long alkyl chain leads to a less efficient thiol dissociation. Vinyl groups remaining in the product appear to be primarily internal vinyl groups, which would be less accessible, especially to sterically hindered species such as dodecanethiol. The excess of dodecanethiol was increased to 1.2 vinyl group equivalents but full functionalisation was still not observed, reaching 91% within one hour. Increasing the thiol excess to 1.5 saw an increase in the conversion at one hour to 93%, the reaction was left overnight and a conversion of >99% was achieved, with only internal vinyl groups remaining (Figure 3.25), highlighting that thiol choice plays an important role in the efficiency of the thiol-Michael addition reaction.

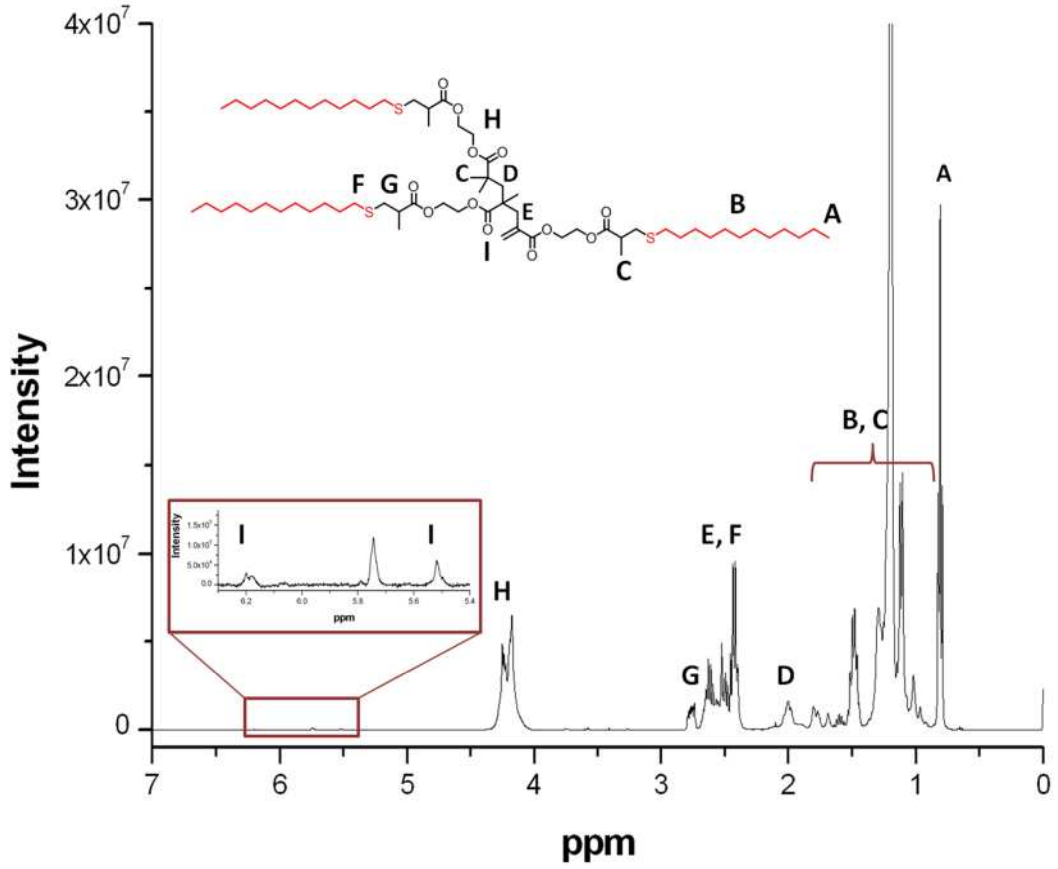

Figure 3.25: ^{1}H NMR of dodecanethiol functionalised polyEGDMA (A8), expansion of 5.4ppm to 6.4ppm displaying remaining vinyl groups

Analysis of polymers **A6**-**A8** *via* SEC a molecular weight increase is only observed for **A8**, functionalisation with dodecanethiol, in which a dramatic increase in molecular weight is observed in line with addition of the long alkyl chain to the polymer. For addition of mercaptoethanol to poly-EGDMA **A** (**A6**) a reduction in M_w is observed. However, on inspection of molecular weight plots it can be seen that a shift to higher molecular weight occurs, but the PDi is narrowed, perhaps due to the increased hydrophilicity of the polymer, due to the addition of the hydroxyl group from mercaptoethanol, causing a contraction in the hydrodynamic volume. This same effect is also observed for **A7**, addition of thioglycerol, but due to the addition of two alcohol functionalities this effect is increased, with a greater contraction in hydrodynamic volume observed when THF was used as the SEC eluent (Table 3.16, Figure 3.26 (left)). Conducting the SEC of **A6** and **A7** in a more hydrophilic solvent, DMF, the expected increase in molecular weight is observed on comparison to poly-EGDMA **A**

(Table 3.16, Figure 3.26 (right)), although the increase in molecular weight for thioglycerol is surprisingly less significant compared to the increase observed for mercaptoethanol functionalisation.

THF eluent				DMF eluent			
Name	M_n ($g.mol^{-1}$)	M_w ($g.mol^{-1}$)	PDi	Name	M_n ($g.mol^{-1}$)	M_w ($g.mol^{-1}$)	PDi
A	1200	2300	2.0	**A**	1100	2200	1.9
A6	1200	2100	1.8	**A6**	2100	3900	1.9
A7	1000	1400	1.4	**A7**	1700	2800	1.7
A8	3100	4900	1.6				

Table 3.16: Molecular weight comparison of EGDMA homopolymer A with functionalised thiol-Michael addition products A6-A8, molecular weights obtained *via* conventional SEC in both THF and DMF eluent (A6 and A7 only). A6 – mercaptoethanol functionalised, A7- thioglycerol functionalised, A8 – dodecanethiol functionalised

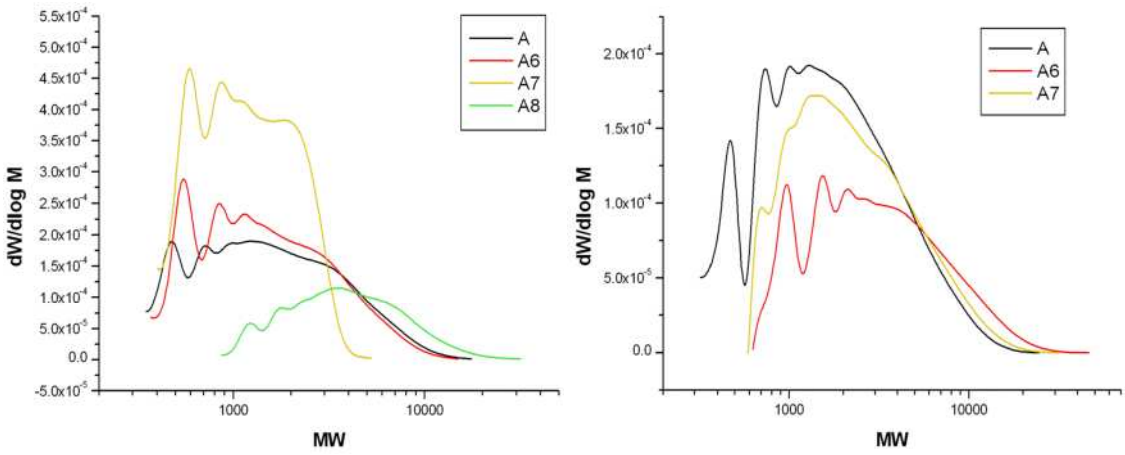

Figure 3.26: (left) SEC comparison of A to A6-A8, THF eluent. Thiol-Michael additions of functional thiols to poly-EGDMA (A). A6 mercaptoethanol, A7 thioglycerol, A8 dodecanethiol. (right) SEC comparison of A to A6-A7, DMF eluent

PDA spectra were obtained for polymers **A6**-**A8** to provide an insight into the level of DMPP-polymer conjugates, as these would have an absorbance in the PDA spectrum whereas the thiols employed are UV inactive. As the level of DMPP used in these reactions is low, 0.05 mole equivalents to vinyl groups, the level of UV absorbance in the polymer region is greatly reduced in comparison to functionalisation with benzyl mercaptan, signifying the functionalisation occurs predominately with the functional thiol, with only low levels of DMPP-polymer conjugation. A typical SEC PDA spectrum is shown in Figure 3.27.

.

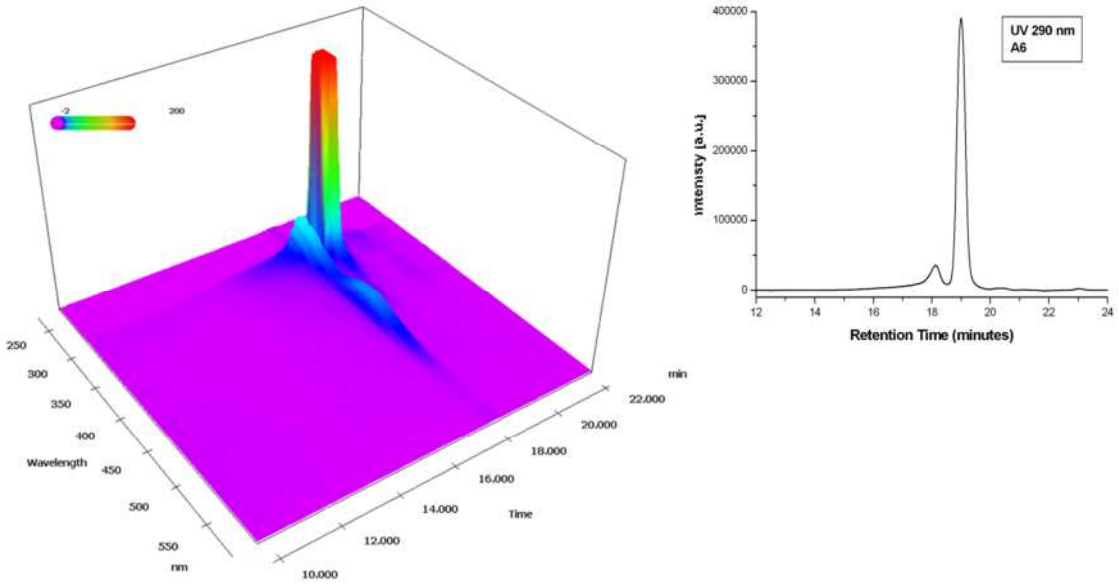

Figure 3.27: (left) Typical SEC PDA spectrum for the functionalisation of poly-EGDMA A with UV inactive thiols (A6). Absorbance at 18 minutes retention time, λ = 290 nm corresponding to THF, absorbance at 17 minutes retention time, λ = 380-500 nm corresponding to CoBF, Low intensity absorbance at 14-17 minutes retention time, λ = 290 nm corresponds to DMPP-polymer conjugates (right) UV chromatogram extraction of data from PDA at λ 290 nm

Investigation of the structural diversity in the products obtained from thiol-Michael addition of mercaptoethanol (**A6**), thioglycerol (**A7**) and dodecanethiol (**A8**) was conducted *via* MALDI-ToF. Use of mercaptoethanol as the functional thiol yielded a similar level of fully functionalised and incomplete functionalisations as previously observed utilising benzyl mercaptan as the functional thiol. Major peaks indicate the full functionalisation of vinyl groups with mercaptoethanol **[A6: 1, 2, 6]** with chains present whereby one DMPP-polymer conjugate is formed **[A6: 3]**. Minor peaks observed correspond to incomplete functionalisation of vinyl groups whereby one vinyl group **[A6: 5]** and two vinyl groups remain unfunctionalised **[A6: 4]** (Figure 3.28, Table 3.17). Although some minor peaks are observed denoting incomplete functionalisation the level of fully functionalised product remains high for mercaptoethanol.

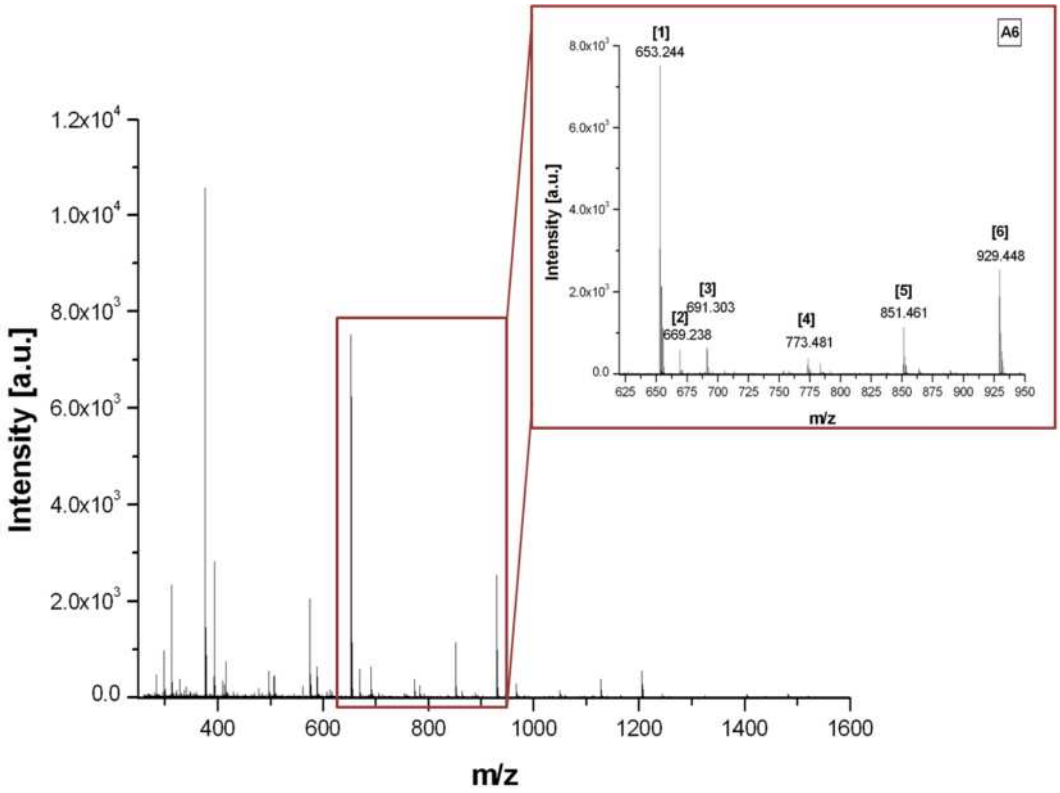

Figure 3.28: MALDI-ToF spectrum of A6, poly-EGDMA thiol-Michael addition with mercaptoethanol (1.0 mol eq. mercaptoethanol, 0.05 mol eq. DMPP to vinyl groups), with zoom region between 620 and 950 Daltons. Annotations correspond to Table 3.17

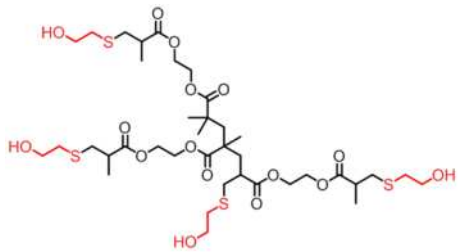

Figure 3.29: Example structure of mercaptoethanol functionalised poly-EGDMA, $(EGDMA)_3(ME)_4$

Name	Corresponding Structure	Theoretical m/z	Measured m/z
[A6: 1]	$(EGDMA)_2(ME)_3Na^+$	653.20	653.24
[A6: 2]	$(EGDMA)_2(ME)_3K^+$	669.18	669.23
[A6: 3]	$(EGDMA)_3(ME)_2(DMPP)_1H^+$	691.27	691.30
[A6: 4]	$(EGDMA)_3(ME)_2Na^+$	773.28	773.48
[A6: 5]	$(EGDMA)_3(ME)_3Na^+$	851.29	851.46
[A6: 6]	$(EGDMA)_3(ME)_4Na^+$	929.31	929.44

Table 3.17: Corresponding structures to MALDI-ToF peaks annotated in Figure 3.28 for mass region 620-950 Daltons, for A6 thiol-Michael addition of mercaptoethanol to poly-EGDMA A in DMSO. ME-mercaptoethanol. Example structure given in Figure 3.29

For thiol-Michael addition of thioglycerol to poly-EGDMA **A** (**A7**) a higher level of incomplete functionalisation products is observed (Figure 3.30, Table 3.18). Major peaks observed correspond to two peak series', whereby one series originates from the full functionalisation of vinyl groups with thioglycerol **[A7: 3]**, with one DMPP adduct per chain. The second peak series arises due to incomplete functionalisation, containing one unfunctionalised vinyl group and one DMPP-polymer conjugate per chain **[A7: 1]**. Fully functionalised chains without DMPP present are observed as minor peaks **[A7: 2]**, with chains whereby two vinyl groups remain unfunctionalised, containing one DMPP-polymer conjugate per chain are also observed as minor peaks **[A7: 4]**. Hence, the efficiency of the thiol-Michael addition of thioglycerol to poly-EGDMA (**A**) under these conditions is lower than previously seen for other thiols, such as benzyl mercaptan and mercaptoethanol, again, highlighting that thiol choice is an important factor in the functionalisation of such polymers. This level of incomplete functionalisation products may explain the less significant increase in molecular weight observed *via* DMF SEC on comparison of **A6** and **A7**. The increase in molecular weight on addition of thioglycerol to the polymer (**A7**) was expected to be greater than for the addition of mercaptoethanol (**A6**), although an increase compared to unfunctionalised poly-EGDMA **A** was observed, the product of **A7** yielded a lower molecular weight compared to **A6** (Table 3.16). Therefore, optimisation reactions should be carried out for each thiol employed, with detailed analysis by MALDI-ToF, as remaining vinyl groups were observed in MALDI-ToF spectra were outside of the limits of ^{1}H NMR detection. Full optimisation for each thiol can be a lengthy process, alternatively employment of high excesses of thiol should increase functionalisation, but this is often undesired due to the toxicity and odour associated with free thiols.

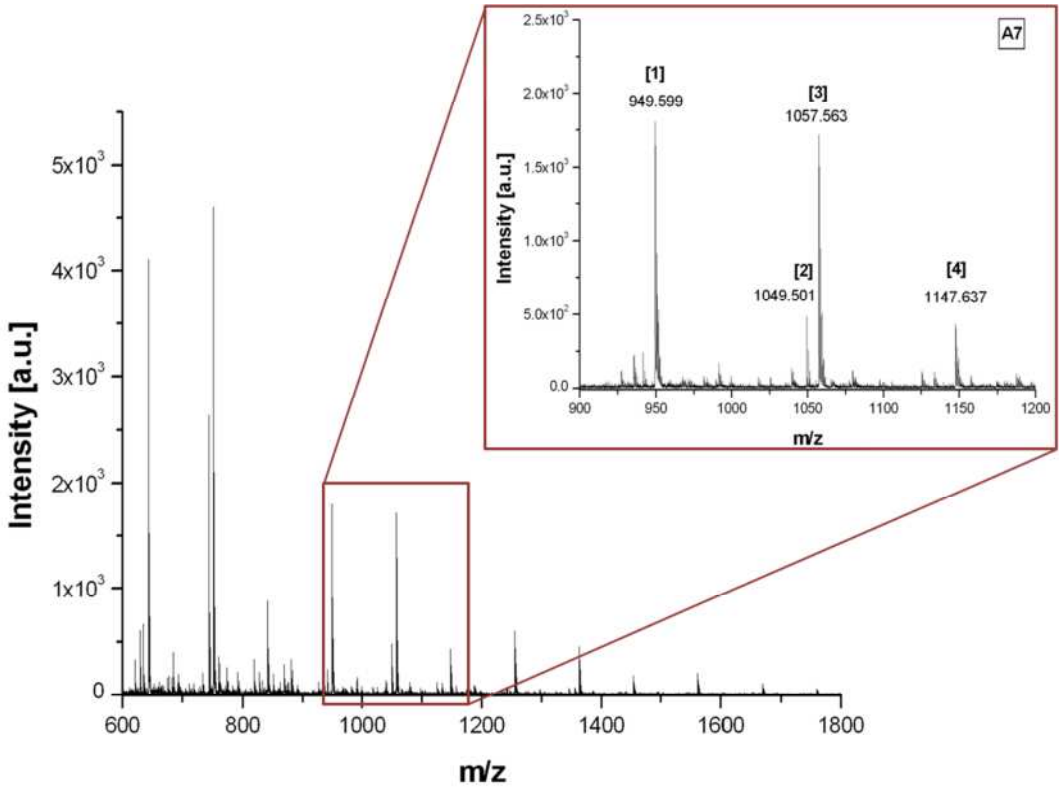

Figure 3.30: MALDI-ToF spectrum of A7, poly-EGDMA thiol-Michael addition with thioglycerol (1.0 mol eq. thioglycerol, 0.05 mol eq. DMPP to vinyl groups), with zoom region between 900 and 1200 Daltons. Annotations correspond to Table 3.18

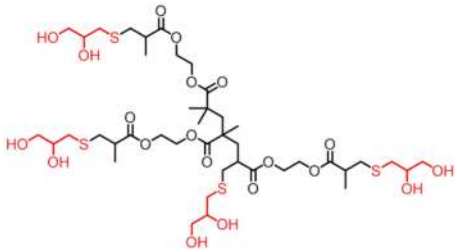

Figure 3.31: Example structure of thioglycerol functionalised poly-EGDMA, $(EGDMA)_3(TG)_4$

Name	Corresponding Structure	Theoretical m/z	Measured m/z
[A7: 1]	$(EGDMA)_3(TG)_2(DMPP)_1H^+$	949.38	949.59
[A7: 2]	$(EGDMA)_3(TG)_4Na^+$	1049.35	1049.50
[A7: 3]	$(EGDMA)_3(TG)_3(DMPP)_1H^+$	1057.40	1057.56
[A7: 4]	$(EGDMA)_4(TG)_2(DMPP)_1Na^+$	1147.47	1147.63

Table 3.18: Corresponding structures to MALDI-ToF peaks annotated in Figure 3.30 for mass region 900-1200 Daltons, for A7 thiol-Michael addition of thioglycerol to poly-EGDMA A in DMSO. TG-thioglycerol. Example structure given in Figure 3.31

As some degree of vinyl group retention was observed *via* ^{1}H NMR for the thiol-Michael addition of dodecanethiol to poly-EGDMA (**A**), it was expected that a higher degree of incomplete functionalisations would be seen *via* MALDI-ToF analysis for **A8**. However, on inspection of the MALDI-ToF spectrum it is found that these unfunctionalised products remain as a minor peak series, whereby one vinyl group remains unfunctionalised **[A8: 4]**, with the major peak series denoting full functionalisation of vinyl groups with dodecanethiol **[A8: 1, 6]** (Figure 3.32, Figure 3.32). As steric hindrance is a likely cause for incomplete functionalisation, this effect will be more significant at higher molecular weights, due to an increased inaccessibility of internal vinyl groups, which are not observed by MALDI-ToF due to high molecular weight discrimination, which is observed in polydisperse samples.[234-236] Other minor peaks observed can be attributed to full functionalisation products whereby single DMPP-polymer conjugates are formed **[A8: 5]**, incorporation of one HEMA unit into the polymer chain **[A8: 3]** and potassiated fully functionalised poly-EGDMA chains **[A8: 2]**. Hence, MALDI-ToF characterisation indicates a high level of fully functionalised chains, despite a low level of vinyl groups (~1%) still observed *via* ^{1}H NMR.

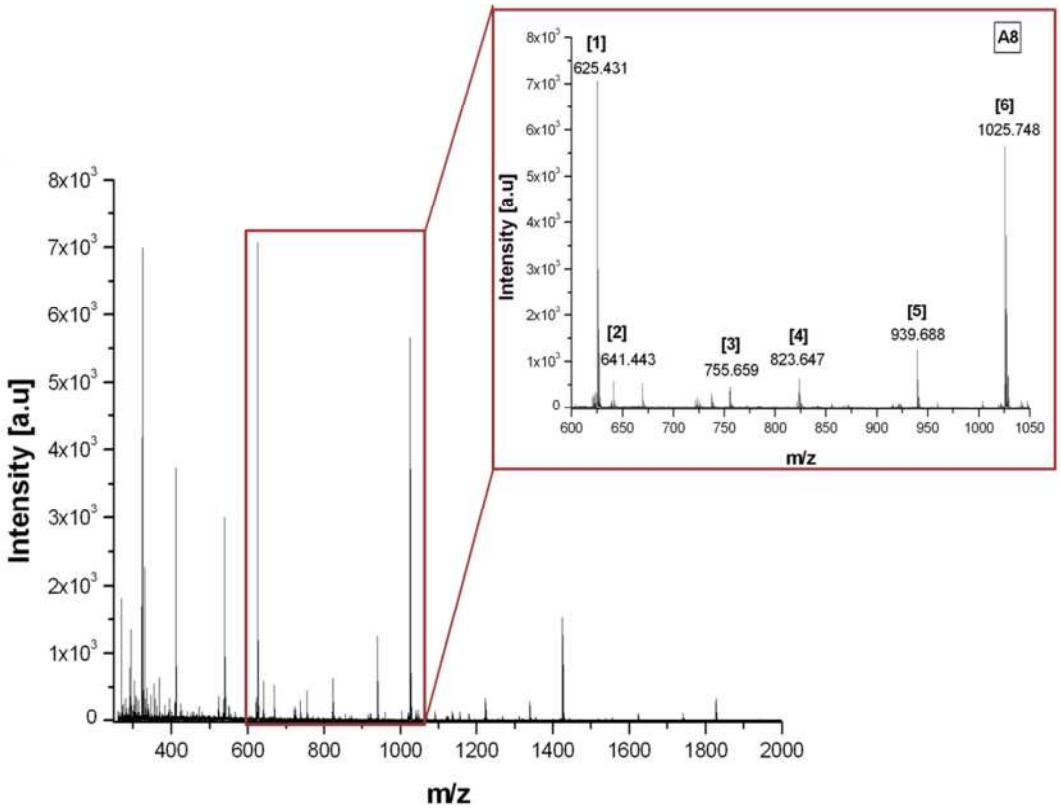

Figure 3.32: MALDI-ToF spectrum of A8, poly-EGDMA thiol-Michael addition with dodecanethiol (1.5 mol eq. thioglycerol, 0.05 mol eq. DMPP to vinyl groups), with zoom region between 600 and 1050 Daltons. Annotations correspond to Table 3.19

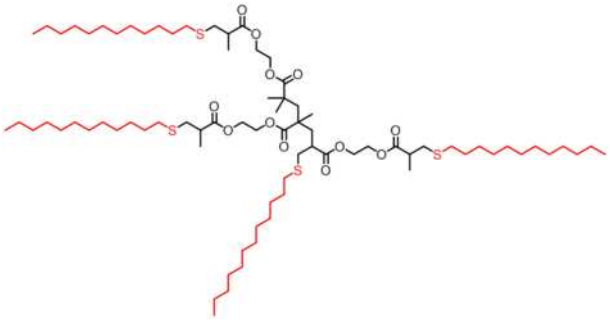

Figure 3.33: Example structure of dodecanethiol functionalised poly-EGDMA, $(EGDMA)_3(DDT)_4$

Name	Corresponding Structure	Theoretical m/z	Measured m/z
[A8: 1]	$(EGDMA)_1(DDT)_2Na^+$	625.42	625.43
[A8: 2]	$(EGDMA)_1(DDT)_2K^+$	641.40	641.44
[A8: 3]	$(EGDMA)_1(HEMA)_1(DDT)_2Na^+$	755.49	755.65
[A8: 4]	$(EGDMA)_2(DDT)_2Na^+$	823.51	823.64
[A8: 5]	$(EGDMA)_2(DDT)_2(DMPP)_1H^+$	939.59	939.58
[A8: 6]	$(EGDMA)_2(DDT)_3Na^+$	1025.69	1025.74

Table 3.19: Corresponding structures to MALDI-ToF peaks annotated in Figure 3.32 for mass region 600-1050 Daltons, for A8 thiol-Michael addition of dodecanethiol to poly-EGDMA A in DMSO. DDT-dodecanethiol. Example structure given in Figure 3.33

3.3 Conclusions

Optimisation of the conditions for the thiol-Michael addition of benzyl mercaptan to poly-EGDMA was conducted; solvent choice proved to be an important factor in the rate of reaction, with DMSO providing a superior solvent, as previously stated in literature, even when biphasic systems are observed. Successful use of as low as 0.01 mole equivalents of DMPP to vinyl groups, which should reduce the level of DMPP-polymer conjugates, and use of approximately equimolar amounts of benzyl mercaptan to vinyl groups saw no detrimental effects in the level of functionalisation achieved, with the retention of high reaction rates. The versatility of this system was tested by use of alternative commercially available functional thiols, covering a range of hydrophobic/hydrophilic functionalities. The importance of thiol choice was highlighted due to the reduced level of functionalisation observed application to both thioglycerol and dodecanethiol, indicating that optimisation of reaction conditions is required for each thiol individually, as the rate of thiol dissociation and steric effects varies with each thiol. Hence, the functionalisation of branched poly-EGDMA via phosphine mediated thiol-Michael addition proved successful for a range of commercial thiols, with a wide scope for the application of this method to a range of alternative functional thiols, providing a facile method for control of polymer functionality by post-polymerisation modification.

3.4 Experimental

General

All reagents were purchased from Aldrich and used as received unless stated. 2, 2-Azobis(2,4-dimethylvaleronitrile) (V-601) was donated from Wako and used as received. CoBF was synthesised according to literature procedure.[244]

Synthetic Procedures

Homopolymerisation of EGDMA (A)

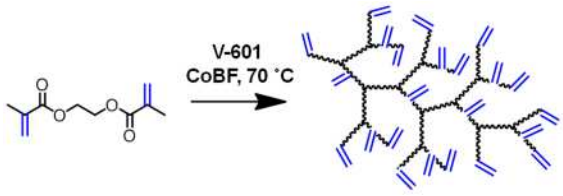

Figure 3.34: General schematic for the CCT homopolymerisation of EGDMA

A Schlenk tube was charged with 50 mL of monomer (EGDMA 0.252 mol) 50 mL dichloroethane. A minimum of three freeze pump thaw cycles were applied and the vessel backfilled with nitrogen. A separate Schlenk tube was charged with 50 mg CoBF (0.1 mmol) and 0.5 g V-601 (2.2 mmol), with magnetic stirring. The vessel was degassed *via* a minimum of three cycles of vacuum/nitrogen, and backfilled with nitrogen. The liquids were cannulated into solids under positive nitrogen pressure and the reaction mixture stirred until homogenous. The vessel was placed in an oil bath (70 ˚C) with stirring and left to react for 6 hours under nitrogen. Solvent was removed in vacuo and the end products characterised by ^{1}H NMR, ^{13}C NMR, IR, MALDI-ToF and SEC.

Phosphine Mediated Thiol-Michael Additions

0.2 g poly-EGDMA (1.2 mmol vinyl groups by SEC, number average calculation) was weighed into a vial with stirring and solvated in 2 mL DMSO. Thiol was added to the reaction mixture with sampling for ^{1}H NMR time zero measurements. DMPP was added *via* microlitre syringe . Reactions carried out under atmospheric conditions and left to react until a complete loss of vinyl functionality was observed by ^{1}H NMR. Volatiles

were removed in vacuo for characterisation by ^{1}H NMR, ^{13}C NMR, IR, MALDI-ToF and SEC

Instruments

^{1}H and ^{13}C NMR

All ^{1}H and ^{13}C NMR were recorded on Bruker DPX-300 and Bruker DPX-400 spectrometers as solutions in $CDCl_3$ or d^6-DMSO. Chemical shifts were calibrated using TMS for $CDCl_3$ and corresponding deuterated solvent signals in all other cases and cited as parts per million (ppm).

Infra Red (IR)

IR was carried out on a Bruker Vector 22 using a Golden Gate diamond attenuated flow cell and analysed using Opus spectroscopy software.

Size Exclusion Chromatography (SEC)

All SEC were performed on Agilent 390-LC multi detector suites equipped with a PL-AS RT/MT autosampler, fitted with a PLgel 5 μm guard column and two PLgel 5 μm Mixed D columns (suitable for separations up to MW = 2.0 x 10^6 g.mol^{-1}). All data was collected and analysed using Cirrus software (Agilent Inc). Any points within the calibration plot with an error greater than 10% were not included in the final calibration. Third order calibration plots were used.

Mobile phases used were THF, $CHCl_3$ and DMF, flow rate 1 mL.min^{-1}, ambient operating temperature (40 ˚C for DMF), 100 μL injection volume. An RI detector was used for conventional SEC. Calibrations were set using PMMA EasiVial standards (690-1944000 g.mol^{-1}), purchased from Agilent, with a minimum of 9 points to form a third order calibration curve. THF SEC was equipped with a Shimadzu photodiode array detector with recorded wavelengths of 200-700 nm, spectra were analysed using LC solutions software.

Matrix-Assisted Laser Desorption and Ionization Time-of-Flight (MALDI-ToF)

Mass spectra were acquired by MALDI-ToF mass spectrometry using a Bruker Daltonics Ultraflex II MALDI-ToF mass spectrometer, equipped with a nitrogen laser delivering 2 ns laser pulses at 337 nm with positive ion ToF detection performed using an accelerating voltage of 25 kV.

2, 5-Dihdroxybenzoic acid (DHB) was used as an organic matrix and sodium iodide (NaI) used as the salt. A layering method was used to spot the MALDI plate. THF or THF/water was used as the solvent for sample preparation.

Characterisation

Characterisation of A (Poly-EGDMA)

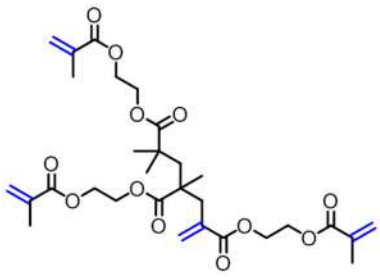

Figure 3.35: Structural representation of CCTP EGDMA trimer

^{1}H NMR (400 MHz, TMS at 25˚C): δ 1.00-1.50 (backbone CH_3), 1.85-2.05 (terminal CH_3), 2.15-2.20 (backbone CH_2), 2.45-2.60 (backbone CH_2), 4.15-4.45 ($OC\underline{H}_2C\underline{H}_2O$), 5.50-5.60 (terminal $C\underline{H}_aH_b$=C + internal $C\underline{H}_aH_b$=C), 6.05-6.15 (terminal $CH_a\underline{H}_b$=C), 6.20-6.35 (internal $CH_a\underline{H}_b$=C)

^{13}C NMR (400 MHz $CDCl_3$ at 25˚C): δ 18.31 (terminal CH_3), 24.82, 27.22 and 30.37 (backbone CH_3), 40.67 (backbone CH_2), 41.58 and 43.05 (backbone quaternary carbons), 46.15 and 48.20 (backbone CH_2), 62.33 (OCH_2CH_2O), 126.04 (terminal $\underline{C}H_2$=C-), 128.63 (internal $\underline{C}H_2$=C-), 135.97 (terminal CH_2=$\underline{C}$-), 137.08 (internal CH_2=$\underline{C}$-), 167.09 (terminal ester carbonyl), 176.70 (internal ester carbonyl)

IR: ν_{max} (neat)/cm^{-1} 2972 (m, CH sp^3), 1715 (s, C=O), 1628 (m, C=C), 1451 (m, CH_2), 1391 (m, CH_3), 1367 (m), 1292 (m), 1141 (s, C-O), 1049 (m), 946 (m), 814 (m)

Conventional SEC: (THF eluent) M_n 1100, M_w 2300, PDi 2.2 (DMF eluent) M_n 1100, M_w 2200, PDi 1.9

Characterisation of A1-A5 (Benzyl Mercaptan functionalised poly-EGDMA)

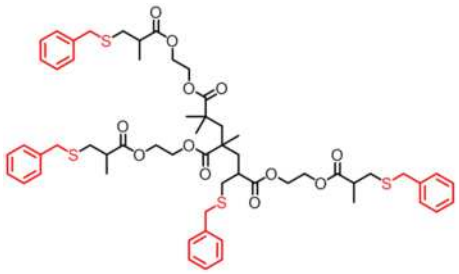

Figure 3.36: Structural representation of thiol-Michael addition product of benzyl mercaptan to EGDMA trimer

^{1}H NMR (400 MHz, TMS at 25˚C): δ 0.95- 1.40 (m, backbone CH_3, terminal CH_3), 1.70-1.80 (m, DMPP CH_3), 1.95-2.10 (br, backbone CH_2), 2.30-2.80 (m, thiol adjacent backbone CH_2, $C\underline{H}_2SCH_2C_6H_5$), 3.60-3.75 (d, $SC\underline{H}_2C_6H_5$), 4.05- 4.35 (m, OCH_2CH_2O), 7.15- 7.30 (m, $SCH_2C_6\underline{H}_5$), 7.45-8.05 (m, DMPP aromatic CH)

^{13}C NMR (400 MHz, $CDCl_3$ at 25˚C): δ 16.84 (terminal CH_3), 24.75, 25.38 (backbone CH_3), 34.46, 34.80 ($\underline{C}H_2SCH_2C_6H_5$), 36.24 ($CH_2S\underline{C}H_2C_6H_5$) 36.62 (thiol adjacent CH_2), 39.83 (quaternary backbone C), 41.66 (backbone CH_2), 42.06 ($\underline{C}HC=O$), 62.30 ($O\underline{C}H_2\underline{C}H_2O$), 127.11 (aromatic para- CH), 128.55 (aromatic meta-CH), 128.90 (aromatic ortho-CH), 138.09 (aromatic quaternary carbon), 174.80 (terminal ester carbonyl), 176.74 (internal ester carbonyl)

IR: u_{max} (neat)/cm^{-1} 2970 (m, CH sp^3), 1729 (m, C=O), 1493 (s), 1453 (s, CH_2), 1283 (s, CH_3), 1233 (s), 1147 (m, C-O), 1071 (s, C-S-C), 942 (s), 875 (s)

Conventional SEC: (THF eluent) **A1** M_n 1400, M_w 2600, PDi 1.8, **A2** M_n 1140, M_w 2600, PDi 1.9, **A3** M_n 1600, M_w 2800, PDi 1.8, **A4** M_n 1600, M_w 2700, PDi 1.8, **A5** M_n 1600, M_w 2700, PDi 1.8

Characterisation of A6 (mercaptoethanol functionalised poly-EGDMA)

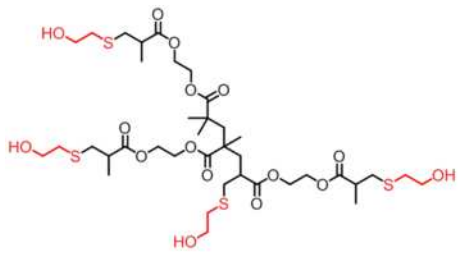

Figure 3.37: Structural representation of thiol-Michael addition product of mercaptoethanol to EGDMA trimer

^{1}H NMR (400 MHz, d^{6}-DMSO at 25˚C): δ 0.90-1.40 (m, terminal CH_3, backbone CH_3, DMPP CH_3), 1.70-1.95 (m, backbone CH_2), 2.50-2.85 (m, $C\underline{H}_2SC\underline{H}_2CH_2OH$, thiol adjacent backbone CH_2), 3.45-3.65 (t, $C\underline{H}_2OH$), 4.10-4.35 (m, $OC\underline{H}_2C\underline{H}_2O$), 4.60-4.90 (br, OH) 7.50-8.00 (m, DMPP aromatic CH)

^{13}C NMR (400 MHz, d^{6}-DMSO at 25˚C): δ 16.40 (internal CH_3), 24.42 (terminal CH_3), 24.97 (DMPP CH_3), 33.97 (external $\underline{C}H_2SCH_2CH_2OH$), 34.30 (internal $\underline{C}H_2SCH_2CH_2OH$), 34.75 (external $S\underline{C}H_2CH_2OH$), 35.05 (internal $S\underline{C}H_2CH_2OH$), 41.10 (backbone CH_2) 41.33 (thiol adjacent backbone CH_2), 42.19 ($\underline{C}HC=O$), 60.82 ($\underline{C}H_2OH$), 61.98, 62.14 ($OCH_2\underline{C}H_2O$), 128.38, 129.56 (DMPP aromatic CH), 174.26, 176.10 (carbonyl)

IR: u_{max} (neat)/cm^{-1} 3341 (br, m, OH H-bonded), 2922 (m, CH sp^3), 1721 (s, C=O), 1455 (m, CH_2), 1389 (m, CH_3), 1154 (s, C-O), 1041 (s, C-S-C), 938 (m), 875 (m)

Conventional SEC: (THF eluent) M_n 1200, M_w 2100, PDi 1.8, (DMF eluent) M_n 2100, M_w 3900, PDi 1.9

Characterisation of A7 (thioglycerol functionalised poly-EGDMA)

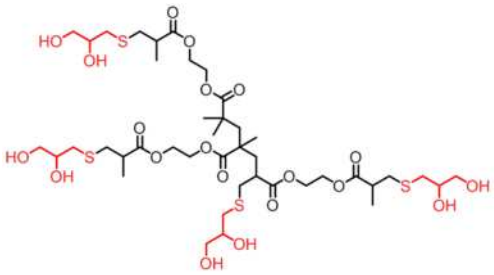

Figure 3.38: Structural representation of thiol-Michael addition product of thioglycerol to EGDMA trimer

^{1}H NMR (400 MHz, d^{6}-DMSO at 25˚C): δ 0.50-1.35 (m, terminal CH_3, backbone CH_3, DMPP CH_3), 1.65-1.95 (m, backbone CH_2), 2.30-2.80 (m, $C\underline{H}_2S C\underline{H}_2CHOH$, thiol adjacent backbone CH_2), 3.20-3.35 (m, $C\underline{H}_2OH$), 3.40-3.55 (br, CHOH), 4.00-4.30 (m, $OC\underline{H}_2C\underline{H}_2O$), 4.45-4.60 (br, OH), 4.65-4.80 (br, OH) 7.45-7.95 (m, DMPP aromatic CH)

^{13}C NMR (400 MHz, d^{6}-DMSO at 25˚C): δ 16.43 (internal CH_3), 24.47 (terminal CH_3), 24.93 (DMPP CH_3), 35.23 (internal $\underline{C}H_2SCH_2CHOH$), 35.32 (external $\underline{C}H_2SCH_2CHOH$), 35.60 (internal $\underline{C}H_2CHOHCH_2OH$) 35.66 (external $\underline{C}H_2CHOHCH_2OH$), 41.13 (backbone CH_2), 41.37 (thiol adjacent CH_2), 42.08 ($\underline{C}HC=O$), 61.95 ($O\underline{C}H_2\underline{C}H_2O$), 64.42 ($CH_2OH$), 71.31 (CHOH), 128.41, 129.56 (DMPP aromatic CH), 174.34, 176.13 (carbonyl)

IR: υ_{max} (neat)/cm^{-1} 3326 (br, s, OH H-bonded), 2918 (m, CH sp^3), 1720 (s, C=O), 1391 (m, CH_2), 1155 (s, C-O), 1068 (s, C-S-C), 1028 (s) 932 (m), 876 (m)

Conventional SEC: (THF eluent) M_n 1000, M_w 1400, PDi 1.4, (DMF eluent) M_n 1700, M_w 2800, PDi 1.7

Characterisation of A8 (dodecanethiol functionalised poly-EGDMA)

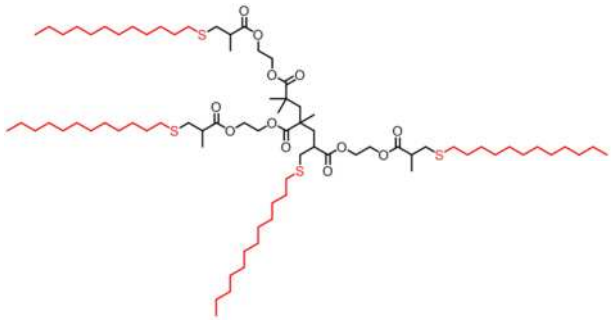

Figure 3.39: Structural representation of thiol-Michael addition product of dodecanethiol to EGDMA trimer

^{1}H NMR (400 MHz, TMS at 25˚C): δ 0.75-0.90 ($(CH_2)_{11}C\underline{H}_3$), 0.95-1.45 (m, terminal CH_3, DMPP CH_3, terminal $(C\underline{H}_2)_{11}CH_3$, internal CH_3), 1.45-1.85 (m, internal $(C\underline{H}_2)_{11}CH_3$), 1.85-2.15 (m, backbone CH_2), 2.35-2.70 (m, thiol adjacent backbone CH_2, $C\underline{H}_2S(CH_2)_{11}CH_3$), 2.75-2.85 (m, $CH_2SC\underline{H}_2(CH_2)_{10}CH_3$), 4.10-4.40 (m, $OC\underline{H}_2C\underline{H}_2O$), 5.45-5.55 (internal $C\underline{H}_aH_b$=C), 6.15-6.25 (internal $CH_a\underline{H}_b$=C)

^{13}C NMR (400 MHz, $CDCl_3$ at 25˚C): δ 14.33 ($(CH_2)_{11}\underline{C}H_3$), 16.78 (terminal CH_3), 22.69 (terminal $(CH_2)_{11}CH_3$), 22.70 (internal CH_3), 18.53, 28.90, 29.35, 29.64, 31.92 (internal $(CH_2)_{11}CH_3$), 35.40 ($S\underline{C}H_2(CH_2)_{10}CH_3$), 39.23 ($CH_2S$), 41.55 (backbone CH_2), 41.92 (thiol adjacent backbone CH_2), 42.49 (CH=O), 62.17 ($O\underline{C}H_2\underline{C}H_2O$), 174.57, 176.76 (carbonyl)

IR: υ_{max} (neat)/cm^{-1} 2921 (s, CH sp^3), 2852 (s, CH sp^3), 1733 (s, C=O), 1457 (m, CH_2), 1376 (m, CH_3), 1247 (m), 1149 (s, C-O), 1066 (m, C-S-C), 9411 (m), 863 (m)

Conventional SEC: (THF eluent) M_n 3100, M_w 4900, PDi 1.6

3.5 References

1. Campos, L. M.; Killops, K. L.; Sakai, R.; Paulusse, J. M. J.; Damiron, D.; Drockenmuller, E.; Messmore, B. W.; Hawker, C. J., *Macromolecules* **2008,** *41* (19), 7063.

2. Yhaya, F.; Sutinah, A.; Gregory, A. M.; Liang, M.; Stenzel, M. H., *J. Polym. Sci., Part A: Polym. Chem.* **2012,** *50* (19), 4085.

3. Flores, J. D.; Treat, N. J.; York, A. W.; McCormick, C. L., *Polym. Chem.* **2011,** *2* (9), 1976.

4. Lima, V.; Jiang, X.; Brokken-Zijp, J.; Schoenmakers, P. J.; Klumperman, B.; Van Der Linde, R., *J. Polym. Sci., Part A: Polym. Chem.* **2005,** *43* (5), 959.

5. Qiu, X.-P.; Winnik, F. M., *Macromol. Rapid Commun.* **2006,** *27* (19), 1648.

6. Nicolaÿ, R., *Macromolecules* **2012,** *45* (2), 821.

7. Li, M.; De, P.; Li, H.; Sumerlin, B. S., *Polym. Chem.* **2010,** *1* (6), 854.

8. Vandenbergh, J.; Junkers, T., *Polym. Chem.* **2012,** *3* (10), 2739.

9. Ho, T. H.; Levere, M.; Soutif, J.-C.; Montembault, V.; Pascual, S.; Fontaine, L., *Polym. Chem.* **2011,** *2* (6), 1258.

10. Roth, P. J.; Davis, T. P.; Lowe, A. B., *Macromolecules* **2012,** *45* (7), 3221.

11. Ho, H. T.; Levere, M. E.; Pascual, S.; Montembault, V.; Soutif, J.-C.; Fontaine, L., *J. Polym. Sci., Part A: Polym. Chem.* **2012,** *50* (8), 1657.

12. Huang, X.; Boyer, C.; Davis, T. P.; Bulmus, V., *Polym. Chem.* **2011,** *2* (7), 1505.

13. Boyer, C.; Davis, T. P., *Chem. Commun.* **2009,** (40), 6029.

14. Boyer, C.; Granville, A.; Davis, T. P.; Bulmus, V., *J. Polym. Sci., Part A: Polym. Chem.* **2009,** *47* (15), 3773.

15. Chan, J. W.; Yu, B.; Hoyle, C. E.; Lowe, A. B., *Polymer* **2009,** *50* (14), 3158.

16. Scales, C. W.; Convertine, A. J.; McCormick, C. L., *Biomacromolecules* **2006,** *7* (5), 1389.

17. Li, M.; De, P.; Gondi, S. R.; Sumerlin, B. S., *J. Polym. Sci., Part A: Polym. Chem.* **2008,** *46* (15), 5093.

18. Boyer, C.; Bulmus, V.; Davis, T. P., *Macromol. Rapid Commun.* **2009,** *30* (7), 493.

19. Hall, D. J.; Van Den Berghe, H. M.; Dove, A. P., *Polym. Int.* **2011,** *60* (8), 1149.

20. Kolb, H. C.; Finn, M. G.; Sharpless, K. B., *Angew. Chem., Int. Ed.* **2001,** *40* (11), 2004.

21. Sumerlin, B. S.; Tsarevsky, N. V.; Louche, G.; Lee, R. Y.; Matyjaszewski, K., *Macromolecules* **2005,** *38* (18), 7540.

22. Geng, J.; Lindqvist, J.; Mantovani, G.; Haddleton, D. M., *Angew. Chem., Int. Ed.* **2008,** *47* (22), 4180.

23. Gao, H.; Matyjaszewski, K., *J. Am. Chem. Soc.* **2007,** *129* (20), 6633.

24. Matyjaszewski, K.; Nakagawa, Y.; Gaynor, S. G., *Macromol. Rapid Commun.* **1997,** *18* (12), 1057.

25. Coessens, V.; Nakagawa, Y.; Matyjaszewski, K., *Polym. Bull.* **1998,** *40* (2), 135.

26. Coessens, V.; Matyjaszewski, K., *Journal of Macromolecular Science, Part A* **1999,** *36* (5-6), 667.

27. Lutz, J.-F.; Börner, H. G.; Weichenhan, K., *Macromol. Rapid Commun.* **2005,** *26* (7), 514.

28. Lutz, J.-F.; BÖrner, H. G.; Weichenhan, K., *Macromolecules* **2006,** *39* (19), 6376.

29. Tsarevsky, N. V.; Sumerlin, B. S.; Matyjaszewski, K., *Macromolecules* **2005,** *38* (9), 3558.

30. Mespouille, L.; Vachaudez, M.; Suriano, F.; Gerbaux, P.; Coulembier, O.; Degée, P.; Flammang, R.; Dubois, P., *Macromol. Rapid Commun.* **2007,** *28* (22), 2151.

31. de Graaf, A. J.; Mastrobattista, E.; van Nostrum, C. F.; Rijkers, D. T. S.; Hennink, W. E.; Vermonden, T., *Chem. Commun.* **2011,** *47* (24), 6972.

32. Garamszegi, L. s.; Donzel, C.; Carrot, G. r.; Nguyen, T. Q.; Hilborn, J. n., *React. Funct. Polym.* **2003,** *55* (2), 179.

33. Liras, M.; García, O.; Quijada-Garrido, I.; París, R., *Macromolecules* **2011,** *44* (6), 1335.

34. Uygun, M.; Tasdelen, M. A.; Yagci, Y., *Macromol. Chem. Phys.* **2010,** *211* (1), 103.

35. Petton, L.; Ciolino, A. E.; Stamenović, M. M.; Espeel, P.; Du Prez, F. E., *Macromol. Rapid Commun.* **2012,** *33* (15), 1310.

36. Norman, J.; Moratti, S. C.; Slark, A. T.; Irvine, D. J.; Jackson, A. T., *Macromolecules* **2002,** *35* (24), 8954.

37. Soeriyadi, A. H.; Boyer, C.; Burns, J.; Becer, C. R.; Whittaker, M. R.; Haddleton, D. M.; Davis, T. P., *Chem. Commun.* **2010,** *46* (34), 6338.

38. Boyer, C.; Soeriyadi, A. H.; Roth, P. J.; Whittaker, M. R.; Davis, T. P., *Chem. Commun.* **2011,** *47* (4), 1318.

39. Nurmi, L.; Lindqvist, J.; Randev, R.; Syrett, J.; Haddleton, D. M., *Chem. Commun.* **2009,** (19), 2727.

40. Zhang, Q.; Slavin, S.; Jones, M. W.; Haddleton, A. J.; Haddleton, D. M., *Polym. Chem.* **2012**.

41. Zhang, Q.; Li, G.-Z.; Becer, C. R.; Haddleton, D. M., *Chem. Commun.* **2012,** *48* (65), 8063.

42. Soeriyadi, A. H.; Li, G.-Z.; Slavin, S.; Jones, M. W.; Amos, C. M.; Becer, C. R.; Whittaker, M. R.; Haddleton, D. M.; Boyer, C.; Davis, T. P., *Polym. Chem.* **2011,** *2* (4), 815.

43. Li, G.-Z.; Randev, R.; Soeriyadi, A. H.; Rees, G.; Boyer, C.; Tong, Z.; Davis, T. P.; Becer, C. R.; Haddleton, D. M., *Polym. Chem.* **2010,** *1*, 1196.

44. Mazzolini, J.; Boyron, O.; Monteil, V.; D'Agosto, F.; Boisson, C.; Sanders, G. C.; Heuts, J. P. A.; Duchateau, R.; Gigmes, D.; Bertin, D., *Polym. Chem.* **2012,** *3* (9), 2383.

45. Robert A. Schoonheydt; Rudi Van Overloop; Mathieu Van Hove; Velinden, J., *Clay Clay Miner.* **1984,** *32* (1), 74.

46. Fessler, M.; Eller, S.; Bachmann, C.; Gutmann, R.; Trettenbrein, B.; Kopacka, H.; Mueller, T.; Brueggeller, P., *Dalton Trans.* **2009,** (8), 1383.

47. Llewellyn, S. A.; Green, M. L. H.; Cowley, A. R., *Inorg. Chim. Acta* **2006,** *359* (11), 3785.

48. Godfrey, S. M.; Lane, H. P.; McAuliffe, C. A.; Pritchard, R. G., *J. Chem. Soc. Dalton Trans.* **1993,** (10), 1599.

49. Stewart, R. C.; Marzilli, L. G., *J. Am. Chem. Soc.* **1978,** *100* (3), 817.

50. Dix, L. R.; Ebdon, J. R.; Hodge, P., *Eur. Polym. J.* **1995,** *31* (7), 653.

51. Lowe, A. B., *Polym. Chem.* **2010,** *1*, 17.

52. Kakwere, H.; Perrier, S. b., *J. Am. Chem. Soc.* **2009,** *131* (5), 1889.

53. Nielen, M. W. F.; Malucha, S., *Rapid Commun. Mass Spectrom.* **1997,** *11* (11), 1194.

54. Schriemer, D. C.; Li, L., *Anal. Chem.* **1997,** *69* (20), 4176.

55. Rashidzadeh, H.; Guo, B., *Anal. Chem.* **1998,** *70* (1), 131.

56. Bakac, A.; Espenson, J. H., *J. Am. Chem. Soc.* **1984,** *106* (18), 5197.

Chapter 4

4. Linear Epoxide Containing Polymers; A Route to the Synthesis of Dual Functional Polymers

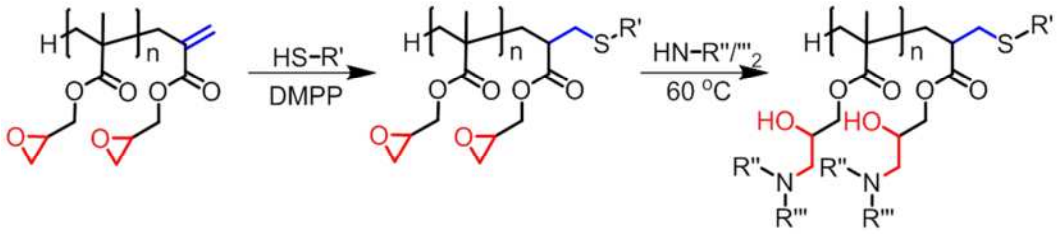

Linear polymers of glycidyl methacrylate were synthesised by CCTP, yielding polymers with two points for post-polymerisation functionalisation; activated vinyl and epoxide groups. Epoxide ring-opening and combinations of thiol-Michael addition and epoxide ring-opening have been used for the functionalisation of these groups with commercial amines and thiols in order to prepare a range of functional polymers.

4.1. Epoxide Containing Polymers for the Synthesis of Functional Materials

4.1.1. A Brief History of Epoxide Containing Polymers in the Literature

In organic chemistry epoxides are recognised as one of the most reactive functional groups due to the high strain associated with the three membered ring, which can ring-open, reacting with a wide range of nucleophiles.[1] One of the most well known uses of epoxide ring-opening reactions employed commercially is the formation of 'epoxy'-resins. These are thermosetting polymers formed from reaction of a poly-epoxide (resin/compound) with a nucleophilic compound such as polyol or polyamine groups (hardeners/activators). On mixing of the two reagents, nucleophilic groups initiate the ring-opening of epoxide moieties and covalent bonds are formed, leading to polymeric structures/networks. The range of 'epoxy' resins available is high and can be tailored for many applications including adhesives, paints and coatings, electrical systems/electronics and aerospace. These products can be cured thermally, or by UV activation, but many can are cured simply on addition of the epoxide compound to the nucleophiles, such as araldite, which uses polyamines, such as diethylenetriamine, to initiate a crosslinking reaction.[2]

The realisation that epoxide containing polymers and copolymers, such as glycidyl methacrylate, can undergo such post-polymerisation modifications occurred in the mid 50's and was patented by DuPont. Copolymers of glycidyl containing monomers were synthesised *via* free radical polymerisation and it was postulated that the resulting polymers, if reacted with functional amines *via* self-catalysed nucleophilic addition, could yield polyamines suitable for use in coating, impregnating, adhesive compositions, as dispersing agents for waxes and oils, and as binders for printing inks and paints.[3] Academic research in this field was carried out in the early 60's by Iwakura *et al*.,[4, 5] with the main focus of their work on ring-opening of epoxide moieties with secondary amines, but work was also done into the functionalisation of copolymer fibres of acrylonitrile and glycidyl methacrylate (GMA) with primary amines.[6] Further expansion of these reactions was undertaken in the mid 70's employing a variety of other functionalities including carboxylic acids, phosphoric acids and thiourea (Figure

4.1), elucidating the scope for the modification of these polymers/copolymers.[7] Although such post-polymerisation modifications cannot necessarily be defined as click chemistry, they can provide a facile route to the synthesis of a wide range of functional polymers from a single polymer precursor, with work based around this concept increasing in the past year.

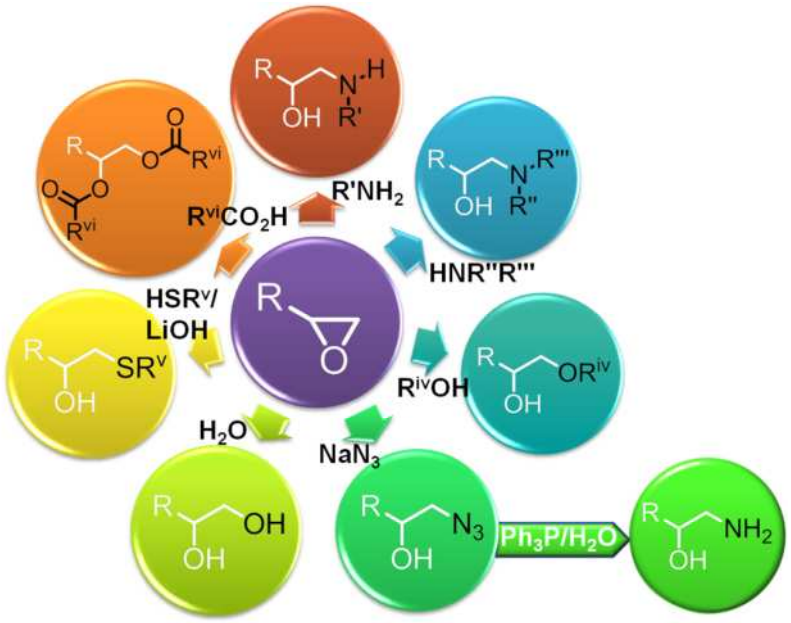

Figure 4.1: Potential reactions of epoxides, ring-opening reactions with a wide range of functional nucleophiles

4.1.2. Recent Literature on Epoxide Containing Polymers

In recent years there has been a resurgence in the number of publications involving epoxide polymers, from reactive surfaces and functional particles,[8-19] through to polymer chain end modifications with small molecule epoxides.[20-22] Tsarevsky *et al*. synthesised copolymers of glycidyl methacrylate and methyl methacrylate *via* ATRP, yielding bromine terminated polymers containing epoxides.[23] Reaction of epoxide and terminal bromine groups with sodium azide, with a subsequent CuAAc reaction with alkyne terminated polymers led to the formation of loosely grafted polymer brushes.[24] Lithium hydroxide has also been employed as a catalyst to facilitate the ring-opening of epoxide groups with functional thiols, with subsequent esterification of the hydroxyl groups formed on ring-opening of epoxides leading to the synthesis of dual functional polymers with great success.[25, 26] Dual functional glycopolymers have also been

achieved using CCTP by Haddleton *et al*. Polymerisation of GMA led to polymers containing epoxide rich side chains and a single terminal vinyl groups per chain. Terminal vinyl groups were exploited using thiol-Michael addition, with subsequent epoxide ring-opening with sugar azides in the formation of dual functional glycopolmyers.[27] Macromonomers formed *via* CCTP have also shown to be susceptible to epoxidation at terminal vinyl groups in work by Heuts *et al*., providing further potential for the functionalisation of such polymers, although attempts to polymerise epoxide terminated macromonomers *via* ring-opening polymerisation did not have the expected results.[21] In parallel to the work outlined below, research into the synthesis of epoxide containing polymers *via* RAFT was investigated, yielding polymers with the potential for dual functionalisation of both the epoxide group, in which functionalisation was conducted with functional amines, and subsequent thiol-ene chemistry on the sulfur end groups obtained from aminolysis of terminal RAFT moieties. These potentially dual functional polymers were used in the synthesis of amphiphilic block copolymers, by copolymerisation of GMA and a range of nucleophile resistant monomers. On functionalisation of poly-GMA block copolymers with hydrophilic functional amines amphiphilic block copolymers, capable of self assembly into micellar structures, were obtained.[28] The scope for post-polymerisation functionalisation has proven to be great for epoxide containing polymers, with many combinations of polymerisations and functionalisations remaining unexplored.

4.2. Results and Discussion

The focus of this current work is the functionalisation of poly-GMA, synthesised by CCTP, *via* epoxide ring-opening with both primary and secondary amines. One of the advantages of using functional amines is due to their strong nucleophilic and basic nature, the majority of primary and secondary amines can take part in epoxide ring-opening reactions without the use of a catalyst, also there is a wealth of primary and secondary amines available commercially. By employing CCTP, not only can the molecular weight of the resulting polymers be controlled, but an *ω*-unsaturated end group is incorporated into the polymer, providing a second reactive handle for functionalisation, either by thiol-ene click chemistry[29, 30] or nucleophilic attack by functional primary amines. By tuning the selectivity of the reactions the optimisation

and generation of dual functional polymers (at the terminus and along the polymer backbone) is possible, which would be difficult to obtain by other methods.

4.2.1. Synthesis of Epoxide Containing Polymers via CCTP

Epoxide containing polymers were synthesised by CCTP of GMA, using CoBF as the chain transfer catalyst, to obtain polymers which posses high levels of epoxide functionality and a single vinyl group per chain (Figure 4.2). The C_s value was measured for GMA in acetonitrile, yielding a value of 6400.[31]

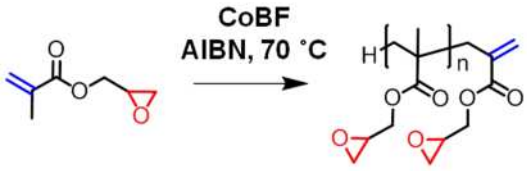

Figure 4.2: Schematic of the synthesis of poly-GMA *via* CCTP, retention of epoxide and vinyl functionality

Variation of the CoBF concentration provides a high level of control over the molecular weight, employing only small amounts (ppm levels) of catalyst. By increasing the CoBF concentration polymer chains of decreasing molecular weight were obtained, which for low molecular weights, contain discernible oligomeric products *via* SEC (Table 4.1, Figure 4.3).

Name	CoBF (mol%)	M_n ($g.mol^{-1}$)	M_w ($g.mol^{-1}$)	PDi	Conversion (%)
A	$7.86x10^{-6}$	800	1400	1.76	90.2
B	$3.94x10^{-6}$	1600	2900	1.86	91.2
C	$1.97x10^{-6}$	3100	5800	1.86	99.0
D	$9.84x10^{-7}$	5000	9100	1.84	93.4

Table 4.1: Linear poly-GMA synthesised. Decreasing CoBF concentrations for the formation of increasing molecular weights. Molecular weights measured by conventional SEC. Conversion measured by GC-FID

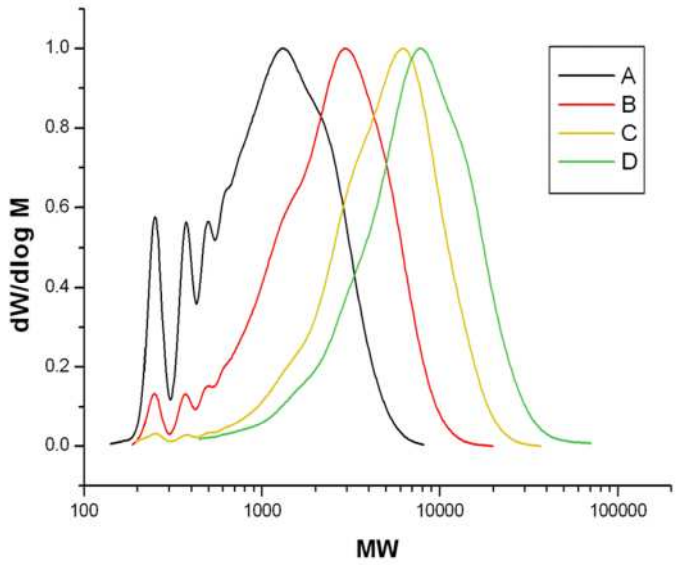

Figure 4.3: Molecular weight comparison of GMA homopolymerisations A-D (A: 7.86x10^{-6} mol% CoBF. B: 3.94x10^{-6} mol% CoBF. C: 1.97x10^{-6} mol% CoBF. D: 9.87x10^{-7} mol% CoBF)

M_w and PDi plots of polymerisations **A**-**D** proceeded in a typical manner for CCTP of monovinyl methacrylates (Figure 4.4). As the [CoBF]/[monomer] ratio is relatively low in the initial stages of the reaction, the highest molecular weights are formed. As the polymerisation proceeds, monomer concentration decreases, hence the relative [CoBF]/[monomer] ratio increases, leading to the formation of lower molecular weight chains. Consequentially a sharp increase in both M_w and PDi is observed *via* SEC in the initial stages of the polymerisation, with these values slowly decreasing as the polymerisation proceeds. Molecular weights obtained from the polymerisations increase on decreasing CoBF concentration, on doubling the concentration of CoBF the molecular weight of the resulting polymer is reduced by half, with PDi's remaining fairly consistent on decreasing CoBF concentration (Figure 4.4).

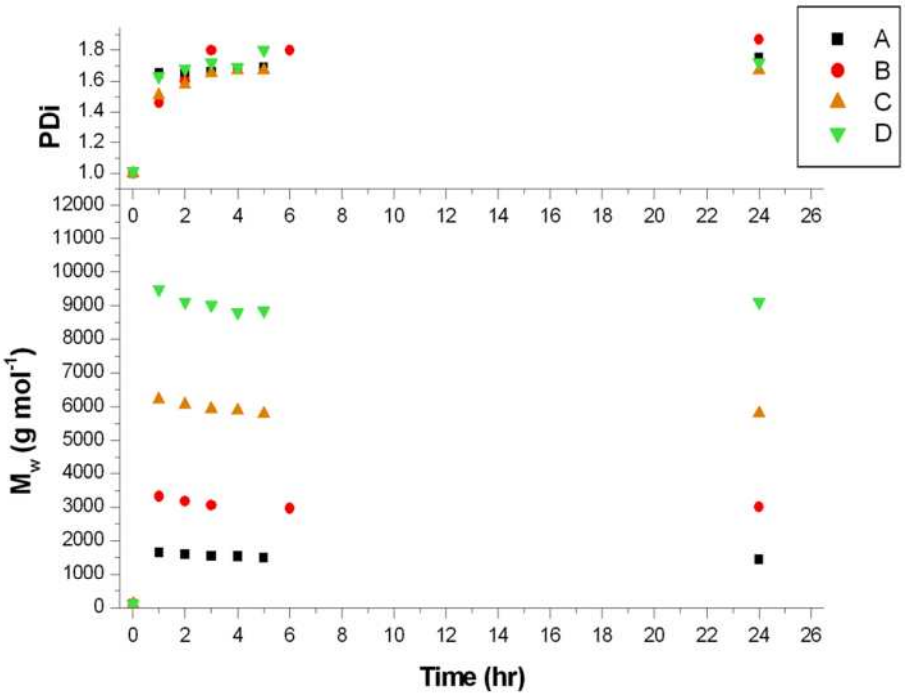

Figure 4.4: SEC data, molecular weight and PDi evolution of GMA polymerisations A-D *via* CCTP (A: 7.86x10^{-6} mol% CoBF. B: 3.94x10^{-6} mol% CoBF. C: 1.97x10^{-6} mol% CoBF. D: 9.87x10^{-7} mol% CoBF)

The resulting polymers possess two sites for further functionalisation; a high level of epoxide functionality, equal to the DP_n of the polymer, and a single terminal vinyl group per chain, both of which can be characterised *via* ^{1}H NMR. A typical ^{1}H NMR spectrum of poly-GMA synthesised *via* CCTP is given in Figure 4.5.

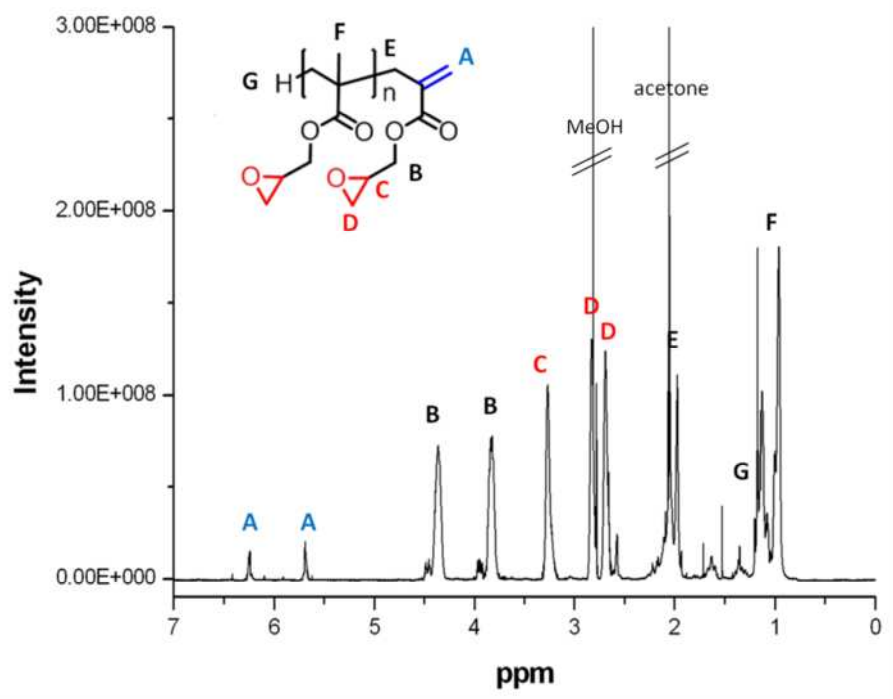

Figure 4.5: Typical ^{1}H NMR spectrum of poly-GMA, synthesised by CCTP, depicting characteristic epoxide and vinyl signals, NMR solvent- d^{6}-acetone

MALDI-ToF analysis of poly-GMA revealed the main product to be increasing molecular weights of [Co(III)-H] initiated poly-GMA **[B: 2, 3 ,5, 6]**, with minor peaks corresponding to incorporation of an unknown impurity (X) of -14 or +128 Daltons to the main peak series **[B: 1 , 4]**. On investigation of the monomer *via* ^{1}H NMR and electrospray ionisation - mass spectrometry (ESI-MS) this impurity X could not be identified. The purity of the monomer as quoted by the supplier is 97%, hence it can be assumed this impurity is present in low quantities. (Figure 4.6, Table 4.2).

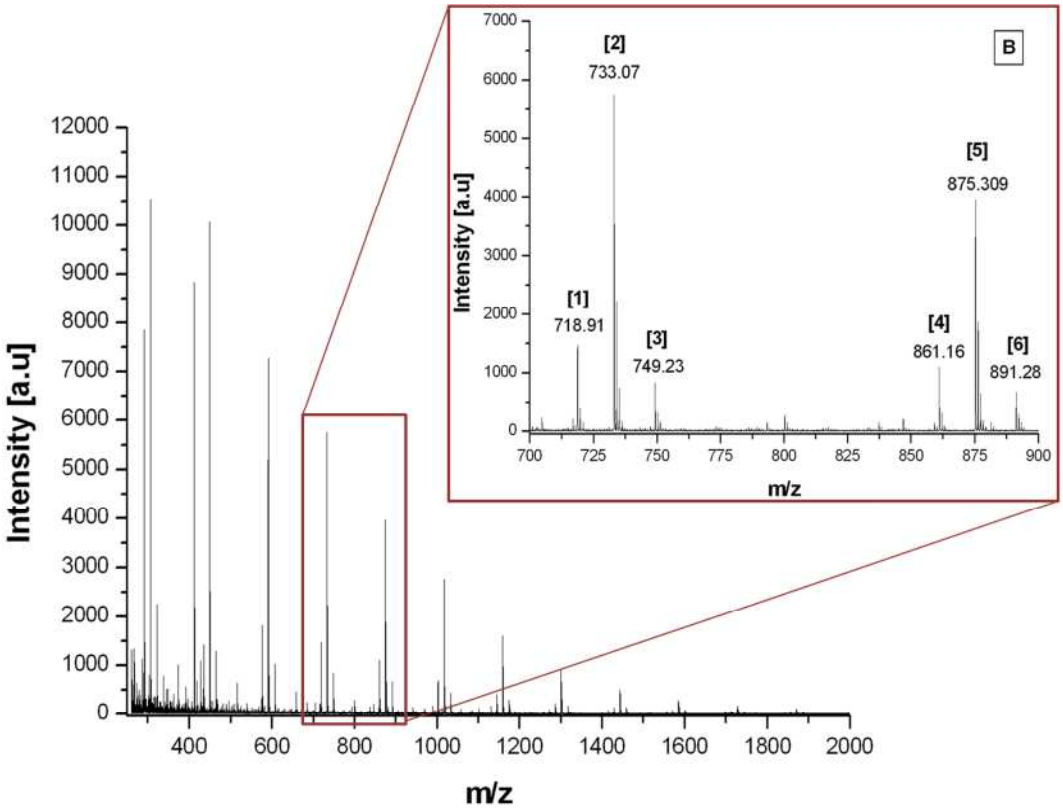

Figure 4.6: MALDI-ToF spectrum of B, poly-GMA, with zoom region between 700-900 Daltons. Annotations correspond to Table 4.2

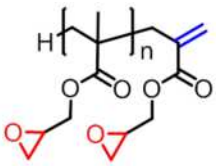

Figure 4.7: Example structure of poly-GMA, $(GMA)_2$ (if n=1)

Name	Theoretical m/z	Measured m/z	Corresponding Structure
[B: 1]	719.19	718.91	$(X)(GMA)_4Na^+$
[B: 2]	733.30	733.07	$(GMA)_5Na^+$
[B: 3]	749.28	749.23	$(GMA)_5K^+$
[B: 4]	861.30	861.16	$(X)(GMA)_5Na^+$
[B: 5]	875.36	875.31	$(GMA)_6Na^+$
[B: 6]	891.34	891.28	$(GMA)_6K^+$

Table 4.2: Corresponding structures to MALDI-ToF peaks annotated in Figure 4.6 for mass region 700-900 Daltons, for poly-GMA B, where X is taken as 128.00 Daltons. Example structure given in Figure 4.7

4.2.2. Initial Study – Reactivity of Epoxide and Vinyl Functionalities to Nucleophilic Attack via Primary Amine

To assess the activity of both epoxide and vinyl groups towards nucleophilic addition of primary amines, a series of reactions were conducted in an attempt to functionalise poly-GMA (**B**) with propylamine, in a self-catalysed manner, with only the addition of a small excess of propylamine (1.2 excess), employing a variety of polar aprotic solvents (Table 4.3). Under these conditions it was found that the vinyl groups were more susceptible to reaction with propylamine than the epoxide, which although surprising considering the ring strain of the epoxide group, has been previously reported in work by Zhang *et al*.[27] Polar aprotic solvents are known to be good solvents for S_N2 ring-opening reactions, yet under these conditions ring-opening of the epoxide is slow, with conversion increasing slowly in line with increasing solvent polarity. Within the time frame of 70 hours complete epoxide conversion does not occur in any solvent tested. Hence, for complete functionalisation at both the epoxide and unsaturated end groups larger excesses of amine were employed in DMSO, which has shown to be a good solvent for both the ring-opening of epoxide moieties and amine addition to vinyl groups. Additionally DMSO provides a good solvent for a wide range of both hydrophobic and hydrophilic primary amines.[29, 32, 33]

Solvent	Epoxide Conversion	Vinyl Group Conversion
MEK	0%	32%
Et. OAc.	0%	65%
DCM	24%	100%
MeCN	35%	31%
DMSO	58%	100%
DMF	64%	100%

Table 4.3: Conversion of both epoxide and vinyl group measured by ^{1}H NMR for the epoxide ring-opening of poly-GMA (A) with propylamine in a variety of polar aprotic solvents, conversion measured after 50 hours reaction time

Ring-opening reactions of poly-GMA with propylamine were carried out using 2-fold, 5-fold and 10-fold excesses of amine to epoxide groups, under ambient conditions in DMSO (Figure 4.8). Conversion of both vinyl and epoxide groups were measured by ^{1}H NMR over the course of 70 hours. Using a 10-fold excess of amine nucleophilic addition to vinyl groups is complete within 1 hour at ambient temperature. A slower rate

of reaction was observed for epoxide ring-opening, which reached 100% conversion within 25 hours. In the cases of 5-fold and 2-fold excess of amine the same trend is observed but the rate of reaction of functionalisation for both epoxide and vinyl groups is reduced, with the use of a 2-fold excess being the slowest. An important observation of these reactions was that in cases where lower amine excesses were used, such as 3-fold excess and below, at ambient temperatures, the products became insoluble/sparingly soluble after several days. This is most likely caused by the use of a primary amine in the ring-opening reaction; primary amines can undergo reaction with two epoxides, causing crosslinking between polymer chains. In addition to this, hydroxyl groups formed on epoxide ring-opening are nucleophilic and can also lead to intra or intermolecular crosslinking.[28] Hence, to decrease the excess of primary amine required in the functionalisation of poly-GMA, subsequent reactions were conducted at 60 ˚C.

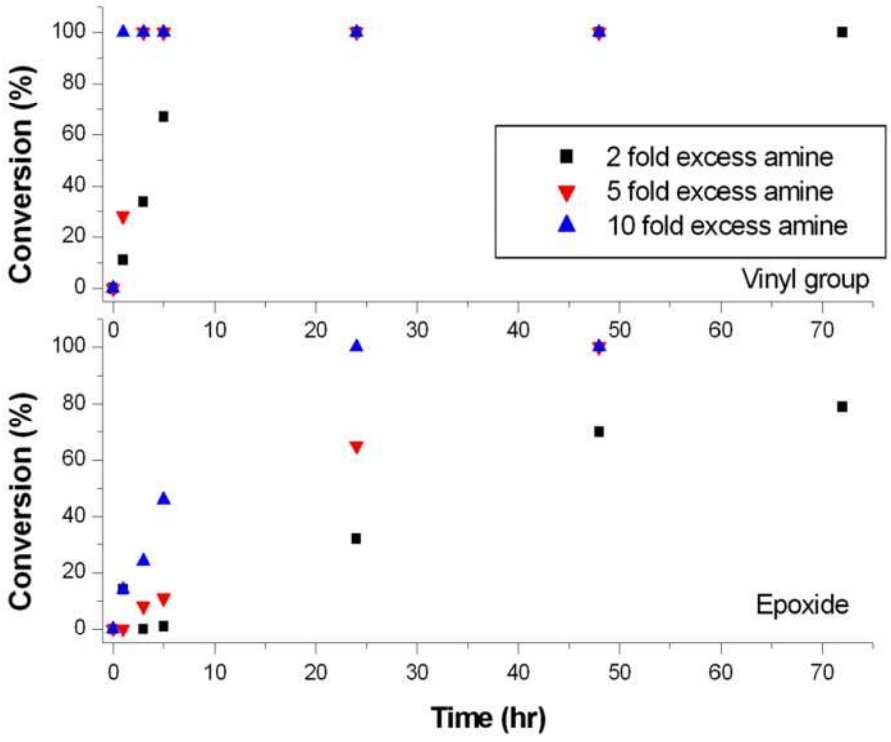

Figure 4.8: Conversions for ring-opening of poly-GMA (B) with propylamine, varying amine excess of 2-, 5- and 10-fold to epoxide groups. Reduction of epoxide and vinyl signals was monitored *via* ^{1}H NMR

Although preliminary reactions at 60 ˚C, using a 10 fold excess of propylamine, displayed a complete loss of epoxide after 4 hours by ^{1}H NMR, however, for long periods of time a crosslinking reaction took place, with products becoming insoluble. It is thought that even as little as 1% unreacted epoxide is enough to affect the solubility of the polymer if intermolecular crosslinking occurs, resulting in functional gels. It was found that by using as little as 1.2 mole equivalent excess of amine to epoxide and vinyl groups, soluble, fully functionalised polymers, at both the vinyl and epoxide groups, could be obtained after 24 hours at 60 ˚C (

Figure 4.9).

4.2.3. Full Functionalisation of poly-GMA with Commercial Primary Amines

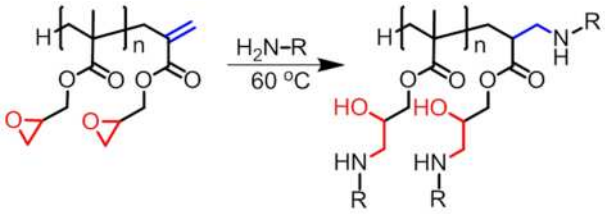

Figure 4.9: General scheme for the full functionalisation of poly-GMA with functional primary amine

Full functionalisation of poly-GMA (**B**) with propylamine was conducted using a 1.0:1.2 ratio of epoxide groups to propylamine at 60 ˚C for 24 hours (**B1**). ^{1}H NMR was utilised to assess the level of functionality achieved. On comparison of the ^{1}H NMR spectra of **B** and **B1** a change in epoxide peaks is observed, with no discernible epoxide peaks remaining after 24 hours. A downfield shift of peaks at 2.6, 2.7 ppm to 2.9 ppm corresponding to oxirane CH_2 peaks is observed, convergence of these two peaks is due to a release in ring-strain. A dramatic shift is also seen in the oxirane CH peak, from 3.2 to 4.3 which, upon ring-opening, becomes adjacent to the newly formed hydroxyl group. Peaks at 3.8 and 4.3 ppm, arising from the constrained OCH_2 adjacent to the epoxide, converge on ring-opening at 4.0 ppm, again indicative of a release of constraint. Peaks corresponding to propylamine are also observed at 2.4, 1.5 and 1.0 ppm confirming its addition to the polymer. A disappearance of vinyl peaks was also observed *via* ^{1}H NMR and the introduction of a peak at approximately 2.6 ppm was

seen, indicating the formation of a CH_2NH group on nucleophilic addition to vinyl groups (Figure 4.10).

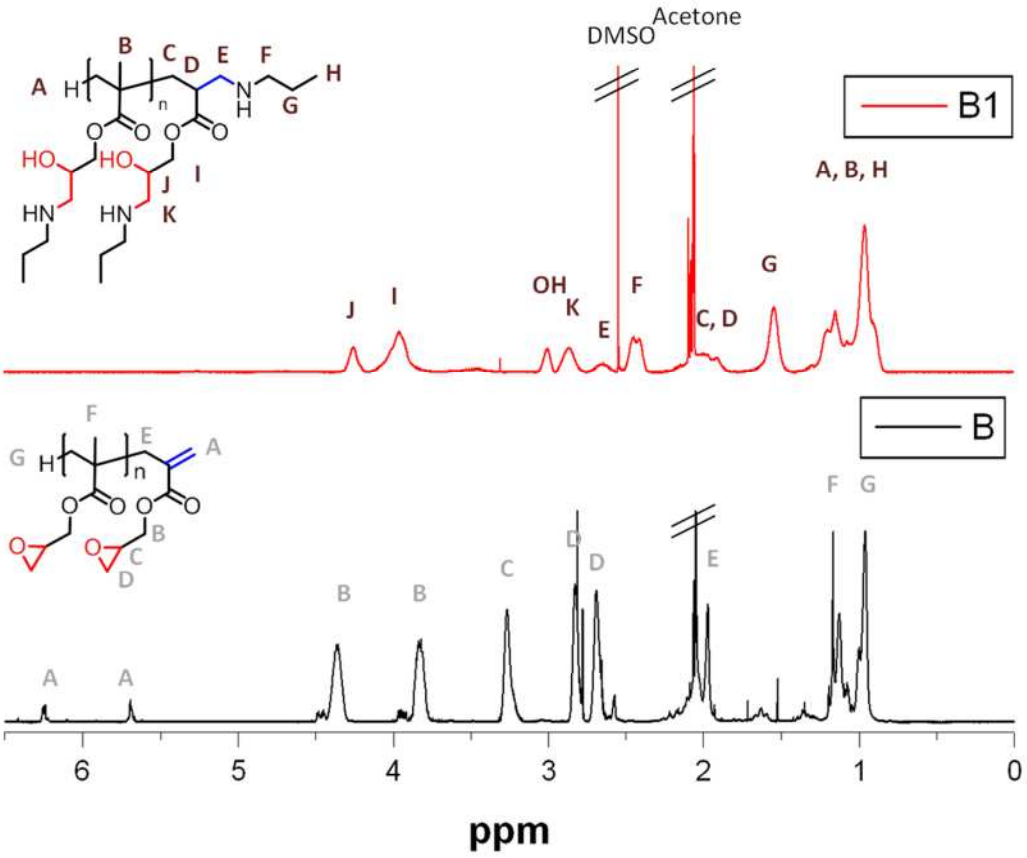

Figure 4.10: ^{1}H NMR comparison of poly-GMA (B) and propylamine functionalised poly-GMA (B1), 1:1.2 molar ratio of epoxide groups to propylamine in d^6-acetone

SEC analysis also confirms the addition of propylamine to the polymer, with a marked increase of measured molecular weight observed on functionalisation of poly-GMA with propylamine from 2800 to 6200 g.mol^{-1} (Table 4.4). No evidence of interchain crosslinking is observed in the SEC spectrum, which would manifest itself by the appearance of high molecular weight species or bimodal peaks and broadening of the PDi.

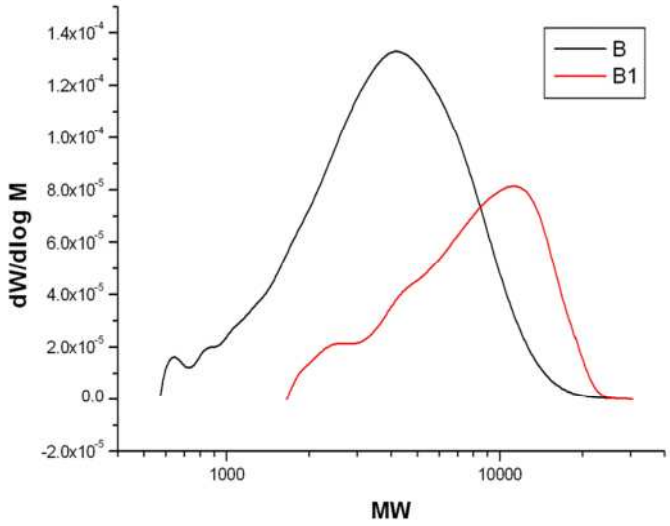

Figure 4.11: SEC comparison of poly-GMA (B) to propylamine functionalised poly-GMA (B1)

Confirmation of epoxide ring-opening is also observed *via* FT-IR analysis, with the loss of peaks corresponding to the asymmetric epoxide stretch at approximately 904 cm^{-1} and emergence of a broad OH peak at 3100-3600 cm^{-1} corresponding to the hydroxyl groups formed on ring-opening of the epoxide (Figure 4.12). Loss of vinyl group functionality cannot be confirmed by FT-IR however, due to an overlapping N-H bend peak arising on the formation of C-N bonds at approximately 1620 cm^{-1}.

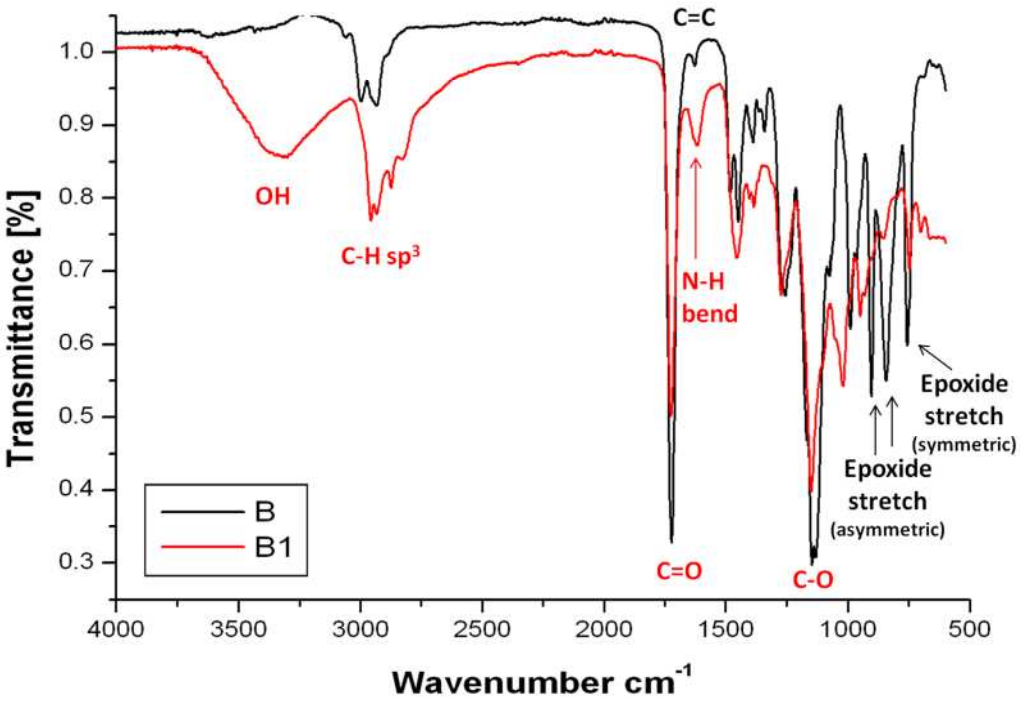

Figure 4.12: FT-IR comparison of poly-GMA (B) with propylamine functionalised poly-GMA (B1)

Functionalisation was extended to a range of commercially available primary amines with varying degrees of success. Reactions with benzylamine (**B2**), 3-amino-1,2-propanediol (**B3**) and decylamine (**B5.1**) all showed full ring-opening of epoxides and full reaction of vinyl groups *via* ^{1}H NMR, with increases in molecular weight observed *via* SEC (Table 4.4, Figure 4.13). On precipitation of benzylamine however, it appeared a low level of vinyl functionality had been retained. Reaction of propargylamine with poly-GMA led to formation of a gel (**B4.1**), which, consequentially could not be characterised by solution techniques. Upon characterisation of the gel by FT-IR no remaining epoxide functionality at 904 cm^{-1} was observed, and a broad peak is observed at 3100-3600 cm^{-1} signifying the formation of a hydroxyl group. It is unclear if the unprotected alkyne groups participated in the crosslinking reaction, as peaks denoting this group would arise at approximately 3300-3400 cm^{-1}, hence, are obscured by the broad OH peak. On repetition of this reaction using a high excess of propargylamine, 5-fold excess to epoxide and vinyl groups, a soluble polymer was yielded (**B4.2**), which showed a retention of alkyne functionality in the product, characterised by a peak in the ^{13}C NMR at approximately 83 ppm, corresponding to the quaternary carbon, however, film formation occurred several weeks after synthesis,

suggesting that the unprotected alkyne functionality is participating in a slow forming side reaction, leading to crosslinking. Ways to circumvent this effect include use of protected alkyne functionality, addition of a protecting group prior to storage, or functionalisation of these groups immediately after synthesis.

Functionalisation with 3-amino-1,2-propanediol led to the formation of a highly hydrophilic species, only soluble in solvents such as water, DMF and DMSO. Conversely, functionalisation with decylamine led to polymer products precipitating out of the DMSO reaction mixture, hence, solvation of the product was limited to hydrophobic solvents, and therefore SEC was performed in $CHCl_3$. On examination of decylamine functionalised poly-GMA *via* SEC a multi-modal polymer peak with a broad PDi was observed, which may be indicative of the occurrence of intermolecular crosslinking, although the solubility is not compromised as in other cases where insoluble products are formed. It is postulated that if intermolecular crosslinking is the cause of the observed PDi broadening, the level of crosslinking is relatively low. A broad PDi may also be an artefact of SEC analysis in an incompatible solvent; however the solubility of decylamine functionalised poly-GMA appeared good in $CHCl_3$, displaying poor solvation in other SEC eluents employed, such as THF and DMF. On repetition of the reaction in DMF rather than DMSO, using a 5 mole equivalent excess of decylamine to epoxide and vinyl groups, a homogenous system was obtained (**B5.2**). Under these conditions a monomodal SEC spectrum was observed (Figure 4.13 (right)), displaying an increased molecular weight compared to unfunctionalised poly-GMA (**B**) (Table 4.4), with no broadening of the PDi. Hence, for certain functional amines higher excesses may be required, highlighting the need for optimisation of each amine employed, especially when functionalisation leads to a dramatic change in the hydrophilicity/hydrophobicity of the polymer.

Name	Functional Amine	Amine Excess (mol %)	M_n (g mol^{-1})	M_w (g mol^{-1})	PDi
		DMF SEC Eluent			
B	Poly-GMA	-	2800	4400	1.6
B1	Propylamine	1.2	6200	8700	1.4
B2	Benzylamine	1.2	7500	15400	2.0
B3	3-Amino-1,2-propanediol	1.2	5600	10600	1.9
B4.1	Propargylamine	1.2		Gel	
B4.2	Propargylamine	5	12700	18100	1.4
		$CHCl_3$ SEC Eluent			
B	Poly-GMA	-	2000	4100	2.1
B5.1	Decylamine	1.2	5800	36200	6.3
B5.2	Decylamine	5	4100	6200	1.5

Table 4.4: SEC comparison of poly-GMA (B) and full amine functionalisation products with a variety of commercially available functional amines

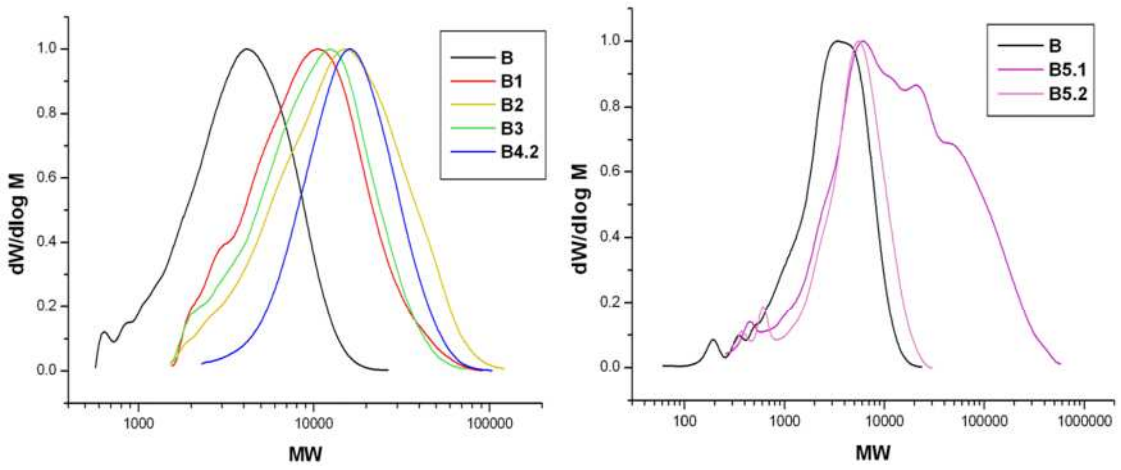

Figure 4.13: (left) SEC comparisons of B to B1-B3, DMF eluent (B poly-GMA, B1 propylamine functionalised poly-GMA, B2 benzylamine functionalised poly-GMA, B3 aminopropanediol functionalised poly-GMA) (right) SEC comparison of B to B5.1 and B5.2, $CHCl_3$ eluent (B poly-GMA, B5 decylamine functionalised poly-GMA)

After purification the resulting polymers were analysed by FT-IR. Epoxide ring-opening was confirmed by a loss of epoxide stretching peaks at approximately 904 cm^{-1}, with the introduction of a broad peak at 3100-3600 cm^{-1} corresponding to the formation of hydroxyl groups. In the case of 3-amino-1,2-propanediol functionalisation a strong OH

peak was observed due to the increased number of hydroxyl groups covalently attached to the polymer.

Polymers were also investigated by MALDI-ToF spectroscopy to ascertain whether homogeneous functionalisation was achieved. The MALDI-ToF spectrum for poly-GMA (**B**) functionalised with propylamine (**B1**) showed two major peak series', one the full functionalisation of both epoxide and vinyl groups **[B1: 2]** and secondly the incomplete functionalisation of products, whereby one epoxide or terminal vinyl group remains in the polymer **[B1: 1, 4]** (Figure 4.14, Table 4.5). A minor peak series is also observed whereby two epoxides or an epoxide and vinyl group remain unfunctionalised **[B1: 3]**, despite the high level of functionalisation suggested by ^{1}H NMR.

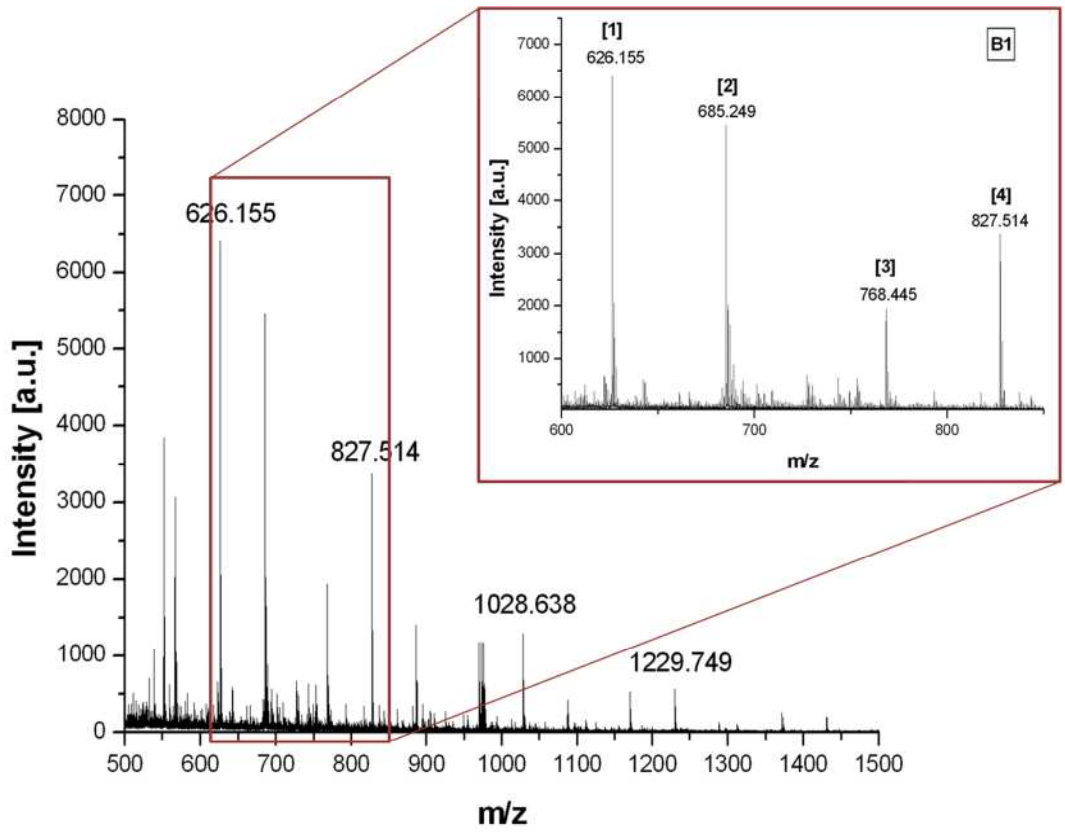

Figure 4.14: MALDI-ToF spectrum of B1, propylamine functionalised poly-GMA (1:1.2 epoxide + vinyl groups to propylamine), with zoom region between 600-900 Daltons. Annotations correspond to Table 4.5

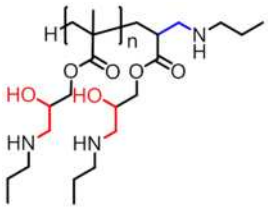

Figure 4.15: Example structure of PGMA functionalised with propylamine, $(GMA)_2(PAm)_3$ (if n=1)

Name	Theoretical m/z	Measured m/z	Corresponding Structure
[B1: 1]	626.40	626.16	$(GMA)_3(PAm)_3Na^+$
[B1: 2]	685.47	685.25	$(GMA)_3(PAm)_4Na^+$
[B1: 3]	768.46	786.45	$(GMA)_4(PAm)_3Na^+$
[B1: 4]	827.54	827.51	$(GMA)_4(PAm)_4Na^+$

Table 4.5: Corresponding structures to MALDI-ToF peaks annotated in Figure 4.14 for mass region 600-900 Daltons, for B1 propylamine functionalised poly-GMA. PAm – propylamine. Example structure given in Figure 4.15

Discrepancies observed in the level of vinyl groups seen *via* ^{1}H NMR and MALDI-ToF may be due to the detection limits of ^{1}H NMR, although precipitated samples were analysed using 600 or 700 MHz spectrometers, which should provide a higher sensitivity. This may also be due to non-quantitative results obtained *via* MALDI-ToF as unfunctionalised polymers may be more readily ionised, hence appear more intense in the spectra. However, a recent publication highlighted the synthesis of heterocycles by reaction of small molecules containing both epoxide and vinyl functionality with primary amines, under similar conditions to those employed in this work.[34] *ω*-Terminal secondary amines formed on epoxide ring opening are in close proximity to activated vinyl groups and may react *via* an aza-Michael type addition, in the formation of eight membered heterocycles (Figure 4.16). This reaction could potentially occur with any functional primary amine and may explain why no remaining vinyl groups are observed *via* ^{1}H NMR, despite apparent incomplete functionalisation products observed *via* MALDI-ToF.

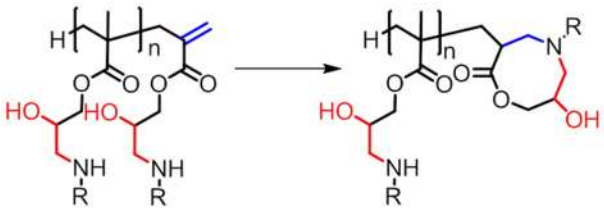

Figure 4.16: Schematic for the formation of terminal heterocycles on epoxide ring-opening with primary amines

Unfortunately, as the peak shifts for any heterocycles formed would be of a similar shift to fully functionalised products, and all peaks are broad due to the polymeric nature of the product, quantification or indeed confirmation of this reaction for the polymer was not possible by NMR. However, MALDI-ToF confirms that full functionalisation at both the epoxide and vinyl groups occurs in addition to incomplete functionalisations; therefore a mixture of terminal functionalities is obtained.

The MALDI-ToF spectrum obtained for benzyl amine functionalised poly-GMA (**B2**) shows a major peak series whereby one group remains unfunctionalised **[B2: 1, 4]**, and minor peak series' corresponding to fully functionalised chains **[B2: 2]** and chains whereby two groups remain unfunctionalised **[B2: 3]** (Figure 4.17, Table 4.6). A lower level of fully functionalised products is observed in comparison to **B1**, but due to the retention of vinyl groups observed in the ^{1}H NMR of the precipitated product, this level of incomplete functionalisation, whereby one group remains, is not unexpected.

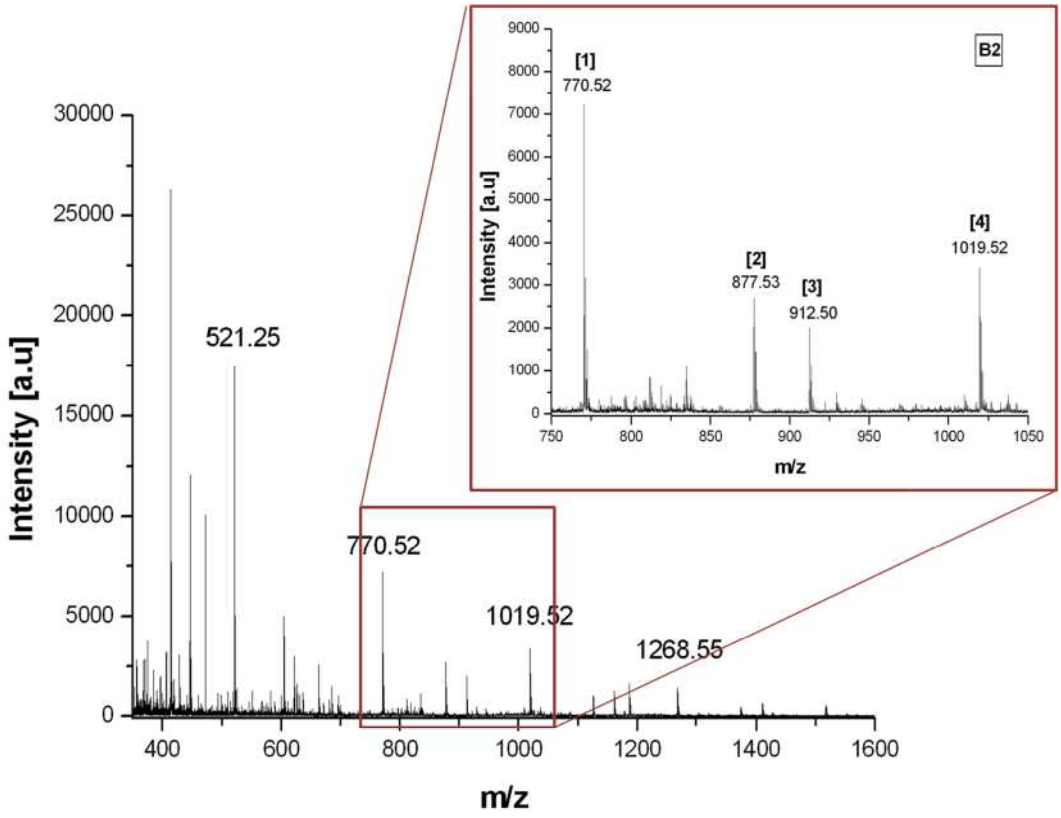

Figure 4.17: MALDI-ToF spectrum of B2, benzylamine functionalised poly-GMA (1:1.2 epoxide + vinyl groups to benzylamine), with zoom region between 750-1050 Daltons. Annotations correspond to Table 4.6

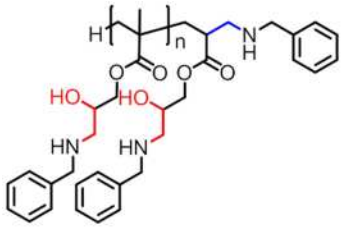

Figure 4.18: Example structure of Poly-GMA functionalised with benzylamine, $(GMA)_2(Bam)_3$ (if n=1)

Name	Theoretical m/z	Measured m/z	Corresponding Structure
[B2: 1]	770.40	770.52	$(GMA)_3(BzAm)_3Na^+$
[B2: 2]	877.47	877.53	$(GMA)_3(BzAm)_4Na^+$
[B2: 3]	912.46	912.50	$(GMA)_4(BzAm)_3Na^+$
[B2: 4]	1019.54	1019.52	$(GMA)_4(BzAm)_4Na^+$

Table 4.6: Corresponding structures to MALDI-ToF peaks annotated in Figure 4.17 for mass region 750-1050 Daltons, for B2 benzylamine functionalised poly-GMA, BzAm-benzylamine. Example structure given in Figure 4.18

The MALDI-ToF obtained of decylamine functionalised poly-GMA (**B5**) also suggested a higher level of products with one epoxide, or vinyl groups, remaining unfunctionalised than observed in ^{1}H NMR, with the major peak series denoting fully functionalised chains **[B5: 1, 5]**, and minor peak series' denoting one **[B5: 3]** and two unfunctionalised groups remaining **[B5: 4]** (Figure 4.19, Table 4.7). MALDI-ToF spectra could not be obtained for 3-amino-1,2-propanediol functionalised poly-GMA (**B3**) and propargylamine functionalised poly-GMA (**B4.2**).

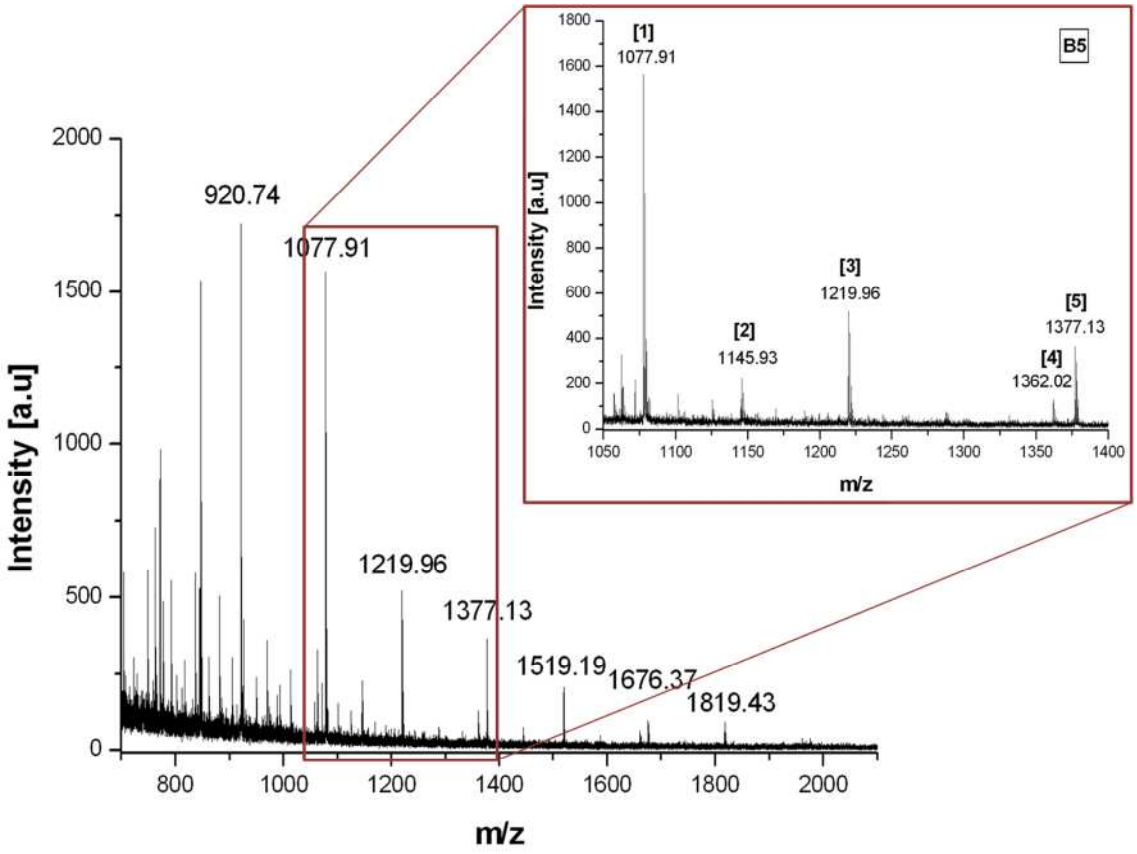

Figure 4.19: MALDI-ToF spectrum of B5, decylamine functionalised poly-GMA (1:1.2 epoxide + vinyl groups to decylamine), with zoom region between 1050-1400 Daltons. Annotations correspond to Table 4.7

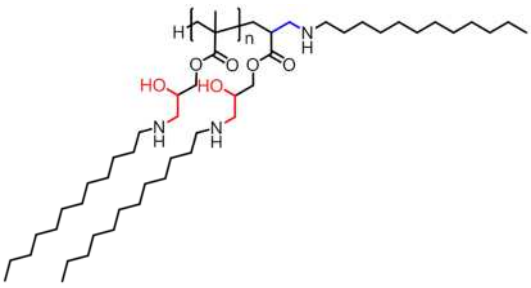

Figure 4.20: Example structure of poly-GMA functionalised with decylamine, $(GMA)_2(Dam)_3$ (if n=1)

Name	Theoretical m/z	Measured m/z	Corresponding Structure
[B5: 1]	1077.91	1077.91	$(GMA)_3(DAm)_4Na^+$
[B5: 2]	1145.96	1145.93	$AIBN\text{-}init(GMA)_3(DAm)_4Na^+$
[B5: 3]	1219.97	1219.96	$(GMA)_4(DAm)_4Na^+$
[B5: 4]	1362.04	1362.02	$(GMA)_5(DAm)_4Na^+$
[B5: 5]	1377.16	1377.13	$(GMA)_4(DAm)_5Na^+$

Table 4.7: Corresponding structures to MALDI-ToF peaks annotated in Figure 4.19 for mass region 1050-1400 Daltons, for B5 decylamine functionalised poly-GMA, DAm-decylamine. Example structure given in Figure 4.20

4.2.4. Dual Functionalisation of Poly-GMA via Thiol-Michael Addition and Epoxide Ring-Opening with Primary Amines

Due to the reactivity of primary amines with terminal vinyl groups for poly-GMA, the thiol-Michael addition of benzyl mercaptan was conducted prior to epoxide ring-opening reactions (Figure 4.21). Thiol-Michael additions were conducted in DMSO, using DMPP as a catalyst, under ambient conditions. Reaction of benzyl mercaptan and poly-GMA (**A**) *via* thiol-Michael addition was successful, with a complete loss of vinyl peaks and the appearance of a multiplet at 2.35 ppm corresponding to hydrothiolation of the vinyl group. No reaction of epoxide groups was observed by ^1H NMR.

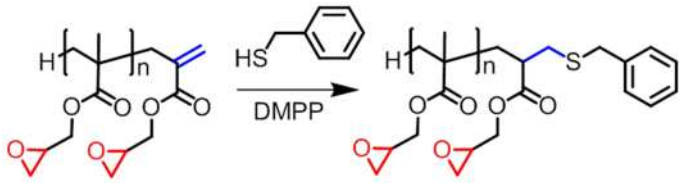

Figure 4.21: General scheme for the phosphine mediated thiol-Michael addition of benzyl mercaptan to poly-GMA

SEC with RI and PDA detection was employed for the analysis of the thiol-Michael addition product of benzyl mercaptan with poly-GMA (**A1**) (Figure 4.22). An increase in molecular weight was observed from 800 to 1200 on functionalisation of poly-GMA with benzyl mercaptan (Figure 4.22 (left), Table 4.8). An absorbance was also observed in the PDA spectrum at approximately 18-15 minutes, 270 nm, corresponding to addition of a chromophore to the polymer, further indicating the successful functionalisation of poly-GMA with benzyl mercaptan (Figure 4.22 (right)).

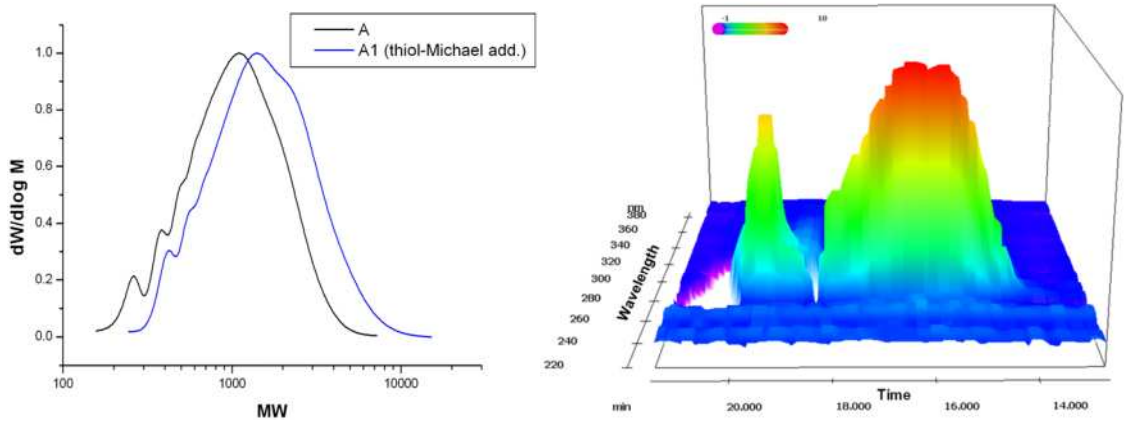

Figure 4.22: (left) SEC comparison of poly-GMA (A) and benzyl mercaptan functionalised poly-GMA (A1) THF eluent (right) PDA spectrum of benzyl mercaptan functionalised poly-GMA (A1) peak at 19 minutes retention 270 nm time corresponding to excess benzyl mercaptan, peak at 14-18 minutes 270 nm corresponding to chromophore addition to the poly-GMA

Name	M_n ($g.mol^{-1}$)	M_w ($g.mol^{-1}$)	PDi
A	800	1200	1.5
A1 (TMA)	1200	1800	1.6

Table 4.8: SEC comparison of poly-GMA (A) with thiol-Michael addition of benzyl mercaptan to poly-GMA (A1 TMA) in THF eluent, TMA-thiol-Michael addition

The successful thiol-Michael addition of benzyl mercaptan to poly-GMA was also confirmed by MALDI-ToF, with the main peak series denoting an increasing molecular weight of poly-GMA with addition of one benzyl mercaptan per chain **[A1 (TMA): 3, 7]** (Figure 4.23, Table 4.9). Incorporation of impurity X is also observed **[A1 (TMA): 2, 6]**, however at this stage inclusion of this impurity in the polymer chain has no detrimental effect on functionalisation *via* thiol-Michael addition, as addition of benzyl mercaptan is still observed. Minor peaks corresponding to unfunctionalised poly-GMA **[A1 (TMA): 4, 8]**, and chains where the addition of two benzyl mercaptan units occurs **[A1 (TMA): 1, 5]** are also present. Although several peak distributions are observed in the MALDI-ToF of the thiol-Michael addition product, only minor peaks correspond to chains whereby the level of functionalisation will lead to inhomogeneous products, containing multiple or no benzyl mercaptan moieties, therefore a high level of purity is obtained.

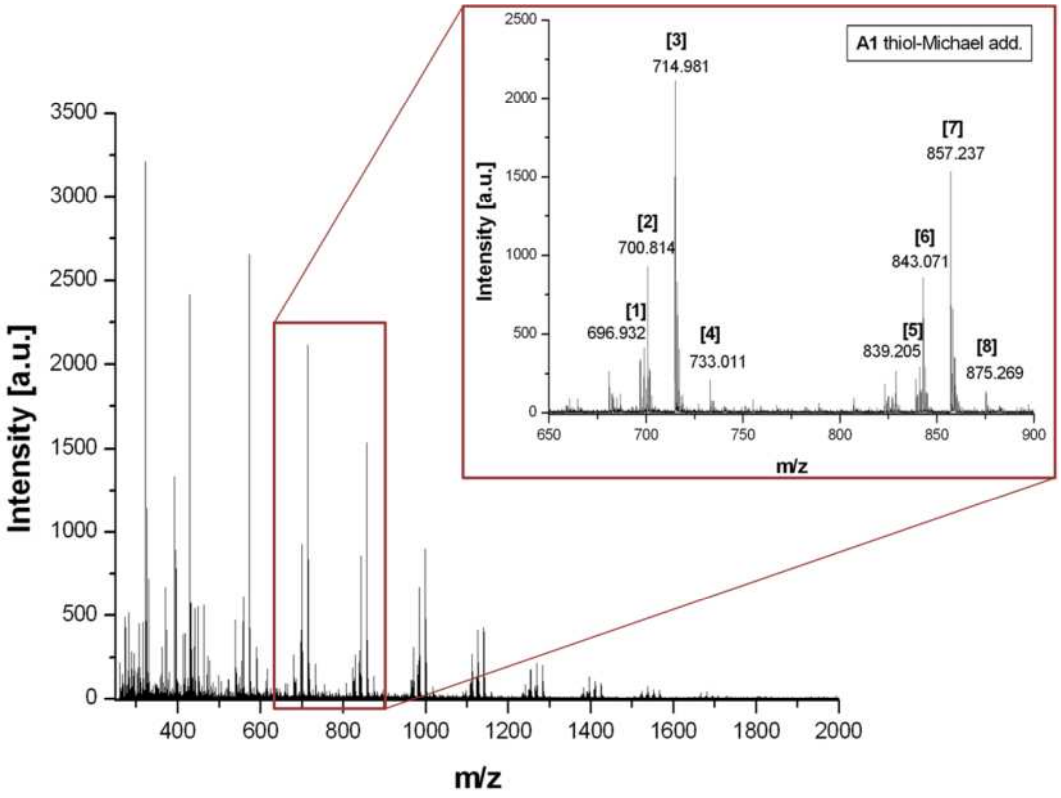

Figure 4.23: MALDI-ToF spectrum of A1, poly-GMA thiol-Michael addition with benzyl mercaptan, with zoom region between 650-900 Daltons. Annotations correspond to Table 4.9

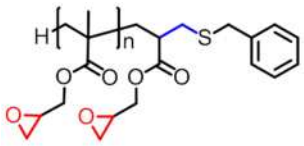

Figure 4.24: Example structure of benzyl mercaptan functionalised poly-GMA, $(GMA)_2(BM)_1$ (if n=1)

Name	Theoretical m/z	Measured m/z	Corresponding Structure
[A1 (TMA): 1]	697.25	696.93	$(GMA)_3(BM)_2Na+$
[A1 (TMA): 2]	701.21	700.81	$(X)(GMA)_3(BM)_1Na+$
[A1 (TMA): 3]	715.28	714.98	$(GMA)_4(BM)_1Na+$
[A1 (TMA): 4]	733.30	733.01	$(GMA)_5Na^+$
[A1 (TMA): 5]	839.31	839.21	$(GMA)_4(BM)_2Na^+$
[A1 (TMA): 6]	843.27	843.07	$(X)(GMA)_4(BM)_1Na^+$
[A1 (TMA): 7]	857.34	857.24	$(GMA)_5(BM)_1Na^+$
[A1 (TMA): 8]	875.36	875.27	$(GMA)_6Na^+$

Table 4.9: Corresponding structures to MALDI-ToF peaks annotated in Figure 4.23 mass region 650-900 Daltons, for A1 thiol-Michael addition of benzyl mercaptan to poly-GMA A. TMA- thiol-Michael addition product, BM- benzyl mercaptan, where X is taken as 128.00 Daltons. Example structure given in Figure 4.24

Due to the retention of epoxide groups post-thiol-Michael addition of benzyl mercaptan, subsequent epoxide ring-opening with functional amines can be used to obtain dual functional polymers, whereby site selective functionality can be achieved and potential cyclisation reactions are circumvented. Upon reaction with propylamine successful epoxide ring-opening was confirmed by ^1H NMR, with a complete loss of epoxide peaks and convergence of OCH_2 peaks on release of ring strain. Due to the change in solubility of the polymer on ring-opening of the epoxide SEC analysis in THF was not suitable, leading to a dramatic decrease in molecular weight from 1200 to 190 (Figure 4.25, Table 4.10). This apparent decrease in molecular weight is most likely due to a contraction in the hydrodynamic volume, as functionalisation of epoxide groups leads to the formation of hydroxyl groups which increase hydrophilicity; as propylamine only has a short alkyl chain, this offers little hydrophobicity to balance this change; hence the polymer becomes more hydrophilic and less THF soluble. As SEC separates by hydrodynamic volume, and not molecular weight directly,[35, 36] this contraction in hydrodynamic volume would give the appearance of a decrease in molecular weight.

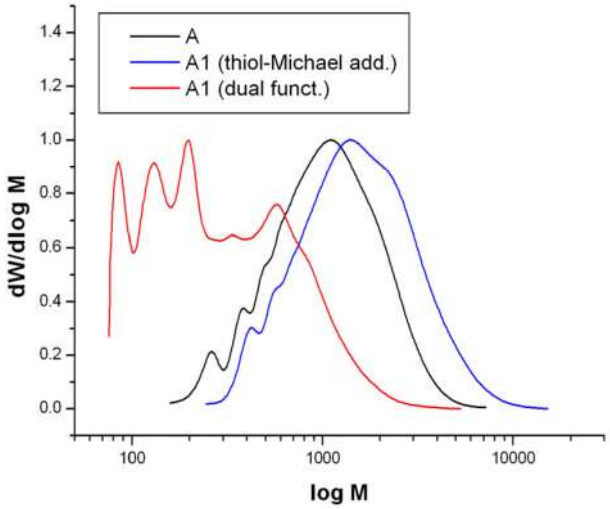

Figure 4.25: SEC comparison, THF eluent, of poly-GMA (A) *via* thiol-Michael addition of benzyl mercaptan to poly-GMA (A1 thiol-Michael addition) and dual functionalised poly-GMA *via* thiol-Michael addition with benzyl mercaptan and epoxide ring-opening with propylamine (A1 dual functionalisation)

THF eluent			
Name	**M_n ($g.mol^{-1}$)**	**M_w ($g.mol^{-1}$)**	**PDi**
A	800	1200	1.5
A1 (TMA)	1200	1800	1.6
A1 (dual funct.)	190	470	2.5

Table 4.10: SEC comparison of poly-GMA (A) *via* thiol-Michael addition of benzyl mercaptan to poly-GMA (A1 TMA) and dual functionalisation product *via* epoxide ring-opening with propylamine (A1 dual funct.) in THF eluent, TMA-thiol-Michael addition, dual funct.-dual functionalised

SEC characterisation using DMF eluent, rather than THF, leads to the expected increase in molecular weight on dual functionalisation. DMF provides a better solvent for the more hydrophilic dual functionalised polymer, however, DMF is a poor solvent for the thiol-Michael addition product, as poly-GMA becomes more hydrophobic on the addition of benzyl mercaptan, hence peak tailing is observed in this spectrum, but a small increase in molecular weight is still observed on comparison to unfunctionalised poly-GMA (**A**) (Figure 4.26, Table 4.11).

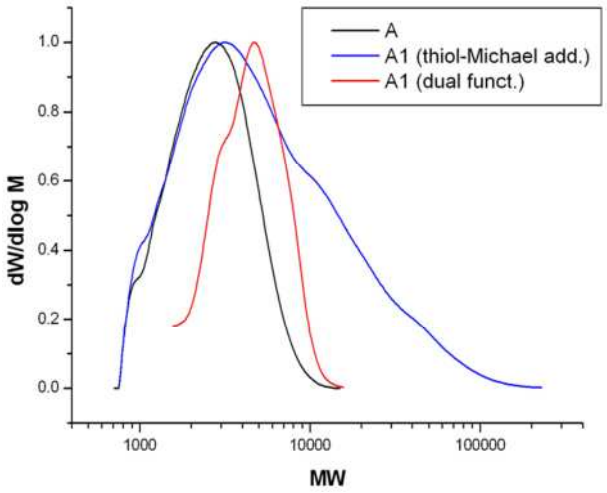

Figure 4.26: SEC comparison, DMF eluent, of poly-GMA (A) *via* thiol-Michael addition of benzyl mercaptan to poly-GMA (A1 thiol-Michael addition) and dual functionalised poly-GMA *via* thiol-Michael addition with benzyl mercaptan and epoxide ring-opening with propylamine (A1 dual functionalisation)

DMF eluent			
Name	**M_n ($g.mol^{-1}$)**	**M_w ($g.mol^{-1}$)**	**PDi**
A	1700	2400	1.4
A1 (TMA)	3200	9100	2.9
A1 (dual funct.)	3900	4800	1.2

Table 4.11: SEC comparison of poly-GMA (A) with thiol-Michael addition of benzyl mercaptan to poly-GMA (A1 TMA) and dual functionalisation product with epoxide ring-opening with propylamine (A1 dual funct.) in DMF eluent, TMA-thiol-Michael addition, dual funct.-dual functionalised

Ring-opening of epoxide groups with propylamine was also confirmed by MALDI-ToF, with the major peak series denoting increasing molecular weights of poly-GMA (**A**), each functionalised with a single benzyl mercaptan unit per chain, and full epoxide ring-opening with propylamine **[A1 dual funct: 1, 4]**. Minor peaks correspond to chains functionalised with two benzyl mercaptan units **[A1 dual funct: 2]** and full functionalisation with propylamine, zero benzyl mercaptan addition **[A1 dual funct: 3]** (Figure 4.27, Table 4.12). Again, although minor peaks are observed for multiple and zero benzyl mercaptan addition, a high level of purity in the dual functionalisation of poly-GMA (**A**) is observed, with no evidence of vinyl or epoxide groups remaining unfunctionalised in the final polymer.

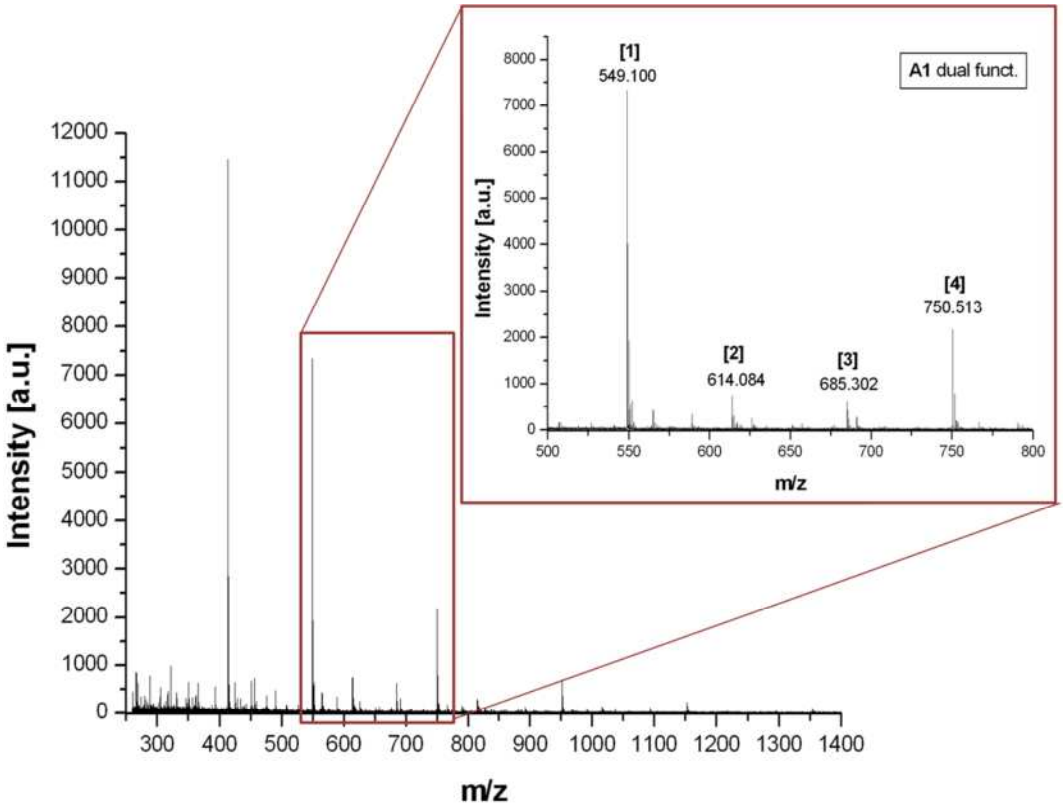

Figure 4.27: MALDI-ToF spectrum of A1 dual functionalised, poly-GMA with thiol-Michael addition with benzyl mercaptan and subsequent epoxide ring-opening with propylamine, with zoom region between 500-800 Daltons. Annotations correspond to Table 4.12

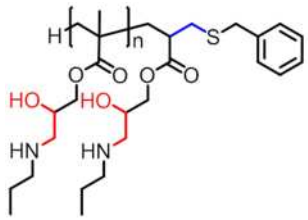

Figure 4.28: Example structure of poly-GMA dual functionalised with benzyl mercaptan and propylamine, $(GMA)_2(BM)_1(PAm)_2$ (if n=1)

Name	Theoretical m/z	Measured m/z	Corresponding Structure
[A1 (dual funct.): 1]	549.30	549.10	$(GMA)_2(BM)_1(PAm)_2Na^+$
[A1 (dual funct.): 2]	614.26	614.08	$(GMA)_2(BM)_2(PAm)_1Na^+$
[A1 (dual funct.): 3]	685.89	685.30	$(GMA)_3(PAm)_4Na^+$
[A1 (dual funct.): 4]	750.43	750.51	$(GMA)_3(BM)_1(PAm)_3Na^+$

Table 4.12: Corresponding structures to MALDI-ToF peaks annotated in Figure 4.27 for mass region 500-800 Daltons, for A1 dual functionalised with thiol-Michael addition with benzyl mercaptan and subsequent epoxide ring-opening with propylamine. BM- benzyl mercaptan, PAm- propylamine. Example structure given in Figure 4.28

4.2.5. Initial Study – Reactivity of Epoxide and Vinyl Functionalities to Nucleophilic Attack via Secondary Amine

Functionalisation of poly-GMA with secondary amines has the advantage over primary amine functionalisation, in that crosslinking of epoxide groups with the tertiary amines formed is not favourable, hence gelation of polymers should be less likely. However, the number of available commercial secondary amines is much less in comparison to primary amines. Ambient temperature experiments using various excesses of secondary amine were conducted, to assess the reactivity of both the epoxide and vinyl groups of poly-GMA (**B**) to nucleophilic attack with diethylamine.

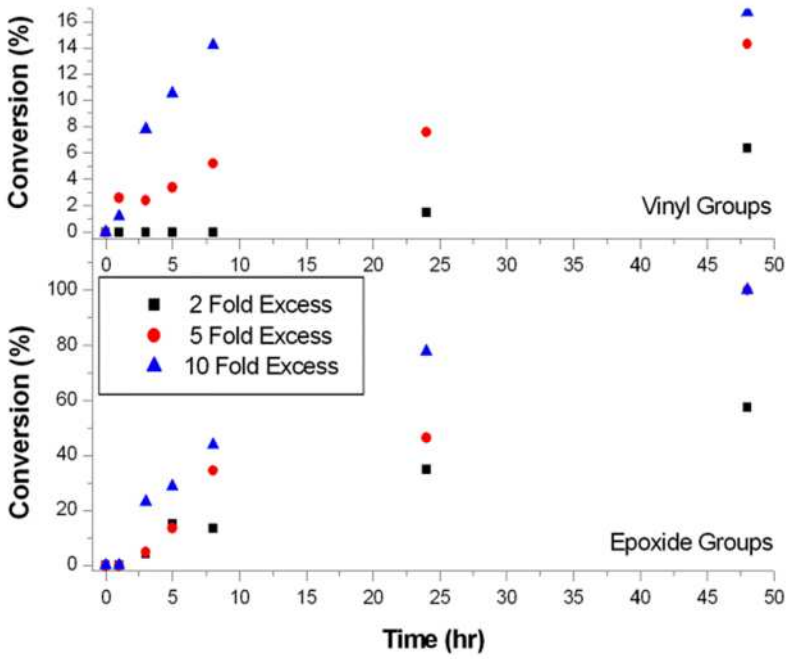

Figure 4.29: Conversion data for ring-opening of poly-GMA (B) with diethylamine, varying amine excess of 2-, 5- and 10-fold to epoxide groups. Reduction of epoxide and vinyl signals was monitored *via* ^{1}H NMR

Reaction of primary amine propylamine with poly-GMA (**B**) saw a high reactivity of vinyl groups to amine addition with a lower rate of epoxide ring-opening (Figure 4.8), using secondary amines however, the opposite trend is observed, with a higher rate observed for epoxide ring-opening than addition to vinyl groups. A rate dependency is observed for amine excess, with increasing amine excesses leading to faster rates for nucleophilic addition to both epoxides and vinyl groups, although addition to both functionalities sees a decreased rate for the use of secondary amines in comparison to primary amines (Figure 4.29).

Vinyl group loss using secondary amines is minimal, with observed values of between 5 and 15%. On increasing the excess of amine the conversion of vinyl groups increases, hence use of a low excess of amines can reduce vinyl loss. Due to the retention of a high level of vinyl groups, there is potential for functionalisation of terminal vinyl groups post ring-opening, adding versatility to the functionalisation of these materials.

4.2.6. Full Functionalisation of Poly-GMA with Commercial Secondary Amines

Reactions of poly-GMA (**B**) with secondary amines, diethylamine (**B6**), diethanolamine (**B7**) and diphenylamine (**B8**) were attempted at 60 ˚C in DMSO, with a 1.2 excess of amine. Reactions with diethylamine and diethanolamine were successful, displaying a shift to higher molecular weight *via* SEC (Table 4.13, Figure 4.31), indicative of addition of the functional amine to the polymer chain, with retention of low PDi's confirming the absence of crosslinking reactions. Resulting polymers contained no discernible epoxide signals *via* ^{1}H NMR with retention of a high level (~90%) of vinyl functionality, an example of which is given in Figure 4.30 for diethanolamine functionalised poly-GMA (**B7**).

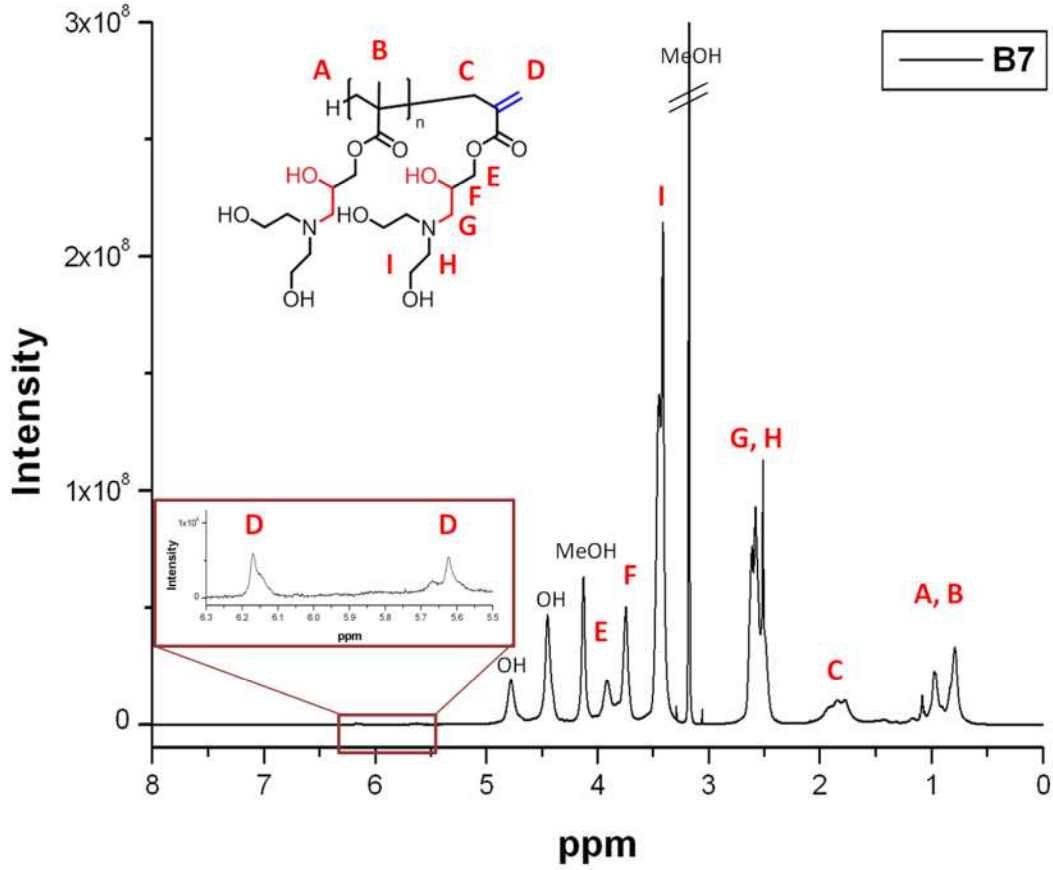

Figure 4.30: Typical ^{1}H NMR spectrum for the epoxide ring-opening reaction of poly-GMA with secondary amines, reaction with diethanolamine (B7) in CD_3OD

However, the reaction of poly-GMA (**B**) with diphenylamine resulted in a low level of epoxide ring-opening, approximately 6% *via* ^{1}H NMR. As nucleophilic attack at the epoxide is an S_N2 reaction, the steric bulk of the phenyl blocks back side attack of the leaving group, hence reactivity is reduced. Reaction of poly-GMA (**B**) under the same conditions with 2-anilinoethanol (**B9**) was attempted, as the steric bulk is reduced, with approximately 15% conversion of epoxide groups observed. Reaction of poly-GMA (**B**) with dibenzylamine (**B10**) was also attempted, as it was postulated that the CH_2 groups between the amine and phenyl ring may reduce the steric hindrance, although approximately 35% amine addition was observed, the majority of epoxide peaks remained, indicating limitations in the full functionalisation of these materials using sterically hindered secondary amines. The low levels of addition of diphenylamine, anilinoethanol and dibenzylamine were all reflected in a small increase in molecular weight, observed *via* SEC, relative to the amount of addition observed *via* ^{1}H NMR (Table 4.13, Figure 4.31).

Name	Functional Amine	M_n (g mol^{-1})	M_w (g mol^{-1})	PDi
B	P-GMA	2800	4400	1.6
B6	Diethylamine	8600	13600	1.6
B7	Diethanolamine	6100	10500	1.7
B8	Diphenylamine	3500	5600	1.6
B9	2-anilinoethanol	3500	5300	1.5
B10	Dibenzylamine	3700	6400	1.7

Table 4.13 SEC data, DMF eluent, epoxide ring-opening of poly-GMA (B) with a range of functional secondary amines

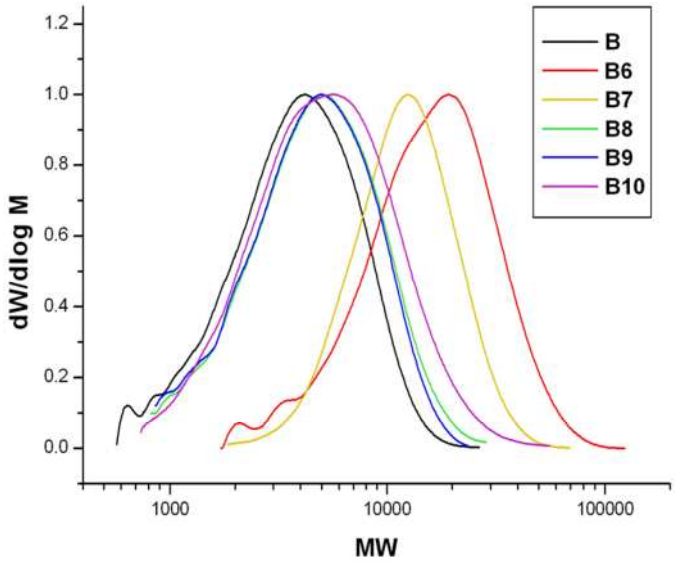

Figure 4.31: SEC comparison of poly-GMA B to epoxide ring-opening products B6-B10. DMF eluent

MALDI-ToF analysis was attempted for the products of poly-GMA ring-opened with diethylamine (**B6**) and diethanolamine (**B7**), but a spectrum could not be obtained for the diethanolamine ring-opened product as it's solubility in suitable solvents for MALDI-ToF was limited. ^{1}H NMR was measured at 600 MHz, with no epoxide peaks observed in the product, signifying a high level of functionalisation.

MALDI-ToF of poly-GMA ring-opened with diethylamine (**B6**) signified a high level of purity in the product. The major peak series denotes an equal level of diethylamine incorporation to epoxide groups **[B6: 1, 5]**, with no evidence of full functionalisation of both epoxide and vinyl groups. Minor peaks correspond to AIBN initiated products **[B6: 2]**, chains containing impurity X, with full functionalisation of epoxide groups **[B6: 4]**, hence impurity X does not contain epoxide functionality, and AIBN initiated chains containing impurity X with incomplete functionalisation of epoxide groups **[B6: 3]**.

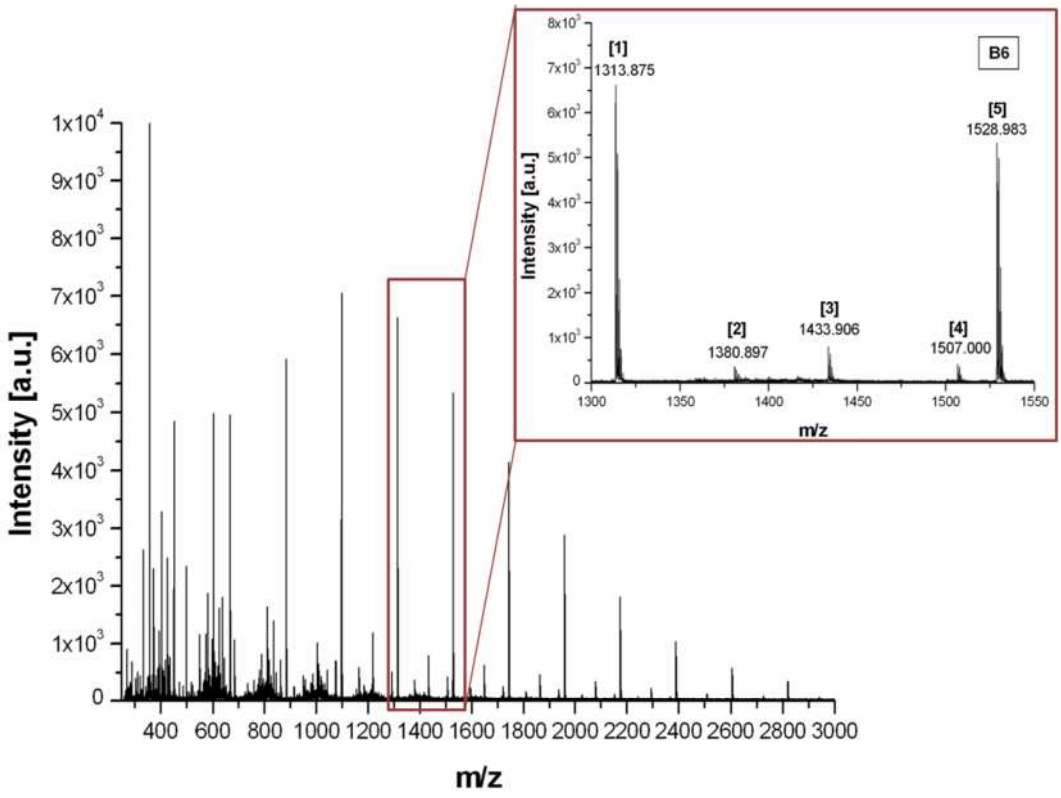

Figure 4.32: MALDI-ToF spectrum of B6, poly-GMA epoxide ring-opened with diethylamine, with zoom region between 1300-1550 Daltons. Annotations correspond to Table 4.14

Figure 4.33: Example structure of poly-GMA functionalised with diethylamine, $(GMA)_2(DEA)_2$ (if n=1)

Name	Theoretical m/z	Measured m/z	Corresponding Structure
[B6: 1]	1313.90	1313.88	$(GMA)_6(DEA)_6Na^+$
[B6: 2]	1380.90	1380.90	AIBN init-$(GMA)_6(DEA)_6Na^+$
[B6: 3]	1435.85	1433.91	AIBN init-$(GMA)_6(X)(DEA)_5Na^+$
[B6: 4]	1508.94	1507.00	AIBN init-$(GMA)_6(X)(DEA)_6Na^+$
[B6: 5]	1529.05	1528.98	$(GMA)_7(DEA)_7Na^+$

Table 4.14: Corresponding structures to MALDI-ToF peaks annotated in Figure 4.32 for mass region 1300-1550 Daltons, for poly-GMA epoxide ring-opened with diethylamine. DEA-diethylamine, AIBN init-AIBN initiated, where X is taken as 128.00 Daltons. Example structure given in Figure 4.33

4.2.7. Dual Functionalisation of Poly-GMA via Thiol-Michael Addition and Epoxide Ring-Opening with Secondary Amines

As vinyl groups are less susceptible to nucleophilic attack by secondary amines; epoxide ring-opening can be conducted prior to or post thiol-Michael addition. Poly-GMA (**B**) epoxide groups were ring-opened with diethylamine (**B6**), with retention of a high level of vinyl groups confirmed by ^{1}H NMR, and an increase in molecular weight observed by SEC, DMF eluent, from 2800 to 8600, in line with the addition of a high level of functionality to the polymer (Figure 4.34, Table 4.1). MALDI-ToF indicated a high level of purity of the polymer, with the majority of products with one remaining functional group, surmised to be vinyl functionality due to the high retention of these groups *via* ^{1}H NMR (Figure 4.32, Table 4.14). Vinyl groups were subsequently functionalised *via* phosphine mediated thiol-Michael addition with benzyl mercaptan to yield a dual functionalised product, confirmed by ^{1}H NMR. A further, less significant, increase in molecular weight observed *via* SEC, from 8600 to 11600, in line with the addition of one benzyl mercaptan group per chain (Figure 4.34, Table 4.15).

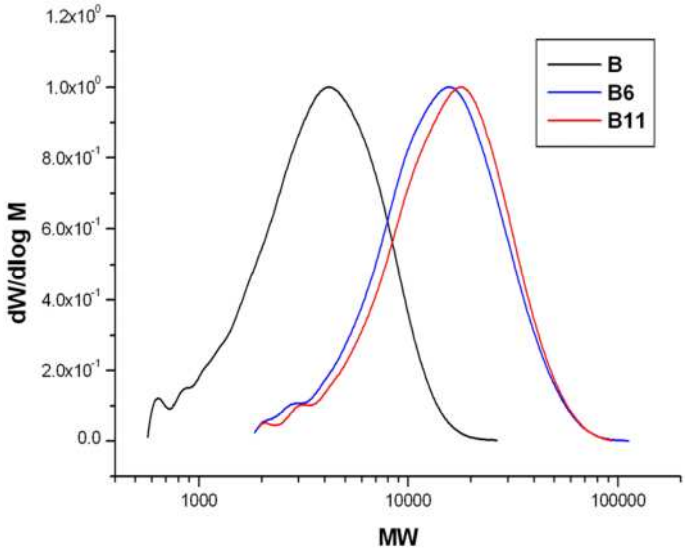

Figure 4.34: SEC comparison of the dual functionalisation products of poly-GMA (B), ring-opening with diethylamine (B6) and subsequent thiol-Michael addition with benzyl mercaptan (B11), DMF eluent

Name	M_n ($g.mol^{-1}$)	M_w ($g.mol^{-1}$)	PDi
B	2800	4400	1.6
B6	8600	13600	1.6
B11	11600	18100	1.6

Table 4.15:SEC comparison of poly-GMA B to epoxide ring-opened poly-GMA with diethylamine B6 and dual functionalised poly-GMA *via* epoxide ring-opening with diethylamine and subsequent thiol-Michael addition with benzyl mercaptan

MALDI-ToF analysis confirmed the addition of benzyl mercaptan to the polymer, with the main peak distribution corresponding to poly-GMA fully ring-opened with diethylamine, with addition of a single unit of benzyl mercaptan per chain **[B11: 2, 5]** (Figure 4.35, Table 4.16). Minor peak series correspond to AIBN initiated chains with the incorporation of impurity X, with full functionalisation of epoxide groups with diethylamine and a single unit of benzyl mercaptan **[B11: 1, 4]**, and chains whereby DP_n-1 diethylamine functionalisation occurs with a single benzyl mercaptan unit per chain **[B11: 3]**, hence, the purity of product remains high.

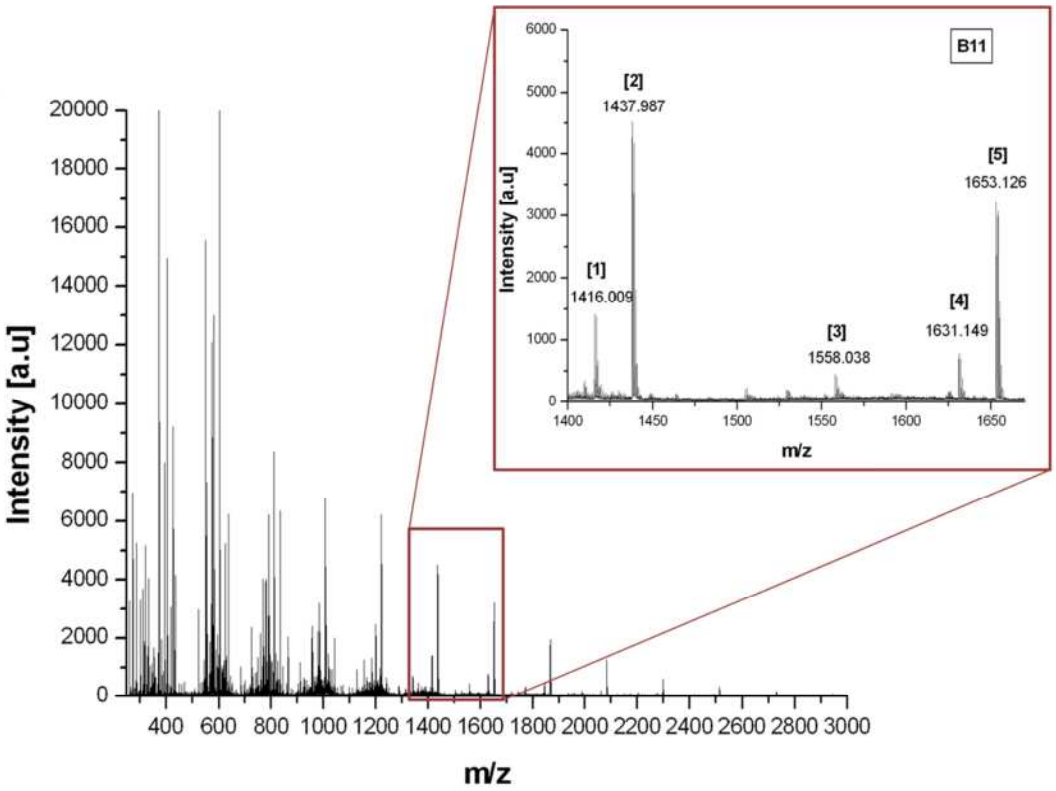

Figure 4.35: MALDI-ToF spectrum of B11, dual functionalisation of poly-GMA, epoxide ring-opening with diethylamine (B6) and subsequent thiol-Michael addition with benzyl mercaptan (B11), zoom region between 1400-1670 Daltons. Annotations correspond to Table 4.16

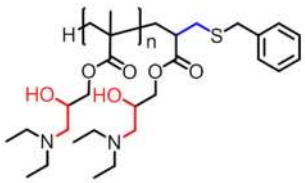

Figure 4.36: Example structure of poly-GMA dual functionalised with benzyl mercaptan and diethylamine, $(GMA)_2(BM)_1(DEA)_2$ (if n=1)

Name	Theoretical m/z	Measured m/z	Corresponding Structure
[B11: 1]		1416.01	AIBN init-$(GMA)_5(X)(DEA)_5(BM)_1Na^+$
[B11: 2]		1437.99	$(GMA)_6(DEA)_6(BM)_1Na^+$
[B11: 3]		1558.04	$(GMA)_7(DEA)_6Na^+$
[B11: 4]		1631.15	AIBN init-$(GMA)_6(X)(DEA)_6(BM)_1Na^+$
[B11: 5]		1653.13	$(GMA)_7(DEA)_7(BM)_1Na^+$

Table 4.16: Corresponding structures to MALDI-ToF peaks annotated in Figure 4.35 for mass region 1400-1670 Daltons, for the dual functionalisation of poly-GMA *via* epoxide ring-opening with diethylamine and subsequent thiol-Michael addition of benzyl mercaptan. AIBN init- AIBN initiated, DEA- diethylamine, BM-benzyl mercaptan. Example structure given in Figure 4.36

4.3. Conclusions

Epoxide containing polymers were synthesised *via* CCTP of glycidyl methacrylate, yielding polymers with a single terminal vinyl group per chain and level of epoxide functionality equal to the DP_n. Control of final molecular weights was accessed by variation in the level of CoBF employed. Reaction of poly-GMA with a range of functional primary amines led to the self-catalysed ring-opening of epoxide groups and nucleophilic addition to activated vinyl groups, obtaining fully functionalised polymers. Terminal vinyl functionality obtained *via* the CCTP mechanism, provides the means for attachment of additional functionality *via* thiol-Michael addition, prior to ring-opening reactions with primary amines, in the formation of dual functional polymers whereby side chain and terminal functionality can be tailored independently. Although the use of primary amines leads to a less versatile system in terms of dual functionalisation of materials, due to nucleophilic addition of the amine to both epoxide and vinyl groups, and the long reaction times required for use of low amine excesses.

Reaction of poly-GMA with secondary amines led to nucleophilic epoxide ring-opening with the retention of a high level of vinyl groups. Hence, by use of secondary amines the functionalisation of vinyl groups can be conducted prior to, or post epoxide ring-opening, increasing the versatility of the system towards dual functionalisation, again with the means to conduct site specific dual functionalisation. For functionalisation of poly-GMA with secondary amines a high product purity of resulting polymers is observed *via* MALDI-ToF, in comparison to poly-GMA functionalised with primary amines. Use of secondary amines also reduces the likelihood of inter/intramolecular crosslinking, however, the number of commercially available secondary amines is

reduced in comparison to the wealth of primary amines, and sterically hindered secondary amines such as diphenylamine lead to incomplete functionalisation products, further reducing the number of applicable secondary amines.

The combination of thiol-Michael addition and self-catalysed functionalisation of poly-GMA with functional amines is a facile way for the introduction of functionality in a site specific manner, which would be difficult to access by other methods and can lead to dramatic changes in the hydrophobicity/hydrophilicity of the resulting polymers. Hydroxyl groups formed on epoxide ring-opening have also been shown to be susceptible to esterification, hence, there is potential for the formation of tri-functional polymers.[25]

4.4. Experimental

General

All reagents were purchased from Aldrich and used as received unless stated. AIBN was recrystallised from methanol. CoBF was synthesised according to literature (RSH).[37]

Poly-GMA synthesis

Stock solutions of CoBF in GMA were made using 4.6 mg CoBF in 25 mL GMA. GMA was freeze pump thawed in a Schlenk tube then cannulated under nitrogen into CoBF degassed thrice *via* vacuum/nitrogen cycle. Stock solutions were stored under nitrogen in a fridge for up to one month. Degassed syringe techniques used for transferring stock solution into reaction mixtures.

A 250 mL round bottom flask was charged with GMA (51 mL, 0.367 mol), acetonitrile (50 mL), AIBN (400 mg, 2.44 mmol) and stirrer bar. The reaction mixture was degassed *via* nitrogen bubbler for 20 minutes prior to addition of CoBF stock solution. Degassed CoBF stock solution was added *via* degassed syringe. The round bottomed flask was immersed in an oil bath at 70 ˚C for 24 hours under nitrogen. Samples were taken hourly (approx 0.1 ml) *via* degassed syringe for 6 hours in order to obtain GPC, GC-FID and ^{1}H NMR measurements, sample taken at 24 hours. Reaction terminated by cooling and introduction of oxygen. Solvent removed *in vacuo*.

Name	CoBF Stock Sol. (mL)	CoBF (mg)	CoBF (mmol)	CoBF (mol %)
A	8	1.47	$2.94x10^{-3}$	$7.86x10^{-6}$
B	4	0.74	$1.47x10^{-3}$	$3.94x10^{-6}$
C	2	0.37	$7.36x10^{-4}$	$1.97x10^{-6}$
D	1	0.18	$3.68x10^{-4}$	$9.84x10^{-7}$

Table 4.17: Concentrations of CoBF employed *via* stock solutions for GMA polymerisations A-D

Full functionalisation of p-GMA with amine

0.5 g p-GMA (1 eq), 1.2 mol eq amine (to moles of epoxide group plus moles of double bond) in 5 mL DMSO. If the boiling point of the amine exceeded reaction temperature, reactions were carried out in 20 mL unsealed vials immersed in an oil bath at 60˚C, with stirring. For amines where the boiling point was lower than reaction temperature a reflux setup was used. Solvent was removed on a Schlenk line, with gentle heating *via* heatgun. SEC's conducted prior to purification by dialysis or precipitation.

Dual Functionalisation

For reaction of poly-GMA with primary amines thiol-Michael addition was conducted first, for reaction with secondary amines thiol-Michael addition could be conducted prior to or post epoxide ring-opening.

Thiol-Michael additions

DMPP stock solutions were used. An ampoule was charged with 8 mL d^6-DMSO and subjected to three cycles of freeze pump thaw, then backfilled with nitrogen (to thaw gentle heating was required *via* heat gun), to which 0.1 mL of DMPP (previously degassed *via* freeze pump thaw) was added using a degassed syringe. Stock solutions were then stored in a fridge for up to 2 months and completely thawed prior to use using gentle heating with heat gun.

Thiol-Michael additions were carried out on a 1 g scale in a large vial. 1:3:0.05 or 1:3:0.1 ratio of double bonds:thiol:DMPP was used. Poly-GMA was dissolved in 5 mL of DMSO, then thiol added (t=0 ^{1}H NMR taken) then DMPP stock solution added *via* degassed syringe (to preserve integrity of stock solution, thiol-ene click conducted under atmospheric conditions). Reactions were checked for completion at 1 hour by ^{1}H NMR. No workup conducted prior to reaction with amine.

Epoxide ring-opening

The ratio of epoxide to amine used was 1:1.2 mol eq. For amines with a lower boiling point than 60 ˚C a reflux setup was used, for higher boiling amines unsealed vials were used as the reaction vessel. Polymer solutions were added to the reaction vessel and functional amine added placing the vessel in an oil bath at 60 ˚C for 24 hours. DMSO was removed *via* Schlenk line. Polymers were precipitated in hexane or petroleum ether 40-60 ˚C or dialysed in methanol or water (1000 and 500-1000 MW cut-off respectively) depending on solubilities/suitability prior to IR, NMR and MALDI-T_OF characterisation.

Characterisation

^{1}H and ^{13}C NMR

NMR was carried out on Bruker DPX-400, Bruker AV III 600 and Bruker AV II 700 spectrometers.

Infra Red (IR)

IR was carried out on a Bruker Vector 22 using a Golden Gate diamond attenuated flow cell and analysed using Opus spectroscopy software.

Size exclusion chromatography (SEC)

All SEC were performed on Agilent 390-LC multi detector suites fitted with two PLgel 5 μm Mixed D columns, plus a guard column. Data was collected and analysed using Cirrus software (Agilent) and all samples calibrated against poly(methyl methacrylate) (PMMA) EasiVial standards, purchased from Agilent. Any points within the calibration plot with an error greater than 10% were not included in the final calibration. Third order calibration plots were used.

A range of SEC eluents was employed, dependant on the solubility of functionalised polymers, including THF, DMF and $CHCl_3$. THF mobile phase: flow rate of 1 mL/min, ambient operating temperature, injection volume 100 μL. The SEC was equipped with a refractive index, light scattering, UV and photodiode array (PDA, Shimadzu) detectors. DMF mobile phase: flow rate of 1 mL/min^{-1}, 40 ˚C operating temperature,

injection volume 100 µL. The SEC was equipped with a refractive index, UV and viscometry detectors. $CHCl_3$ mobile phase: flow rate of 1 mL/min-1, an ambient operating temperature, injection volume 100 µL. The SEC was equipped with a refractive index, light scattering and viscometry detectors.

Matrix-Assisted Laser Desorption and Ionisation Time-of-Flight (MALDI-ToF)

Mass spectra were acquired by MALDI-ToF (matrix-assisted laser desorption and ionisation time-of-flight) mass spectrometry using a Bruker Daltonics Ultraflex II MALDI-ToF mass spectrometer, equipped with a nitrogen laser delivering 2 ns laser pulses at 337 nm with positive ion ToF detection performed using an accelerating voltage of 25 kV.

2,5-Dihdroxybenzoic acid (DHB) or trans-2-[3-(4-tert-butylphenyl)-2-methyl-2-propenylidene]malononitrile (DCTB) were used as an organic matrix and sodium iodide (NaI) used as the salt. Calibrations were conducted using polyethylene glycol methyl ether of average molecular weight 1,100 and 2,000. A layering method was used to spot the MALDI plate. THF or THF/water was used as the solvent for sample preparation.

Gas chromatograph – Flame ionisation detector (GC-FID)

GC-FID analysis was performed using a Varian 450. A FactorFour^{TM} capillary column VF-1 ms, of 15 m × 0.25 mm I.D., film thickness 0.25 µm from Varian was used. The oven temperature was programmed as follows: 40 °C (hold for 1 min) at 25 °C min^{-1} to 200 °C. The injector was operated at 200 °C and the FID was operated at 220 °C. Nitrogen was used as carrier gas at a flow rate of 1 mL min^{-1} and a split ratio of 1:100 was applied. Chromatographic data were processed using Galaxie Chromatography data system, version 1.9.302.530 software.

Characterisation of Polymers

Poly-GMA

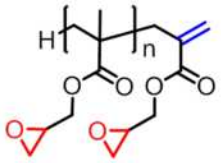

Figure 4.37: Linear poly-GMA synthesised via CCTP

Name	CoBF (mol%)	[CoBF:GMA] (mol)	M_n (g/mol^{-1})	M_w (g/mol^{-1})	PDi	Conversion* (%)
A	7.86x10^{-6}	[1:98K]	800	1400	1.76	90.2
B	3.94x10^{-6}	[1:195K]	1600	2900	1.86	91.2
C	1.97x10^{-6}	[1:391K]	3100	5800	1.86	99.0
D	9.84x10^{-7}	[1:783K]	5000	9100	1.84	93.4

*Conversion measured by GC-FID

Table 4.18: Molecular weights and conversion of polymerisations A-D with decreasing CoBF concentration

^{1}H NMR (400 MHz, TMS at 25 ˚C): δ 0.85-1.15 (CH_3, backbone and terminal), 1.80-2.35 (backbone CH_2), 2.57 (CH epox), 2.77 (CH epox), 3.16 (CH epox), 3.70-3.95 (O-C$\underline{H}_2$-epox), 4.20-4.40 (O-C$\underline{H}_2$-epox), 5.50-5.60 (C=C$\underline{H}_2$), 6.20-6.25 (C=C$\underline{H}_2$)

^{13}C NMR (400 MHz $CDCl_3$ at 25 ˚C): δ 16.49, 21.28, 24.68, 29.62 (CH_3, backbone and terminal), 44.44 (CH_2, epoxide), 49.11 (CH, epoxide), 51.62 (C, tertiary backbone), 53.36 (CH_2, backbone), 65.73 (OCH_2), 128.74, 129.52 ($\underline{C}H_2$=C), 136.62 (C=CH_2), 166.52 (carbonyl)

IR: υ_{max} (neat)/cm^{-1} 2972 (m, CH sp^3), 1724 (s, C=O), 1628 (m, C=C), 1485 (s), 1448 (m, CH_2), 1246 (s), 1146 (s, C-O), 992 (m), 905 (s, epoxide), 846 (m), 757 (m)

SEC (THF eluent): **A**: M_n 800, M_w 1400, PDi 1.8 **B**: M_n 1600, M_w 2900, PDi 1.8 **C**: M_n 3100, M_w 5800, PDi 1.9 **D**: M_n 5000, M_w 9100, PDi 1.8

GC-FID (conversion): **A**: 90.2% **B**: 91.2% **C**: 99.0% **D**: 93.4%

Propylamine Functionalised Poly-GMA (B1)

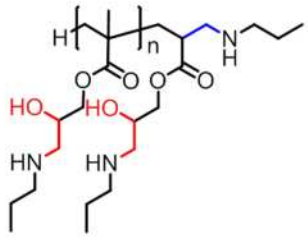

Figure 4.38: Propylamine functionalised poly-GMA

^{1}H NMR (700 MHz, d^{6}-acetone at 25 ˚C): 0.80-1.40 (C<u>H</u>$_3$CH$_2$CH$_2$NH, backbone CH$_3$, terminal CH$_3$), 1.45-1.70 (NHCH$_2$C<u>H</u>$_2$CH$_3$), 1.80-2.20 (backbone CH$_2$, CHC=O), 2.40-2.50 (NHC<u>H</u>$_2$CH$_2$), 2.60-2.75 (C<u>H</u>$_2$NH), 2.75-2.95 (CH(OH)C<u>H</u>$_2$NH), 2.95-3.10 (NH/OH), 3.80-4.15 (OCH$_2$), 4.15-4.35 (C<u>H</u>(OH))

^{13}C NMR (700 MHz d^{6}-acetone at 25 ˚C): 11.30 (<u>C</u>H$_3$CH$_2$CH$_2$NH), 21.10 (terminal CH$_3$), 22.31 (NHCH$_2$<u>C</u>H$_2$), 23.30 (backbone CH$_3$), 40.41 (<u>C</u>HC=O), 44.59 (backbone CH$_2$), 50.38 (NHCH$_2$), 51.73 (CH(OH)<u>C</u>H$_2$NH), 54.00 (terminal CH(OH)<u>C</u>H$_2$NH), 66.69 (OCH$_2$), 72.28 (CH(OH)), 94.78 (backbone quaternary C), 177.01 (carbonyl)

IR: υ_{max} (neat)/cm^{-1} 3317 (v, OH/NH), 2957 (m, CH sp^3), 1724 (s, C=O), 1616 (m, N-H bend), 1455 (m, CH$_2$), 1272 (m, C-N), 1148 (m, C-O), 1020 (m), 950 (m), 748 (m)

SEC (DMF eluent): M$_n$ 6200, M$_w$ 8700, PDi 1.4

Benzylamine Functionalised Poly-GMA (B2)

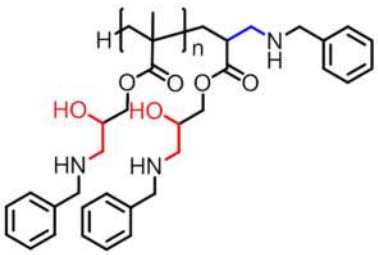

Figure 4.39: Benzylamine functionalised poly-GMA

^{1}H NMR (700 MHz, TMS at 25 ˚C): 0.80-1.20 (backbone CH$_3$), 1.25-1.35 (terminal CH$_3$), 1.60-2.15 (backbone CH$_2$, CHC=O), 2.60-2.80 (CHC<u>H</u>$_2$NH), 2.80-2.90

(CH(OH)C<u>H</u>$_2$NH), 3.65-3.80 (C<u>H</u>$_2$C$_6$H$_5$), 2.85-4.10 (OCH$_2$), 4.15-4.25 (C<u>H</u>(OH)), 7.10-7.40 (C<u>6</u>H<u>5</u>)

^{13}C NMR (700 MHz CDCl$_3$ at 25 ˚C): 22.80 (terminal CH$_3$), 23.10 (backbone CH$_3$), 41.66 (<u>C</u>HC=O), 45.00 (NH<u>C</u>H$_2$C$_6$H$_5$), 51.32 (CH(OH)<u>C</u>H$_2$NH), 53.71 (OCH$_2$), 67.84 (CH(OH)), 127.20 (para aromatic C-H), 128.52 (meta aromatic C-H), 129.01 (ortho aromatic C-H), 138.07 (quaternary aromatic), 177.59 (carbonyl)

IR: υ_{max} (neat)/cm^{-1} 3351 (v, OH/NH), 2940 (m, CH sp^3), 1721 (s, C=O), 1603 (m, N-H bend), 1452 (m), 1267 (m, C-N), 1149 (s, C-O), 1027 (m), 738 (m), 697 (s, =C-H bend)

SEC (DMF eluent): M_n 7500, M_w 15400, PDi 2.0

Aminopropanediol Functionalised Poly-GMA (B3)

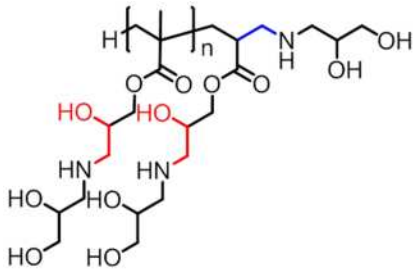

Figure 4.40 Aminopropanediol functionalised poly-GMA

^{1}H NMR (600 MHz, d^6-DMSO at 25 ˚C): 0.60-1.00 (backbone CH$_3$), 1.00-1.25 (terminal CH$_3$), 1.60-2.10 (backbone CH$_2$, CH(C=O)), 2.25-2.75 (terminal and internal NHC<u>H</u>$_2$CH(OH)), 3.15-3.40 (terminal and internal CH(OH)C<u>H</u>$_2$OH), 3.45-3.60 (OCH$_2$), 3.60-4.30 (terminal and side chain C<u>H</u>(OH))

^{13}C NMR (600 MHz d^6-DMSO at 25 ˚C): 15.96, 22.40 (backbone CH$_3$), 29.64 (terminal CH$_3$), 40.97 (<u>C</u>HC=O), 44.48 (backbone CH$_2$), 52.66 (terminal and side chain NHC<u>H</u>$_2$CH(OH)), 64.37 (CH(OH)), 67.13 (internal C<u>H</u>(OH)), 70.14 (terminal C<u>H</u>(OH)), 177.33 (carbonyl)

IR: υ_{max} (neat)/cm^{-1} 3314 (v, OH/NH), 2931 (m, CH sp^3), 1719 (s, C=O), 1613 (m, N-H bend), 1450 (m), 1272 (m, C-N), 1151 (s, C-O), 1035 (m), 930 (m), 862 (m), 747 (m)

SEC (DMF eluent): M_n 5600, M_w 10600, PDi 1.9

Propargylamine Functionalised Poly-GMA (B4.2)

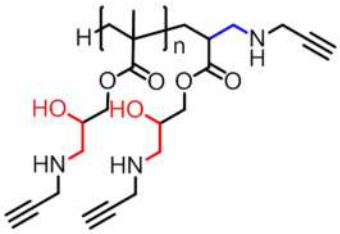

Figure 4.41: Propargylamine functionalised poly-GMA

^{1}H NMR (500 MHz, d^{6}-DMSO at 25 ˚C): 0.6-1.10 (backbone CH_3), 1.10-1.30 (terminal CH_3), 1.60-2.10 (backbone CH_2, CHC=O), 2.40-2.80 (NHC$\underline{H}_2$CH(OH)), 2.90-3.05 (C≡CH), 3.05-3.60 (OCH_2, NH$\underline{C}H_2$C≡CH), 3.60-4.00 (CH(OH))

^{13}C NMR (500 MHz d6-DMSO at 25 ˚C): 16.42 (terminal, backbone CH_3), 18.57 (backbone CH_3), 38.06 (CH_2, propargylamine), 44.54 (backbone CH_2), 51.45 (CH(OH)$\underline{C}H_2$NH), 67.61 (CH(OH), 67.81 (C≡$\underline{C}$H), 74.03 (O$\underline{C}H_2$), 83.42 ($\underline{C}$≡CH), 177.55 (carbonyl)

SEC (DMF eluent): M_n 12700, M_w 18100, PDi 1.4

Decylamine Functionalised Poly-GMA (B5)

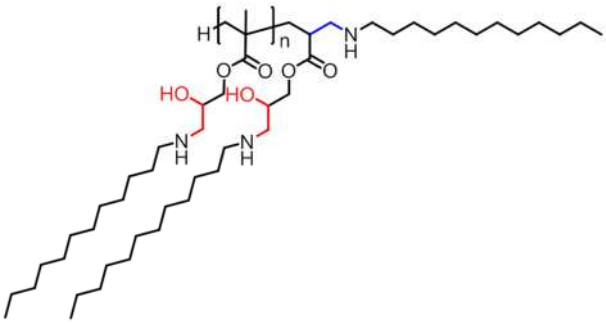

Figure 4.42: Decylamine functionalised poly-GMA

^{1}H NMR (700 MHz, TMS at 25 ˚C): 0.8-1.0 (CH_3-decylamine, backbone CH_3), 1.0-1.15 (terminal CH3), 1.40-1.65 (NHC$\underline{H}_2CH_2$), 1.80-2.15 (backbone CH_2, CHC=O), 2.30-2.90 (NHC$\underline{H}_2$CH(OH), CHC$\underline{H}_2$NH), 3.70-4.20 (OCH_2, CH(OH))

^{13}C NMR (700 MHz $CDCl_3$ at 25 ˚C): 14.07 (terminal, backbone, amino CH_3), 22.65 ($\underline{C}H_2CH_3$), 27.00 (CH_2 decylamine, terminal), 29.33, 29.62 (decylamine CH_2), 32.15 (NHCH2, terminal), 34.13 ($NHCH_2$), 40.92 ($\underline{C}HC=O$), 45.02 (backbone CH_2), 49.95 ($CH(OH)\underline{C}H_2NH$), 51.98 (OCH_2), 177.53 (carbonyl)

IR: υ_{max} (neat)/cm^{-1} 3334 (v, OH/NH), 2922 (s, CH sp^3), 1727 (s, C=O), 1618 (m, N-H bend), 1457 (m), 1378 (m), 1271 (m, C-N), 1149 (s, C-O), 990 (m), 934 (m), 887 (m), 748 (m)

SEC ($CHCl_3$ eluent): M_n 4100, M_w 6200, PDi 1.5

Benzyl Mercaptan, Propylamine Functionalised Poly-GMA (A1)

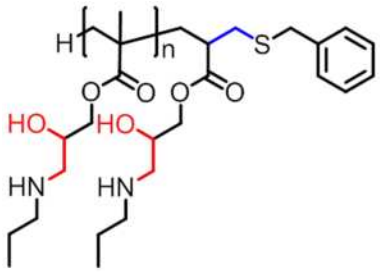

Figure 4.43: Poly-GMA dual functionalised with benzyl mercaptan and propylamine

^{1}H NMR (400 MHz, TMS at 25 ˚C): 0.75-0.95 ($NHCH_2CH_2C\underline{H}_3$), 0.95-1.10 (backbone CH_3), 1.10-1.20 (terminal CH_3), 1.35-1.65 ($NHCH_2C\underline{H}_2CH_3$), 1.75-2.20 (backbone CH_2), 2.35-2.45 ($C\underline{H}_2SCH_2C_6H_5$), 2.45-2.65 ($CH(OH)C\underline{H}_2NH$), 2.70-2.85 ($NHC\underline{H}_2CH_2CH_3$), 3.30-3.45 ($SC\underline{H}_2C_6H_5$), 3.75-4.10 ($OCH_2$), 4.10-4.30 (CH(OH)), 7.25-7.45 (aromatic CH), 7.55-7.65 (aromatic CH (DMPP)), 7.80-7.85 (aromatic CH (DMPP))

^{13}C NMR (400 MHz $CDCl_3$ at 25 ˚C): 11.65 ($CH_2CH_2\underline{C}H_3$), 17.91 (backbone CH_3), 22.48 ($NHCH_2\underline{C}H_2CH_3$), 30.64 (terminal CH_3), 41.59 (backbone CH_2), 44.01 ($\underline{C}H_2SCH_2C_6H_5$), 51.18 ($CH(OH)\underline{C}H_2$), 52.17 ($NH\underline{C}H_2CH_2CH_3$), 58.37 ($S\underline{C}H_2C_6H_5$), 66.93 (CH(OH)), 126.75 (para aromatic C-H), 128.37 (meta aromatic C-H), 128.81 (ortho aromatic C-H), 131.27 (quaternary aromatic C), 176.78 (carbonyl)

IR: υ_{max} (neat)/cm^{-1} 3302 (m, OH/NH), 2958 (m, CH sp^3), 1722 (s, C=O), 1618 (N-H bend), 1454 (m), 1384 (m), 1261 (m, C-N), 1149 (s, C-O), 991 (m), 933 (m), 862 (m), 804 (m), 749 (m), 701 (m)

SEC(THF eluent): **A1** thiol-Michael addition product M_n 1200, M_w 1800, PDi 1.6, **A1** dual functionalised M_n 190, M_w 470, PDi 2.5

SEC (DMF eluent): **A1** thiol-Michael addition product M_n 3200, M_w 9100, PDi 2.9 **A1** dual functionalised M_n 3900, M_w 4800, PDi 1.2

Diethylamine Functionalised Poly-GMA (B6)

Figure 4.44: Diethylamine functionalised poly-GMA

^{1}H NMR (600 MHz, d^6-DMSO at 25 ˚C): 0.70-0.90 (backbone CH_3), 0.90-1.05 ($N(CH_2\underline{C}H_3)_2$), 1.05-1.10 (terminal CH_3), 1.60-2.05 (backbone CH_2), 2.30-2.45 ($CH(OH)\underline{C}H_2NH$), 2.45-2.55 ($N(\underline{C}H_2CH_3)_2$), 3.35-3.60 (teminal OCH_2), 3.60-3.85 (terminal CH(OH)), 3.85-4.05 (internal OCH_2), 4.05-4.15 (internal CH(OH)), 5.50-5.15 (CH_2=C), 6.10-6.20 (CH_2=C)

^{13}C NMR (600 MHz, d^6-DMSO at 25 ˚C): 11.82 ($N(CH_2\underline{C}H_3)_2$, 15.92 (backbone CH_3), 17.74 (terminal CH_3), 44.48 (backbone CH_2), 47.04 ($N(\underline{C}H_2CH_3)_2$), 55.91 ($CH(OH)\underline{C}H_2N$), 61.15 (internal OCH_2), 66.59 (internal CH(OH)), 67.32 (terminal CH(OH)), 73.01 (terminal OCH_2), 128.25 ($\underline{C}H_2C$), 135.94 ($\underline{C}$=CH_2), 176.81 (carbonyl)

IR: υ_{max} (neat)/cm^{-1} 3362 (m, OH/NH), 2967 (m, CH sp^3), 1715 (s, C=O), 1449 (m), 1385 (m), 1270 (m, C-N), 1152 (s, C-O), 1062 (m)

SEC (DMF eluent): M_n 8600, M_w 13600, PDi 1.6

Diethanolamine Functionalised Poly-GMA (B7)

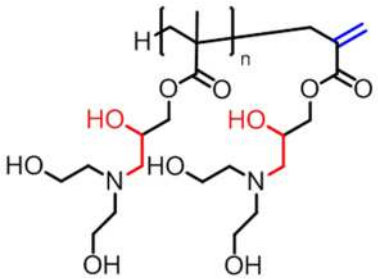

Figure 4.45: Diethanolamine functionalised poly-GMA

^{1}H NMR (600 MHz, d^{6}-DMSO at 25 ˚C): 0.65-1.25 (m, backbone CH_3, terminal CH_3), 1.65-2.10 (br, backbone CH_2), 2.50-2.70 (br, m, $NC\underline{H}_2CH_2OH$), 3.30-3.60 (br, m, $NCH_2C\underline{H}_2OH$), 3.65-3.95 (br, C<u>H</u>(OH)), 3.85-4.00 (br, OCH_2), 4.35-4.60 (br, amino-OH), 4.65-4.90 (br, CH(O<u>H</u>)), 5.55-5.70 (CH_2=C), 6.10-6.20 (CH_2=C)

^{13}C NMR (600 MHz d^{6}-DMSO at 25 ˚C): 16.36 (terminal CH_3), 18.32 (backbone CH_3), 44.56, 45.02 (backbone CH_2), 57.00 ($NH\underline{C}H_2CH_2OH$), 58.74 (CH(OH)<u>C</u>H_2NH), 59.60 ($NHCH_2\underline{C}H_2OH$), 66.81 (<u>C</u>H(OH)), 67.73 (OCH_2), 177.74 (carbonyl)

IR: u_{max} (neat)/cm^{-1} 3346 (s, OH/NH), 2947 (m, CH sp^3), 1719 (s, C=O), 1450 (m), 1271 (m, C-N), 1152 (s, C-O), 1033 (s), 877 (m), 747 (m)

SEC (DMF eluent): M_n 6100, M_w 10500, PDi 1.7

Benzyl Mercaptan, Diethylamine Functionalised Poly-GMA (B11)

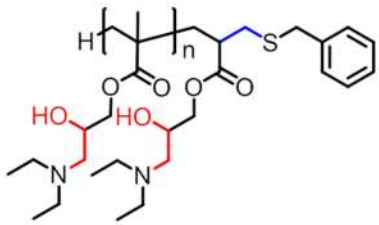

Figure 4.46: Poly-GMA dual functionalised with benzyl mercaptan and diethylamine

^{1}H NMR (400 MHz, TMS at 25 ˚C): 0.70-0.85 (backbone CH_3), 0.85-1.05 ($N(CH_2C\underline{H}_3)_2$), 1.05-1.15 (terminal CH_3), 1.70-2.05 (backbone CH_2, CHC=O), 2.30-2.45 (CH(OH)C<u>H</u>$_2$NH, $C\underline{H}_2SCH_2C_6H_5$), 2.45-2.65 ($N(C\underline{H}_2CH_3)_2$), 3.45-3.55 ($SC\underline{H}_2C_6H_5$),

3.55-3.85 (OCH_2), 3.85-4.15 (C<u>H</u>(OH)), 7.20 (C_6H_5), 7.50-7.60 (C_6H_5 (DMPP)), 7.75-7.85 (C_6H_5 (DMPP))

^{13}C NMR (400 MHz $CDCl_3$ at 25 ˚C): 11.62 (($NCH_2\underline{C}H_3)_2$), 17.91 (backbone CH_3), 23.73 (terminal CH_3), 44.07 ($\underline{C}H_2SCH_2C_6H_5$), 45.13 (backbone CH_2), 47.06 ($N(\underline{C}H_2H_3)_2$), 55.88 ($CH(OH)\underline{C}H_2NH$), 60.63 ($S\underline{C}H_2C_6H_5$), 66.23 (CH(OH)), 67.32 ($COOCH_2$), 126.72 (para aromatic C-H), 128.33 (meta aromatic C-H), 128.81 (ortho aromatic C-H), 129.58 (quaternary aromatic), 177.04 (carbonyl)

IR: u_{max} (neat)/cm^{-1} 3385 (m, OH/NH), 2968 (m, CH sp^3), 1724 (C=O), 1601 (N-H bend), 1453 (m), 1385 (m), 1245 (m, C-N), 1151 (s, C-O), 1063 (m), 993 (m), 934 (m), 805 (m), 767 (m), 702 (m)

SEC (DMF eluent): M_n 11600, M_w 18100, PDi 1.6

4.5. References

1. Clayden, J.; Greeves, N.; Warren, S.; Wothers, P., *Organic Chemistry*. 1st ed.; Oxford University Press: Oxford, 2001.
2. Odian, G., *Principles of Polymerisation*. 4th ed.; John Wiley & Sons: 2004.
3. DuPont **1955**.
4. Iwakura, Y.; Kurosaki, T.; Nakabayashi, N., *Makromol. Chem.* **1961,** *44* (1), 570.
5. Iwakura, Y.; Kurosaki, T.; Ariga, N.; Ito, T., *Makromol. Chem.* **1966,** *97* (1), 128.
6. Iwakura, Y.; Kurosaki, T.; Imai, Y., *Makromol. Chem.* **1965,** *86* (1), 73.
7. Kalal, J.; Švec, F.; Maroušek, V., *J. Polym. Sci: Pol. Sym.* **1974,** *47* (1), 155.
8. Wang, S.; Shao, L.; Song, Z.; Zhao, J.; Feng, Y., *J. Appl. Polym. Sci.* **2012,** *124* (6), 4827.
9. Ekenseair, A. K.; Boere, K. W. M.; Tzouanas, S. N.; Vo, T. N.; Kasper, F. K.; Mikos, A. G., *Biomacromolecules* **2012,** *13* (6), 1908.
10. Wei, D.; Zhou, R.; Guan, Y.; Zheng, A.; Zhang, Y., *J. Appl. Polym. Sci.* **2012,** (In Print), DOI:10.1002/app.37849.
11. Zhao, P.; Yan, Y.; Feng, X.; Liu, L.; Wang, C.; Chen, Y., *Polymer* **2012,** *53* (10), 1992.
12. Bondar', Y.; Han, D., *Russ. J. Appl. Chem.* **2012,** *85* (2), 272.
13. Sung, D.; Park, S.; Jon, S., *Langmuir* **2012,** *28* (9), 4507.
14. Barbey, R.; Kauffmann, E.; Ehrat, M.; Klok, H.-A., *Biomacromolecules* **2010,** *11* (12), 3467.
15. Barbey, R.; Klok, H.-A., *Langmuir* **2010,** *26* (23), 18219.

16. Rahane, S. B.; Hensarling, R. M.; Sparks, B. J.; Stafford, C. M.; Patton, D. L., *J. Mater. Chem.* **2012,** *22* (3), 932.

17. Ende, A. E. v. d.; Kravitz, E. J.; Harth, E., *J. Am. Chem. Soc.* **2008,** *130* (27), 8706.

18. Abdelrahman, A. I.; Thickett, S. C.; Liang, Y.; Ornatsky, O.; Baranov, V.; Winnik, M. A., *Macromolecules* **2011,** *44* (12), 4801.

19. de la Fuente, J. L.; Cañamero, P. F.; Fernández-García, M., *J. Polym. Sci., Part A: Polym. Chem.* **2006,** *44* (6), 1807.

20. Harvison, M. A.; Davis, T. P.; Lowe, A. B., *Polym. Chem.* **2011,** *2* (6), 1347.

21. Sanders, G. C.; van Ravensteijn, B. G. P.; Duchateau, R.; Heuts, J. P. A., *Polym. Chem.* **2012,** *3* (8), 2200.

22. Li, C.; Ge, Z.; Fang, J.; Liu, S., *Macromolecules* **2009,** *42* (8), 2916.

23. Tsarevsky, N. V.; Bencherif, S. A.; Matyjaszewski, K., *Macromolecules* **2007,** *40* (13), 4439.

24. Tsarevsky, N. V.; Jakubowski, W., *J. Polym. Sci., Part A: Polym. Chem.* **2011,** *49* (4), 918.

25. De, S.; Khan, A., *Chem. Commun.* **2012,** *48* (25).

26. De, S.; Stelzer, C.; Khan, A., *Polym. Chem.* **2012,** *3* (9), 2342.

27. Zhang, Q.; Slavin, S.; Jones, M. W.; Haddleton, A. J.; Haddleton, D. M., *Polym. Chem.* **2012**.

28. Benaglia, M.; Alberti, A.; Giorgini, L.; Magnoni, F.; Tozzi, S., *Polym. Chem.* **2012**, Accepted Manuscript.

29. Lowe, A. B., *Polym. Chem.* **2010,** *1*, 17.

30. Hoyle, C. E.; Bowman, C. N., *Angew. Chem., Int. Ed.* **2010,** *49* (9), 1540.

31. McEwan, K. A.; Slavin, S.; Tunnah, E.; Haddleton, D. M., *Polym. Chem. Submitted*.

32. Dix, L. R.; Ebdon, J. R.; Hodge, P., *Eur. Polym. J.* **1995,** *31* (7), 653.

33. Kakwere, H.; Perrier, S. b., *J. Am. Chem. Soc.* **2009,** *131* (5), 1889.

34. Wang, M.; Wang, Y.; Qi, X.; Xia, G.; Tong, K.; Tu, J.; Pittman, C. U.; Zhou, A., *Org. Lett.* **2012,** *14* (14), 3700.

35. Striegel, A.; Yau, W.; Kirkland, J.; Bly, D., *Modern Size-Exclusion Liquid Chromatography: Practice of Gel Permeation and Gel Filtration Chromatography* 2nd ed.; Wiley: 2009.

36. Hiemenz, P. C.; Lodge, T. P., *Polymer Chemistry*. 2nd ed.; CRC Press: Taylor & Francis Group: 2007.

37. Bakac, A.; Espenson, J. H., *J. Am. Chem. Soc.* **2002,** *106* (18), 5197.

Chapter 5

5. Synthesis and Functionalisation of Branched Epoxide Containing Polymers

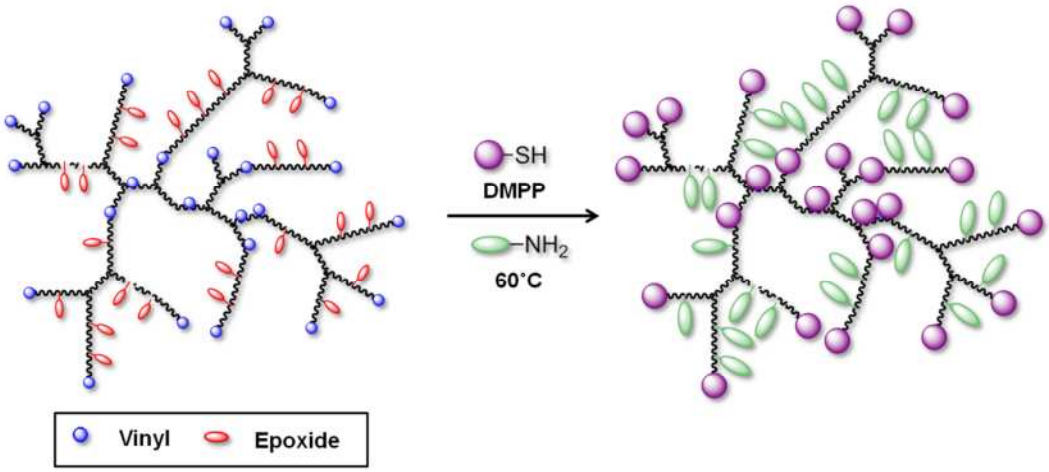

Branched polymers containing epoxide functionality were obtained from copolymerisations of divinyl monomer ethylene glycol dimethacrylate (EGDMA) and glycidyl methacrylate (GMA) by CCTP. Resulting polymers possess both epoxide and vinyl functionality, available for post-polymerisation modification leading to the formation of dual functionalised polymers in a site selective manner, with the potential for self assembly.

5.1. Branched Epoxide Containing Polymers in the Literature

Copolymerisation of monomers capable of introducing branching with epoxide containing monomers such as GMA, whereby epoxide functionality is retained during polymerisation process appear only in literature for the synthesis of macroporous crosslinked structures and the synthesis of crosslinked networks.

Traditionally, emulsion and suspension polymerisation are used in the formation of polymer particles, however, other methods can be utilised such as precipitation polymerisation, the main benefit of this is that reactions can be conducted in the absence of surfactant or stabilisers. However, for control over sphere/particle size, often solids contents as low as 3% are required. For the synthesis of fully crosslinked epoxide containing microspheres, the most common method is the copolymerisation of GMA with branching monomers such as DVB or EGDMA,[1-4] however, *grafting from* methods have been explored by the modification of microspheres, incorporating ATRP initiating groups and subsequent grafting from polymerisation of GMA, in the formation of microspheres with reactive epoxide chains.[5, 6] The use of GMA as a comonomer is particularly attractive due to the high reactivity of epoxide groups to a wide range of functionalities, providing a broad scope for the application of such materials.

The wide ranging and facile epoxide ring-opening reactions that can be performed on epoxide containing polymer beads has led to such uses as packing material for HPLC columns, HPLC chiral columns;[7-9] electroactive, degradable gels with tunable conductivity;[10] supports for catalysts and biocatalysts,[11-13] and metal binding, particularly pertechnetate for such diverse applications including water purification.[14]

As previously discussed branched polymers possess many desirable properties relative to their linear counterparts,[15-17] coupled with the ability to functionalise the branched polymers by ring-opening reactions of epoxide functionalities, towards nucleophilic reactions,[18-23] leads to a vast potential for the synthesis of branched functional polymers form a small, commercial monomer set.

5.2. Results and Discussion

The focus of this work is the copolymerisation of the branching monomer EGDMA and epoxide containing monomer GMA, for the synthesis of branched epoxide containing polymers by CCTP. It envisages that the resulting copolymers should possess high levels of both activated vinyl groups and epoxide moieties, dependant on the ratio of comonomers employed. CCTP has shown to be a facile technique for the synthesis of branched EGDMA homopolymers which retain high levels of internal and external vinyl functionality, which proved susceptible to functionalisation *via* thiol-Michael addition. Copolymerisation of EGDMA with GMA adds a further handle for functionalisation, *via* epoxide moieties, providing the means for the creation of branched dual functional polymers, whereby functionalisation can be site selective.

5.2.1. Copolymerisation of EGDMA and GMA via CCTP

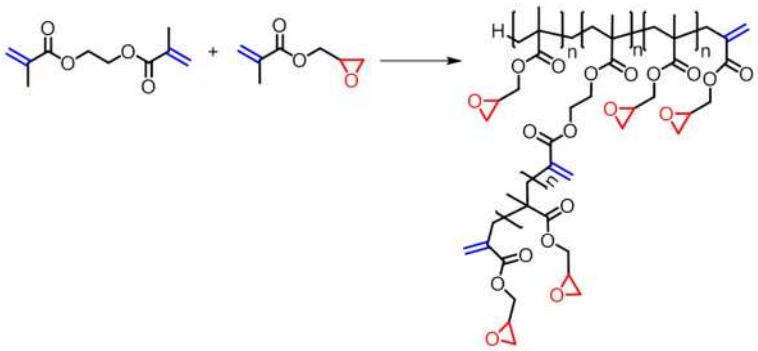

Figure 5.1: General schematic for the copolymerisation of EGDMA and GMA in the formation of branched epoxide containing copolymers

Copolymerisation of EGDMA and GMA 10/90 mol % under the conditions used in Chapter 2, 50% solids in 1,2-dichloroethane, for the copolymerisation of EGDMA and MMA, yielded insoluble gels within several hours (Figure 5.2). The gels obtained displayed a retention of epoxide functionality on analysis by FT-IR at approximately 907 cm^{-1} and a disappearance of peaks at approximately 1620 cm^{-1}, corresponding to C=C groups, indicating that crosslinking occurs *via* vinyl groups rather than epoxides, leading to the formation of epoxide functional gels, which are capable of swelling in organic solvents.

As the chain transfer efficiency of CoBF for GMA is lower than MMA, 6800 and 20000-40000 respectively (Appendix, Table 1), the CoBF concentration was increased. At higher CoBF concentrations gelation was delayed, but ultimately higher levels of CoBF than deemed necessary were required, with the products still forming insoluble gels after long time scales, hence an alternative solvent was investigated. As acetonitrile proved to be a good solvent for the homopolymerisation of GMA, this was investigated as a solvent.

Figure 5.2: Gel formed on polymerisation of EGDMA/GMA (90/10 mol%) in 1,2-dichloroethane, swollen in additional 1,2-dichloroethane

Copolymerisation of EGDMA and GMA, 10/90 mole % in acetonitrile at 50 wt% solids led to precipitation polymerisation within hours of initiation, forming large particles which could not be solubilised (Figure 5.3). As with the gels formed in dichloroethane, epoxide functionality is retained, as observed *via* FT-IR. Increasing the concentration of CoBF delayed precipitation polymerisation, most likely due to a reduction in the molecular weight, but did not circumvent this effect indefinitely, with the formation of precipitate occurring for long timescales. As previously mentioned, copolymerisation of EGDMA and GMA has been frequently used for the synthesis of epoxide containing microspheres by precipitation polymerisation.[3, 4] Precipitation polymerisations use high levels of solvent, commonly acetonitrile, to control the size of the crosslinked polymer spheres produced. Monomer levels as low as 1 wt% solids are used in order to control the microsphere size obtained from these polymerisations.

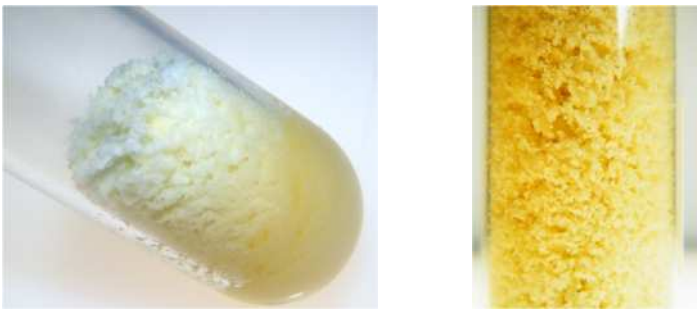

Figure 5.3: Polymer precipitate formed in CCTP of EGDMA/GMA (10/90 mol%) in acetonitrile, 50% solids

Investigation of the literature describing microspheres by precipitation polymerisation also shows a size dependency on the level of EGDMA incorporated, with high levels decreasing the particle size. Use of a 50/50 mol ratio of EGDMA relative to GMA a reduction in particle size was observed (Figure 5.4), but particles did not remain suspended in solvent. To investigate if sphere size would decrease on decreasing solids EGDMA/GMA 50/50 mol % at 20% solids was attempted and a soluble resulted after 24 hours.

Figure 5.4: Polymer from the CCTP of EGDMA/GMA (50/50 mol%) in acetonitrile, 50% solids, after precipitation in hexane

Although these reactions were surprising, in that particles were obtained using relatively high solids, an investigation of these effects were outside of the scope of this work, hence due to the high levels of solvent required to form soluble branched polymers using acetonitrile, further investigation of solvent choice was required. Precipitation polymerisations often use Hildebrand solubility parameters for solvent choice,[24] based on a good solubility for the mono-functional monomer and poorer solubility for the branching monomer. As molecular weight increases, the decreasingly soluble polymer precipitates from solution and further polymerisation takes place from

initiator and monomer absorbing in the polymer phase. In essence, Hildebrand solubility parameters are based on a like dissolves like principle, using the square root of the cohesive energy density to measure each solvent/reagents solubility value (δ). The Hildebrand solubility parameters for EGDMA, GMA and a range of solvents attempted are given in Table 5.1. Fully soluble polymer products were obtained in toluene, which has approximately the same δ value as EGDMA, no polymer precipitation was observed, even after long timescales.

	Hildebrand solubility parameter (δ)
EGDMA	18.2
GMA	19.4
1,2-Dichloroethane	20.2
Acetonitrile	24.6
MEK	19.0
Chloroform	18.7
Toluene	18.2

Table 5.1: Hildebrand solubility parameters for monomers and solvents utilised for the copolymerisation of EGDMA and GMA *via* CCTP[24]

5.2.2. Synthesis of Branched Epoxide Containing Polymers by CCTP

Copolymerisation of EGDMA and GMA in toluene resulted in soluble branched copolymers containing a high level of both activated vinyl functionality and epoxide groups observable by ^{1}H NMR, Figure 5.5. Variation in the ratio of EGDMA to GMA was used in order to vary both the level of branching in the product and the ratio of vinyl to epoxide groups. Copolymerisations using 50 mol% EGDMA and above required early termination in order to circumvent gelation. Increasing the level of CoBF would also have the same effect by limiting the molecular weight further, although as polymerisations could be taken to high conversion within 9 hours under these conditions, the CoBF level was kept constant and the reaction time reduced (Table 5.2).

Name	CoBF (mol%)	EGDMA/GMA (mol%)	M_n ($g.mol^{-1}$)	M_w ($g.mol^{-1}$)	PDi	Total conversion (%)	Duration (hr)
A	$3.8x10^{-5}$	25/75	900	2400	2.7	95	24
B	$3.8x10^{-5}$	50/50	1100	2400	2.2	89	9
C	$3.8x10^{-5}$	75/25	1500	4100	2.7	91	9

Table 5.2: Copolymerisation of EGDMA and GMA, varying monomer ratios. SEC data obtained from conventional SEC, conversion obtained *via* GC-FID

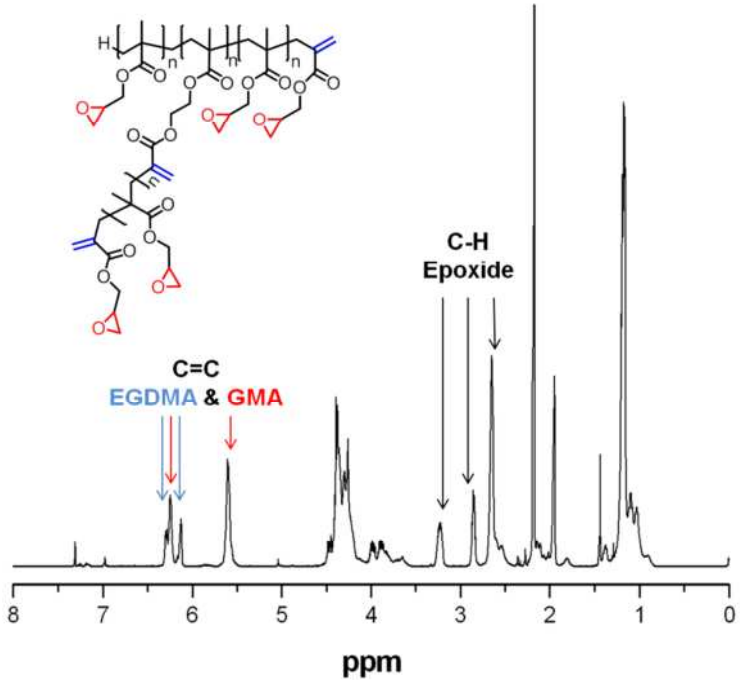

Figure 5.5: Example ^{1}H NMR spectrum of EGDMA/GMA (50/50 mol%) copolymer B in $CDCl_3$

The molecular weight evolution in copolymerisations **A**, 25 mol% EGDMA, displays a controlled linear increase as the reaction proceeds. However, for copolymerisations **B** and **C**, employing 50 and 75 mol% EGDMA respectively, sharper increases in both molecular weight and PDi are observed between 6 and 9 hours, indicative of the onset of gelation (Figure 5.6).

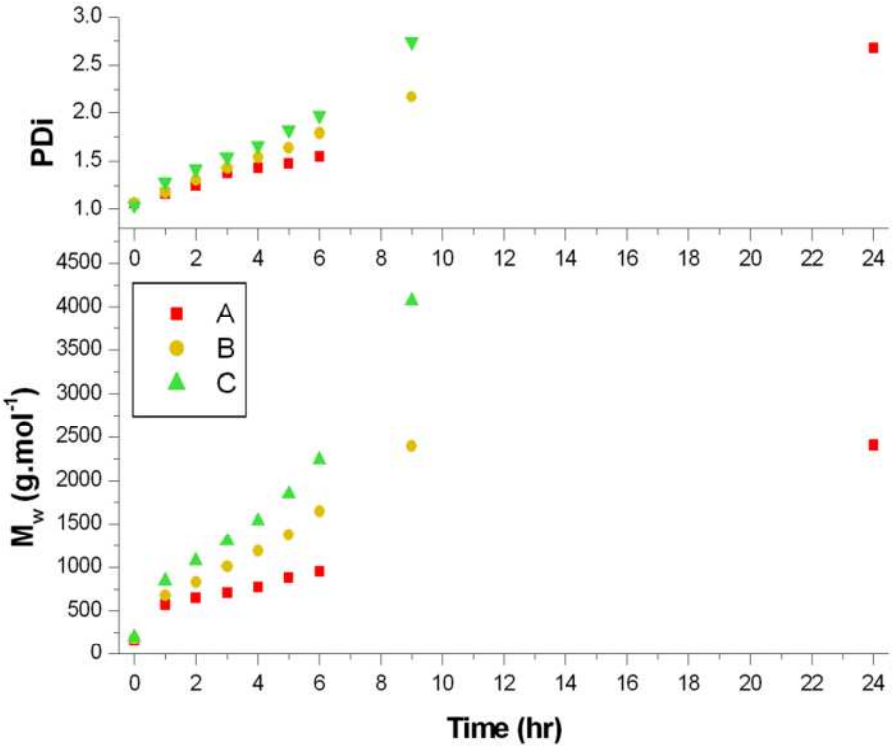

Figure 5.6: Molecular weight evolution of copolymerisations A-C (A: EGDMA/GMA 25/75 mole%, B: EGDMA/GMA 50/50 mole%, C: EGDMA/GMA 75/25 mole%), molecular weights obtained *via* conventional SEC

Although the molecular weight evolution displays an apparent loss of control for copolymerisations **B** and **C** between 6 and 9 hours the total conversions of all polymerisations proceed in the same manner, indicating the rate of polymerisation is unaffected but that crosslinking of chains is likely to be responsible for the increase in molecular weight observed (Figure 5.7).

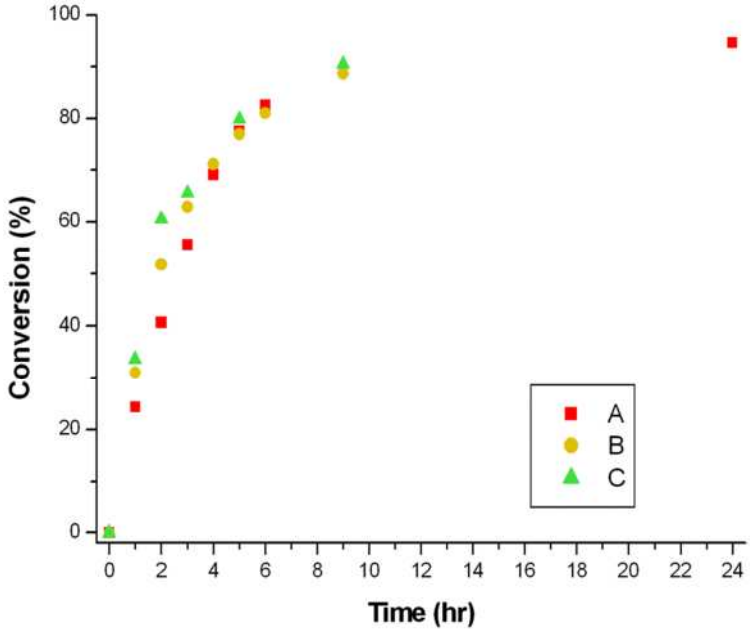

Figure 5.7: Total conversions of copolymerisations A-C, conversion measured by GC-FID

In all copolymerisations of EGDMA and GMA the conversion of EGDMA proceeded at a higher rate than that of GMA, from GC-FID, hence the polymers formed, providing homopolymerisation does not dominate, are likely to have a more densely branched 'core' than the periphery (Figure 5.8, Figure 5.9).

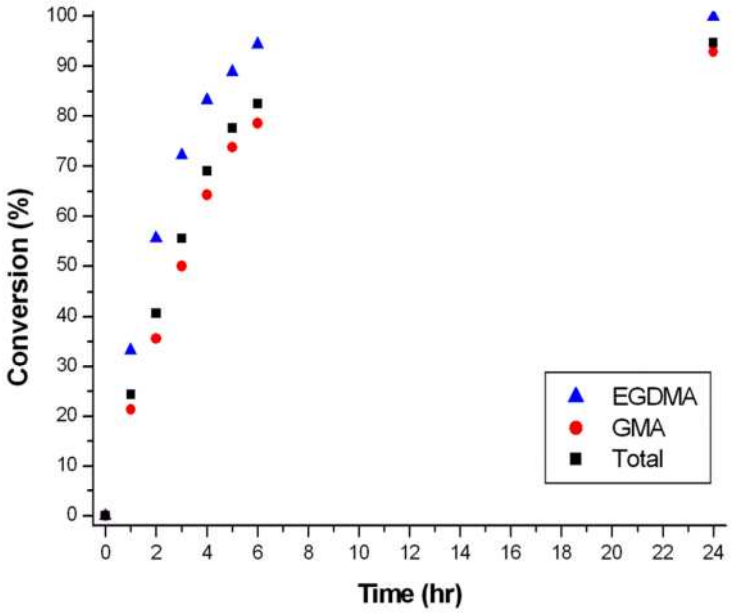

Figure 5.8: Individual monomer conversions for copolymerisation A (EGDMA/GMA 25/75 mol%), conversion measured by GC-FID

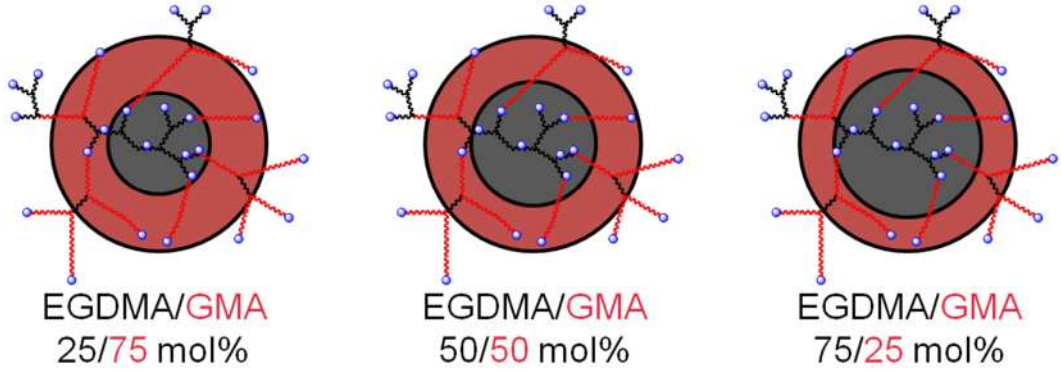

Figure 5.9: Generalised "branched core" schematic of the resulting copolymers of EGDMA (black) and GMA (red), retention of a high level of vinyl groups (blue)

Although soluble polymers were obtained post-polymerisation, it was found that on leaving under ambient conditions insoluble gels were formed after only a few days. Gelation of EGDMA homopolymers was also observed, as discussed in Chapter 2. However, in the case of EGDMA homopolymers gelation occurred over several weeks and was prevented indefinitely by the addition of low levels of antioxidant/ inhibitor BHT. Gelation of EGDMA/GMA copolymers was not circumvented by the addition of radical inhibitor BHT; hence, it is believed that epoxide ring-opening arising from nucleophilic impurities in toluene was the cause of gelation. Investigation of the gels formed, by FT-IR, shows the retention of both vinyl C=C bonds and epoxide groups, with only a minor peak observed for the formation of hydroxyl groups on ring-opening. Formation of hydroxyl groups following ring-opening with nucleophilic impurities in the solvent could lead to a cascade of epoxide ring-opening with the hydroxyl groups formed, leading to the formation of additional C-O bonds, to which a small increase in this region of the FT-IR is observed at approximately 1000-1100 cm^{-1} (Figure 5.10). Only a low level of epoxide crosslinking is required to cause the gelation of products, possibly explaining the retention of epoxide peaks observed *via* FT-IR. On removal of toluene immediately after polymerisation, by precipitation and removal of solvents in vacuo, gelation can be avoided, however, BHT was added as a precaution and the polymers kept away from natural light in an effort to limit post-polymerisation crosslinking.

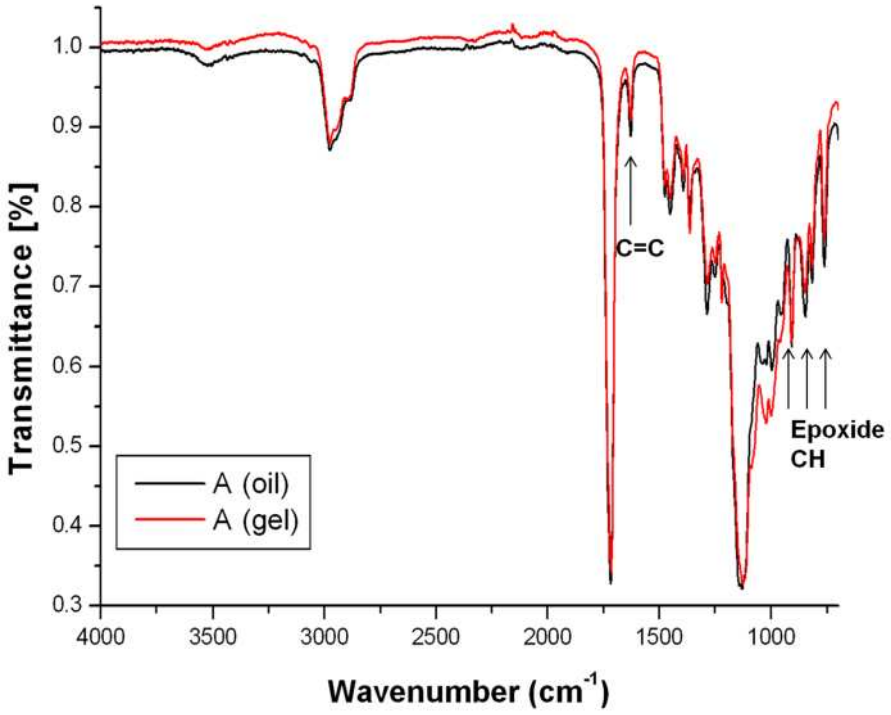

Figure 5.10: FT-IR of EGDMA/GMA copolymer A, oil (uncrosslinked) compared with the gel (crosslinked) product

MALDI-ToF analysis of copolymers **A**-**C** revealed spectra with a multitude of peak distributions, signifying a high level of variety in the products, however, this was not unexpected as the PDi of these materials, measured by conventional SEC, was approximately 3. As the PDi's of these materials are relatively high, it is likely that high molecular weight exclusion will be observed in the MALDI-ToF spectra.[25-27] Surprisingly, the major MALDI-ToF peak series in copolymer **A** denotes roughly equivalent incorporations of EGDMA and GMA (**[2]**, **[4]**, **[10]** and **[11]**), despite the high molar ratio of GMA employed. Minor peak series correspond to further EGDMA/GMA combinations (**[6]** and **[8]**) and the incorporation of low levels of impurities, such as HEMA, originating from EGDMA, and an unknown impurity, X, originating from GMA, as previously observed in Chapter 4 (**[1]**, **[3]**, **[5]**, **[7]** and **[9]**). No evidence of homopolymer formation is observed for copolymer **A**.

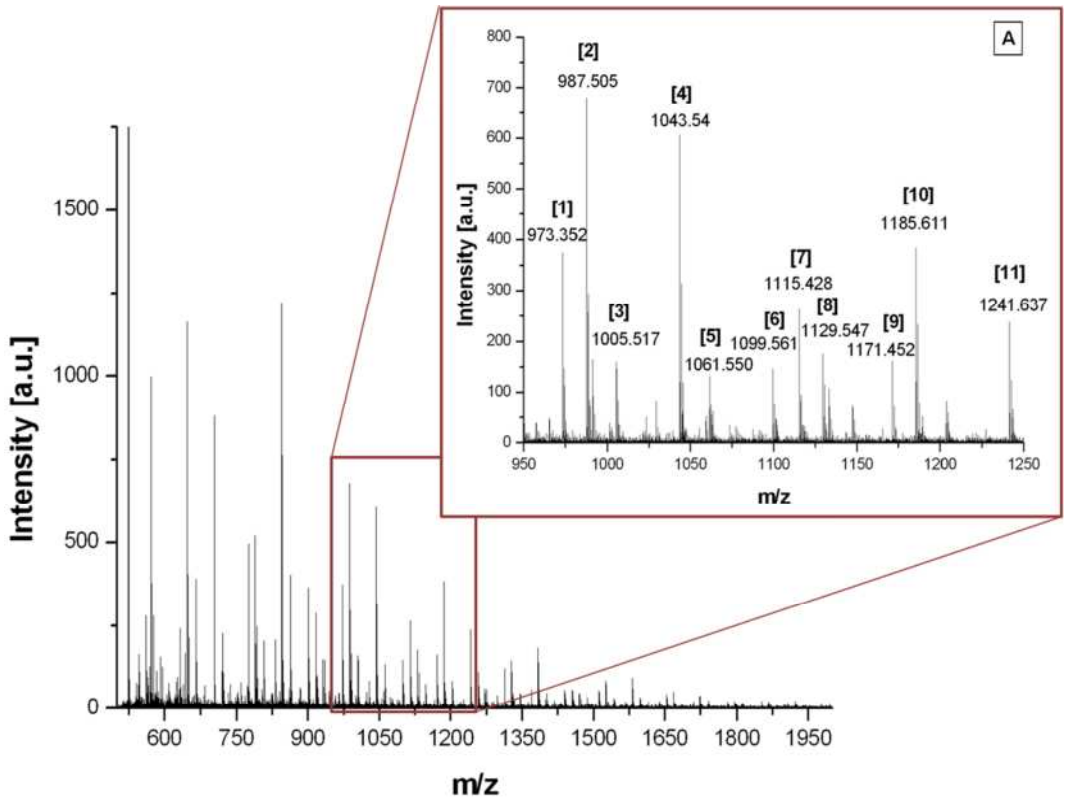

Figure 5.11: MALDI-ToF spectrum of A, poly-EGDMA/GMA copolymer (25/75 mol%). Zoom region between 950 and 1250 Daltons. Annotations correspond to Table 5.3

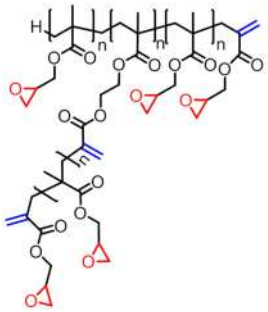

Figure 5.12: Example structure of EGDMA/GMA copolymer $(EGDMA)_1(GMA)_5$ (if n=1)

Name	Theoretical m/z	Measured m/z	Corresponding Structure
[1]	973.35	973.35	$(EGDMA)_2(GMA)_3(X)Na^+$
[2]	987.41	987.51	$(EGDMA)_2(GMA)_4Na^+$
[3]	1005.41	1005.52	$(GMA)_6(HEMA)_1Na^+$
[4]	1043.44	1043.54	$(EGDMA)_3(GMA)_3Na^+$
[5]	1061.44	1061.55	$(EGDMA)_1(GMA)_5(HEMA)_1Na^+$
[6]	1099.47	1099.56	$(EGDMA)_4(GMA)_2Na^+$
[7]	1115.41	1115.43	$(EGDMA)_2(GMA)_4(X)Na^+$
[8]	1129.47	1129.55	$(EGDMA)_2(GMA)_5Na^+$
[9]	1171.44	1171.45	$(EGDMA)_3(GMA)_3(X)Na^+$
[10]	1185.50	1185.61	$(EGDMA)_3(GMA)_4Na^+$
[11]	1241.53	1241.64	$(EGDMA)_4(GMA)_3Na^+$

Table 5.3: Corresponding structures to MALDI-ToF peaks annotated in Figure 5.11 for A, poly-EGDMA/GMA copolymer (25/75 mol%). Mass region 950-1250 Daltons. Example structure given in Figure 5.12

Copolymer **B** had an equivalent molar ratio of EGDMA/GMA and correspondingly, the major peaks series contain higher levels of EGDMA in comparison to copolymer **A [1]**, **[6]**, **[7]**, **[8]**, **[12]**. Minor peaks again correspond to further combinations of EGDMA and GMA **[3]** and **[10]** and incorporations of low levels of monomer impurity X **[2]**, **[5]**, **[9]** and **[11]**. Low levels of EGDMA homopolymer are observed using this higher mole equivalent of EGDMA **[4]**.

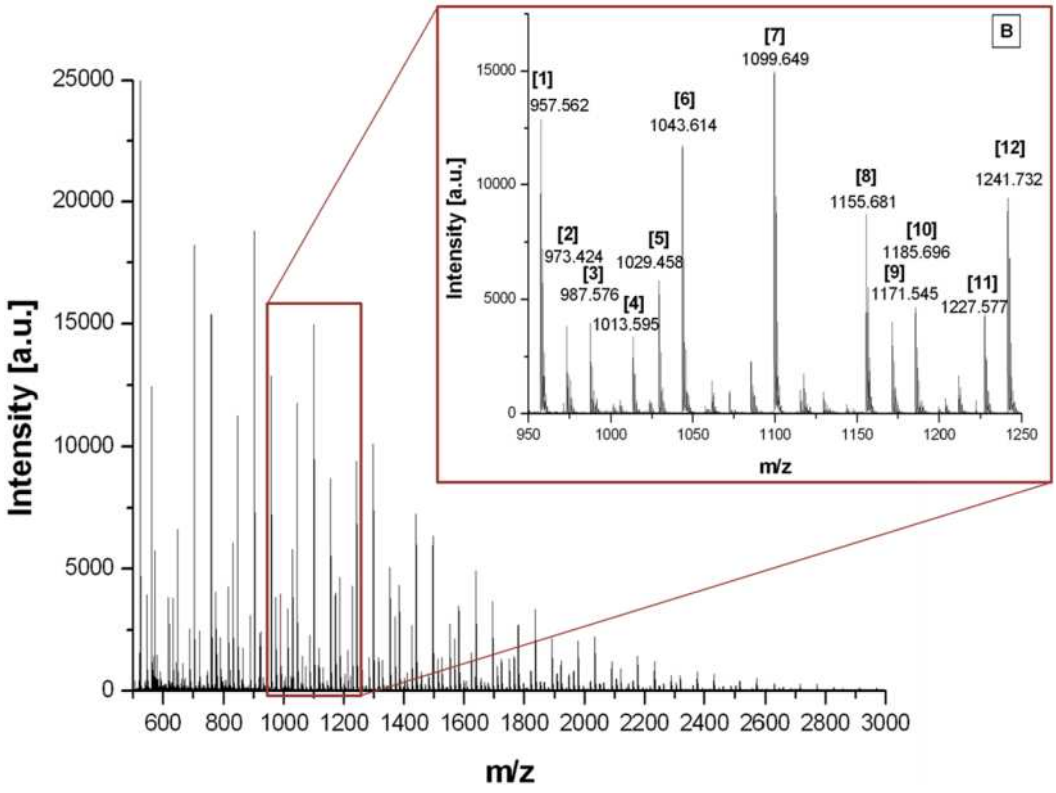

Figure 5.13: MALDI-ToF spectrum of B, EGDMA/GMA copolymer (50/50 mol%). Zoom region between 950 and 1250 Daltons. Annotations correspond to Table 5.4

Name	Theoretical m/z	Measured m/z	Corresponding Structure
[1]	957.41	957.56	$(EGDMA)_4(GMA)_1Na^+$
[2]	973.35	973.42	$(EGDMA)_2(GMA)_3(X)Na^+$
[3]	987.41	987.58	$(EGDMA)_2(GMA)_4Na^+$
[4]	1013.44	1013.60	$(EGDMA)_5Na^+$
[5]	1029.30	1029.46	$(EGDMA)_3(GMA)_2(X)Na^+$
[6]	1043.44	1043.61	$(EGDMA)_3(GMA)_3Na^+$
[7]	1099.47	1099.65	$(EGDMA)_4(GMA)_2Na^+$
[8]	1155.50	1155.68	$(EGDMA)_5(GMA)_1Na^+$
[9]	1171.44	1171.55	$(EGDMA)_3(GMA)_3(X)Na^+$
[10]	1185.50	1185.70	$(EGDMA)_3(GMA)_4Na^+$
[11]	1227.47	1227.58	$(EGDMA)_4(GMA)_2(X)Na^+$
[12]	1241.53	1241.73	$(EGDMA)_4(GMA)_3Na^+$

Table 5.4: Corresponding structures to MALDI-ToF peaks annotated in Figure 5.13 for B, poly-EGDMA/GMA copolymer (50/50 mol%). Mass region 950-1250 Daltons. Example structure given in Figure 5.12

Copolymer **C** employed the highest level of EGDMA, which again is reflected in the MALDI-ToF spectrum, with the major peak series denoting EGDMA homopolymer and

the incorporation of a single unit of GMA **[1]**, **[3]**, **[6]** and **[8]**. Minor peak series correspond to further GMA incorporation **[4]**. Low level incorporations of monomer impurity HEMA are also observed **[2]**, **[5]** and **[7]**.

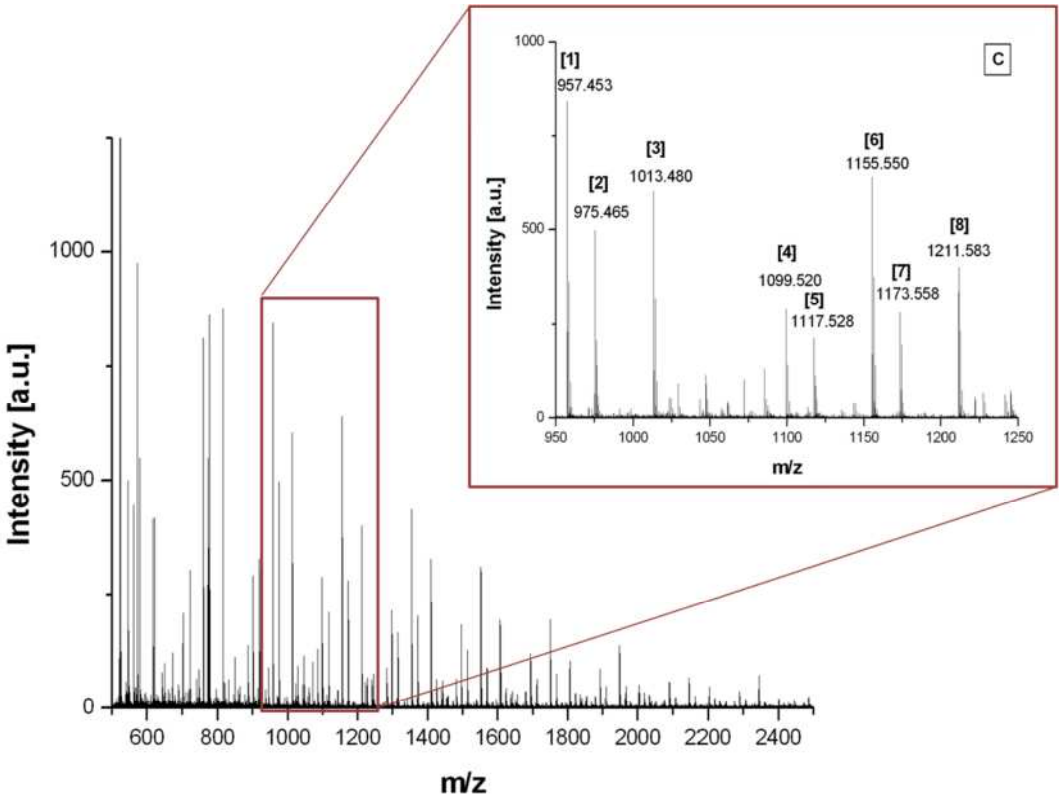

Figure 5.14: MALDI-ToF spectrum of C, EGDMA/GMA copolymer (75/25 mol%). Zoom region between 950 and 1250 Daltons. Annotations correspond to Table 5.5

Name	Theoretical m/z	Measured m/z	Corresponding Structure
[1]	957.41	957.45	$(EGDMA)_4(GMA)_1Na^+$
[2]	975.41	975.47	$(EGDMA)_2(GMA)_3(HEMA)_1Na^+$
[3]	1013.44	1013.48	$(EGDMA)_5Na^+$
[4]	1099.47	1099.52	$(EGDMA)_4(GMA)_2Na^+$
[5]	1117.47	1117.53	$(EGDMA)_2(GMA)_4(HEMA)_1Na^+$
[6]	1155.50	1155.55	$(EGDMA)_5(GMA)_1Na^+$
[7]	1173.50	1173.56	$(EGDMA)_3(GMA)_3(HEMA)_1Na^+$
[8]	1211.53	1211.58	$(EGDMA)_6Na^+$

Table 5.5: Corresponding structures to MALDI-ToF peaks annotated in Figure 5.14 for C, poly-EGDMA/GMA copolymer (75/25 mol%). Mass region 950-1250 Daltons. Example structure given in Figure 5.12

5.2.3. Multidetector SEC Analysis of EGDMA/GMA Copolymers

Universal calibration was employed to investigate the branching in EGDMA/GMA copolymers **A**-**C**, by comparison of their α values to α values of linear poly-GMA over the same molar mass range. As previously discussed in chapter 2, previous literature exists on the applicability of universal calibration and the Mark-Houwink relationship to polymers of low molecular weight, which describes a deviation from the linear relationship between log[η] and log M for low molecular weights (<10000).[28-31] This deviation is also observed in linear PGMA standards synthesised for the analysis of copolymers **A**-**C** due to their low molecular weights, hence molecular weight averages are unlikely to be a reflection of the true molecular weight but, provided a linear standard of the same molar mass is used, should still indicate trends in both the molecular weight and branching.

A clear reduction in α values are observed for copolymers **A**-**C** compared to their linear counterparts, indicative of a contraction in hydrodynamic volume on branching (Table 5.6).

Name	M_n ($g.mol^{-1}$)	M_w ($g.mol^{-1}$)	PDi	α
PGMA 1	2300	4900	2.1	0.30
A	1000	4500	4.7	0.24
B	1400	3200	2.3	0.27
PGMA 2	5500	9800	1.8	0.41
C	2100	7800	3.8	0.28

Table 5.6: Molecular weights and α values derived from universal calibration for branched EGDMA/GMA copolymers A-C and linear poly-GMA homopolymers 1 and 2 (A: EGDMA/GMA 25/75 mol%, B: EGDMA/GMA 50/50 mol%, C: EGDMA/GMA 75/25 mol%)

The reduction in α on comparison of **A** and **B** indicates that **A** possesses a higher level of branching, contrary to the lower amount of branching monomer incorporated (25 and 50 mol% respectively). However, this may be due to the early termination of **B** yielding lower molecular weight products, with less significant changes in the hydrodynamic volume expected for low molecular weights (Table 5.6). The molecular weight distribution plot for **A** shows a high molecular weight shoulder that was not present in SEC's obtained on termination of the polymerisation, hence a small amount of chain crosslinking may have occurred, which may further reduce the α value (Figure 5.15).

Copolymer **C** shows the most significant decrease in α compared to its linear counterpart, which is expected due to the high level of branching monomer.

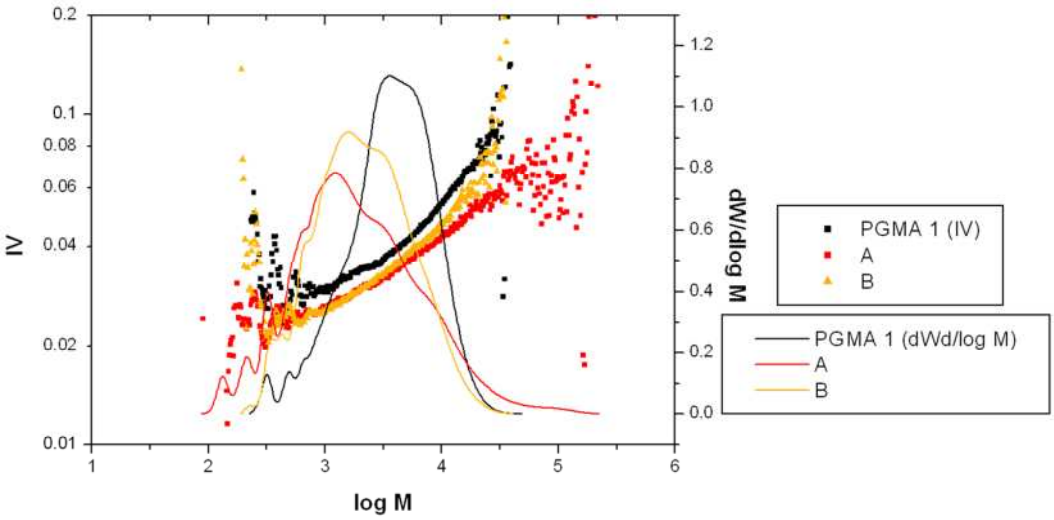

Figure 5.15: Mark-Houwink plots for copolymerisations A and B (A: EGDMA/GMA 25/75 mol%, B: EGDMA/GMA 50/50 mol%) compared to linear PGMA 1

Mark-Houwink plots of **A** and **B** compared to linear **PGMA 1** over the same molar mass range indicate a lower solution viscosity of both branched polymers over the whole molecular weight distribution. The gradients of the IV plots increase in a non-linear fashion, which could be an indication of the variation in branching formed on copolymerisation, but as linear **PGMA 1** also displays this inconsistent gradient, it may also be an artefact caused by the low molecular weights (Figure 5.15).

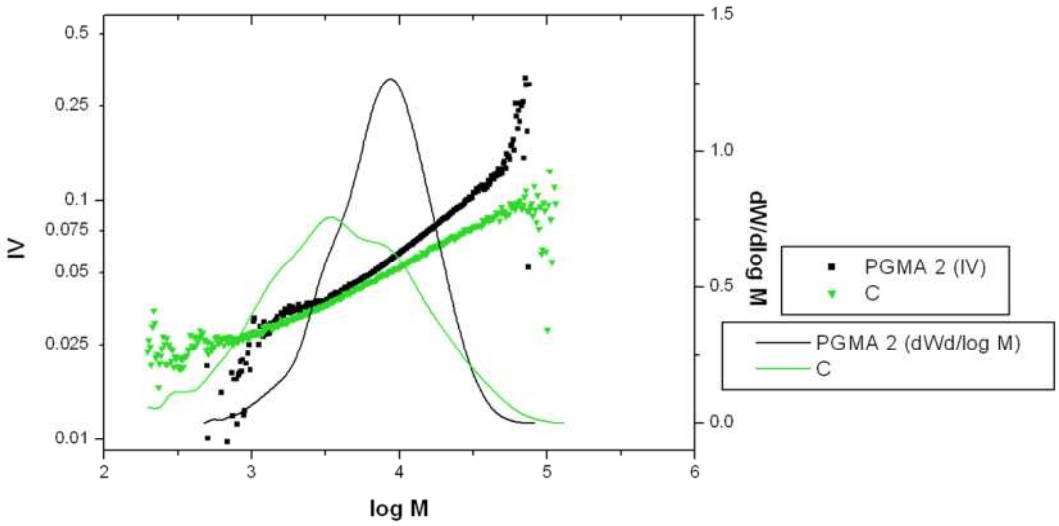

Figure 5.16: Mark-Houwink plots for copolymerisation C (EGDMA/GMA 75/25 mol%) compared to linear PGMA 2

On comparison of the Mark-Houwink plot of copolymer **C** to linear **PGMA 2** a reduction in the solution viscosity is also observed throughout the entire molecular weight distribution. The gradient of the IV plot for **C** displays a higher level of linearity than IV plots of **A** and **B**, indicating the variation in branching is lower, this may be due to the high levels of branching monomer employed (75 mol%) leading to more homogenous branching and the higher level of EGDMA homopolymer observed *via* MALDI-ToF.

A further indication of branching is displayed by a reduction in g' for copolymers **A**-**C** (Figure 5.17). The gradients of the g' plots are non-linear, signifying that branching is not uniform over the distribution, which is expected due to the copolymerisation of branching and non-branching monomers. A reduction in g' is observed with increasing molecular weight, indicative of an increase in branching as molar mass increases. As indicated by the Mark-Houwink plots (Figure 5.15, Figure 5.16), copolymer **A** appears more branched than copolymer **B**, despite employing a higher level of branching monomer, this is most likely due to the early termination of copolymerisation **B** in order to prevent gelation, leading to the formation of lower molecular weights, this is confirmed by the g' plots (Figure 5.17), as a more pronounced reduction is observed for **A** than for **B**. In agreement with Mark-Houwink plots copolymer **C** displays the highest level of branching, with the greatest reduction in g', most likely due to its increased molecular weight and higher incorporation of branching monomer.

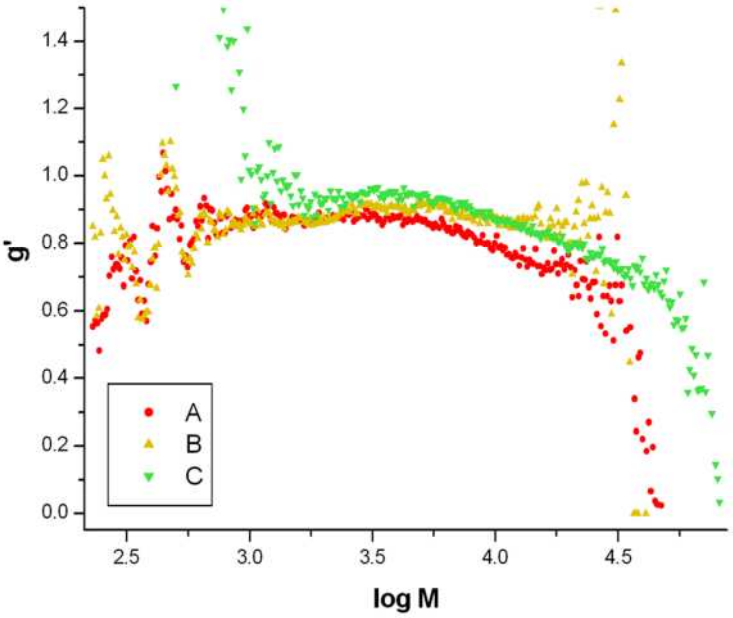

Figure 5.17: g' plots for copolymers A-C (A: EGDMA/GMA 25/75 mol%, B: EGDMA/GMA 50/50 mol%, C: EGDMA/GMA 75/25)

As with linear poly-GMA synthesised *via* CCTP, there should be several routes for functionalisation of such polymers, due to the presence of both vinyl and epoxide functionality in the products; full functionalisation with functional amines, functionalisation of vinyl groups *via* thiol-Michael addition and dual functionalisation, combining both functionalisation techniques.

5.2.4. Full Amine Functionalisation of EGDMA/GMA copolymers

Calculation of the level of vinyl groups becomes more complicated in copolymerisations; hence, it was approximated from the conversion, with the assumption that each EGDMA unit retains a single vinyl group. The vinyl groups retained as terminal GMA units is approximated from the $M_n/M_{r,GMA}$ and the level of epoxide functionality is calculated based on conversion by GC-FID. All of these calculations are approximations however, and most likely provide an overestimation of the level of functionalisable groups.

As the functionalisation of epoxide containing polymers (Chapter 4) proved more successful with a wide variety of primary amines, only primary amines were investigated in this study. In previous work it was shown that terminal vinyl groups

formed in the CCTP of poly-GMA were susceptible to Michael type addition of primary amines, hence, functionalisations were attempted with propylamine, benzylamine and aminopropanediol to EGDMA/GMA copolymer **A**, using the same conditions as outlined in Chapter 4 for linear poly-GMA, 1.0:1.2 excess of amine to epoxide and vinyl groups in DMSO, 60 ˚C, 24 hours. However, after 24 hours reaction time vinyl peaks were still present in the ^{1}H NMR, and due to a multitude of peaks arising between 2.0 and 4.5 the level of epoxide functionalisation was difficult to ascertain from the reaction solution. All primary amines attempted, failed to completely functionalise vinyl groups, with an average of approximately 50% remaining in the product (Table 5.7).

Name	Functional Amine	Vinyl Conversion (%)
A1	Propylamine	56
A2	Benzylamine	32
A3	Aminopropanediol	62

Table 5.7: Vinyl conversion for attempts to fully functionalise EGDMA/GMA copolymer A with functional amines. Vinyl conversion measured by ^{1}H NMR

It was postulated that as full functionalisation occurs in linear poly-GMA homopolymers, it may be the vinyl groups arising from EGDMA that are retained, perhaps due to internal vinyl groups in the core being more sterically hindered; or perhaps reactions at terminal vinyl groups on GMA are being catalysed by epoxide ring-opening reactions, such as in the cyclisation reactions discussed in Chapter 4 (Figure 5.18).

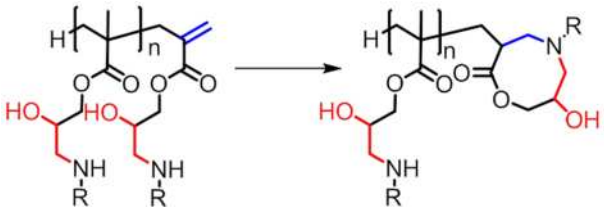

Figure 5.18: Potential cyclisation reaction on ring-opening of ω-epoxide group and subsequent aza-Michael type addition to ω-vinyl group.

To ascertain the reactivity of EGDMA vinyl groups to self-catalysed nucleophilic attack by primary amines, under these conditions, EGDMA homopolymers were reacted with propylamine, benzylamine and aminopropanediol. EGDMA homopolymers are bright yellow/orange in colour, due to the level of CoBF employed to circumvent crosslinking in the polymerisation. On addition of functional amine all polymer solutions displayed a colour change to green/blue, additionally on heating a colour change from green/blue

to red was observed. It is postulated that the amines are coordinating with the CoBF as axial ligands, leading to this initial colour change, then being oxidised, resulting in a further colour change from green/blue to red (Figure 5.19).

Figure 5.19: Colour change of poly-EGDMA homopolymer (yellow) on addition of functional primary amines (green/blue) and colour change on heating solution at 60 ˚C for 24 hours (red)

Despite the vinyl conversion observed for poly-GMA homopolymers, very little conversion of poly-EGDMA vinyl groups is observed *via* ^{1}H NMR (Table 5.8), indicating that perhaps these vinyl groups are not susceptible to nucleophilic attack of primary amines under these conditions. Therefore, addition of amines to GMA vinyl groups must be promoted by the close proximity of the epoxide groups. Hence, it is likely that the vinyl groups remaining in EGDMA/GMA copolymers functionalised with primary amines originate from EGDMA.

Functional Amine	Vinyl Conversion (%)
Propylamine	0
Benzylamine	6
Aminopropanediol	17

Table 5.8: Vinyl conversion for attempts to fully functionalise EGDMA homopolymer with functional amines, by ^{1}H NMR

The addition of functional amines to epoxide, and some degree of vinyl, groups is also characterised by an increase in molecular weight observed by SEC (Figure 5.20, Table 5.9).

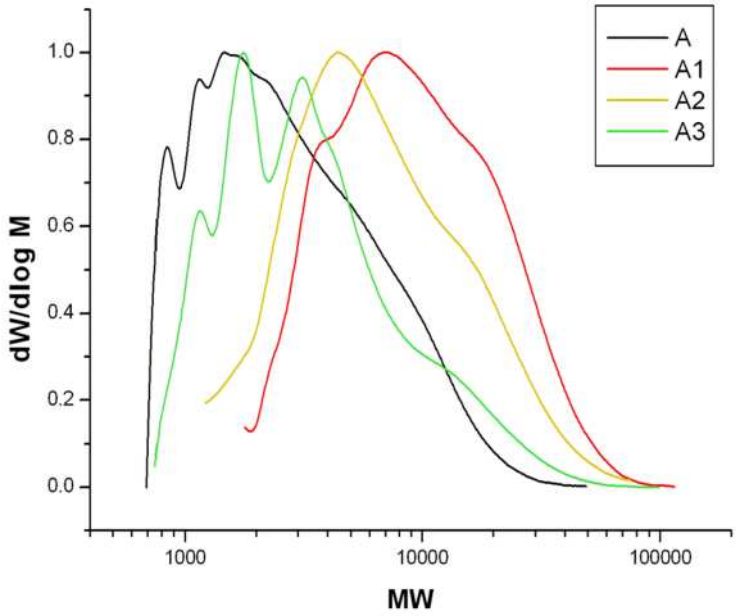

Figure 5.20: SEC comparisons of copolymer A to A1-A3, DMF eluent (A: EGDMA/GMA 25/75 mol% copolymer, A1 copolymer A functionalised with propylamine, A2 copolymer A functionalised with benzylamine, A3 copolymer A functionalised with aminopropanediol)

Name	Functionality	M_n ($g.mol^{-1}$)	M_w ($g.mol^{-1}$)	PDi
A	None	2000	3800	1.92
A1	Propylamine	6700	12000	1.78
A2	Benzylamine	4600	8800	1.90
A3	Aminopropanediol	2500	4900	2.02

Table 5.9: SEC comparisons of copolymer A to A1-A3, DMF eluent (A: EGDMA/GMA 25/75 mol% copolymer, A1 copolymer A functionalised with propylamine, A2 copolymer A functionalised with benzylamine, A3 copolymer A functionalised with aminopropanediol)

5.2.5. Dual Functionalisation of EGDMA/GMA copolymers

Due to the retention of vinyl groups for amine functionalised copolymers **A1**-**A3**, attempts were made to functionalise these remaining vinyl groups *via* thiol-Michael addition. Copolymer **A2**, EGDMA/GMA copolymer (25/75 mol%) ring-opened with benzylamine, was chosen as this copolymer displayed the highest retention of vinyl groups and functionalised with thioglycerol *via* thiol-Michael addition, **A2.1**. Although a reduction in remaining vinyl groups was observed on thiol-Michael addition with thioglycerol, the retention of approximately 25% of remaining vinyl groups was observed in the final product, indicating that perhaps steric hindrance, on conducting

the epoxide ring-opening reaction prior to thiol-Michael addition, is leading to the incomplete addition of thioglycerol to remaining vinyl groups. An increase in molecular weight by SEC was observed, indicating the addition of thioglycerol to the polymer (Figure 5.21, Table 5.10).

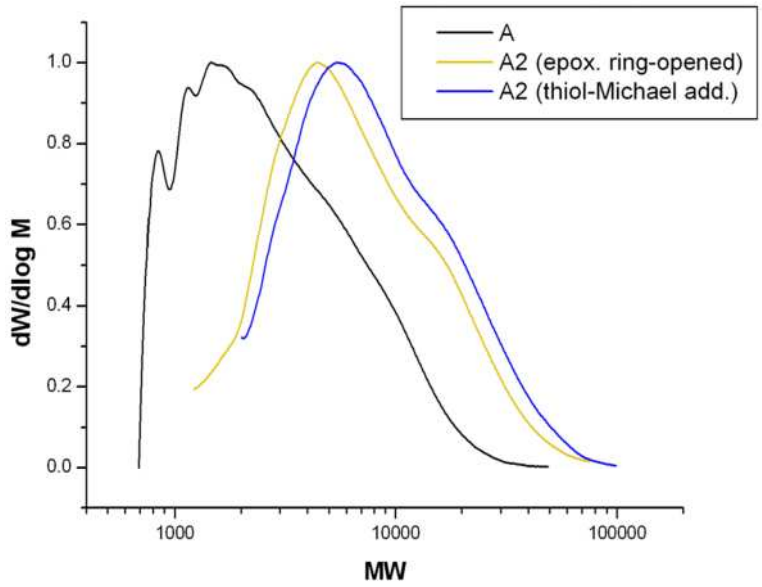

Figure 5.21: SEC comparison of copolymer A to benzylamine functionalised A2 and dual functionalised A2 thiol-Michael addition with thioglycerol. DMF eluent

Name	Functionality	M_n (g.mol^{-1})	M_w (g.mol^{-1})	PDi
A	None	2000	3800	1.9
A2	Benzylamine	4600	8800	1.9
A2.1	Benzylamine + thioglycerol	6000	10800	1.8

Table 5.10: SEC comparison of copolymer A to benzylamine functionalised A2 and dual functionalised A2 thiol-Michael addition with thioglycerol. DMF eluent

Due to the limited reactivity of the remaining vinyl groups to thiol-Michael addition post-epoxide ring-opening, the thiol-Michael addition was attempted prior to ring-opening. Thiol-Michael addition of benzyl mercaptan to copolymer **B** saw a complete disappearance of all vinyl peaks within 1 hour, as measured by ^{1}H NMR. Hence, there appears to be no steric hindrance effects at the "core" when epoxide groups remain unfunctionalised, even for higher EGDMA incorporations, which should produce a more densely branched structure. An increase in molecular weight is also observed *via* SEC, using THF eluent, on addition of benzyl mercaptan to copolymer **B** (Figure 5.22, Table

5.11) and the addition of a chromophore at approximately 270 nm corresponding to the polymer region was observed *via* PDA detection (Figure 5.23).

Ring-opening of epoxide groups for **B1** thiol-Michael addition product with aminopropanediol (**B1** dual functionalised) was carried out to obtain copolymers of amphiphilic, site selective functionality. Upon ring-opening with aminopropanediol a complete loss of epoxide functionality was observed *via* ^{1}H NMR, and an increase in the molecular weight was observed by SEC using THF eluent (Figure 5.22, Table 5.11). PDA of dual functionalised **B1** also confirms the retention of a chromophore in the polymer region at approximately 270 nm (Figure 5.23).

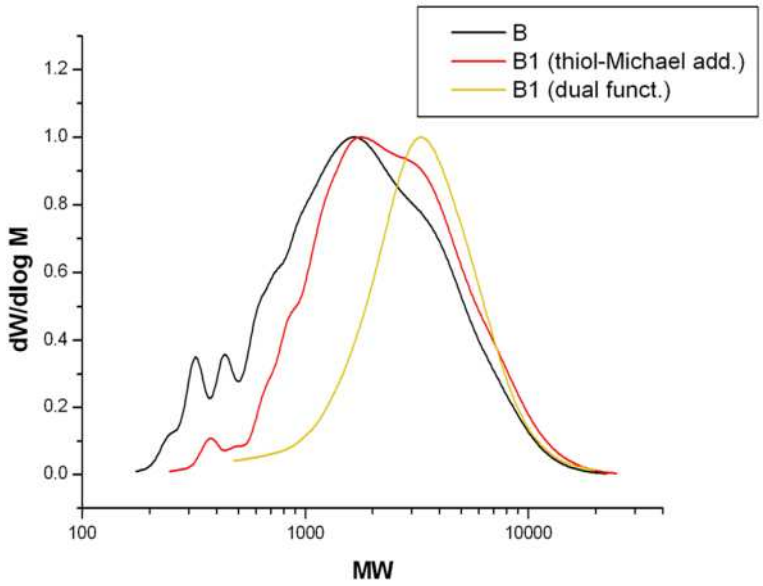

Figure 5.22: SEC comparison of EGDMA/GMA 50/50 mol% copolymer B with B1 thiol-Michael addition product with benzyl mercaptan, and B1 dual functionalised with benzyl mercaptan and aminopropanediol. THF eluent

Name	Functionality	M_n ($g.mol^{-1}$)	M_w ($g.mol^{-1}$)	PDi
B	None	1200	2400	2.1
B1 Thiol-Michael add.	Benzyl mercaptan	1700	3000	1.7
B1 Dual funct.	Aminopropanediol	2700	3900	1.4

Table 5.11: SEC comparison of EGDMA/GMA 50/50 mol% copolymer B with B1 thiol-Michael addition product with benzyl mercaptan, and B1 dual functionalised with benzyl mercaptan and aminopropanediol. THF eluent

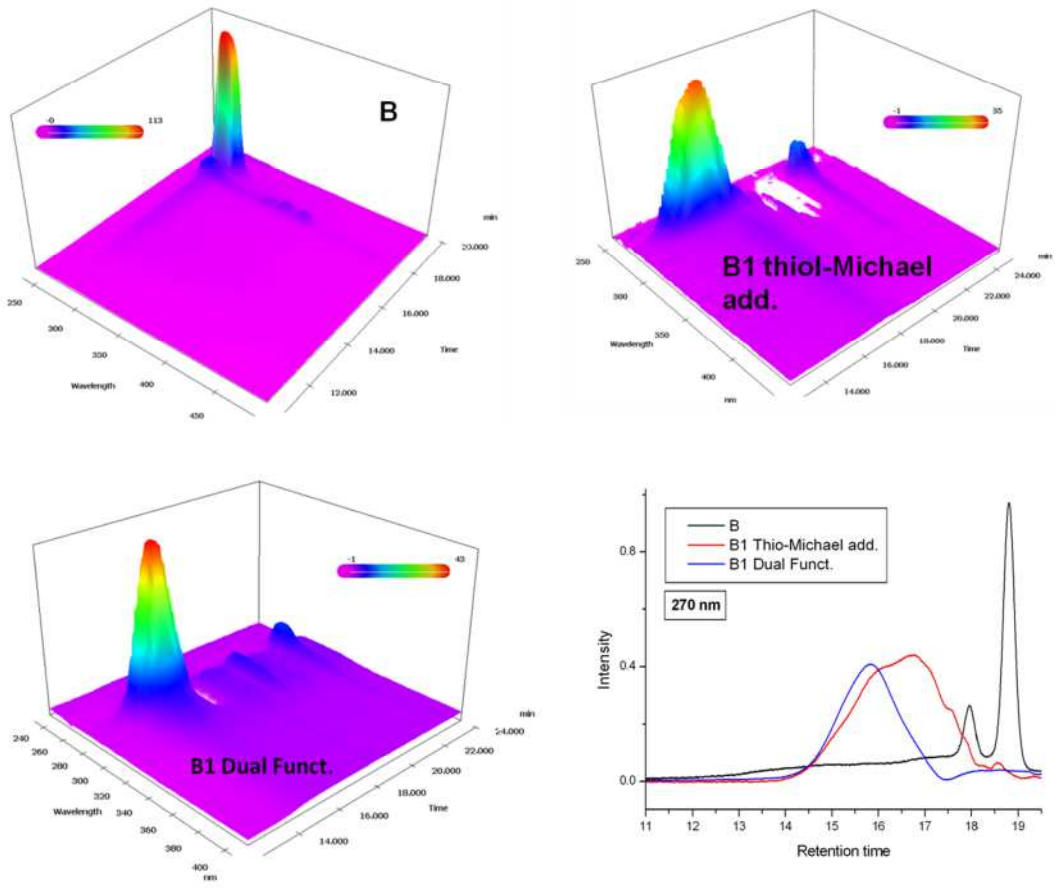

Figure 5.23: (Top left) SEC with PDA detection for copolymer B, no chromophore observed in the polymer region. (Top right) PDA detection for B1 thiol-Michael addition with benzyl mercaptan, chromophore observed for the polymer region 14-18 minutes retention time, 270 nm (Bottom left) PDA detection for B1 dual functionalised with benzyl mercaptan and aminopropanediol, chromophore observed for polymer region 14-17 minutes retention time, 270 nm (Bottom right) UV chromatogram overlay for B, B1 thiol-Michael addition and B1 dual functionalised at 270 nm

Functionalisation of **B** with benzyl mercaptan (**B1** thiol-Michael add.) and aminopropanediol (**B1** dual funct.) were investigated by SEC, DMF eluent. On addition of benzyl mercaptan (**B1** thiol-Michael add.) a reduction is seen in the molecular weight using SEC with DMF eluent, this is most likely due to the increasing hydrophobicity of the polymer on attachment of benzyl mercaptan causing a reduction in the hydrodynamic volume. For **B1** (dual funct.) a greater increase in molecular weight is observed on dual functionalisation, using SEC DMF eluent, as it provides a much better solvent for the addition of hydrophilic aminopropanediol, hence contraction in the hydrodynamic volume on addition of this functionality is not expected, as it may be with THF eluent (Figure 5.24, Table 5.12).

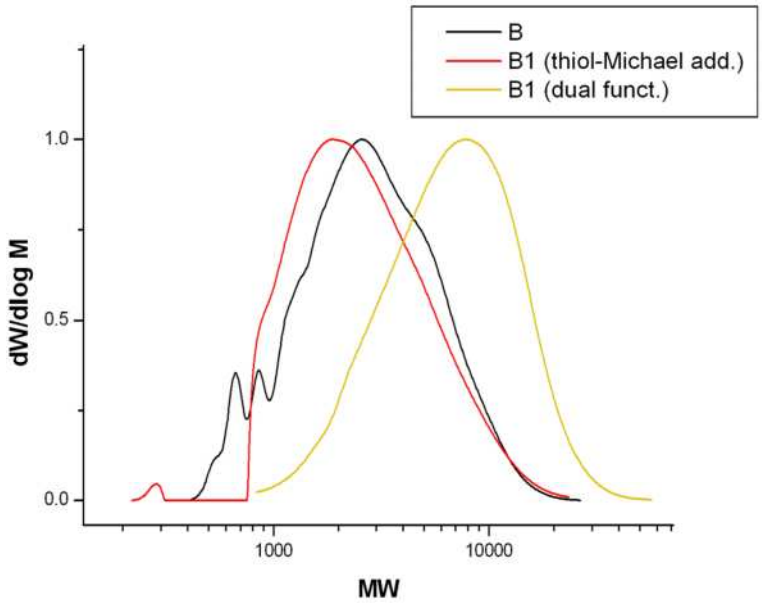

Figure 5.24: SEC comparison of EGDMA/GMA 50/50 mol% copolymer B with B1 thiol-Michael addition product with benzyl mercaptan, and B1 dual functionalised with benzyl mercaptan and aminopropanediol. DMF eluent

Name	Functionality	M_n ($g.mol^{-1}$)	M_w ($g.mol^{-1}$)	PDi
B	None	2000	3400	1.7
B1 Thiol-Michael add.	Benzyl mercaptan	2000	3200	1.6
B1 Dual funct.	Aminopropanediol	5000	8000	1.6

Table 5.12: SEC comparison of EGDMA/GMA 50/50 mol% copolymer B with B1 thiol-Michael addition product with benzyl mercaptan, and B1 dual functionalised with benzyl mercaptan and aminopropanediol. DMF eluent

MALDI-ToF was attempted for both the thiol-Michael addition product and dual functionalised product of **B1**; however, due to the reduced solubility of the dual functionalised product in solvents suitable for MALDI-ToF, a spectrum was not obtained. Due to the already high number of peak distributions based on the many combinations of monomer available in the copolymerisation of EGDMA and GMA, and the broad PDi of the copolymers in question, the peak distributions for **B1** thiol-Michael addition product with benzyl mercaptan are diverse (Figure 5.25, Table 5.13).

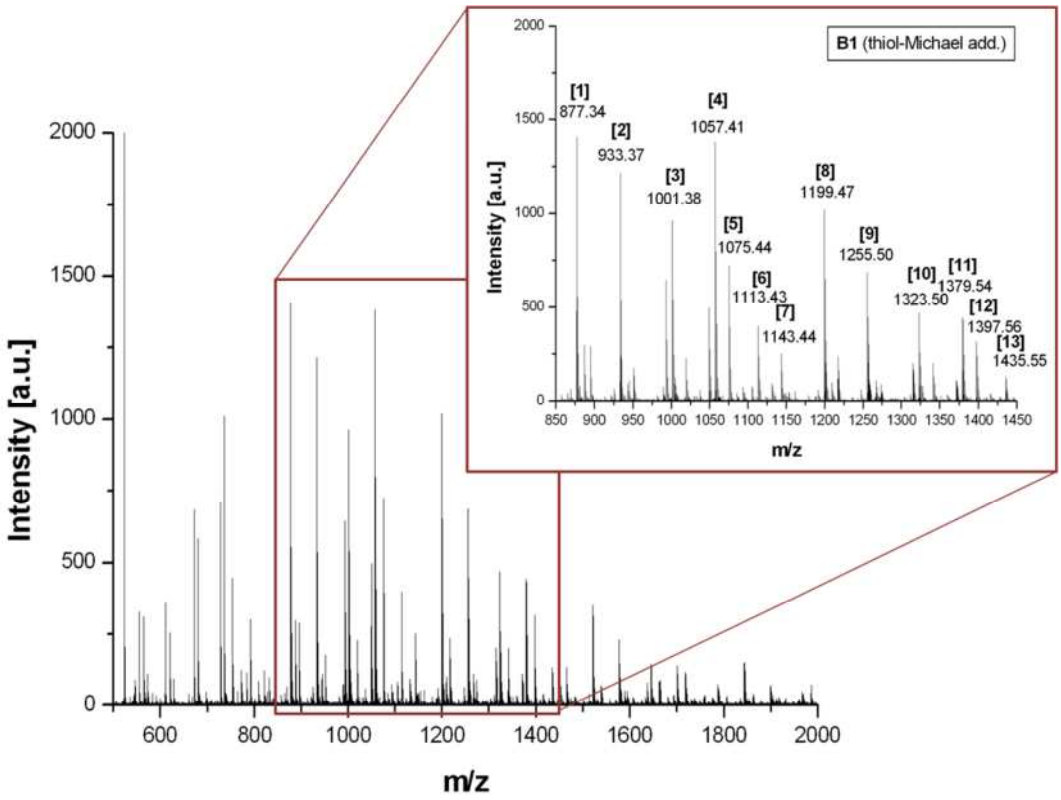

Figure 5.25: MALDI-ToF spectrum of B1 thiol-Michael addition product with benzyl mercaptan. Zoom region between 850 and 1450 Daltons. Annotations correspond to Table 5.13

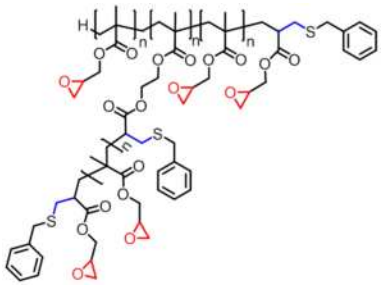

Figure 5.26: Example structure of EGDMA/GMA copolymer functionalised *via* thiol-Michael addition with benzyl mercaptan $(EGDMA)_1(GMA)_5(BM)_3$ (if n=1)

Name	Theoretical m/z	Measured m/z	Corresponding structure
[1]	877.29	877.34	$(EGDMA)_1(BM)_3(GMA)_2Na^+$
[2]	933.32	933.37	$(EGDMA)_2(BM)_3(GMA)_1Na^+$
[3]	1001.32	1001.38	$(EGDMA)_1(BM)_4(GMA)_2Na^+$
[4]	1057.35	1057.41	$(EGDMA)_2(BM)_4(GMA)_1Na^+$
[5]	1075.38	1075.44	$(EGDMA)_2(BM)_3(GMA)_2Na^+$
[6]	1113.38	1113.43	$(EGDMA)_3(BM)_4Na^+$
[7]	1143.38	1143.44	$(EGDMA)_1(BM)_4(GMA)_3Na^+$
[8]	1199.41	1199.47	$(EGDMA)_2(BM)_4(GMA)_2Na^+$
[9]	1255.44	1255.50	$(EGDMA)_3(BM)_4(GMA)_1Na^+$
[10]	1323.44	1323.50	$(EGDMA)_2(BM)_5(GMA)_2Na^+$
[11]	1379.49	1379.54	$(EGDMA)_3(BM)_5(GMA)_1Na^+$
[12]	1397.50	1397.56	$(EGDMA)_3(BM)_4(GMA)_2Na^+$
[13]	1435.50	1435.55	$(EGDMA)_4(BM)_5Na^+$

Table 5.13: Corresponding structures for MALDI-ToF of B1 thiol-Michael addition of benzyl mercaptan to copolymer B (EGDMA/GMA 50/50 mole%). Example structure given in Figure 5.26

Predicting the level of vinyl functionality per chain for EGDMA/GMA copolymers becomes more difficult, as it depends on the monomer sequence. The potential maximum and minimum levels of vinyl functionality can however be approximated as maximum vinyl groups = $(EGDMA)_{n+1}$ + $(GMA)_n$ and minimum vinyl groups = $(EGDMA)_{n+1}$ + $(GMA)_1$. Using this method to calculate the minimum and maximum levels of vinyl functionality potentially available, no functionalisations with benzyl mercaptan exceed the maximum observed *via* MALDI-ToF characterisation, with most functionalisations showing a level of benzyl mercaptan functionalisation within the maximum and minimum. However, peaks at [**B1** thiol-Michael add.: **2, 9, 12**] show a level of benzyl mercaptan functionality below the calculated minimum, suggesting one or more vinyl groups remain unfunctionalised (Figure 5.25, Table 5.13).

Dual functionalisation of copolymer **B** was also attempted using the corresponding thiol to aminopropanediol, thioglycerol, and the corresponding amine to benzyl mercaptan, benzyl amine, in order to reverse the hydrophobic/hydrophilic groups by site specific functionalisation. Hence, if the "core" model postulated is correct, this choice of functionalities should produce a more hydrophilic core, with a more hydrophobic shell. For the thiol-Michael addition of thioglycerol to copolymer **B** a complete loss of vinyl peaks is observed within one hour, with the retention of epoxide functionality observed by ^{1}H NMR (**B2** thiol-Michael add.). An increase in molecular weight was observed on addition of thioglycerol (Figure 5.27, Table 5.14), and the change in solubility of the

resulting polymer limited SEC eluent choice to DMF, as complete dissolution was only observed in DMF and DMSO.

Ring-opening of epoxide groups with benzyl amine was conducted post-thiol-Michael addition with thioglycerol, with a complete loss of epoxide peaks observed *via* ^{1}H NMR, and a further increase in molecular weight observed *via* SEC (Figure 5.27, Table 5.14).

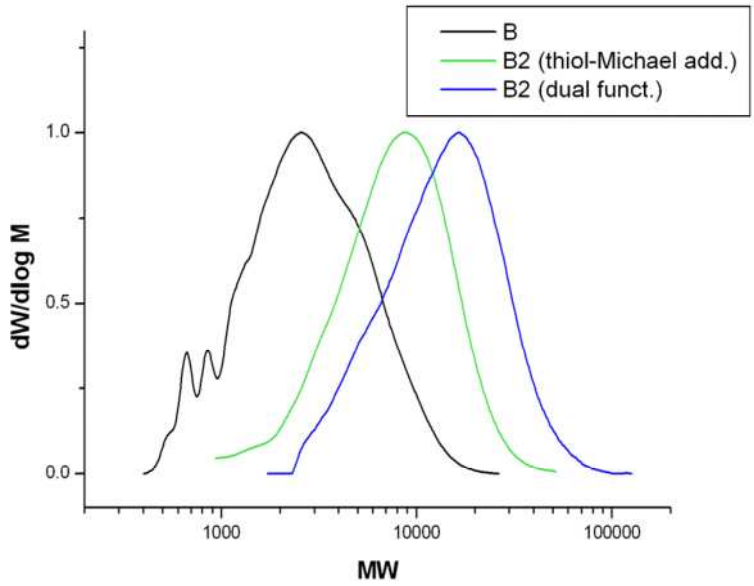

Figure 5.27: SEC comparison of copolymer B with B2 (thiol-Michael addition) and B2 (dual functionalised) (B: EGDMA/GMA copolymer 50/50 mol%, B2 thiol-Michael add.: copolymer B functionalised *via* thiol-Michael addition with thioglycerol, B2 dual functionalised: copolymer B functionalised *via* thiol-Michael addition with thioglycerol and epoxide ring-opened with benzylamine) DMF eluent

Name	Functionality	M_n ($g.mol^{-1}$)	M_w ($g.mol^{-1}$)	PDi
B	None	2000	3400	1.7
B2 (thiol-Michael add.)	Thioglycerol	5800	9000	1.6
B2 (dual funct.)	Thioglycerol + benzylamine	10500	16300	1.6

Table 5.14: SEC comparison of copolymer B with B2 (thiol-Michael addition) and B2 (dual functionalised) (B: EGDMA/GMA copolymer 50/50 mol%, B2 thiol-Michael add.: copolymer B functionalised *via* thiol-Michael addition with thioglycerol, B2 dual functionalised: copolymer B functionalised *via* thiol-Michael addition with thioglycerol and epoxide ring-opened with benzylamine) DMF eluent

Recent literature has shown that (hyper)branched polymers containing both hydrophobic and hydrophilic functionalities can self assemble due to the flexibility of the polymer backbone, with some even displaying inversion of conformation dependant on the solvent choice.[32-34] This area of research again has stemmed from the costly synthesis of amphiphilic dendrimers,[35] leading to investigation of (hyper)branched polymers as a cheaper, less synthetically demanding analogues, to which a variety of conformations have been obtained including micelles, monolayers, bilayers, nanofibres and disklike structures.[34, 36-38] Therefore, the ability to attach both hydrophobic and hydrophilic functionalities to EGDMA/GMA copolymers in a site selective manner could provide a route to the facile synthesis of amphiphilic polymers capable of self assembly, examples of such strategies are relatively few in the literature but have been termed Janus hybramers or self-adapting amphiphilic hyperbranched polymers.[32, 35]

Dual functional polymers **B1** and **B2** were investigated by dynamic light scattering (DLS). To solubilise them in water a solvent switch from DMSO to water was attempted. **B1** remained clear on addition to water, whereas **B2** formed an opaque solution. Both dual functionalised copolymers displayed a single peak in DLS measurements (Figure 5.28, Figure 5.29). **B1** had an average Z size of 220 nm, PDi 0.13 (Figure 5.28 (left)), which may be an indication of aggregation of the particles in solution, rather than self assembly. Therefore, it may be that the hydrophobic/hydrophilic functionalities are not influential enough to drive self assembly in this case. By use of longer chain hydrophobic/hydrophilic functionalities the influence of these substituents would be larger. The intensity, volume and number plots *vs*. size correlate well suggesting a single size distribution (Figure 5.28 (right)).

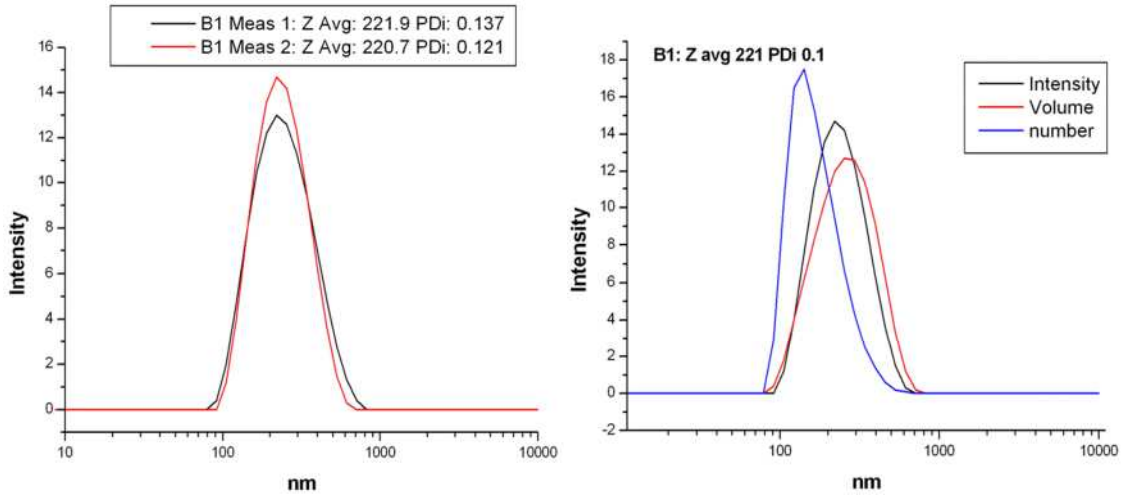

Figure 5.28: (left) Repeat DLS measurements of B1 in water intensity *vs*. size (right) DLS measurements of B1 in water intensity, volume and number *vs*. size plot

B2 possessed a smaller average Z size of 79 nm, PDi 0.22 (Figure 5.29 (left)). DLS measurements of **B2** have an increased PDi relative to **B1**, which on investigation of intensity, volume number *vs*. size plots (Figure 5.29 (right)) appears to be due to a small number of larger particles. The number *vs*. size plot indicates the majority of particles are of approximately 40 nm, in the micellar region. Although these results show some promise for self assembly through DLS measurements, in that particles are obtained, it was postulated a greater effect could be induced by use of longer chain hydrophobic/hydrophilic functionalities.

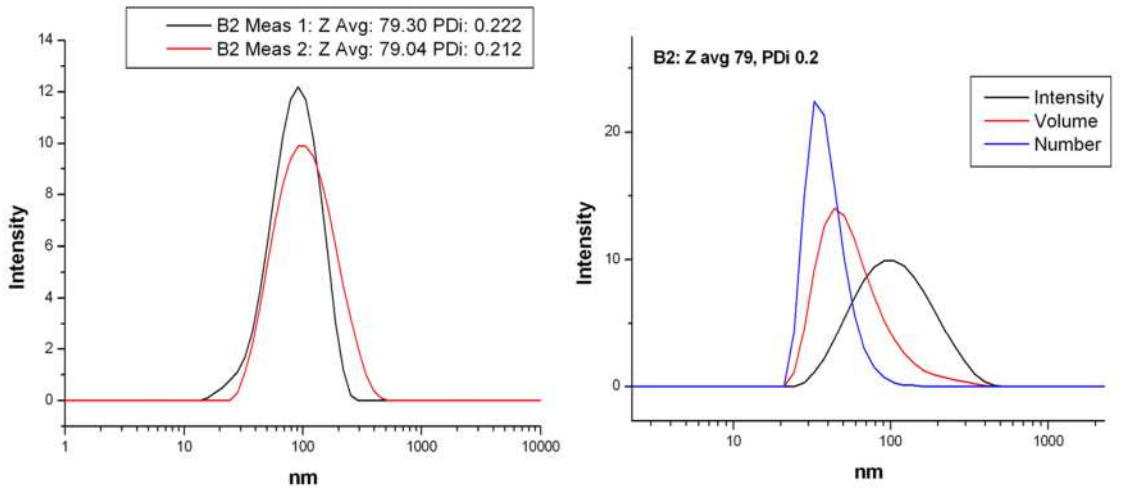

Figure 5.29: (left) Repeat DLS measurements of B2 in water, intensity *vs*. size plot (right) DLS measurements of B2 in water, intensity, volume and number *vs*. size plot

Attempts to conduct dual functionalisation of EGDMA/GMA **B** with dodecanethiol and *O*-(2-aminopropyl)-*O'*-(2-methoxyethyl) polypropylene glycol$_{500}$ (PPG amine) were unsuccessful. Thiol-Michael addition of dodecanethiol displayed a complete loss of vinyl peaks by ^{1}H NMR within one hour; however, ring-opening of this product with PPG amine was unsuccessful. It was postulated this may be due to the additional steric bulk of dodecane groups hindering epoxide ring-opening, however, attempts to functionalise EGDMA/GMA **B** with PPG amine alone was unsuccessful, even with the addition of 20 mole% catalysts such as TEA and LiOH, suggesting that perhaps the steric bulk of the PPG amine itself is hindering ring-opening of epoxides. Hence, dodecanethiol functionalised EGDMA/GMA **B** was ring-opened with aminopropanediol (**B3**). Ring-opening of dodecanethiol functionalised **B** was confirmed by both a complete loss of epoxide peaks *via* ^{1}H NMR, and loss of the epoxide signal at approximately 908 cm^{-1} *via* FT-IR, with the introduction of a strong peak at approximately 3400 cm^{-1}, indicating both the formation of a hydroxyl group on epoxide ring-opening and the addition of hydroxyl functionality to the polymer.

The addition of thiol and amine functionality to the polymers was also confirmed by SEC, in both DMF and THF eluents. Due to the addition of hydrophobic dodecanethiol to poly-EGDMA/GMA **B**, a large decrease in molecular weight is observed for the thiol-Michael addition product in DMF (Figure 5.30, Table 5.15), which is most likely due to DMF being an unsuitable solvent for this system. On dual functionalisation of **B3** thiol-Michael addition with aminopropanediol a large increase in molecular weight is observed, indicative of the addition of functionality to the polymer, and a reduction in the hydrophobicity of the polymer on addition of this more polar group.

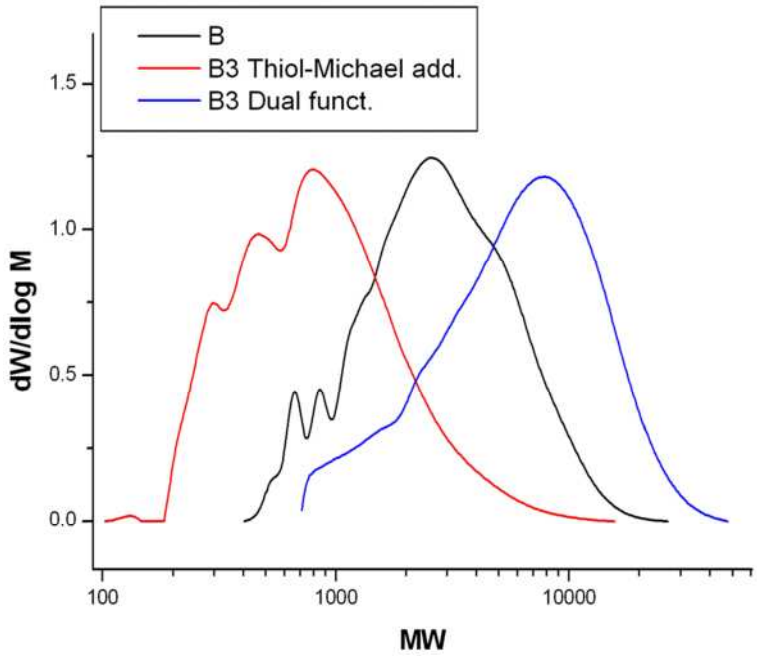

Figure 5.30: SEC comparison of copolymer B with B3 (thiol-Michael addition) and B3 (dual functionalised) (B: EGDMA/GMA copolymer 50/50 mol%, B3 thiol-Michael add.: copolymer B functionalised *via* thiol-Michael addition with dodecanethiol, B3 dual functionalised: copolymer B functionalised *via* thiol-Michael addition with dodecanethiol and epoxide ring-opened with aminopropanediol) DMF eluent

Name	M_n ($g.mol^{-1}$)	M_w ($g.mol^{-1}$)	PDi
B	2000	3400	1.7
B3 thiol-Michael add.	600	1100	1.8
B3 dual funct.	4000	7600	1.9

Table 5.15: SEC comparison of copolymer B with B3 (thiol-Michael addition) and B3 (dual functionalised) (B: EGDMA/GMA copolymer 50/50 mol%, B3 thiol-Michael add.: copolymer B functionalised *via* thiol-Michael addition with dodecanethiol, B3 dual functionalised: copolymer B functionalised *via* thiol-Michael addition with dodecanethiol and epoxide ring-opened with aminopropanediol) DMF eluent

Use of THF as the SEC eluent provides a better solvent system for the hydrophobic thiol-Michael addition product with dodecanethiol, and the expected increase in molecular weight is observed on its addition to the polymer (Figure 5.31, Table 5.16). A less significant increase in molecular weight is observed for dual functionalisation with aminopropanediol.

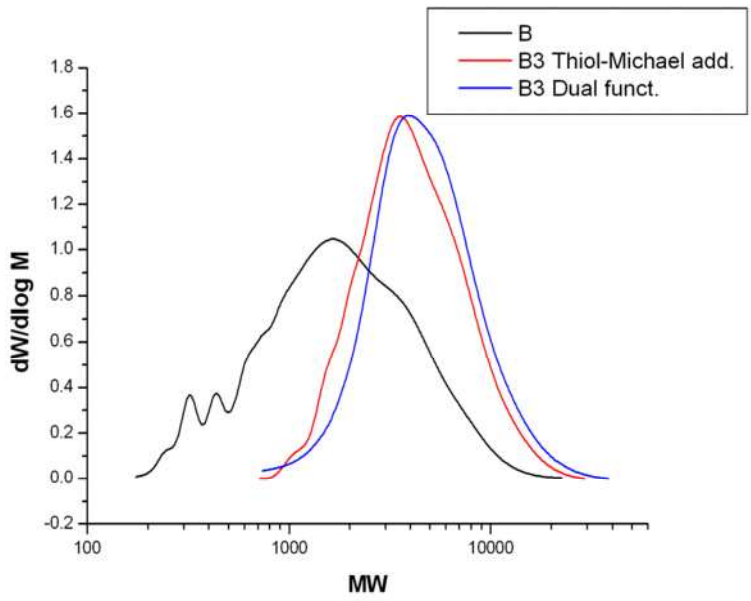

Figure 5.31: SEC comparison of copolymer B with B3 (thiol-Michael addition) and B3 (dual functionalised) (B: EGDMA/GMA copolymer 50/50 mol%, B3 thiol-Michael add.: copolymer B functionalised *via* thiol-Michael addition with dodecanethiol, B3 dual functionalised: copolymer B functionalised *via* thiol-Michael addition with dodecanethiol and epoxide ring-opened with aminopropanediol) THF eluent

Name	M_n ($g.mol^{-1}$)	M_w ($g.mol^{-1}$)	PDi
B	1200	2400	2.1
B3 thiol-Michael add.	3400	4500	1.4
B3 dual funct.	3900	5500	1.4

Table 5.16: SEC comparison of copolymer B with B3 (thiol-Michael addition) and B3 (dual functionalised) (B: EGDMA/GMA copolymer 50/50 mol%, B3 thiol-Michael add.: copolymer B functionalised via thiol-Michael addition with dodecanethiol, B3 dual functionalised: copolymer B functionalised via thiol-Michael addition with dodecanethiol and epoxide ring-opened with aminopropanediol) THF eluent

Initial DLS measurements of **B3** in water indicate a large particle size in comparison to **B1** and **B2** of approximately 450 nm, which is larger than the particle size for typical micellar structures; a narrower PDi of approximately 0.1 is obtained (Figure 5.32 (left)). Intensity, volume, number *vs*. size plots correlate well, denoting the formation of monodisperse particles (Figure 5.32 (right)). This large particle size may be a sign of aggregation, due to the longer alkyl chain in comparison to hydroxyl groups. However, literature on amphiphilic core *shell* hyperbranched polymers describes the polymers as

unimolecular micelles smaller than 10 nm in solution;[39-41] whereas self assembly is described as the formation of large micelles above 100 nm, through direct interconnection of unimolecular micelles without phase separation.[42-44] Hence, more extensive studies would be required to assess any self assembly capabilities of these materials.

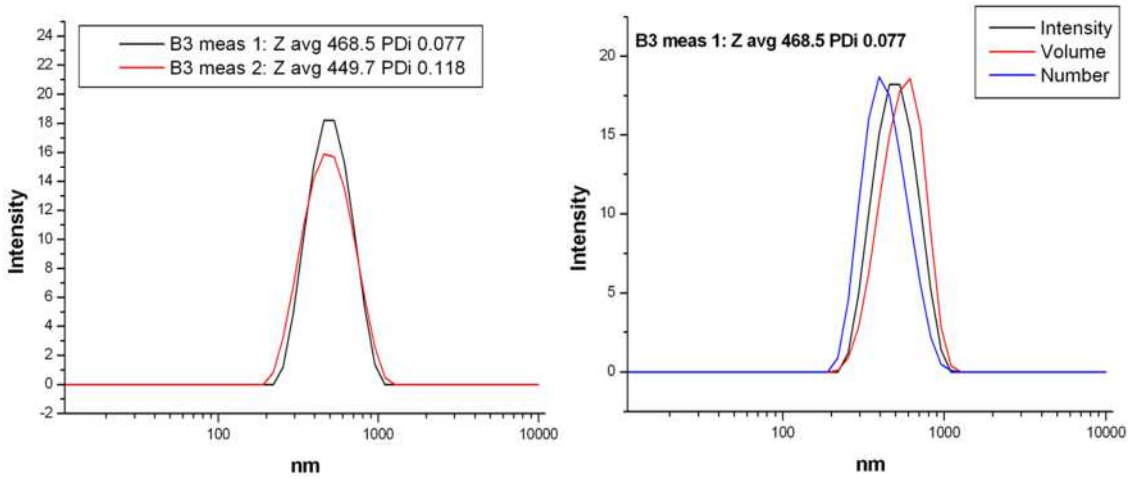

Figure 5.32: (left) Repeat DLS measurements of B3 in water, intensity *vs*. size plot (right) DLS measurements of B3 in water, intensity, volume and number *vs*. size plot

5.3. Conclusions

The polymerisation of branching monomer EGDMA and epoxide functional GMA was successfully performed by CCTP, yielding soluble branched copolymers containing both vinyl and epoxide functionalities. However, solvent choice was key to obtaining soluble polymers. Tailoring of the levels of vinyl to epoxy groups was accessed *via* monomer ratio and molecular weight control, and to a certain degree branching, controlled *via* the CoBF concentration. The level of branching for copolymers formed was characterised *via* universal calibration, with the generation of Mark-Houwink and g' plots confirming the lower solution viscosities of branched copolymers in comparison to their linear counterparts and providing an insight into the relative levels of branching, however due to the low molecular weight of polymers investigated a non linear relationship between hydrodynamic volume and IV was observed, meaning a true reflection of the molecular weight averages was not obtained and only trends in the molecular weights and branching of polymers **A**-**C** could be obtained.

Attempts to fully functionalise EGDMA/GMA copolymers with primary amines led to the retention of vinyl functionality, which was not as prevalent in previous work on the functionalisation of linear poly-GMA, with attempts to conduct thiol-Michael addition on previously epoxide ring-opened copolymers also displaying a retention of vinyl groups. Conducting thiol-Michael addition prior to epoxide ring-opening proved more successful, with the capability to functionalise with both hydrophobic and hydrophilic groups in a site specific manner. Preliminary DLS studies indicate that particles are obtained in all cases of amphiphilic dual functionalised copolymers. However, the particle size was large, with a low PDi only obtained for **B3**, indicating the formation of micellar structures is unlikely. It must be noted however that further work would be required in order to confirm any self assembly, as DLS only provides a very basic analysis of particles, and should ideally be used in conjunction with imaging techniques. However, it is believed that the copolymers described here show potential for self assembly, based on these initial results.

5.4. Experimental

General

All reagents were purchased from Aldrich and used as received unless stated. CoBF was synthesised according to literature (RSH).[45]

Poly-EGDMA/GMA copolymer synthesis

A 250 mL two-neck round bottom flask was charged with GMA, toluene (20 mL), V-601 (250 mg, 1.08 mmol) and stirrer bar. The reaction mixture was degassed *via* nitrogen bubbler for 20 minutes prior to addition of CoBF (25 mg, 0.05 mmol) under positive nitrogen pressure. The solution was degassed for a further 10 minutes. The round bottomed flask was immersed in an oil bath at 70 ˚C for 24 hours under nitrogen. Samples were taken hourly (approx 0.1 ml) *via* degassed syringe for 6 hours in order to obtain SEC, GC-FID and ^{1}H NMR measurements, sample taken at 24 or 9 hours, dependant on termination time. Reaction terminated by cooling and introduction of oxygen. Polymers precipitated from reaction mixture into hexane.

Name	EGDMA/GMA (mol)	EGDMA/GMA (mL)	EGDMA/GMA (mol%)	Duration (hr)
A	0.0331/0.0997	6.3/13.6	25/75	24
B	0.0663/0.0660	12.5/9.0	50/50	9
C	0.0997/0.0330	18.8/4.5	75/25	9

Table 5.17: EGDMA/GMA ratios employed for copolymerisations A-C

Thiol-Michael additions

Thiol-Michael additions were carried out on a 0.5-1.0 g scales in a large vial under ambient conditions. 1:3:0.05 or 1:3:0.1 ratio of double bonds:thiol:DMPP was used. Poly-GMA was dissolved in 5-10 mL of DMSO, then thiol added *via* syringe (t=0 ^{1}H NMR taken) then DMPP added *via* microlitre syringe. Reactions were checked for completion at 1 hour by ^{1}H NMR. Products precipitated in hexane or dialysed in methanol or water (1000 and 500-1000 MW cut-off respectively) prior to epoxide ring-opening reactions.

Epoxide ring-opening

Ratio of epoxide to amine used was 1:1.2 mol eq. For amines with a lower boiling point than 60 ˚C a reflux setup was used, for higher boiling amines unsealed vials were used as the reaction vessel. Polymer solutions were added to the reaction vessel and functional amine added placing the vessel in an oil bath at 60 ˚C for 24 hours. DMSO was removed *via* Schlenk line. Polymers were precipitated in hexane or petroleum ether 40-60 ˚C or dialysed in methanol or water (1000 and 500-1000 MW cut-off respectively) depending on solubilities/suitability prior to IR, NMR and MALDI-T_OF characterisation.

Characterisation

^{1}H and ^{13}C NMR

NMR was carried out on Bruker DPX-400, Bruker DRX-500, Bruker AV III 600 and Bruker AV II 700 spectrometers.

Infra Red (IR)

IR was carried out on a Bruker Vector 22 using a Golden Gate diamond attenuated flow cell and analysed using Opus spectroscopy software.

Size exclusion chromatography (SEC)

All SEC were performed on Agilent 390-LC multi detector suites fitted with two PLgel 5 μm Mixed D columns, plus a guard column. Data was collected and analysed using Cirrus software (Agilent) and all samples calibrated against poly(methyl methacrylate) (PMMA) EasiVial standards, purchased from Agilent. Any points within the calibration plot with an error greater than 10% were not included in the final calibrations. Third order calibration plots were used for both conventional SEC and when conducting universal calibration.

A range of SEC eluents was employed, dependant on the solubility of functionalised polymers, including THF, DMF and $CHCl_3$.

THF mobile phase: flow rate of 1 mL/min, ambient operating temperature, injection volume 100 μL. The SEC was equipped with a refractive index, light scattering, UV and photodiode array (PDA, Shimadzu) detectors.

DMF mobile phase: flow rate of 1 mL/min^{-1}, 40 ˚C operating temperature, injection volume 100 μL. The SEC was equipped with a refractive index, UV and viscometry detectors.

$CHCl_3$ mobile phase: flow rate of 1 mL/min-1, an ambient operating temperature, injection volume 100 μL. The SEC was equipped with a refractive index, light scattering and viscometry detectors.

Matrix-Assisted Laser Desorption and Ionisation Time-of-Flight (MALDI-ToF)

Mass spectra were acquired by MALDI-ToF (matrix-assisted laser desorption and ionisation time-of-flight) mass spectrometry using a Bruker Daltonics Ultraflex II MALDI-ToF mass spectrometer, equipped with a nitrogen laser delivering 2 ns laser pulses at 337 nm with positive ion ToF detection performed using an accelerating voltage of 25 kV.

2,5-Dihdroxybenzoic acid (DHB) or trans-2-[3-(4-tert-butylphenyl)-2-methyl-2-propenylidene]malononitrile (DCTB) were used as an organic matrix and sodium iodide (NaI) used as the salt. Calibrations were conducted using polyethylene glycol methyl ether of average molecular weight 1,100 and 2,000. A layering method was used to spot the MALDI plate. THF or THF/water was used as the solvent for sample preparation.

Gas chromatograph – Flame ionisation detector (GC-FID)

GC-FID analysis was performed using a Varian 450. A FactorFour^{TM} capillary column VF-1 ms, of 15 m × 0.25 mm I.D., film thickness 0.25 µm from Varian was used. The oven temperature was programmed as follows: 40 °C (hold for 1 min) at 25 °C min^{-1} to 200 °C. The injector was operated at 200 °C and the FID was operated at 220 °C. Nitrogen was used as carrier gas at a flow rate of 1 mL min^{-1} and a split ratio of 1:100 was applied. Chromatographic data were processed using Galaxie Chromatography data system, version 1.9.302.530 software

Dynamic light scattering measurements (DLS)

DLS was measured on a Malvern zetasizer Nano S90 at a concentration of approximately 1 mg /mL. Two measurements of 12 sub-runs each were obtained at a 173˚ backscatter measuring angle. Equilibrated at 25 ˚C

Characterisation of Polymers

Characterisation of linear **PGMA 1** and **2** can be found in Chapter 4, Experimental 4.4.

Characterisation of Copolymers A-C (**A**: EGDMA/GMA copolymer 25/75 mol%, **B**: EGDMA/GMA copolymer 50/50 mol%, **C**: EGDMA/GMA copolymer 75/25 mol%)

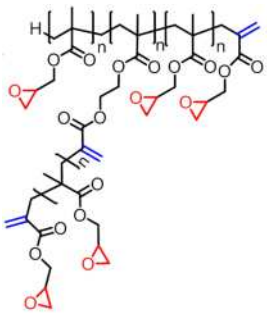

Figure 5.33: General structure of polymers A-C, EGDMA/GMA copolymers

^{1}H NMR (400 MHz, TMS at 25 ˚C): 0.90-1.30 (backbone CH_3), 1.30-1.45 (terminal CH_3), 1.90-2.10 (terminal CH_3, EGDMA), 2.20-2.25 (backbone CH_2, GMA), 2.45-2.65 (backbone CH_2, EGDMA), 2.55-2.70 (epoxide CH), 2.75-2.85 (epoxide CH), 3.15-3.30 (epoxide CH), 3.55-4.05 (OCH_2, GMA), 4.10-4.50 (OCH_2CH_2O, OCH_2 GMA), 5.50-5.65 ($C=CH_2$, EGDMA internal and terminal, GMA), 6.10-6.20 ($C=CH_2$, EGDMA terminal), 6.20-6.35 ($C=CH_2$, EGDMA internal, GMA)

^{13}C NMR (400 MHz $CDCl_3$ at 25 ˚C): 18.24 (terminal CH_3, EGDMA), 21.69 (terminal CH_3, GMA), 24.75 (backbone CH_3), 40.74 (backbone CH_2), 42.94 (backbone quaternary C), 44.59 (epoxide CH_2), 49.33 (epoxide CH), 62.48 ($O\underline{C}H_2\underline{C}H_2O$), 65.43 ($OCH_2$), 126.05 ($\underline{C}H_2=C$, EGDMA terminal, GMA), 128.77 ($\underline{C}H_2=C$, EGDMA internal, GMA), 135.94 ($\underline{C}=CH_2$, EGDMA terminal), 136.84 ($\underline{C}=CH_2$, EGDMA internal, GMA), 176.65 (carbonyl)

IR: u_{max} (neat)/cm^{-1} 3529 (br, OH), 2949 (br, CH sp^3), 1716 (s, C=O), 1448, (m, CH_2), 1360 (m), 1132 (s, C-O), 996 (m), 952 (m), 908 (m, C-H epoxide), 847 (m, C-H epoxide), 815 (C-H epoxide), 761 (m)

Conventional SEC ($CHCl_3$ eluent): **A**: M_n 900, M_w 2400, PDi 2.7 **B**: M_n 1100, M_w 2400, PDi 2.2 **C**: M_n 1500, M_w 4100, PDi 2.7

Universal calibration ($CHCl_3$ eluent): **A**: M_n 1000, M_w 4500, PDi 4.7 **B**: M_n 1400, M_w 3200, PDi 2.3 **C**: M_n 2100, M_w 7800, PDi 3.8

GC-FID (conversion): **A**: EGDMA 99.9, GMA 92.9, total 94.7 **B**: EGDMA 95.3, GMA 82.1, total 88.7 **C**: EGDMA 95.6, GMA 75.0, total 90.5

Characterisation of A1 (Propylamine functionalised EGDMA/GMA copolymer **A** (25/75 mol%))

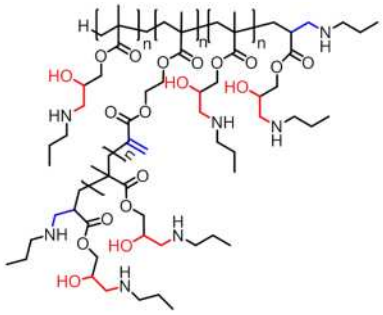

Figure 5.34: General structure of A1, propylamine functionalised EGDMA/GMA copolymer A

^{1}H NMR (700 MHz, TMS at 25 ˚C): 0.75-0.95 ($CH_3CH_2CH_2NH$), 0.95-1.30 (backbone CH_3, terminal CH_3, GMA), 1.40-1.70 ($CH_3CH_2CH_2NH$), 1.70-1.80 (terminal CH_3, EGDMA), 1.90-2.25 (backbone CH_2, terminal $NHCH_2$, $NHCH_2CH_2CH_3$), 2.35-2.80 ($CH(OH)CH_2NH$), 3.20-4.40 (OCH_2CH_2O, OCH_2, $CH(OH)$), 5.40-5.70 ($C=CH_2$), 6.10-6.30 ($C=CH_2$)

^{13}C NMR (700 MHz $CDCl_3$ at 25 ˚C): 11.12, 11.60 ($CH_3CH_2CH_2NH$), 18.19 (terminal CH_3, EGDMA), 20.17, 22.63 ($CH_3CH_2CH_2NH$), 21.28 (terminal CH_3, GMA), 24.72, 27.35, 28.02, 29.52 (backbone CH_3), 38.18, 39.00 40.38 (backbone CH_2), 41.26 ($CHC=O$), 44.77 (backbone quaternary C), 49.14 ($NHCH_2CH_2CH_3$), 51.50 ($CH(C=O)CH_2NH$), 62.25 (OCH_2CH_2O), 67.03 (OCH_2), 70.79 ($CH(OH)$), 125.85 (terminal $CH_2=C$), 128.19 (internal $CH_2=C$), 136.88 ($C=CH_2$), 176.56, 178.00 (carbonyl)

IR: u_{max} (neat)/cm^{-1} 3392 (br, OH/NH), 2959 (m, CH sp^3), 1720 (s, C=O), 1618 (m, C=C, N-H bend), 1455 (m, CH_2),1386 (m), 1136 (s, C-O), 756 (m)

SEC (DMF eluent): M_n 6700, M_w 12000, PDi 1.8

Characterisation of A2 (Benzylamine functionalised EGDMA/GMA copolymer **A** (25/75 mol%))

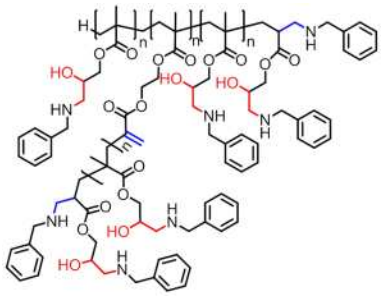

Figure 5.35: General structure of A2, benzylamine functionalised EGDMA/GMA copolymer A

^{1}H NMR (400 MHz, TMS at 25 ˚C): 0.80-1.00 (backbone CH_3, GMA), 1.00-1.30 (terminal CH_3), 1.70-1.80 (terminal CH_3, EGDMA), 1.90-2.05 (backbone CH_2, GMA, CHC=O), 2.50-2.65 (backbone CH_2, EGDMA), 2.75-2.90 (CH(OH)C$\underline{H_2}$NH), 3.65-3.90 (C$\underline{H_2}C_6H_5$), 3.80-4.40 (OCH_2, OCH_2CH_2O, CH(OH)), 5.40-5.65 (C=C$\underline{H_2}$), 6.05-6.25 (C=C$\underline{H_2}$), 7.15-7.40 (C_6H_5)

^{13}C NMR (400 MHz $CDCl_3$ at 25 ˚C): 18.25 (terminal CH_3, EGDMA), 23.04 (terminal CH_3 GMA), 24.73 (backbone CH_3), 40.69 (backbone CH_2), 41.47 (CHC=O), 42.84 (backbone quaternary C), 51.81 (CH(OH)C$\underline{H_2}$NH), 53.12 (C$\underline{H_2}C_6H_5$), 62.42 (OCH_2CH_2O), 66.36 (OCH_2), 72.54 (CH(OH)), 126.98 (para aromatic C-H, $\underline{C}H_2$=C), 128.19 (meta aromatic C-H, $\underline{C}H_2$=C), 129.08 (ortho CH aromatic,), 136.95 ($\underline{C}$=CH_2), 139.28 (quaternary aromatic), 176.57 (carbonyl)

IR: υ_{max} (neat)/cm^{-1} 3434 (br, OH/NH), 2974 (m, C-H sp^3), 1715 (s, C=O), 1625 (m, C=C, N-H bend), 1453, 1362 (m, C-H aromatic), 1143 (s, C-O), 734 (m), 698 (m)

SEC (DMF eluent): M_n 4600, M_w 8800, PDi 1.9

Characterisation of A2.1 (Dual functionalised (benzylamine + thioglycerol) EGDMA/GMA copolymer **A** (25/75 mol%))

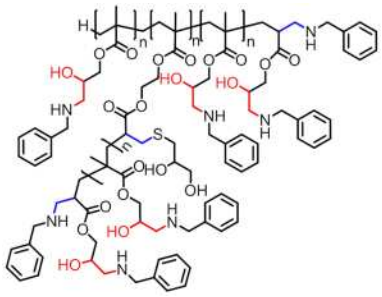

Figure 5.36: General structure of A2.1, Dual functionalised EGDMA/GMA copolymer A, epoxide ring-opening with benzylamine, thiol-Michael addition with thioglycerol

^{1}H NMR (500 MHz, d^{6}-DMSO at 25 ˚C): 0.80-1.00 (backbone CH_3, GMA), 1.00-1.30 (terminal CH_3), 1.70-1.80 (terminal CH_3, EGDMA), 1.90-2.05 (backbone CH_2, CHC=O), 2.30-2.75 ($C\underline{H_2}SC\underline{H_2}$), 3.30-3.65 ($CH_2OH$, CH_2NH), 3.65-3.90 ($C\underline{H_2}C_6H_5$), 3.80-4.40 (OCH_2, OCH_2CH_2O, CH(OH)), 5.40-5.65 ($C=C\underline{H_2}$), 6.05-6.25 ($C=C\underline{H_2}$), 7.15-7.40 (C_6H_5)

^{13}C NMR (500 MHz, d^{6}-DMSO at 25 ˚C): 18.22 (terminal CH_3 EGDMA), 21.52 (terminal CH_3, GMA), 24.84 (backbone CH_3), 35.85 (SCH_2), 40.48 (backbone CH_2), 41.31 (CHC=O), 41.81 (backbone quaternary carbon), 49.06 (CH(OH)), 51.85 ($SC\underline{H_2}CH(OH)$), 53.54 ($CH_2C_6H_5$), 62.50 (OCH_2CH_2O), 64.92 (OCH_2), 67.76 ($\underline{C}H(OH)$), 71.72 (CH(OH)), 127.46 (para aromatic C-H, $\underline{C}H_2=C$), 128.43 (meta aromatic C-H, $C=CH_2$), 128.57 (ortho aromatic C-H), 140.78 (quaternary aromatic), 176.55 (carbonyl)

IR: υ_{max} (neat)/cm^{-1} 3345 (br, OH/NH), 2925 (m, CH sp^3), 1723 (s, C=O), 1626 (m, C=C, N-H bend), 1453, 1367 (m, C-H aromatic), 1150 (s, C-O), 1022 (s), 1000 (s), 881 (m), 747 (m), 699 (m)

SEC (DMF eluent): M_n 6000, M_w 10800, PDi 1.8

Characterisation of A3 (Aminopropanediol functionalised EGDMA/GMA copolymer **A** (25/75 mol%))

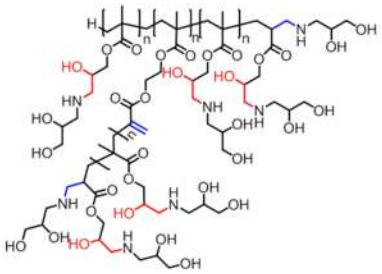

Figure 5.37: General structure of A3, aminopropanediol functionalised EGDMA/GMA copolymer A

^{1}H NMR (600 MHz, d^{6}-DMSO at 25 ˚C): 0.70-1.20 (backbone CH_3), 1.20-1.30 (terminal CH_3, GMA), 1.55-2.05 (terminal CH_3, EGDMA, CHC=O, backbone CH_2, CH(C=O)C$\underline{H}_2$NH terminal), 2.30-2.80 (NHC$\underline{H}_2$CH(OH)), 3.20-3.50 (CH(OH)C$\underline{H}_2$OH), 3.50-4.60 (OC$\underline{H}_2$C$\underline{H}_2$O, OCH_2, C$\underline{H}$OH), 5.55-5.65 (CH_2=C), 6.10-6.20 (CH_2=C)

^{13}C NMR (600 MHz, d^{6}-DMSO at 25 ˚C): 21.56 (terminal CH_3, GMA), 22.44, 25.32, 27.73, 28.64 (backbone CH_3), 40.42 (backbone CH_2), 42.58, 42.74 (backbone quaternary C), 50.62, 51.11 (terminal CH(C=O)C$\underline{H}_2$NH), 52.21, 52.37 (NHC$\underline{H}_2$CH(OH)), 53.12, 53.47 (CH(OH)C$\underline{H}_2$OH), 63.33, 64.09 (OC$\underline{H}_2$C$\underline{H}_2$O), 64.64, 64.83 (OCH_2), 69.17, 70.44 (CHOH), 127.09 (C$\underline{H}_2$=C), 128.44 (C$\underline{H}_2$=C), 141.59 (C$\underline{=}$CH_2), 175.29, 177.47 (carbonyl)

IR: υ_{max} (neat)/cm^{-1} 3318 (br, OH/NH), 2932 (m, C-H sp^3), 1717 (m, C=O), 1602 (C=C, N-H bend), 1453, 1393 (m, O-H), 1264 (m), 1033 (s, C-O), 860 (m)

SEC (DMF eluent): M_n 2500, M_w 4900, PDi 2.0

Characterisation of B1 (Dual functionalised (benzyl mercaptan + aminopropanediol) EGDMA/GMA copolymer **B** (50/50 mol%))

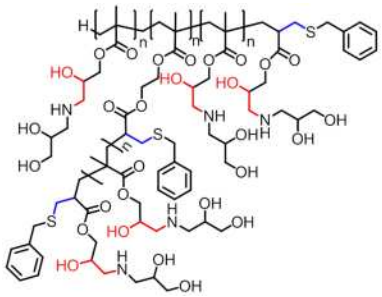

Figure 5.38: General structure of B1, dual functionalised EGDMA/GMA copolymer B, thiol-Michael addition with benzyl mercaptan, epoxide-ring opening with aminopropanediol

^{1}H NMR (400 MHz, d^{6}-DMSO at 25 ˚C): 0.80-1.00 (terminal CH_3, GMA), 1.00-1.30 (backbone CH_3), 1.70-1.80 (terminal CH_3, EGDMA), 1.90-2.05 (backbone CH_2, CHC=O), 2.30-2.75 ($C\underline{H}_2SCH_2C_6H_5$, $NHC\underline{H}_2CH(OH)$), 3.30-3.65 (CH_2OH), 3.65-3.90 ($C\underline{H}_2C_6H_5$), 3.80-4.40 (OCH_2, OCH_2CH_2O, CH(OH)), 7.15-7.40 (C_6H_5)

^{13}C NMR (400 MHz, d^{6}-DMSO at 25 ˚C): 16.40 (terminal CH_3 EGDMA), 25.11 (terminal CH_3, GMA), 30.59 (backbone CH_3), 34.27 (CH_2S), 35.25 ($S\underline{C}H_2C_6H_5$), 41.05 (backbone CH_2), 41.59 ($\underline{C}HC=O$), 41.25 (backbone quaternary carbon), 52.78 ($NH\underline{C}H_2CH(OH)$), 62.13 (CH_2OH), 64.55 (OCH_2CH_2O), 67.01 (OCH_2), 67.77 (internal CH(OH)), 70.48 (terminal CH(OH)), 126.85 (aromatic para C-H), 128.33 (aromatic meta C-H), 128.75 (aromatic ortho C-H), 138.00 (quaternary aromatic) 176.55 (carbonyl)

IR: υ_{max} (neat)/cm^{-1} 3386 (br, OH/NH), 2950 (m, C-H sp^3), 1725 (s, C=O), 1631 (m, N-H bend), 1474 (m, C=C aromatic), 1453, 1391 (m, C-H aromatic), 1240 (m), 1141 (s, C-O), 1070 (m), 1027 (m), 735 (m), 700 (m)

SEC (THF eluent): M_n 800, M_w 1200, PDi 1.5

SEC (DMF eluent): M_n 1600, M_w 2200, PDi 1.4

Characterisation of B2 (Dual functionalised (thioglycerol + benzylamine) EGDMA/GMA copolymer **B** (50/50 mol%))

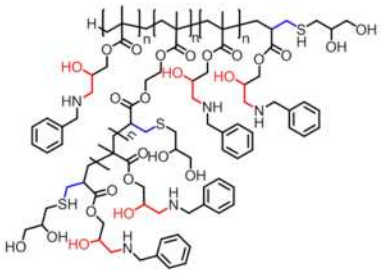

Figure 5.39: General structure of B2, EGDMA/GMA copolymer B dual functionalised, thiol-Michael addition with thioglycerol, epoxide ring-opening with benzylamine

^{1}H NMR (400 MHz, d^6-DMSO at 25 ˚C): 0.80-1.30 (CH_3, terminal GMA, backbone), 1.60-1.75 (backbone CH_2, GMA), 1.80-2.05 (terminal CH_3, EGDMA, CHC=O), 2.30-2.50 (backbone CH_2 EGDMA), 2.50-2.75 ($C\underline{H}_2SC\underline{H}_2$), 3.25-3.60 ($CH(OH)C\underline{H}_2OH$), 3.60-3.80 ($C\underline{H}_2C_6H_5$, CH(OH)), 3.80-4.35 ($OCH_2$, OCH_2CH_2O), 7.10-7.35 (C_6H_5)

SEC (DMF eluent): M_n 10500, M_w 163000, PDi 1.6

Characterisation of B3

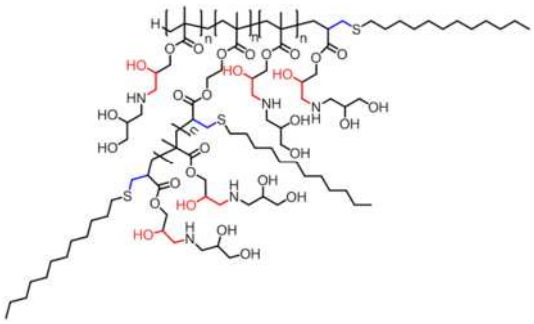

Figure 5.40: General structure of B3, EGDMA/GMA copolymer B dual functionalised, thiol-Michael addition with dodecanethiol, epoxide ring-opening with aminopropanediol

^{1}H NMR (400 MHz, d^7-DMF at 25 ˚C): 0.80-1.00 ($C\underline{H}_3(CH_2)_{11}$), 1.10-1.50 (terminal and backbone CH_3), 1.30-1.40 ($CH_2(C\underline{H}_2)_{10}CH_3$), 1.55-1.70 ($C\underline{H}_2(CH_2)_{11}CH_3$), 1.90-2.25 (backbone CH_2, CHC=O), 2.55-3.00 ($C\underline{H}_2S(CH_2)_{11}CH_3$, $NHC\underline{H}_2CH(OH)$), 3.45-3.70 (OCH_2), 3.70-3.80 ($C\underline{H}OH$), 4.30-4.45 ($OC\underline{H}_2C\underline{H}_2O$)

^{13}C NMR (400 MHz, d^7-DMF at 25 ˚C): 13.83 ($\underline{C}H_3(CH_2)_{11}$), 16.42 (terminal CH_3), 22.61 ($S(CH_2)_{10}$ $\underline{C}H_2CH_3$), 25.13 (backbone CH_3), 29.61, 31.90 ($S(\underline{C}H_2)_{10}CH2CH_3$), 40.41 (CHC=O), 41.83 (backbone CH_2), 42.62 (backbone quaternary C), 53.56 $NH\underline{C}H_2CH(OH)$, 62.49 ($O\underline{C}H_2\underline{C}H_2O$), 65.35 ($OCH_2$), 68.10, 70.96 (CHOH), 174.32 (carbonyl)

IR: υ_{max} (neat)/cm^{-1} 3389 (br, OH/NH), 2922, 2852 (s, C-H sp^3), 1729 (s, C=O), 1655 (m, N-H bend), 1457 (m, CH_2), 1391 (m), 1248 (m), 1145 (s, C-O), 1028 (m), 872 (m), 720 (m)

SEC (THF eluent): M_n 3900, M_w 5500, PDi 1.4

SEC (DMF eluent): M_n 4000, M_w 7600, PDi 1.9

5.5. References

1. Smigol, V.; Svec, F. e., *J. Appl. Polym. Sci.* **1993,** *48* (11), 2033.
2. Wang, R.; Zhang, Y.; Ma, G.; Su, Z., *J. Appl. Polym. Sci.* **2006,** *102* (5), 5018.
3. Jin, J. M.; Lee, J. M.; Ha, M. H.; Lee, K.; Choe, S., *Polymer* **2007,** *48* (11), 3107.
4. Jiang, X.; Tu, W., *J. Appl. Polym. Sci.* **2010,** *115* (2), 963.
5. Bicak, N.; Gazi, M.; Galli, G.; Chiellini, E., *J. Polym. Sci., Part A: Polym. Chem.* **2006,** *44* (23), 6708.
6. Jonsson, M.; Nyström, D.; Nordin, O.; Malmström, E., *Eur. Polym. J.* **2009,** *45* (8), 2374.
7. Svec, F.; Frechet, J. M. J., *Anal. Chem.* **1992,** *64* (7), 820.
8. Liu, Y.; Juneau, K. N.; Svec, F.; Fréchet, J. M. J., *Polym. Bull.* **1998,** *41* (2), 183.
9. Petro, M.; Svec, F.; Fréchet, J. M. J., *Biotechnol. Bioeng.* **1996,** *49* (4), 355.
10. Guo, B.; Finne-Wistrand, A.; Albertsson, A.-C., *Chem. Mater.* **2011,** *23* (5), 1254.
11. Yuan, D.; Huang, B., *Catal. Commun.* **2012,** *18* (0), 126.
12. Miletić, N.; Vuković, Z.; Nastasović, A.; Loos, K., *J. Mol. Catal. B: Enzym.* **2009,** *56* (4), 196.
13. Miletić, N.; Rohandi, R.; Vuković, Z.; Nastasović, A.; Loos, K., *React. Funct. Polym.* **2009,** *69* (1), 68.
14. Hercigonja, R. V.; Maksin, D. D.; Nastasović, A. B.; Trifunović, S. S.; Glodić, P. B.; Onjia, A. E., *J. Appl. Polym. Sci.* **2012,** *123* (2), 1273.
15. Odian, G., *Principles of Polymerisation*. 4th ed.; John Wiley & Sons: 2004.
16. Voit, B. I.; Lederer, A., *Chem. Rev.* **2009,** *109* (11), 5924.

17. England, R. M.; Rimmer, S., *Polym. Chem.* **2010,** *1* (10), 1533.

18. Clayden, J.; Greeves, N.; Warren, S.; Wothers, P., *Organic Chemistry*. 1st ed.; Oxford University Press: Oxford, 2001.

19. Iwakura, Y.; Kurosaki, T.; Imai, Y., *Makromol. Chem.* **1965,** *86* (1), 73.

20. Iwakura, Y.; Kurosaki, T.; Ariga, N.; Ito, T., *Makromol. Chem.* **1966,** *97* (1), 128.

21. Kalal, J.; Švec, F.; Maroušek, V., *J. Polym. Sci: Pol. Sym.* **1974,** *47* (1), 155.

22. Tsarevsky, N. V.; Jakubowski, W., *J. Polym. Sci., Part A: Polym. Chem.* **2011,** *49* (4), 918.

23. De, S.; Khan, A., *Chem. Commun.* **2012,** *48* (25).

24. Belmares, M.; Blanco, M.; Goddard, W. A.; Ross, R. B.; Caldwell, G.; Chou, S. H.; Pham, J.; Olofson, P. M.; Thomas, C., *J. Comput. Chem.* **2004,** *25* (15), 1814.

25. Schriemer, D. C.; Li, L., *Anal. Chem.* **1997,** *69* (20), 4176.

26. Nielen, M. W. F.; Malucha, S., *Rapid Commun. Mass Spectrom.* **1997,** *11* (11), 1194.

27. Rashidzadeh, H.; Guo, B., *Anal. Chem.* **1998,** *70* (1), 131.

28. Dondos, A.; Benoit, H., *Polymer* **1977,** *18* (11), 1161.

29. Dondos, A.; Skordilis, V., *Journal of Polymer Science: Polymer Physics Edition* **1985,** *23* (4), 615.

30. Mrkvičková, L., *J. Liq. Chromatogr. Relat. Technol.* **1997,** *20* (3), 403.

31. Gruendling, T.; Junkers, T.; Guilhaus, M.; Barner-Kowollik, C., *Macromol. Chem. Phys.* **2010,** *211* (5), 520.

32. Samuel, A. Z.; Ramakrishnan, S., *Macromolecules* **2012,** *45* (5), 2348.

33. Wang, Y.; Grayson, S. M., *Adv. Drug Delivery Rev.* **2012,** *64* (9), 852.

34. Saha, A.; Ramakrishnan, S., *J. Polym. Sci., Part A: Polym. Chem.* **2009,** *47* (1), 80.

35. Aathimanikandan, S. V.; Savariar, E. N.; Thayumanavan, S., *J. Am. Chem. Soc.* **2005,** *127* (42), 14922.

36. Ornatska, M.; Bergman, K. N.; Goodman, M.; Peleshanko, S.; Shevchenko, ValeriyÂ V.; Tsukruk, V. V., *Polymer* **2006,** *47* (24), 8137.

37. Ornatska, M.; Peleshanko, S.; Genson, K. L.; Rybak, B.; Bergman, K. N.; Tsukruk, V. V., *J. Am. Chem. Soc.* **2004,** *126* (31), 9675.

38. Zhou, Y.; Yan, D., *Chem. Commun.* **2009,** (10), 1172.

39. Sunder, A.; Krämer, M.; Hanselmann, R.; Mülhaupt, R.; Frey, H., *Angew. Chem., Int. Ed.* **1999,** *38* (23), 3552.

40. Krämer, M.; Stumbé, J.-F.; Türk, H.; Krause, S.; Komp, A.; Delineau, L.; Prokhorova, S.; Kautz, H.; Haag, R., *Angew. Chem., Int. Ed.* **2002,** *41* (22), 4252.

41. Kumar, K. R.; Brooks, D. E., *Macromol. Rapid Commun.* **2005,** *26* (3), 155.

42. Mai, Y.; Zhou, Y.; Yan, D., *Macromolecules* **2005,** *38* (21), 8679.

43. Hong, H.; Mai, Y.; Zhou, Y.; Yan, D.; Cui, J., *Macromol. Rapid Commun.* **2007,** *28* (5), 591.

44. Radowski, M. R.; Shukla, A.; von Berlepsch, H.; Böttcher, C.; Pickaert, G.; Rehage, H.; Haag, R., *Angew. Chem., Int. Ed.* **2007,** *46* (8), 1265.

45. Bakac, A.; Espenson, J. H., *J. Am. Chem. Soc.* **2002,** *106* (18), 5197.

Chapter 6

6. Conclusions

The main aims of this body of work was to synthesise branched functional polymers from commercially available materials, whereby factors such as molecular weight, branching and functionality could be controlled. This had the potential to lead to a facile and inexpensive synthetic method of synthesising branched polymers, which would be in direct contrast to the expensive and synthetically demanding synthesis of dendrimers.

Previous literature highlighted the CCTP of EGDMA as a potential industrially viable route to the synthesis of branched polymers, with a wide scope for copolymerisation or application of this technique to further di or multivinyl monomers. The salient advantages of CCTP are that relatively low amounts of chain transfer agent required to circumvent gelation, compared to conventional chain transfer, and the retention of high levels of activated vinyl groups in the polymers, which provide a reactive handle for functionalisation via click chemistry techniques, which has been exploited previously for linear polymers synthesised via CCTP.

Initial work focused on tuning the homopolymerisation of EGDMA. It was found that the molecular weight and in turn the level of branching could be controlled, to a certain degree, by the concentration of CoBF used in the reaction. High levels of CoBF reduced the molecular weight and hence less branched products were obtained. Whereas decreasing the CoBF concentration led to an increase in molecular weight and branching, as indicated by Mark-Houwink data. However below a critical CoBF concentration gelation could no longer be circumvented, only delayed, and insoluble polymers resulted.

Changes in the solids content also provided a means for controlling the molecular weight, and hence the level of branching. As the solids content was increased to bulk the molecular weights vs conversion showed a dramatic increase, which in the cases of high solids contents and bulk led to gelation of the polymer within a few hours. Reduction of the solids content provided a higher level of control over the molecular weight, but the likelihood of cyclisation reactions increases at low solids, hence it was

established that 50% solids would provide adequate control over the molecular weight and reduce the liklihood of cyclisations.

Copolymerisations of EGDMA with monovinyl monomer MMA and trivinyl monomer TMPTMA and homopolymerisations of TMPTMA were also explored as a means to control branching. Copolymerisations of EGDMA and MMA led to a control of branching through EGDMA incorporation, with low incorporations of EGDMA leading to less branched products. This also had the effect of increasing the maximum molecular weight achieveable prior to gelation. The branching was also increased by copolymerisation with TMPTMA, again with a lower incorporation of TMPTMA leading to less branched products. A TMPTMA homopolymer was also synthesised which displayed a high level of branching, indicated by Mark-Houwink data. However, on increasing branching, limitations on the maximum molecular weight achieveable prior to gelation are observed.

End group fidelity was also probed using MALDI-ToF for poly-EGDMA due to the importance of these groups in further functionalisation steps, which proved to be high at approximately 99% vinyl group retention.

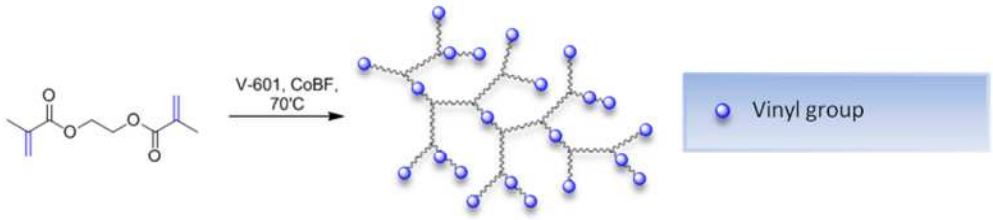

With the means to control the molecular weight and branching, through both CoBF concentration monomer choice and copolymerisation, and high vinyl end group fidelity in the polymer product, the functionalisation of an EGDMA homopolymer was investigated via thiol-Michael addition. The thiol-Michael addition was found to be greatly enhanced by use of DMSO as the solvent. Quantitative conversions were obtained for reactions, using as low as 0.01 mole equivalents of DMPP and a molar equivalent amount of benzyl mercaptan to vinyl groups, as estimated by GPC. The versatility of this system was further tested by use of alternative commercially available functional thiols, covering a range of hydrophobic/hydrophilic functionalities. Using this combination of CCTP and thiol-Michael addition a range of functional materials were

obtained from a single polymer precursor, with a wide scope for application to further branched polymers synthesised via CCTP.

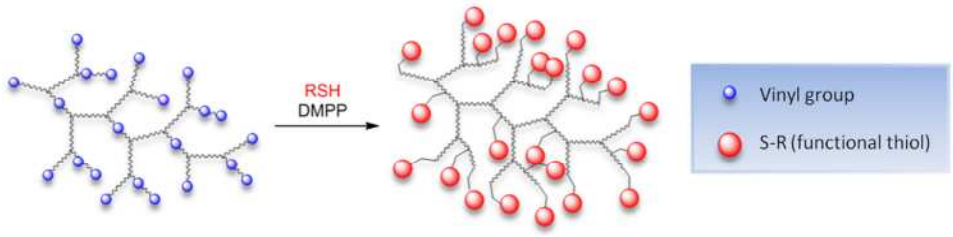

Progression from this point was spurred on by the popularity of GMA as a functional monomer in the literature, and the wide range of ring-opening methods demonstrated, which could be applied in the synthesis of functional polymers. However, no literature on the CCTP of GMA and its functionalisation existed at that time, therefore, although the aim of this work was to produce functional branched polymers, the application of CCTP to the synthesis of linear GMA homopolymers and ring-opening of these polymers with a range of amines was tested first, in order to ascertain the applicability of this monomer to a branched CCTP system.

Linear homopolymers of GMA were synthesised by CCTP, yielding polymers of low molecular weight, with a single terminal vinyl group and a level of epoxide equal to the DP_n, with no discernible loss of epoxide groups during the polymerisation; providing the means for the synthesis of dual functional polymers via combinations of thio-Michael addition and epoxide ring-opening reactions. Molecular weights and hence epoxide functionality could be controlled by the level of CoBF, whereby decreases in the CoBF concentration led to increases in molecular weight.

The viability of epoxide ring-opening with both primary and secondary amines was examined, to which it was found reactions could proceed to completion without the need for catalysis, with as little as a 1.2 excess of amine to epoxide groups. Results showed that primary amines predominantly led to full functionalisation of both epoxide and vinyl groups, whereas functionalisation with secondary amines led to full epoxide functionalisation with minimal vinyl loss. Therefore, for the synthesis of dual functional polymers using primary amines, it was necessary to conduct the thio-Michael addition prior to the epoxide ring-opening reaction, whereas for use of secondary amines, dual

functionalisation proved more versatile in that epoxide ring-opening reactions could be conducted prior to or post thio-Michael addition.

A higher level of purity was observed via MALDI-ToF for products of the dual functionalisation of poly-GMA using secondary amines in comparison to primary amines, although some restrictions to functionalisation with secondary amines was observed on use of sterically hindered amines, such as diphenylamine, additionally the number of commercially available secondary amines is reduced in comparison to primary amines, leading to advantages and disadvatages to both routes of functionalisation. However, the combination of thiol-Michael addition and self-catalysed functionalisation of poly-GMA with functional amines is a facile way for the introduction of functionality in a site specific manner and can lead to dramatic changes in the hydrophobicity/hydrophilicity of the resulting polymers. Hydroxyl groups formed on epoxide ring-opening have also been shown to be susceptible to esterification, hence, there is potential for the formation of tri-functional polymers and the potential for application of this monomer to branched systems via CCTP.

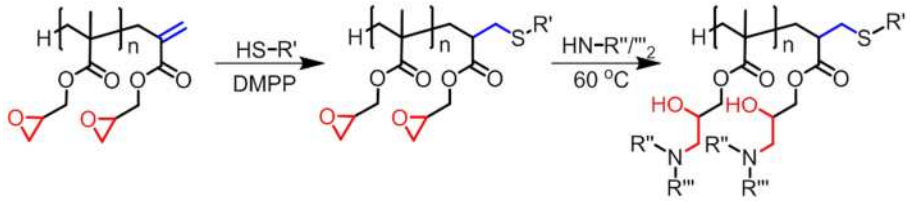

Due to the success of the CCTP of linear GMA and its dual functionalisation, copolymerisations of GMA and branching monomer GMA were investigated in order to synthesise branched polymers containing high levels of both vinyl and epoxide groups for further functionalisation. Initial reactions led to micro and macrogelation of products due to solvent choice, once this was adressed however, soluble copolymers containing both vinyl and epoxide functionalities were obtained, hence solvent choice is a key parameter for copolymerisations of GMA and EGDMA.

The ratio of vinyl to epoxide groups was accessed by the comonomer ratios, which in turn affects the branching of the polymers, providing a facile method for tailoring the properties of the resulting polymers. The level of branching for copolymers formed was characterised *via* universal calibration, with the generation of Mark-Houwink and g' plots confirming the lower solution viscosities of branched copolymers in comparison to

their linear counterparts and providing an insight into the relative levels of branching, however, due to the low molecular weight of polymers investigated, a non-linear relationship between hydrodynamic volume and IV was observed, meaning a true reflection of the molecular weight averages was not obtained and only trends in the molecular weights and branching of polymers could be obtained.

On investigation of the conversion for individual monomers the incorporation of EGDMA was found to be higher than that of GMA, which would likely lead to the formation of star like polymers. This combined with the potential for dual functionalisation led to investigation of amphiphilic dual functionalisation and self assembly of these products. Conducting thiol-Michael addition prior to epoxide ring-opening proved successful, enabling dual functionalisation with both hydrophobic and hydrophilic groups in a site specific manner, which can have a dramatic effect over the solubility of the resulting polymers. Preliminary DLS studies indicated that particles were obtained in all cases of amphiphilic dual functionalised copolymers. However, the particle size was large, indicating the formation of micellar structures was unlikely. However, it is believed that the copolymers described in this work show potential for self assembly.

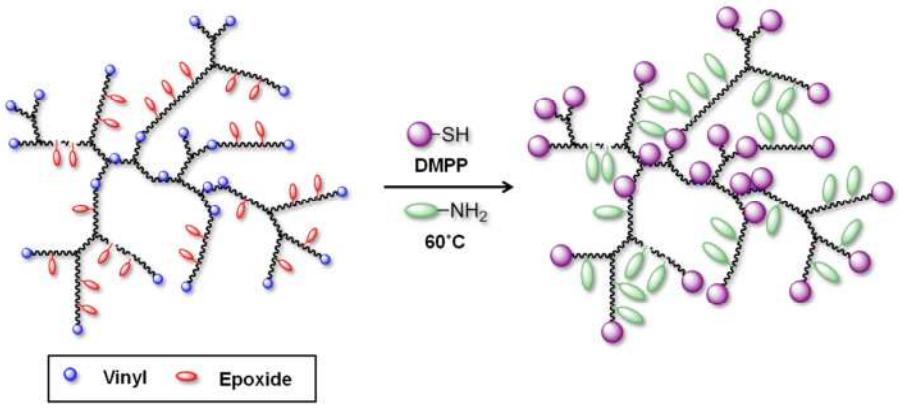

To conclude a method for the facile synthesis of branched polymers from commercially available materials was established, using relatively low levels of chain transfer agent. Control over branching and molecular weight was accessed by the CoBF concentration, the level of crosslinking monomer for copolymerisations and/or the level of vinyl functionality of the crosslinking monomer. Functionalisation of these materials was also achieved by thiol-Michael addition, exploiting the high level of vinyl groups retained via the CCTP mechanism, and by copolymerisation with epoxide functional

monomer GMA and subsequent ring-opening reactions, enabling dual functionalisation of these materials in a site specific manner, which would be difficult to achieve using alternative polymerisation techniques.

Future work on this project would widen the scope of the functionalisation of GMA, exploring more methods for the functionalisation of this material through ring-opening techniques and examine further functional monomers, such as propargyl methacrylate, for the exploitation of CuAAc chemistry and other routes to introduce further functionality. Additionally, it has been shown that dual functionalisation in a site specific manner provides an opportunity to create amphiphilic branched polymers, further work into the self-assembly of these materials would be a point of interest.

Appendix

Table 1: Selection of monomers employed in CCT homopolymerizations and associated reaction conditions

Monomer	Catalyst[a]	C_s	Solvent	Temp. (°C)	Ref.
Methyl methacrylate	CoBF	24 000- 40 000 (40000)	Bulk	60	1-6
	CoPhBF	18 000- 24 000	Bulk	60	1, 2, 7, 8
	$Co(dmg)_2$	2 200- 20 000 (2 200)	Bulk	60	9
	cycCoBF	13 700	Bulk	60	1
	CoP	3 600	Bulk	60	2, 10
	CoTMHP	2 400	Bulk	60	11
	CoBF	41 000- 60 000	Toluene	60	12
	CoBF	26 500	Butanone	60	1
	CoBF	10 100	Methanol	60	1
	CoBF	16000- 25000	Ethanol	60	13
	CoPhBF	110000	$ScCO_2$	50	14
	CoTFPP	1300	$ScCO_2$	60	15
	Co(ipp)BF	32000	Bulk	60	16
	$Co(L_S)$	17.5	Butanone	70	17-19
	TAPCo	--	$CDCl_3$	60	20
Ethyl methacrylate	CoBF	27000	Bulk	60	2
***n*-Butyl methacrylate**	CoBF	16000- 28000	Bulk	60	21
	CoTMHP	670	Bulk	60	22, 23
	CoPhBF	11900- 46700[b]	$ScCO_2$	50	24
	CoPhBF	13200- 43000[b]	$ScCO_2$	60	24
***t*-Butyl methacrylate**	CoBF	14000- 16800	Bulk	60	1
Hexyl methacrylate	CoTMHP	430	Bulk	60	22, 23
Heptyl methacrylate	CoTMHP	250	Bulk	60	

Octyl methacrylate	CoTMHP	250	Bulk	60	
Nonyl methacrylate	CoTMHP	150	Bulk	60	
Decyl methacrylate	CoTMHP	110	Bulk	60	
Hexadecyl methacrylate	CoTMHP	130	Bulk	60	
2-Hydroxy ethyl methacrylate	CoBF	600	Bulk	60	[16]
	Co(ipp)BF	900	Water	60	[25]
	CoBF	1100	Water/MeOH (2:1)	80	[20]
	TAPCo	--	$CDCl_3$	60	[26]
2-Phenoxyethyl methacrylate	CoPhBF	2 000	Bulk	60	[27]
3-[Tris(trimethylsilyloxy)silyl]propyl methacrylate	CoBF	800- 1700	Toluene	60	[28]
	CoBF	~7500	2-Butanone	60	[28]
3-(Trimethoxysilyl) propyl methacrylate	CoBF	~27000	2-Butanone	60	[28]
2-[3-(2H-Benzotriazol-2-yl)-4-hydroxyphenyl]ethyl methacrylate	CoBF	~4000	Toluene	60	[28]
Lauryl methacrylate	CoBF	~20000	2-Butanone	60	[29]
2-Dimethylaminoethyl methacrylate	CoBF	~4400	Bulk	70	[30]
2-Phthalimidoethyl methacrylate	CoBF	500	Toluene	80	[31]
Glycidyl methacrylate	CoBF	--	MIBK	105	[32]
	CoBF	6400	Acetonitrile	60	[25]
3-O-Methacryloyl-1,2:5,6-di-O-isopropylidene-D-glucofuranose	CoBF	--	Distilled water	80	[33]
Benzyl methacrylate	CoBF	5700- 6900	Bulk	60	[34]
2-Ethyl hexyl methacrylate	CoBF	11900	Bulk	60	[35]
ethyl α-hydroxymethacrylate	CoBF	700	Bulk	60	[36, 37]
Trimethylsilane-protected propargylmethacrylate	CoBF	--	Toluene	60	[25]
Glycerol methacrylate	CoBF	1000	Water/MeoH (2:1)	80	

Methacrylic acid	CoBF	1100	Water	55	[25]
Dimethyl itaconate	CoBF	7300- 9500	Bulk	60	[38]
Styrene	CoBF	350- 8300 (~8000)	Bulk	60	[1, 3, 4, 34, 39]
	TAPCo	--	$CDCl_3$	60	[20]
	CoPhBF	100- 1200[b]	$ScCO_2$	50	[24]
α-Methyl styrene	CoBF	89300	Bulk	50	[39]
Phenyl allyl alcohol	CoBF	138000- 157000	10% in MMA	60	[40]
Methyl acrylate	CoBF	8- 22	Bulk	60	[5, 33]
	TAPCo	--	$CDCl_3$	60	[20]
Butyl acrylate	CoBF	700	Bulk	60	[34]
Acrylamide	CoBF	100	Acetic acid	60	[41]
Di(ethylene glycol) methyl ether methacrylates	CoBF	7600	Acetonitrile	70	[42]
Poly(ethylene glycol)$_{475}$ methyl ether methacrylate	CoBF	1800	Acetonitrile	70	[42]
	Co(ipp)BF	--	Water	60	[16]
Poly(ethylene glycol)$_{1100}$ methyl ether methacrylate	CoBF	180	Acetonitrile	70	[42]
Poly(ethylene glycol)$_{2000}$ methyl ether methacrylate	Co(ipp)BF	15-20	Water	60	[16]
Ethylene glycol dimethacrylate	CoBF	--	1,2-Dichloroethane	55	[43, 44]
	CoTMHP	--	--	--	[45]
Triethylene glycol dimethacrylate	CoTMHP	--	--	--	[46]
1,4-Butanediol dimethacrylate	CoTMHP	--	Bulk	60	[47]
1,4-Butanediol diacrylate	CoTMHP	--	Bulk	60	[47]
Methylolpropane trimethacrylate	CoBF	--	1,2-Dichloroethane	70	[44]
Poly(ethylene glycol)$_{4000}$ dimethacrylate	Co(ipp)BF	--	Water	60	[16]

Methacrylonitrile	TAPCo	--	$CDCl_3$	60	[20]
2-Methacryloxyethyl phosphoryl choline	CoBF	--	Water/MeoH (2:1)	80	[25]
2-Aminoethyl methacrylate hydrochloride	CoBF	--	Water	80	[25]
1,1,2,2-Tetrahydroperfluoroalkyl methacrylate	CoBF	110	Acetone	65	[48, 49]
Cyclohexene	TAPCo	--	$CDCl_3$	60	[20]
Methyl crotonate	TAPCo	--	$CDCl_3$	60	[20]
Vinyl acetate	TAPCo	--	$CDCl_3$	60	[20]
Cis-2-pentenenitrile	TAPCo	--	$CDCl_3$	60	[20]
Vinyl benzoate	TAPCo	--	$CDCl_3$	60	[20]

[a] CoBF= bis[(difluoroboryl)dimethylglyoximato] cobalt(II); CoPhBF=bis[(difluoroboryl)diphenyl glyoximato] cobalt (II); $Co(dmg)_2$=bis[dimethyl glyoximato]cobalt(II); cycCoBF=bis[(difluoroboryl) cyclobutylglyoximato]cobalt(II); CoP= cobalt(*meso*-Ph_4-porphyrin); CoTMHP= tetra methyl ether of cobalt hematoporphyrin IX; CoTFPP= cobalt tetrafluorophenyl porphyrin; CoPc= cobalt(II) 2,16-bis(4-butanamidoyl)phthalocyanine; MIBK= methyl isobutyl ketone; TAPCo tetrakis(*p*-methoxyphenyl)porphyrinato)cobalt (II); Co(ipp)BF bis(boron difluoro-dimethylglyoximato)isopropyl-pyridine Co(II); (--) indicates C_s value hasn't been determined $Co(L_s)$= Co(II) thiophenolate complex; [b] value dependent on pressure

References

1. Haddleton, D. M.; Maloney, D. R.; Suddaby, K. G.; Muir, A. V. G.; Richards, S. N., Macromol. Symp. ***1996,*** *111, 37.*

2. Heuts, J. P. A.; Forster, D. J.; Davis, T. P., Macromolecules ***1999,*** *32 (12), 3907.*

3. Kukulj, D.; Davis, T. P., Macromol. Chem. Phys. ***1998,*** *199 (8), 1697.*

4. Suddaby, K. G.; Maloney, D. R.; Haddleton, D. M., Macromolecules ***1997,*** *30 (4), 702.*

5. Pierik, B.; Masclee, D.; Herk, A. v., Macromol. Symp. ***2001,*** *165 (1), 19.*

6. Sanayei, R. A.; Odriscoll, K. F., J. Macromol. Sci. Chem. ***1989,*** *A26 (8), 1137.*

7. Heuts, J. P. A.; Forster, D. J.; Davis, T. P., Macromol. Rapid Commun. ***1999,*** *20 (6), 299.*

8. Heuts, J. P. A.; Forster, D. J.; Davis, T. P.; Yamada, B.; Yamazoe, H.; Azukizawa, M., Macromolecules ***1999,*** *32 (8), 2511.*

9. Burczyk, A. F.; Odriscoll, K. F.; Rempel, G. L., J. Polym. Sci., Part A: Polym. Chem. ***1984,*** *22 (11), 3255.*

10. Vollmerhaus, R.; Pierik, S.; van Herk, A. M., Macromol. Symp. ***2001,*** *165 (1), 123.*

11. Enikolopyan, N. S.; Smirnov, B. R.; Ponomarev, G. V.; Belgovskii, I. M., J. Polym. Sci., Chem. Ed. ***1981,*** *19 (4), 879.*

12. Pierik, S. C. J.; Herk, A. M. v., J. Appl. Polym. Sci. ***2004,*** *91 (3), 1375.*

13. Forster, D. J.; Heuts, J. P. A.; Lucien, F. P.; Davis, T. P., Macromolecules ***1999,*** *32 (17), 5514.*

14. Zwolak, G.; Jayasinghe, N. S.; Lucien, F. P., J. Supercrit. Fluids ***2006,*** *38 (3), 420.*

15. Mang, S. A.; Dokolas, P.; Holmes, A. B., Org. Lett. ***1999,*** *1 (1), 125.*

16. Kazanskii, K. S.; Rakova, G. V.; Kozlov, S. I.; Stegno, E. V.; Lapienis, G., Vysokomol. Soedin., Ser. A Ser. B ***2004,*** *46 (3), 390.*

17. Wang, W. X.; Stenson, P. A.; Irvine, D. J.; Howdle, S. M., Polym. Prepr. (Am. Chem. Soc., Div. PMSE) ***2004,*** *228, 572.*

18. Wang, W.; Stenson, P. A.; Irvine, D. J.; Howdle, S. M., Polym. Prepr. (Am. Chem. Soc., Div. PMSE) ***2004,*** *91, 1051.*

19. Wang, W. X.; Stenson, P. A.; Marin-Becerra, A.; McMaster, J.; Schroder, M.; Irvine, D. J.; Freeman, D.; Howdle, S. M., Macromolecules ***2004,*** *37 (18), 6667.*

20. Morrison, D. A.; Davis, T. P.; Heuts, J. P. A.; Messerle, B.; Gridnev, A. A., J. Polym. Sci., Part A: Polym. Chem. ***2006,*** *44 (21), 6171.*

21. Pierik, S. C. J.; Vollmerhaus, R.; van Herk, A. M., Macromol. Chem. Phys. ***2003,*** *204 (8), 1090.*

22. Mironychev, V. Y.; Mogilevich, M. M.; Smirnov, B. R.; Shapiro, Y. Y.; Golikov, I. V., Vysokomol. Soedin., Ser. A ***1986,*** *28 (9), 1891.*

23. Mironychev, V. Y.; Mogilevich, M. M.; Smirnov, B. R.; Shapiro, Y. Y.; Golikov, I. V., Polymer Science U.S.S.R. ***1986,*** *28 (9), 2103.*

24. Zwolak, G.; Lucien, F. P., Macromolecules ***2006,*** *39 (25), 8669.*

25. Haddleton, D. M. D., E.; Kelly, E. J.; Kukukj, D.; Morsley, S. R.; Bon, S. A. F.; Eason, M. D.; Steward, A. G., J. Polym. Sci., Part A: Polym. Chem. ***2001,*** *39, 2378.*

26. Forster, D. J.; Heuts, J. P. A.; Davis, T. P., Polymer ***2000,*** *41 (4), 1385.*

27. Muratore, L. M.; Heuts, J. P. A.; Davis, T. P., Macromol. Chem. Phys. ***2000,*** *201 (9), 985.*

28. Steward, A. G.; haddleton, D. M.; Muir, A. V. G.; Willis, S. L., Polym. Prepr. (Am. Chem. Soc., Div. Polym. Chem.) ***1998,*** *39 (2), 459.*

29. Eason, M. D.; Haddleton, D. M.; Khoshdel, E., Polym. Prepr. (Am. Chem. Soc., Div. Polym. Chem.) ***1998,*** *39 (2), 455.*

30. Kelly, E. J.; Haddleton, D. M.; Khoshdel, E., Polym. Prepr. (Am. Chem. Soc., Div. Polym. Chem.) ***1998,*** *39 (2), 453.*

31. Kodo, K. S., Hidenori JP2002212512, ***2002****.*

32. McEwan, K. A.; Slavin, S.; Tunnah, E.; Haddleton, D. M., Polym. Chem. Submitted.

33. Roberts, G. E.; Heuts, J. P. A.; Davis, T. P., Macromolecules ***2000,*** *33 (21), 7765.*

34. Pierik, S. C. J.; Vollmerhaus, R.; van Herk, A. M.; German, A. L., Macromol. Symp. ***2002,*** *182, 43.*

35. Davis, T. P.; Zammit, M. D.; Heuts, J. P. A.; Moody, K., Chem. Commun. ***1998,*** *(21), 2383.*

36. Nurmi, L.; Lindqvist, J.; Randev, R.; Syrett, J.; Haddleton, D. M., Chem. Commun. ***2009,*** *(19), 2727.*

37. Gou, Y.; Haddleton, D. M., Polym. Prepr. (Am. Chem. Soc., Div. Polym. Chem.) ***2010,*** *51 (2), 229.*

38. Roberts, G. E.; Davis, T. P.; Heuts, J. P. A.; Ball, G. E., Macromolecules ***2002,*** *35 (27), 9954.*

39. Kukulj, D.; Heuts, J. P. A.; Davis, T. P., Macromolecules ***1998,*** *31 (18), 6034.*

40. Morrison, D. A.; Eadie, L.; Davis, T. P., Macromolecules ***2001,*** *34 (23), 7967.*

41. Martchenko, A.; Bremner, T.; Odriscoll, K. F., Eur. Polym. J. ***1997,*** *33 (5), 713.*

42. Soeriyadi, A. H.; Li, G.-Z.; Slavin, S.; Jones, M. W.; Amos, C. M.; Becer, C. R.; Whittaker, M. R.; Haddleton, D. M.; Boyer, C.; Davis, T. P., Polym. Chem. ***2011,*** *2 (4), 815.*

43. Guan, Z., J. Am. Chem. Soc. ***2002,*** *124 (20), 5616.*

44. Haddleton, D. M.; McEwan, K.; Menzel, J. P., Polym. Prepr. (Am. Chem. Soc., Div. Polym. Chem.) ***2010,*** *51 (1), 310.*

45. Kurmaz, S. V.; Bubnova, M. L.; Perepelitsina, E. O.; Roshchupkin, V. P., Vysokomol. Soedin., Ser. A Ser. B ***2003,*** *45 (3), 373.*

46. Golokov, I. V.; Semyannikov, V. A.; Mogilevich, M. M., Vysokomol. Soedin., Ser. A Ser. B ***1985,*** *27 (4), 304.*

47. Kurmaz, S.; Perepelitsina, E., Russ. Chem. Bull. ***2006,*** *55 (5), 835.*

48. Romack, T.; Harrelson, S.; Kenward, A., Abstracts, 55th Southeast Regional Meeting ACS, Atlanta, US ***2003****, 1093.*

49. Romack, T. J.; Kaur, G.; Weaver, S. F.; Harrelson, S. K.; Kenward, A. G., J. Polym. Sci., Part A: Polym. Chem. ***2006,*** *44 (13), 4136.*

Publications

Peer Reviewed:

Combining catalytic chain transfer polymerisation (CCTP) and thio-Michael addition: enabling the synthesis of peripherally functionalised branched polymers
McEwan, K. A.; Haddleton, D. M. *Polymer Chemistry,* **2011**, *2*, 1992-1999

Dual-functional materials via CCTP and selective orthogonal thio-Michael addition/epoxide ring-opening reactions
McEwan, K. A.; Slavin. S.; Tunnah, E.; Haddleton, D. M., *Polymer Chemistry*, **2013** advance article

Non-Peer Reviewed:

Synthesis of hyperbranched polymers via cobalt-catalyzed chain transfer and functionalization by thiol-ene click chemistry
McEwan, K. A.; Haddleton, D. M. Abstracts of Papers, 240th ACS National Meeting, Boston, MA, United States, August 22-26, **2010**, POLY-432

Book Chapter:

Cobalt Catalyzed Chain Transfer Polymerization: A Review
Slavin, S.; McEwan, K. A.; Haddleton, D. M. In *Polymer Science: A Comprehensive Reference*; 1st ed.; Matyjaszewski, K., Möller, M., Eds.; Elsevier: **2012**; Vol. 3, p 249-275